

APPENDIX B-2

**INVESTIGATION AND
BENCH-SCALE TREATABILITY STUDIES
TO EVALUATE REMOVAL OF PERCHLORATE
FROM JPL GROUNDWATER**

TABLE OF CONTENTS

	Page
LIST OF TABLES	B2-iii
LIST OF FIGURES	B2-iv
EXECUTIVE SUMMARY	B2-v
1.0 INTRODUCTION	B2-1
2.0 BACKGROUND	B2-2
2.1 REDUCTION	B2-2
2.2 ADSORPTION	B2-3
2.2.1 Granular Activated Carbon (GAC)	B2-4
2.2.2 Biologically Activated Carbon	B2-4
2.2.3 Ion Exchange Resins	B2-4
2.2.4 Activated Alumina	B2-4
2.3 MEMBRANE SEPARATION	B2-4
2.4 PRECIPITATION	B2-5
3.0 APPROACH	B2-5
4.0 SCOPE AND OBJECTIVES	B2-6
4.1 EXPERIMENT 1: INITIAL SCREENING	B2-6
4.2 EXPERIMENT 2: RANGE FINDING	B2-6
4.3 EXPERIMENT 3: ISOTHERM GENERATION	B2-7
5.0 MATERIALS AND METHODS	B2-7
5.1 EXPERIMENT 1: INITIAL SCREENING	B2-7
5.2 EXPERIMENT 2: RANGE FINDING	B2-9
5.3 EXPERIMENT 3: GENERATION OF ISOTHERMS	B2-9
6.0 RESULTS AND DISCUSSION	B2-10
6.1 EXPERIMENT 1: INITIAL SCREENING	B2-10
6.1.1 Activated Alumina	B2-10
6.1.2 Metal Catalysts	B2-11
6.1.3 Ion Exchange Resins	B2-11
6.1.4 Granular Activated Carbon (GAC)	B2-11
6.1.5 Chemical Reductants	B2-11
6.1.6 Biological Reduction	B2-11
6.1.7 Summary of Findings	B2-12
6.2 EXPERIMENT 2: RANGE FINDING	B2-12
6.3 EXPERIMENT 3: ISOTHERM GENERATION	B2-13
6.3.1 Summary of Findings	B2-13
6.3.2 Application to Full Scale Design	B2-13

TABLE OF CONTENTS

(Continued)

	Page
7.0 CONCLUSIONS.....	B2-15
8.0 REFERENCES	B2-16

APPENDICES

Appendix A	Experimental Plans/Laboratory Reports - Experiment 1
Appendix B	Experimental Plans/Laboratory Reports - Experiment 2
Appendix C	Experimental Plans/Laboratory Reports - Experiment 3

LIST OF TABLES

<u>TABLE NUMBER</u>	<u>TITLE</u>
1	Summary of General Water Quality Data
2	Materials Tested – Screening Experiment (Experiment 1)
3	Resin Loading Rates – Range Finding Experiment (Experiment 2)
4	Anion Exchange Resins – Isotherm Experiment (Experiment 3)
5	Comparison of ClO_4^- Concentrations – Method Blanks and Associated Influent
6	Perchlorate Removal – Boiling/Glucose Amendment
7	Summary of Results – Experiment 1
8	Summary of Results – Experiment 3

LIST OF FIGURES

<u>FIGURE NUMBER</u>	<u>TITLE</u>
1	Removal of Perchlorate by Activated Alumina (5 and 50 g/L) from JPL Groundwater
2	Removal of Perchlorate by Activated Alumina (5 and 50 g/L) from Deionized Water
3	Removal of Perchlorate by Metal Catalysts (5 and 50 g/L) from JPL Groundwater
4	Removal of Perchlorate by Metal Catalysts (5 and 50 g/L) from Deionized Water
5	Removal of Perchlorate by Ion Exchange Resins (5 and 50 g/L) from JPL Groundwater
6	Removal of Perchlorate by Ion Exchange Resins (5 and 50 g/L) from Deionized Water
7	Removal of Perchlorate by Activated Carbon (5 and 50 g/L) from JPL Groundwater
8	Removal of Perchlorate by Activated Carbon (5 and 50 g/L) from Deionized Water
9	Removal of Perchlorate by Soluble Reducing Agents (1 g/L) from JPL Groundwater
10	Removal of Perchlorate by Soluble Reducing Agents (1 g/L) from Deionized Water
11	Resin Loading Ranges – Amberlite IRA400 Cl
12	Contact Time Ranges – Amberlite IRA400 Cl
13	Perchlorate Removal from JPL Groundwater and Deionized Water by Amberlite IRA400 Cl for different Resin Loadings – 2 hour Contact Time
14	Freundlich Isotherm –Amberlite IRA400 Cl (SBA)
15	Freundlich Isotherm – Dowex MSA-1 (SBA)
16	Freundlich Isotherm – Dowex MS 500A (SBA)
17	Freundlich Isotherm – Ionac AFP-329 (WBA)
18	Freundlich Isotherm – Ionac A-305B (WBA)
19	Freundlich Isotherm – Ionac A-641 (SBA)

APPENDIX B-2

INVESTIGATION AND BENCH-SCALE TREATABILITY STUDIES TO EVALUATE REMOVAL OF PERCHLORATE FROM JPL GROUNDWATER

EXECUTIVE SUMMARY

This report summarizes research conducted to identify and assess adsorbents and reductants with potential to remove the perchlorate ion (ClO_4^-) from groundwater sampled at the Jet Propulsion Laboratory (JPL). Three experiments were conducted as follows (i) screening experiment (Experiment 1), (ii) range finding experiment (Experiment 2), and (iii) isotherm generation (Experiment 3).

The screening experiment consisted of testing a number of adsorbents and reductants that were deemed potentially feasible for removing ClO_4^- from groundwater after conducting an initial information and literature search. These included various activated alumina preparations, metal catalysts, anion exchange resins, activated carbons, and chemical reductants. The screening experiment consisted of a series of flask tests, in which two specified quantities of these materials were contacted with ClO_4^- contaminated JPL groundwater, and ClO_4^- concentrations in the effluent measured after 3 hours. This test indicated that ion exchange resins had the greatest potential to remove ClO_4^- from the JPL groundwater. In a parallel experiment, bioreduction was also found to be capable of removing ClO_4^- from the JPL groundwater.

Based on the success of ion exchange resins, Experiments 2 and 3 were initiated to confirm the findings of Experiment 1, and to obtain preliminary performance information. A total of six resins were selected for Experiments 2 and 3. These were selected based on their compatibility with drinking water as indicated by the manufacturers of these resins.

The second and third experiments focused mainly on generating isotherms for the six selected resins, and thereby determining the maximum ClO_4^- loading capacities for these resins. These consisted of several flask tests. Of the resins tested, four resins were of the strong base anion (SBA) type and two were of the weak base anion (WBA) type. The generated isotherms indicated ClO_4^- loading capacities ranged from 79 to 515 $\mu\text{g ClO}_4^-/\text{g resin}$. In general, the SBA resins performed better than the WBA resins. This data was used to confirm the results of the initial study, specify the best resin to use in a column study, and estimate preliminary design parameters for the column study (volumetric loading rates, resin volumes, testing durations).

1.0 INTRODUCTION

The US Environmental Protection Agency (EPA) has identified the perchlorate ion (ClO_4^-) as a potential environmental health risk (EPA, 1992, 1995). Studies by the California Department of Health Services (DHS) indicate that the primary mechanism of toxicity in humans appears to be the inhibition of iodine uptake by the thyroid gland, leading to decreased production of thyroid hormones (DHS, 1997). Perchlorate has recently been detected in groundwater at the Jet Propulsion Laboratory (JPL). Although no federal or state drinking water standards currently exist for ClO_4^- , the DHS has recommended an interim action level of 18 $\mu\text{g/L}$ (micrograms per liter), which is considered to be protective of public health (DHS, 1997). Perchlorate has been detected in the JPL groundwater monitoring wells at concentrations ranging from below detection limits (4 $\mu\text{g/L}$) to as high as 615 $\mu\text{g/L}$. The presence of ClO_4^- in the groundwater has caused the shutdown of one down-gradient drinking water production well, and is currently threatening another. Clearly, an efficient, cost-effective technique for removing ClO_4^- from contaminated groundwater is needed.

This report presents the findings of a study conducted by Foster Wheeler Environmental Corporation (Foster Wheeler) to investigate techniques for removal of ClO_4^- from groundwater at JPL. Initially, a broad range of potentially applicable treatment techniques used for water treatment were identified, primarily reduction (chemical and biological), adsorption, membrane separation, and precipitation. Based on the chemistry of the ClO_4^- ion, our experience with treatment of similar ions, literature reviews, and discussions with academia and industry, the potentially ineffective treatment techniques were eliminated. The remainder, which consisted primarily of adsorption and chemical reduction were retained and tested on a laboratory scale. Biological reduction was also tested concurrently, since literature reviews indicated that it presented significant potential.

The remainder of this report is organized as follows:

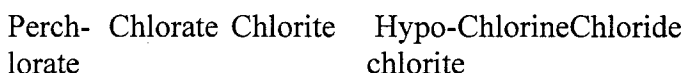
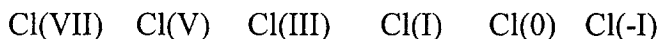
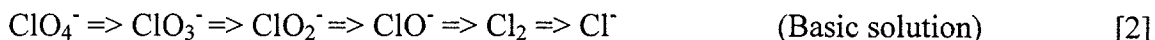
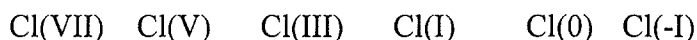
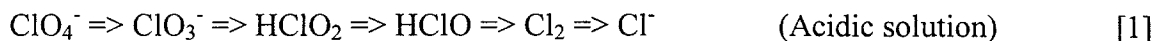
- Section 2.0 – Background
- Section 3.0 – Approach
- Section 4.0 – Scope and Objectives
- Section 5.0 – Materials and Methods
- Section 6.0 – Results and Discussions
- Section 7.0 – Conclusions
- Section 8.0 - References

2.0 BACKGROUND

Research regarding behavior and/or transformations of ClO_4^- in groundwater is lacking, probably because ClO_4^- contamination has only recently been reported. Speciation and oxidation states of chlorine (Cl), including its oxyanionic forms, are given below (Ebbing, 1987):

OXIDIZED

REDUCED



The most stable Cl species/compounds are those in which the element is in its highest or lowest oxidation state (Greenwood and Earnshaw, 1985). As indicated above, ClO_4^- contains Cl in its highest oxidation state. While ClO_4^- is a powerful oxidizing agent when heated, at room temperature (characteristic of JPL groundwater), aqueous solutions of ClO_4^- are not notable oxidizers and are extremely stable (Greenwood and Earnshaw, 1985). Although information regarding the behavior of ClO_4^- in environmental matrices is virtually nonexistent, it appears that spontaneous reduction to more innocuous forms such as Cl^- may be unlikely in the time frame of interest, and this undermines potential clean-up actions based on strategies such as natural attenuation. There are, however, several options (which are currently being applied to other oxyanions) with the potential to remove ClO_4^- from contaminated water, or convert it to less toxic forms. Four basic removal processes are potentially applicable: reduction, adsorption, membrane separation, and precipitation. Below are brief discussions of each of these processes as they apply to treating ClO_4^- contaminated water.

2.1 Reduction

Complete reduction of ClO_4^- to Cl^- represents destruction of ClO_4^- , and effectively eliminates its toxicity. Hypochlorite and Cl_2 , which are potential intermediates in this reaction, are commonly added to wastewater for disinfection, and residuals have traditionally been removed by reduction to Cl^- using granular activated carbon (GAC), or sulfur dioxide (SO_2) (Mecalf and Eddy, 1979). Therefore, a non-intrusive means of reducing ClO_4^- may be effective, even if the reaction is not complete, since further reduction of the reaction products may be accomplished through traditional means. Chemical reduction is widely used in treatment of drinking water and biological reduction is steadily gaining acceptance. However, these reactions are usually sensitive to environmental conditions such as pH and temperature.

In addition to reducing ClO_4^- and Cl_2 to Cl^- , GAC has been shown to remove ClO_2^- and ClO_3^- from solution (Gonce and Voudrias, 1994). However, while reduction to Cl^- was shown to be the mechanism for removal of ClO_2^- , ClO_3^- was not reduced, but was physically and reversibly adsorbed. Based on this finding and the reported stability of ClO_4^- at typical groundwater temperatures, reduction of ClO_4^- by GAC seems unlikely. However, other chemical reductants have been used in treating oxyanions in contaminated water. For example, sodium dithionite ($\text{Na}_2\text{S}_2\text{O}_4$) has been used to remove arsenic oxyanions from solution at the former Rhone Poulenc facility, Southgate, CA (A. Eloskof, Foster Wheeler, personal communication, 1997), and removal of aqueous chromate (CrO_4^{2-}) has been accomplished through reduction by Fe(II) (Eary and Rai, 1988). Other reducing agents commonly used for water treatment are sodium sulfite (Na_2SO_3) and sodium thiosulfate ($\text{Na}_2\text{S}_2\text{O}_3$). Soluble chemical reductants can only be used to treat drinking water in cases where they are easy to remove, are not a potential threat themselves, or can be effective when added at very low concentrations (below their regulatory limits).

The dynamic surface chemistry, which characterizes insoluble forms of many metals, is known to catalyze reduction reactions. For example, a study currently being conducted has demonstrated reduction (and removal from solution) of CrO_4^{2-} and selenate (SeO_4^{2-}) by a treatment system which utilizes zero-valent iron (Fe^0) as the reductant (C. Amrhein, Professor of Soil Chemistry, University of California, Riverside, personal communication, 1997). Nickel (Ni) and palladium (Pd) is also used in various reduction reactions (Bailey and Bailey, 1985). Metal catalysts may also have applicability with regard to reduction of ClO_4^- .

Bioreduction represents another possible mechanism for bringing about reduction of oxidized Cl species. This does not refer to degradative processes whereby organic contaminants such as petroleum hydrocarbons are utilized as carbon/energy sources. Rather, it is based on the hypothesis that ClO_4^- may be reduced enzymatically as a terminal electron acceptor in microbial respiration as O_2 becomes limiting, analogous to NO_3^- and SO_4^{2-} reduction in soils and water. In addition, other microbial uptake/reduction mechanisms may bring about reduction of ClO_4^- , or remove it from solution. Bacterial reduction of numerous oxyanions, including those containing Cr(VI) and Se(VI), is known to occur (Losi et al., 1994; Losi and Frankenberger, 1997). Because many of these mechanisms are enzymatic in nature, reaction rates can be very rapid. Bacterial reduction of ClO_4^- has been demonstrated, and the organisms which carry out the reaction may be ubiquitous (van Ginkel, 1997; Logan, 1997). Such organisms may be useful as part of a treatment scheme to remove ClO_4^- from groundwater.

2.2 Adsorption

Adsorption is another means for removing anions from solution by collecting them on a suitable interface. The main advantages of this technique are its amenability to flow-through systems (rather than batch), and minimal need for reagents. As with reduction reactions, parameters such as pH and temperature may exert a strong influence on adsorptive processes. A wide variety of adsorptive materials are commercially available, as discussed below.

2.2.1 Granular Activated Carbon (GAC)

GAC is the most inexpensive and widely used adsorbent for treating contaminated water. Many preparations of GAC are available which vary widely in terms of the material from which they were manufactured, porosity, surface area, means of activation, and reactivity (surface properties). These are generally used for removing organic compounds, but some preparations remove inorganic contaminants as well. In some cases, removal is accomplished purely through reversible or irreversible adsorption mechanisms, while in others, reactions which transform the contaminants are operative. In most cases, these two processes may operate in tandem to varying degrees. As mentioned above, ClO_4^- and Cl_2 may be reduced to Cl^- by GAC, but evidence suggests that the more oxidized chloro-oxyanions are subject only to reversible adsorption in GAC systems (Gonce and Voudrias, 1994).

2.2.2 Biologically Activated Carbon

Biologically activated carbon (BAC) is a variation that combines the reactive capabilities of microorganisms with the adsorptive properties of GAC to enhance contaminant removal efficiency. Biologically activated carbon technology was pioneered in Europe and is now widely used for treating drinking water (Dussert and Van Stone, 1994). There are reports in the literature of enhanced destruction of a target compound by GAC inoculated with a specific degrader organism (Feakin et al., 1995). Since bacterial growth is observed in virtually all activated carbon systems, effluent disinfection is usually a concern whether or not the carbon has been inoculated with a specific organism (Faust and Aly, 1987).

2.2.3 Ion Exchange Resins

Ion exchange resins have been used since the early 1900s to remove contaminants from water (Owens, 1995). The ion exchange process consists of removing ions from solution, and replacing them with ions from a solid phase. Ion exchange resins are commonly used in 4 different forms: Weak Acid Cation (WAC), Weak Base Anion (WBA), Strong Acid Cation (SAC) and Strong Base Anion (SBA), depending on the type of ion that needs to be removed. For ClO_4^- , either the SBA or WBA type of resin would be the most appropriate.

2.2.4 Activated Alumina

Activated alumina has been used since the 1930s to remove fluoride ions from drinking water, (Metcalf and Eddy, 1979). It functions similar to ion exchange resins. Exchange is very pH specific, with anion exchange occurring up to a pH of about 9.5, and cation exchange above 9.5. Process design of activated alumina is very similar to that of ion exchange, with NaOH being used as the regenerant.

2.3 **Membrane Separation**

Several pressure-, or gradient-driven membrane separation techniques are now widely applied to treat drinking and wastewaters. The technique best suited to removing anionic solutes such as

ClO_4^- is hyperfiltration (or reverse osmosis). Hyperfiltration techniques may have an advantage of anion selectivity, and are generally considered to be comparable to other techniques in terms of both technical and economic feasibility (Geckeler and Volchek, 1996). In addition, systems can be designed to treat relatively clean feeds containing few contaminants (such as groundwater at JPL) with minimal production of waste product. However, long residence times with slow flow rates may be required to treat water with very low ClO_4^- concentrations relative to those of other anions. Nevertheless, in the absence of other feasible remedial alternatives, hyperfiltration may eventually merit investigation.

2.4 Precipitation

Finally, chemical precipitation involves addition of chemicals to convert a soluble compound to an insoluble precipitate, which is then removed by sedimentation, or filtration. This (as is the case with addition of chemical reductants) must be carefully controlled, and is feasible only when the chemicals are added at levels which do not exceed drinking water standards, or can be quantitatively recovered in the precipitate. Additionally, in most applications chemical precipitation reactions are very complex, and are often incomplete, or subject to numerous side reactions and interferences. Precipitation techniques are commonly used in removal of phosphates and bicarbonates in water treatment (Metcalf and Eddy, 1979). The potassium ion (K^+) is reportedly used to precipitate ClO_4^- in gravimetric analysis with a notable lack of interferences (Harris, 1987). Furthermore, a recent paper has reported the synthesis of a reagent that selectively removes dichromate ($\text{Cr}_2\text{O}_7^{2-}$) and ClO_4^- from aqueous solution (Kopchinsky and Meloan, 1996).

3.0 APPROACH

Our approach was to conduct a series of batch experiments to evaluate the potential of the methods listed in Section 2.0 for removal of ClO_4^- from JPL groundwater. These included commercially available solid phase adsorbents or reactants.

It was originally conceived that laboratory bench-scale continuous flow column experiments would be conducted. This work was to be conducted jointly with US Filter/Westates (USF/W) at their facility in Vernon California. Dr. Jim Graham and Abe Goldhaar of USF/W indicated that they had knowledge of, and access to catalysts (later disclosed to be Raney Nickel) which they indicated would be successful in reducing ClO_4^- in a groundwater matrix.¹ Initial contractual negotiations with USF/W proved unsuccessful because Foster Wheeler could not guarantee USF/W patent rights regarding any invention that might result from the research (due to Foster Wheeler's contractual obligations to JPL). Following consultation with Charles Buriel of JPL, it was decided that the work would be carried out solely by Foster Wheeler personnel at a

¹ As will be discussed in subsequent sections, this was one of the materials that we tested, and found to be ineffective, with a ClO_4^- removal of less than 16% (compared to 100% for ion exchange resins).

laboratory with no vested interest in the project (CET Environmental Laboratories, Tustin, CA). It was also agreed that due to the wide variety of promising materials (adsorbents), and the lack of information regarding potential chemical processes, laboratory batch testing should preclude column studies to facilitate efficient and economical screening of the available materials. This approach was confirmed in consultation with Dr. Andrew Chang (Professor of Agricultural Engineering/Water Quality, University of California, Riverside). Also, since chemical reductants were also targeted for investigation, use of columns for such techniques would be impracticable.

Hence, our approach to the study was modified to use flask tests instead of column studies.

4.0 SCOPE AND OBJECTIVES

The main objectives of this study were:

1. To identify and study a process which can be used to remove ClO_4^- from the groundwater at existing municipal production well heads in conjunction with air stripping systems (already in place) which remove volatile organics. The process should be capable of treating large volumes of water with minimal pre- or post-treatments.
2. Upon identification of such a process, perform laboratory studies to confirm feasibility in treating actual JPL water.
3. Establish design parameters for additional laboratory scale studies, future field scale pilot testing and/or full-scale implementation. Given the scarcity of actual implementation experience in treating ClO_4^- contaminated water, it is envisioned that additional laboratory studies and field scale pilot studies would be required prior to full-scale implementation.

The scope of work required to meet these objectives is discussed below.

4.1 Experiment 1: Initial Screening

An initial batch screening study was conducted to evaluate various materials and determine their potential for removing ClO_4^- from JPL groundwater. These materials included adsorbents, catalysts and chemical reductants that were deemed potentially feasible in an initial information and literature search, as discussed in Section 2.0. This experiment was intended to identify the most promising material(s) for further study.

4.2 Experiment 2: Range Finding

Results from Experiment 1 suggested that ion exchange resins were capable of removing ClO_4^- from the JPL matrix and showed the most promise for use in a treatment process. Experiment 2 consisted of a range finding experiment to (i) determine the range of resin concentrations which would yield useful isotherm data, (ii) assess the time required for the system to reach equilibrium and thus determine a meaningful contact time for the isotherm experiment, and (iii) estimate the extent to which the JPL matrix interferes with the adsorption process.

4.3 Experiment 3: Isotherm Generation

Based on the results of Experiment 2, Experiment 3 was conducted to generate adsorption isotherms, which would: (i) allow for comparison of various resins or resin types as to their ability to remove ClO_4^- from the JPL groundwater, and (ii) provide estimates of preliminary design parameters for a future column study (volumetric loading rates, resin volumes, testing durations).

5.0 MATERIALS AND METHODS

All experimental work was performed at CET Environmental Laboratories under the direction of Dr. Mark Losi of Foster Wheeler. Perchlorate analysis was conducted by ion chromatography (EPA 300.0, modified; limit of detection-4 $\mu\text{g/L}$) at E. S. Babcock and Sons (Babcock) Laboratory, Riverside, CA. Babcock Laboratory is certified by the California Department of Health Services to perform ClO_4^- analysis. For Experiment 1, level III data reporting was specified as a cautionary measure because we suspected that several of the materials could potentially interfere with the analysis, particularly the soluble chemical reductants. No such interferences were noted: soluble reductants did not remove ClO_4^- , influent and effluent concentrations were within 15% of each other for 6 of the 8 comparisons made (see results, Figures 9 and 10), and effluent concentrations actually exceeded influent for the two pairs that were outside this range, probably due to analytical variation. In any case, ion exchange, which is not expected to cause matrix interferences, was selected for further experimentation. For these reasons, level I data reporting was specified for subsequent analytical work. Laboratory quality assurance/quality control (QA/QC) is the same for Levels I and III, however, in Level III reporting, the laboratory provides all raw data including chromatograms and calibration curves in addition to analytical and QA/QC results, whereas for Level I only analytical and QA/QC results are provided.

5.1 Experiment 1: Initial Screening

In this experiment, ClO_4^- removal by a variety of materials was assessed from two water samples (feeds): actual JPL groundwater, and deionized water (DIW) spiked with NaClO_4 to a ClO_4^- concentration similar to that of the JPL groundwater. The spiked DIW feed was formulated at CET. The JPL groundwater used in all experiments described herein was pumped from JPL monitoring well MW-7 on 11/17/97 using existing, dedicated pumping equipment. This water will be referred to in this report as the JPL groundwater. Prior to collecting the water, the well was purged by pumping three casing volumes to ensure collection of a representative sample. Ten gallons were then collected in two 5-gal polyethylene bottles that were rinsed twice with the groundwater prior to filling. The sample was visually inspected and determined to have very low turbidity. Immediately following sampling, a subsample was submitted to Babcock Laboratory for ClO_4^- analysis, and the containers were stored at 5°C at CET. The results from Babcock Laboratory were received on 11/19/97 and indicated a ClO_4^- concentration of 840 $\mu\text{g/L}$ (two influent samples were subsequently submitted for ClO_4^- analysis along with the experimental

samples, and ClO_4^- concentration were reported at 590 and 650 $\mu\text{g/L}$). Two influent samples of the spiked DIW were also analyzed along with the experimental samples, and ClO_4^- levels were 820 and 680 $\mu\text{g/L}$.

Monitoring well MW-7 is periodically being sampled and the water analyzed by Montgomery Watson Laboratories as part of the ongoing quarterly groundwater monitoring program. A summary of the general water quality data from the five most recent samplings for Well MW-7 is presented in Table 1.

Because of the observed consistency, these values are assumed to reflect the composition of the MW-7 water sample used in our experiments. Water from MW-7 has also historically contained chromium (Cr) at concentrations of 0.007 to 0.019 mg/L, and volatile organic compounds (VOCs), mainly carbon tetrachloride and trichloroethene, at levels ranging from 39 to 170 $\mu\text{g/L}$ and 22 to 39 $\mu\text{g/L}$ respectively. For these experiments, the effects of the Cr on adsorption were assumed to be minimal, and were not addressed. Similarly, the VOCs were assumed to have undergone some degree of volatilization during handling and experimentation. For this reason, and because it was assumed that in practice, ClO_4^- removal would follow air stripping, the effects of organics were not addressed in this study.

From 11/14/97 to 12/14/97, various materials were procured based on numerous telephone conversations with academia and industry. Materials included three activated alumina preparations, four metal catalysts [active nickel (Ni) (Raney 2800), active chromium promoted Ni (Raney 2800), and palladium (Pd)-impregnated carbon and alumina], three anion exchange resins, two GACs, and four chemical reductants [ascorbic acid, Na_2SO_3 , $\text{Na}_2\text{S}_2\text{O}_3$, sodium dithionite ($\text{Na}_2\text{S}_2\text{O}_4$)]. A summary of materials (and relevant information) tested in the screening experiment is given in Table 2.

Quantities of these materials were weighed into 250-mL Erlenmeyer flasks containing 100 mL of either the JPL groundwater or the spiked DIW. Loading rates were 5 and 50 g/L for all solid reductants/adsorbents (materials 1-12, Table 2), and 1 g/L for the soluble chemical reductants (materials 13-16, Table 2) in both feeds. The flasks were agitated on a rotary shaker at 200 RPM for 3 hours. The suspensions were then filtered through Whatman No.1 filter paper directly into polyethylene laboratory sample containers to remove the solid adsorbents/reductants. No filtering was necessary for the chemical reductants. The samples were immediately refrigerated (5°C), and promptly submitted to Babcock for ClO_4^- analysis by ion chromatography (EPA 300.0, modified, limit of detection, 4 $\mu\text{g/L}$). The experimental work was conducted from 12/2/97 to 12/4/97, and the samples were submitted to the analytical laboratory on 12/8/97. A total of four method blanks were submitted (two per feed, two feeds total). These blanks consisted of the designated feed carried through the procedure, but with no addition of materials/chemicals. This was to ensure that any observed removal was due to the respective material/chemical. As mentioned, one influent sample for each feed used on each day was submitted for analysis to establish the influent ClO_4^- concentration (two per feed, two feeds total). A summary of the experimental plan is included in Appendix A.

In a parallel experiment, 100 mL aliquots of the JPL groundwater and the spiked DIW sample were amended with 0.5 g glucose (an electron-rich compound) and boiled for 10 minutes. In addition, a sample of the JPL groundwater was submitted to Dr. W. T. Frankenberger (University of California, Riverside) to test the ability of a recently isolated ClO_4^- reducing bacterium to biologically reduce the ClO_4^- in the JPL matrix. Results are included in Appendix A.

5.2 Experiment 2: Range Finding

This experiment was conducted to select a range of ion exchange resin loading rates and a contact time for the isotherm experiment, and to estimate interferences caused by other components of the JPL groundwater matrix. One resin (Amberlite IRA400 Cl) was used, and the feed consisted of the MW-7 JPL groundwater sample. Prior to initiating this experiment (1/20/98), a subsample of the JPL groundwater was submitted to Babcock Laboratory for ClO_4^- analysis, and a result of 650 $\mu\text{g/L}$ was obtained. Quantities of the resin were weighed into four sets of 250 mL Erlenmeyer flasks (10 flasks per set), each containing 100 mL of the JPL groundwater. These four sets represented four different contact times. Resin loading rates for the 10 flasks within each set are given in Table 3.

The flasks were agitated on a rotary shaker at 200 rpm. One set of 10 flasks was sampled at each of the following times: 0.25 h, 0.5 h, 1.0 h, and 2.0 h (filtered through No. 1 Whatman filter paper directly into a polyethylene sample container provided by the analytical laboratory, and immediately refrigerated, 5° C).

To estimate the interference due to the JPL matrix, an additional set of 10 flasks containing spiked dionized water (~700 $\mu\text{g ClO}_4^-/\text{L}$) was prepared for the above masses of resin. This set was sampled (as described above) after a 2.0 h contact time and the results compared with the set containing the JPL groundwater which was sampled at 2 h. All samples were delivered to Babcock Laboratories for ClO_4^- analysis. The experimental design for Experiment 2 is included in Appendix B.

5.3 Experiment 3: Generation of Isotherms

In this experiment, isotherms describing adsorption of ClO_4^- in the JPL matrix were generated using six resins. Resins included in the isotherm experiment are shown in Table 4. One hundred-mL aliquots of the JPL groundwater were equilibrated with resin concentrations of 50, 100, 300, 500, 800, 1100, 1300, and 1500 mg/L in 250 mL flasks for 1.5 h, as determined in Experiment 2. The flasks were agitated on a rotary platform shaker, and samples were removed, filtered and refrigerated as in Experiments 1 and 2. When experimentation was complete, samples were transported on ice to Babcock Laboratories for ClO_4^- analysis. The general experimental design is given in Appendix C. From the resultant data, an isotherm was plotted for each resin, and Freundlich coefficients were determined according to Weber (1972). This is explained below.

The Freundlich adsorption isotherm is expressed as follows:

$$x/M = k * C^{1/n}$$

Where: x = Mass of solute (ClO₄⁻)
 M = Mass of resin
 C = Equilibrium concentration of solute
 k,n = Experimental Constants

For each resin, the x/M is plotted against the equilibrium concentration on a log-log scale to determine k and n. Once these are determined, the equation can be solved for mass of ClO₄⁻ per mass of resin, given the target value of ClO₄⁻ in the treated effluent, which we have assumed to be 2 µg/L (half the current detection limit).

6.0 RESULTS AND DISCUSSION

6.1 Experiment 1: Initial Screening

Perchlorate concentrations measured in the influent samples and associated method blanks are shown in Table 5 along with the percent recoveries. Based on this data, we can make the assumption that essentially no ClO₄⁻ loss occurred independent of the adsorbent/reductant (method blank ClO₄⁻ levels exceeding those of the influent are due to analytical variation, n=1).

Results of the screening experiment are presented graphically for each material at the two loading rates with each feed in Figures 1 through 10, and will be discussed by individual material (refer to Table 2 for additional explanation of materials). In these figures, effluent ClO₄⁻ for each material is shown along side the influent concentration associated with that batch for comparison. In some cases, effluent ClO₄⁻ concentration exceeded that of the influent, and this is attributed to analytical variation (n=1). The raw data for Experiment 1 is compiled in Appendix A.

6.1.1 Activated Alumina

Figures 1 and 2 show removal of ClO₄⁻ from the JPL groundwater and DIW feeds, respectively, by three activated alumina preparations at loadings of 5 or 50 g/L. No appreciable removal was observed for the DD-2 and the A-2 at either loading. A small amount of ClO₄⁻ in the JPL groundwater may have been removed by the AHTC-24 at 5 g/L, and approximately 65% removal was noted by this material at 50 g/L. This was confirmed by similar (slightly higher) removal rates achieved by AHTC-24 from the DIW. Although activated alumina can reportedly be used to adsorb arsenic and selenium oxyanions, our data suggests that very limited ClO₄⁻ adsorption occurred, even from DIW. It is possible that 3 hours was insufficient for equilibrium to be reached, and that the capacity for ClO₄⁻ adsorption by activated alumina was not fully realized. However adsorption rates must be rapid for the technology to be useful. In addition, the pH optimum for ClO₄⁻ adsorption by activated alumina may be different from the pH of the feed. However, pH adjustment would be impractical for the JPL application. For these reasons activated alumina is considered unacceptable for the JPL application.

6.1.2 Metal Catalysts

Influent and effluent ClO_4^- concentrations for feeds contacted with metal catalysts are shown in Figures 3 and 4. For the JPL groundwater and spiked DIW feeds, no appreciable removal was noted, with the possible exception of the Pd-impregnated GAC. However, since similar removal was observed for GAC (see below), and removal was not observed for the Pd-impregnated activated alumina, it is likely that the removal in this treatment is due to adsorption by the GAC and not reduction by the Pd. Alternatively, limited, adsorption-influenced ClO_4^- reduction by the Pd may be occurring on the carbon surface, but this is doubtful. Dr. C. Amrhein of the University of California, Riverside has been conducting experiments to study oxyanion removal by another potential catalyst/reductant, Fe^0 . Although successful in removing several other oxyanions, he has reported no success in ClO_4^- reduction/removal, even with Pd-treated Fe^0 , and he has abandoned the ClO_4^- portion of the project (C. Amrhein, University of California, Riverside, personal communication). In light of this information, metal catalysts do not warrant further investigation for the JPL application.

6.1.3 Ion Exchange Resins

Figures 5 and 6 show ClO_4^- removal from feeds contacted with ion exchange resins. The three resins tested (both loading rates) adsorbed ClO_4^- in both feeds, lowering concentrations to below detection limits in all cases. Ion exchange resins are thus identified as being potentially applicable in treatment of JPL groundwater.

6.1.4 Granular Activated Carbon (GAC)

Perchlorate removal by the GAC is depicted in Figures 7 and 8. The data indicate that adsorption did occur, but to a lesser extent than was observed with anion exchange resins, and the interim action level ($18 \mu\text{g/L}$) was met only for the spiked DIW at the low loading (by the COL L 60) and only at the high loading (also by the COL L 60) for the JPL groundwater. Other researchers have also found that ClO_4^- is weakly adsorbed by GAC, and rapid breakthroughs are commonly observed (Harding Lawson, 1997). Hence, GAC is not retained for consideration.

6.1.5 Chemical Reductants

Figures 9 and 10 reflect influent and effluent ClO_4^- concentrations for feeds contacted with chemical reductants. None of the chemicals tested removed ClO_4^- . The chemicals were added in excess of the quantity needed to remove all soluble oxygen (assuming saturation, $8 \text{ mg O}_2/\text{L}$) as well as ClO_4^- . Soluble reductants are thus not being considered for continued study. Table 6 shows ClO_4^- recoveries for JPL and spiked DIW samples before and after amendment with 5-g glucose/L and boiling. Recoveries indicate that no ClO_4^- reduction occurred, and underscores the stability of this compound in groundwater.

6.1.6 Biological Reduction

Dr. W. T. Frankenberger (University of California, Riverside) reported complete ClO_4^- reduction (to Cl^-) in the JPL matrix (to $<4 \mu\text{g/L}$) by a microbial consortium, which is now known to be a

single isolate (see Appendix A). Frankenberger incubated the JPL groundwater sample anaerobically for 3 days following addition of acetate (energy source), protein, and several inorganic nutrients. This is an interesting finding for several reasons, given the apparent aqueous stability ClO_4^- .

While not well suited to treating large volumes of drinking water at flow rates required for primary treatment, a batch-type bioreactor may be applicable in a treatment train to treat much smaller quantities of wastewater generated by primary treatment techniques. Further, *in-situ* treatment technologies can be envisioned whereby a carbon source is injected into the plume to stimulate ClO_4^- bioreduction by naturally occurring microorganisms. As stated in Frankenberger's letter, ClO_4^- is believed to serve as an alternate electron acceptor in anaerobic respiration, which is analogous to the reductive dechlorination of chlorinated organics. It is now well known that if a suitable energy source is available, this process can be used as an *in situ* remedial technique to treat water contaminated with chlorinated organics.

6.1.7 Summary of Findings

Table 7 summarizes ClO_4^- removal from both feeds by all materials at the two loading rates. As shown in Table 7, anion exchange resins show the greatest promise for adsorbing ClO_4^- and thereby reducing concentrations in JPL groundwater to below the interim action level ($18 \mu\text{g L}^{-1}$) recommended by the California Department of Health Services. Previous work has also suggested that ion exchange resins may be useful for treating ClO_4^- contaminated water (Velayudham and Sastry, 1988), but very little information is presently available, and no established methodology currently exists.

In a technology screening report, ion exchange was identified as being potentially preferred for treating ClO_4^- contaminated groundwater in the San Gabriel Basin, second in cost effectiveness only to biological reduction (Harding Lawson, 1997). However, virtually all parameters related to a full-scale treatment method have not been adequately investigated in the laboratory, including selection of resins, resin capacities with respect to specific matrix interferences, regeneration, and leakage. Perchlorate adsorption data is currently unavailable from resin vendors. The resins we tested effectively removed ClO_4^- from the JPL groundwater matrix, indicating potential matrix compatibility. In addition, ion exchange can be used to treat potable water, and the technology is amenable to well head treatment, both of which suit the needs of JPL.

6.2 Experiment 2: Range Finding

In order to assess the feasibility of ion exchange, knowledge of resin capacities for ClO_4^- in the JPL groundwater matrix is integral to modeling and ultimately scaling up the process. An initial estimate of resin loading rates can be obtained by generating adsorption isotherms in flask studies. In Experiment 2, we determined the resin loading rates and contact time necessary to generate the adsorption isotherms, as well as estimating the degree of interference caused by other components of the JPL matrix.

As discussed earlier, the most common isotherm model used in this type of analysis is the Freundlich model. Finding the proper range of resin loading rates is crucial to insure that enough data points are obtained to determine the experimental constants as discussed in Section 5.3. For example, if eight resin loading rates are tested and complete ClO_4^- removal is observed for seven of these rates, then only two points are possible, and a meaningful isotherm can not be generated. Figure 11 shows ClO_4^- removal by resin at loading rates ranging from 5 to 5000 mg/L. From Figure 11, we observe that 50-1500 mg resin/L is range over which variable final ClO_4^- concentrations will be obtained. This range was selected and used in Experiment 3.

All isotherm models are based on the assumption that when concentrations are measured, sufficient time has elapsed such that the sorbate (ClO_4^-) is in equilibrium with the adsorbent (resin). Figure 12 shows final ClO_4^- concentrations at each resin loading rate as a function of time. From this graph, 1.5 h was selected as reasonably approximating equilibrium, accounting for the range suggested by resin vendor technical support personnel (0.5-1 h), and for analytical variation.

A major unknown regarding this process was the degree that other anions would interfere with ClO_4^- adsorption. Substantial interference could explain low adsorption capacities, and lead to rapid breakthrough times, which would undermine the usefulness of the technology. Figure 13 shows a comparison of ClO_4^- removal from the JPL groundwater and from the spiked DIW by Amberlite IRA400 Cl for various resin loads. Potentially competing anions in the JPL groundwater and their approximate concentrations are given in Table 1 and for the spiked, DIW no competing anions were present. It is evident from Figure 13 that interference is minor, and suggests that ClO_4^- is adsorbed with reasonable efficiency from the JPL matrix. This is somewhat surprising, and contradicts what resin vendor technical personnel had predicted.

6.3 Experiment 3: Isotherm Generation

6.3.1 Summary of Findings

As discussed earlier, isotherm generation (Freundlich) consists of plotting the mass of solute/mass of resin against the equilibrium solute concentrations on a log-log scale. These are shown on Figures 14 through 19 for the six resins tested. Based on these isotherms, and a target treatment level of 2 $\mu\text{g/L}$, the amount of ClO_4^- that can be exchanged by 1 gram of resin is shown in Table 8 for the six resins tested. As shown in Table 8, Amberlite IRA400 Cl showed the highest exchange capacity of approximately 500 μg (i.e. 0.5 mg) per gram of resin. Studies by other researchers for ClO_4^- removal with a number of different resins had also shown Amberlite IRA400 Cl to have higher removal rates compared to six other resins (Velayudham and Sastry, 1988).

6.3.2 Application to Full Scale Design

It should be noted that this exchange capacity was derived entirely from flask experiments, which basically ensure complete mixing. Performance in a column setting, as in a full-scale

system may be different, and some amount of column testing (on a laboratory scale) is warranted. This exchange capacity does however serve as a starting point for a laboratory column study, as follows.

Assume a 2-inch diameter column.

$$\text{Surface Area} = \frac{\pi}{4} \times (2)^2 = 3.14 \text{ in}^2$$

Assume a bed depth of 24 inches

$$\therefore \text{Resin Volume} = 75.36 \text{ in}^3 = 0.44 \text{ ft}^3$$

Recommended volumetric loading = 2 to 4 gpm/ft³, assume 2

$$\therefore \text{Allowable flow} = 2 \times 0.44 = 0.88 \text{ gpm}$$

$$\begin{aligned} \text{Surface loading} &= \frac{0.88 \text{ gpm}}{3.14 \text{ in}^2} = \frac{0.88 \text{ gpm}}{0.0218 \text{ ft}^2} \\ &= 40 \text{ gpm/ft}^2 \end{aligned}$$

Recommended surface loading = 1 to 8 gpm/ft² (Owens, 1995)

Therefore surface loading is acceptable.

Based on a resin density of 45 lb/ft³, mass of resin is:

$$M = 45 \times 0.44 \text{ ft}^3 = 19.8 \text{ lbs} = 899 \text{ grams}$$

Based on 0.5 mg/g loading capacity, the amount of ClO₄⁻ to breakthrough:

$$= 0.5 \frac{\text{mg}}{\text{g}} \times 899 \text{ g} = 449.5 \text{ mg}$$

Assuming an influent loading of 1,000 µg/L (1 mg/L) in the feed, the amount of ClO₄⁻ per minute:

$$= 0.5 \text{ mg/minute}$$

$$= 1 \frac{\text{mg}}{\text{L}} \times 0.132 \text{ gpm} \times 3.785 \frac{\text{liters}}{\text{gallon}}$$

Time for 449.5 mg of ClO₄⁻ to flow through column =

$$\frac{449.5 \text{ minutes}}{0.5} = 899 \text{ minutes} = 15 \text{ hours}$$

Hence, theoretically, the time to break through would be 15 hours. Once the column study is completed, depending on the actual time to break through, the above design methodology can be used to size the full-scale system. The actual breakthrough time during the column study is expected to be less than 15 hours, and, if the column is designed to be geometrically similar to the full-scale system; the full-scale system can be expected to have this same lower breakthrough time. Thus, column studies would be required prior to designing a full-scale system.

Another factor that will have to be understood prior to the design of the full-scale system is the regeneration of the spent brine. Based on ion exchange resin vendor information, 4 to 10% brine would be required to regenerate the resin. The volume of brine required is expected to be approximately 1% of the water feed rate. The disposal of this brine (which will contain 200 to 400 mg/L of ClO_4^-) will be a major operational issue. Again, the column study can be used to study the effect of different brine concentrations on regeneration efficiency. Additional testing of the brine would be required in order to formulate treatment methods for the brine (e.g. bioreduction).

Thus, laboratory column testing prior to field scale pilot operation is required in order to design an effective system, as well as to provide a feasible solution for treatment of the brine generated. Once the column studies are completed, the results can then be used to obtain bids from established ion exchange equipment manufacturers for field scale pilot test units. This approach will help reduce the pitfalls associated with application of the ion exchange technology to a relatively unknown contaminant.

7.0 CONCLUSIONS

The relevant conclusions of our research and experiments are as follows:

1. The ClO_4^- ion is fairly stable in water, and does not degrade even with boiling in conjunction with addition of glucose
2. Anion exchange resins appear to be capable of removing ClO_4^- from JPL groundwater.
3. GAC and to some extent activated alumina can also remove ClO_4^- from JPL groundwater.
4. Metal catalysts and chemical reduction had little, if any effect.
5. Biological reduction can remove ClO_4^- from JPL groundwater, and may be useful in a treatment train, or as an *in situ* treatment.
6. Strong base anion exchange showed the highest ClO_4^- removal per gram of resin - of these, Amberlite IRA400 Cl showed the required removal (to below 4 $\mu\text{g/L}$) at a loading of 515 μg of ClO_4^- per gram of resin.
7. Comparison of removal rates in JPL groundwater and spiked DIW indicate minimal interference by other anions.

Based on these conclusions, Foster Wheeler recommends the following:

1. Perform preliminary column studies to establish design parameters for field and/or full scale systems - column sizing, breakthrough curves, and regeneration efficiencies.
2. Perform concurrent laboratory studies to study treatment techniques for brine, primarily biological reduction.
3. Depending on preliminary column studies, move to either secondary column studies or field scale pilot studies to establish full-scale design parameters. If field scale pilot studies are the next step, use the information from the column studies to solicit bids from established ion exchange equipment manufacturers.

8.0 REFERENCES

- Amrhein. 1997. C. University of California, Riverside. Personal communication.
- Bailey, P. S. and C. A. Bailey. 1985. Organic Chemistry. Allyn and Bacon, Inc. Boston. P. 86, 338.
- California Department of Health Services. 1997. Perchlorate in California Drinking Water. Division of Drinking Water and Environmental Mgmt., Drinking Water Program.
- Dussert, B. W. and G. R. Van Stone. 1994. The Biological Activated Carbon Process for Water Purification. Water Engineering Management. 12:22-24.
- Eary, L. E. and D. Rai, 1988. Chromate Removal from Aqueous Waste by Reduction with Ferrous Iron. Environmental Science Technology. 22:972-977.
- Ebbing, D. D. 1987. General Chemistry. Houghton Mifflin Co. Boston.
- Eloskof, A. 1997. Foster Wheeler. Personal communication.
- Faust, S. A. and O. M. Aly. 1987. Absorption Processes for Water Treatment. Butterworths. Boston, MA.
- Feakin, S. J., E. Blackburn, and R. G. Burns. 1995. Inoculation of Granular Activated Carbon in a Fixed Bed with S-triazine-degrading Bacteria as a Water Treatment Process. Water Resources 3:819-825.
- Geckeler, K. E. and K. Volchek. 1996. Removal of Hazardous Substances from Water using Ultrafiltration in Conjunction with Soluble Polymers. Environ. Sci. & Technol. 3:725-734.
- Gonce, N. and E. A. Voudrias. 1994. Removal of Chlorite and Chlorate Ions from Water using Granular Activated Carbon. Water Resources. 5:1059-1069.
- Greenwood, N. N. and A. Earnshaw. 1985. Chemistry of the Elements. Pergammon. New York.
- Harding Lawson Associates. 1997. Transmittal of Technology Screening for the Treatability of Perchlorate in Groundwater, Baldwin Park Operable Unit (BPOU), San Gabriel Basin. Prepared for the BPOU Steering Committee.

- Harris, D. C. 1987. Quantitative Chemical Analysis. W. H. Freeman and Company.
- Kopchinsky, A. F. and C. E. Meloan. 1996. The Synthesis, Characterization, and Testing of a Reagent for the Selective Removal of Dichromate and Perchlorate from Aqueous Solution. *Separation Science and Technology*. 1:133-140.
- Logan, B. 1997. Growth Kinetics of Chlorate-respiring Microorganisms. Presented at the USEPA Symposium on the Biological and Chemical Reduction of Chlorate and Perchlorate. Contact: E. Urbansky, 26 W. Martin Luther King Dr., MS-681. Cincinnati, OH. 45268.
- Losi, M. E., C. Amrhein, and W. T. Frankenberger, Jr. 1994. Bioremediation of Chromate-Contaminated Groundwater by Reduction and Precipitation in Surface Soils. *Journal of Environmental Quality*. 6:1141-1150.
- Losi, M. E. and W. T. Frankenberger, Jr. 1997. Reduction of Selenium Oxyanions by *Enterobacter Cloacae* SLD1a-1: Isolation and Growth of the Bacterium, and its Expulsion of Selenium Particles. *Applied Environmental Microbiology*. In Press.
- Metcalf and Eddy. 1979. *Wastewater Engineering: Treatment, Disposal, Reuse*. McGraw-Hill Book Company. New York.
- Owens, D.L. 1995. *Ion Exchange*. Tall Oaks Publishing, Inc. Littleton, CO.
- US EPA. 1992. Provisional Non-cancer and Cancer Toxicity Values for Potassium Perchlorate (CASRN 7778-74-7) (Aerojet General Corp./CA). Memorandum from Joan S. Dollarhide, Superfund Health Risk Technical Support Center, Environmental Criteria and Assessment Office, Office of Research and Development, to Dan Stralka, US EPA Region IX.
- US EPA. 1995. Correspondence from Joan S. Dollarhide, National Center for Environmental Assessment, Office of Research and Development, to Mike Girrard, Chairman, Perchlorate Study Group.
- van Ginken, C. G. 1997. Microbial Transformations of Chlorooxo Acids. Presented at the USEPA Symposium on the Biological and Chemical Reduction of Chlorate and Perchlorate. Contact: E. Urbansky, 26 W. Martin Luther King Dr., MS-681. Cincinnati, OH. 45268.
- Velayuham B. and C. A. Sastry. 1988. Mathematical Model for Perchlorate Removal from Wastewater by Ion Exchange. *Indian Journal of Environmental Protection*. Vol. 8, No. 9, September.
- Weber, W. J. 1972. *Physiochemical Processes for Water Quality Control*. Wiley-Interscience. New York.

TABLES

TABLE 1
SUMMARY OF GENERAL WATER QUALITY DATA
(FROM JPL QUARTERLY GROUNDWATER MONITORING PROGRAM)
 (All concentrations are mg/L)

Sampling	Cl ⁻	CO ₃ ²⁻	HCO ₃ ⁻	NO ₃ ⁻ -N	SO ₄ ²⁻	Na ⁺	Mg ²⁺	K ⁺	Ca ²⁺	Fe	ALK ^(a)	pH	TDS ^(b)
Aug/Sep 1996	19	0.38	146	6	39	20	18	2.8	52	<0.10	120	7.6	280
Oct/Nov 1996	20	0.36	177	5.7	36	18	15	2.6	47	0.41	145	7.5	250
Feb/Mar 1997	20	0.35	171	5.7	44	18	17	2.4	52	0.15	140	7.5	280
Jun/Jul 1997	24	0.57	175	6.5	48	17	17	2.8	54	0.16	145	7.7	300
Sep/Oct 1997	22	0.46	177	6.3	44	18	16	3	55	<0.10	145	7.6	320
MEAN	21	0.42	169	6.0	42.2	18.2	17	2.7	52	0.24	139	7.6	286
STDEV	2.0	0.1	13.2	0.4	4.7	1.1	1.1	0.2	3.1	0.10	10.8	0.1	26.1

(a) Alkalinity

(b) Total dissolved solids

TABLE 2**MATERIALS TESTED -
SCREENING EXPERIMENT (EXPERIMENT 1)**

Classification	Material	Manufacturer	Process
Activated alumina	AHTC-24	ALCOA	Adsorption
Activated alumina	DD-2	ALCOA	Adsorption
Activated alumina	A-2	LaRoche	Adsorption
Metal catalyst	Raney Ni 2400	Davidson Chem.	Reduction
Metal catalyst	Raney Ni 2800	Davidson Chem.	Reduction
Metal catalyst	Pd/Act. Alum.	Precious Metals Corp.	Red/Ads
Metal catalyst	Pd/Act. Carbon	Precious Metals Corp.	Red/Ads
Anion exchange resin	Amberlite IRA400Cl	Rohm&Hass	Adsorption
Anion exchange resin	DOWEX 550A(OH-)	Dow Chem.	Adsorption
Anion exchange resin	Ionac AFP-329	Sybron Chem.	Adsorption
Activated Carbon	COC L 60	Carbon Activated Co.	Adsorption
Activated Carbon	COL L 60	Carbon Activated Co.	Adsorption
Chemical	Ascorbic Acid	Fisher Scientific	Reduction
Chemical	Sodium Sulfite (Na_2SO_3)	Fisher Scientific	Reduction
Chemical	Sodium Thiosulfate ($\text{Na}_2\text{S}_2\text{O}_3$)	Fisher Scientific	Reduction
Chemical	Sodium Dithionite ($\text{Na}_2\text{S}_2\text{O}_4$)	Fisher Scientific	Reduction

TABLE 3

RESIN LOADING RATES -

RANGE FINDING EXPERIMENT (EXPERIMENT 2)

Flask Number	Resin Concentration (mg/L)	Resin Loading (mg/ 100 mL)
1	0	0
2	5	0.5
3	50	5
4	100	10
5	250	25
6	500	50
7	750	75
8	1000	100
9	2500	250
10	5000	500

TABLE 4**ANION EXCHANGE RESINS -
ISOTHERM EXPERIMENT (EXPERIMENT 3)**

No.	Manufacturer	Product	Class	AEC, meq/ml
1	Rohm and Hass	Amberlite IRA400 Cl	Type 1, Strong Base	1.4
2	Dow	Dowex MSA-1	Type 1, Strong Base	1.0
3	Dow	Dowex 550A	Type 1, Strong Base	1.1
4	Sybron	Ionac AFP-329	Weak Base	1.5
5	Sybron	Ionac A-305B	Weak Base	1.9
6	Sybron	Ionac A-641	Type 1, Strong Base	1.2

TABLE 5**COMPARISON OF ClO_4^- CONCENTRATIONS -
METHOD BLANKS AND ASSOCIATED INFLUENT**

Associated influent [ClO_4^-], mg/L	Method blank [ClO_4^-], mg/L	% Recovery
	JPL Groundwater	
650	560	86.2
590	650	110.2
	SPIKED dionized Water	
820	870	106.1
680	860	126.5
Average Recovery		107.3

TABLE 6**PERCHLORATE REMOVAL – BOILING/GLUCOSE AMENDMENT**

Associated influent [ClO ₄], mg/L	Glucose-amended/boiled [ClO ₄], mg/L	% Recovery
	JPL Groundwater	
590	680	115.2
	SPIKED dionized Water	
820	780	95.2

TABLE 7

SUMMARY OF RESULTS – EXPERIMENT 1

No.	Group	Material Loading (g/L)	% ClO ₄ ⁻ Removal	
			JPL Groundwater	Spiked DIW
1	Activated Alumina	5	10.8	16.7
		50	17.9	12.7
2	Metal Catalysts	5	15.8	27.7
		50	15.1	14.6
3	Anion Exchange Resins	5	100.0*	100.0*
		50	100.0*	100.0*
4	Granular Activated Carbons	5	84.7	88.9
		50	98.2	98.1
5	Chemical Redcuction (ascorbic acid, sodium sulfite, sodium thiosulphate, sodium dithiomite)	1	0	0
6	Boiling/Glucose Amendment	5	0	4.9
7	Biological Reduction/Acetate	5	100.00*	--

*Based on removal below detection limit of 4 µg/L.

TABLE 8
SUMMARY OF RESULTS – EXPERIMENT 3

No.	Manufacturer	Product	Class	Perchlorate Removed, µg/gram of resin
1	Rohm and Hass	Amberlite IRA400 Cl	Type 1, Strong Base	515
2	Dow	Dowex MSA-1	Type 1, Strong Base	239
3	Dow	Dowex 550A	Type 1, Strong Base	169
4	Sybron	Ionac AFP-329	Weak Base	220
5	Sybron	Ionac A-305B	Weak Base	74
6	Sybron	Ionac A-641	Type 1, Strong Base	280

Note: Perchlorate removals estimated based on Freundlich Isotherms, and target effluent perchlorate concentrations of 2 µg/L.

FIGURES

Figure 1. Removal of Perchlorate by Activated Alumina (5 and 50 g/L) from JPL Groundwater
(Refer to Table 2 for details regarding alumina preparations)

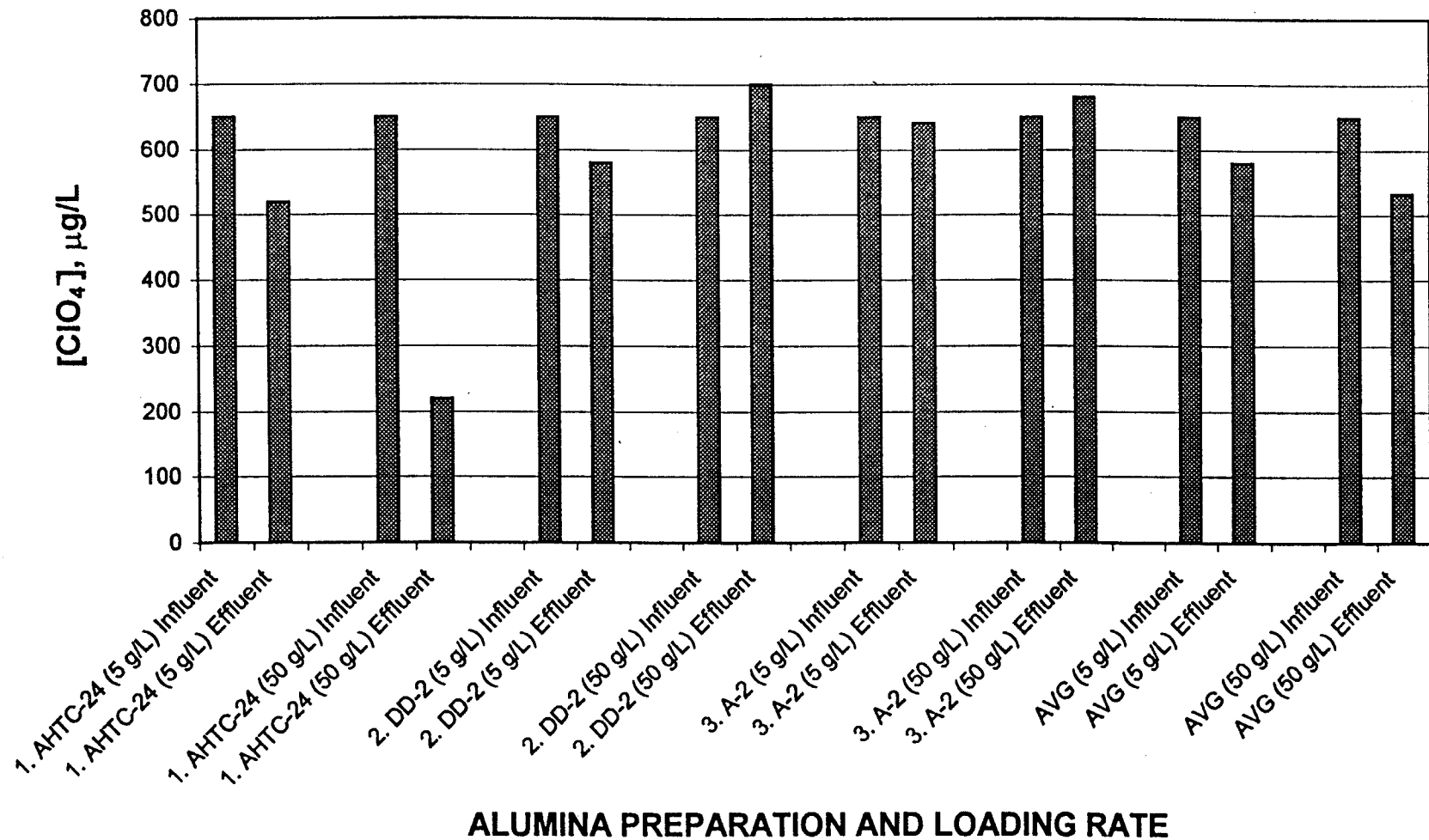


Figure 2. Removal of Perchlorate by Activated Alumina (5 and 50 g/L) from Deionized Water
(Refer to Table 2 for details regarding alumina preparations)

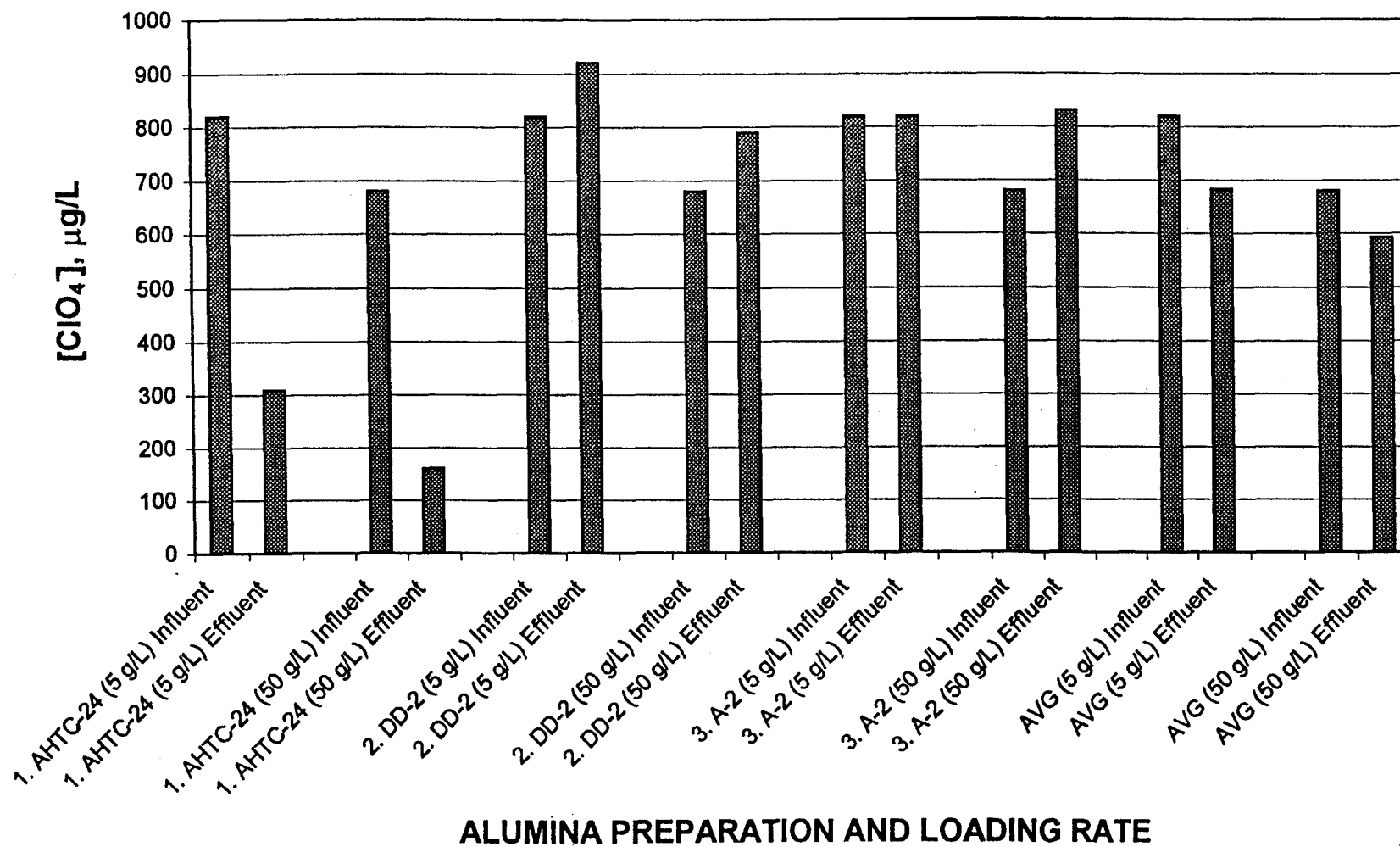


Figure 3. Removal of Perchlorate by Metal Catalysts (5 and 50 g/L) from JPL Groundwater
(Refer to Table 2 for details regarding metal catalysts)

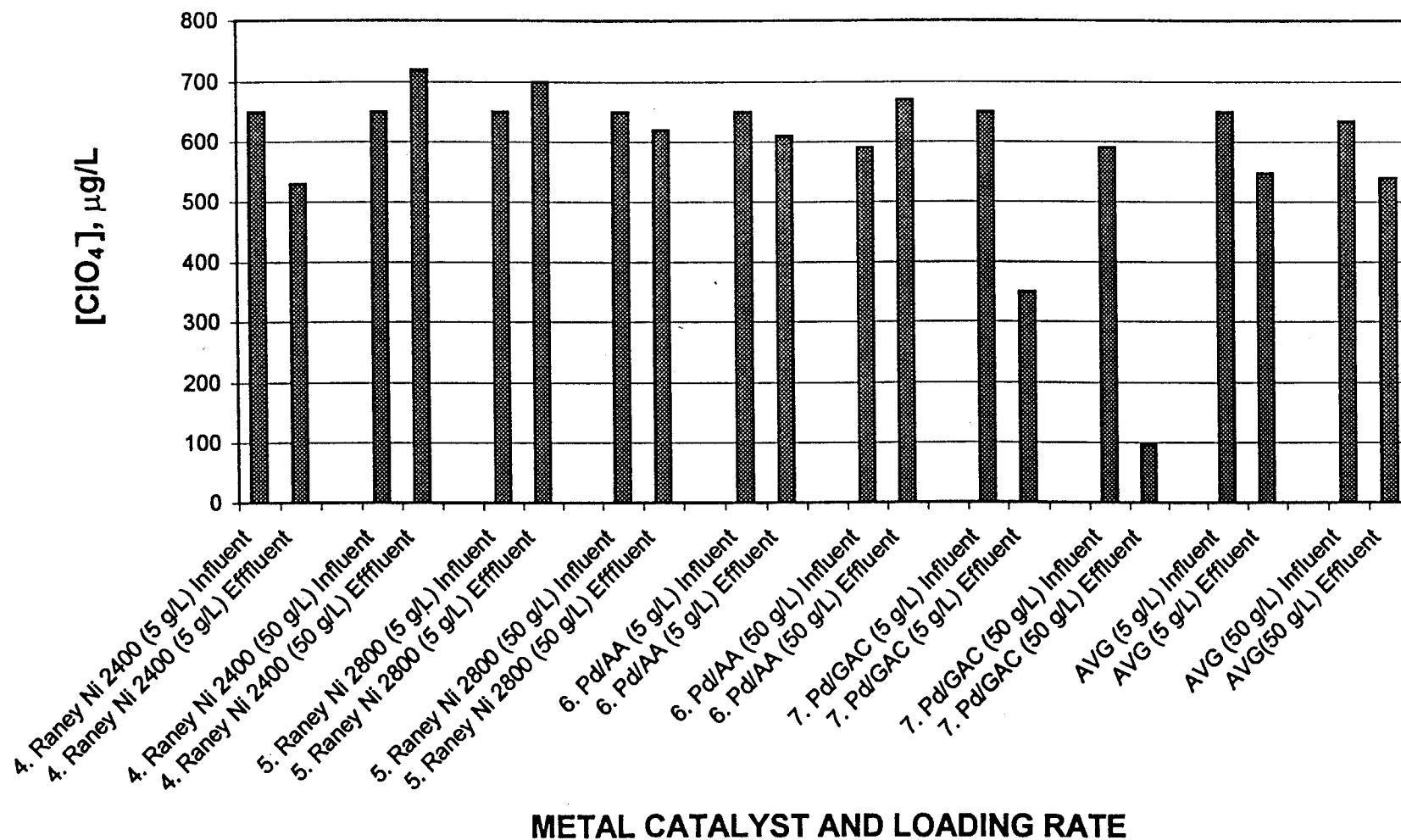


Figure 4. Removal of Perchlorate by Metal Catalysts (5 and 50 g/L) from Deionized Water
(Refer to Table 2 for details regarding metal catalysts)

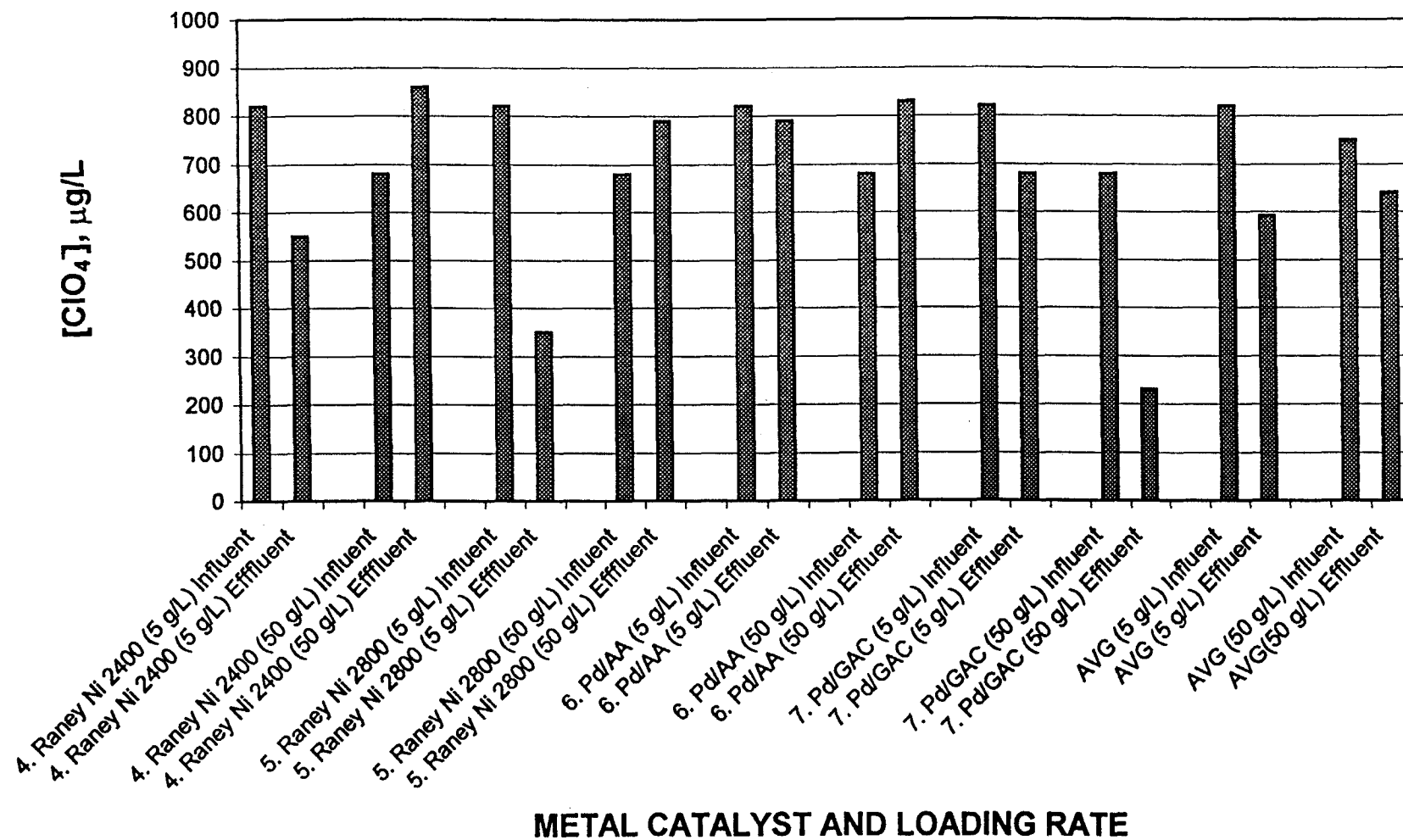


Figure 5. Removal of Perchlorate by Anion Exchange Resins (5 and 50 g/L) from JPL Groundwater

(Refer to Table 2 for details regarding anion exchange resins)

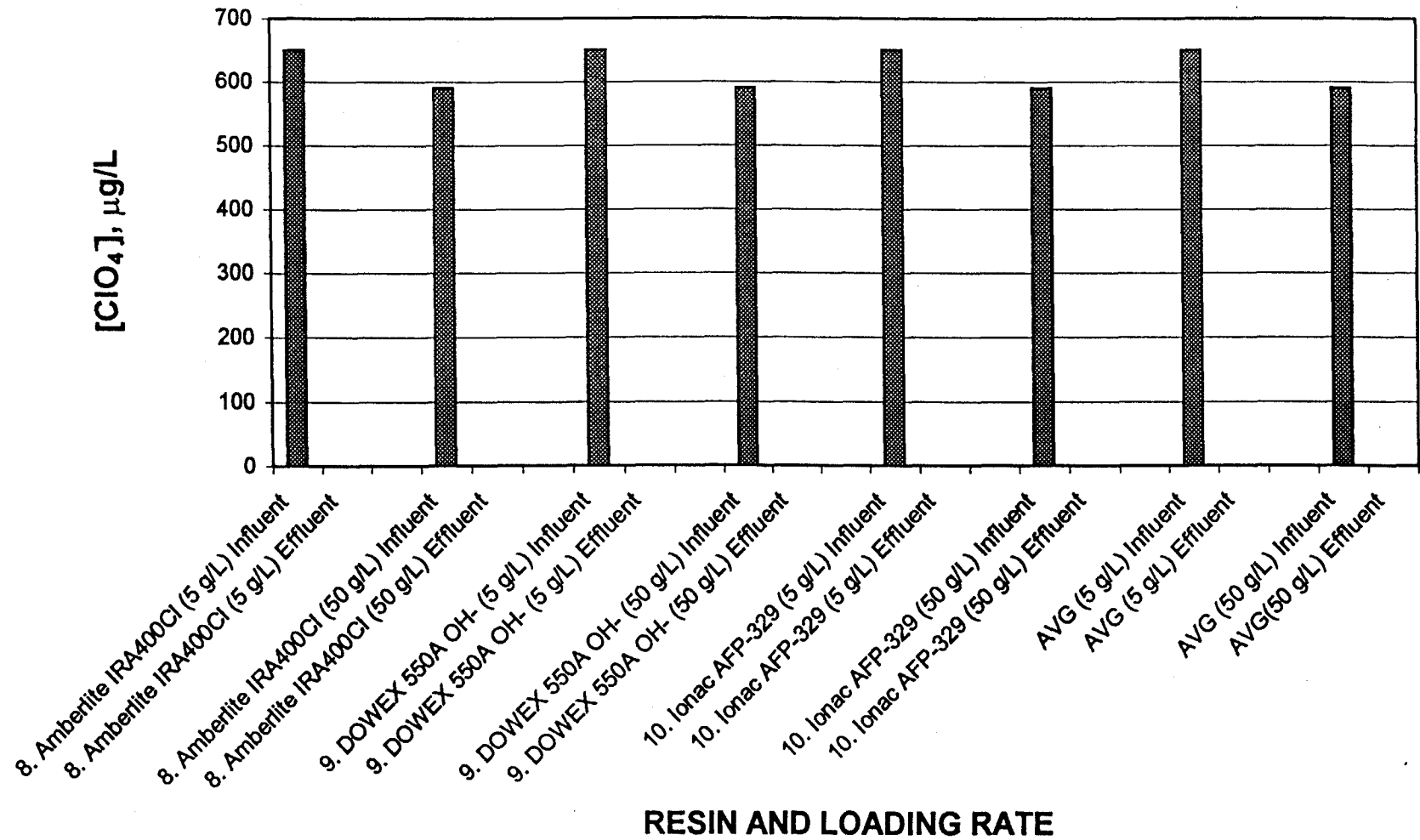
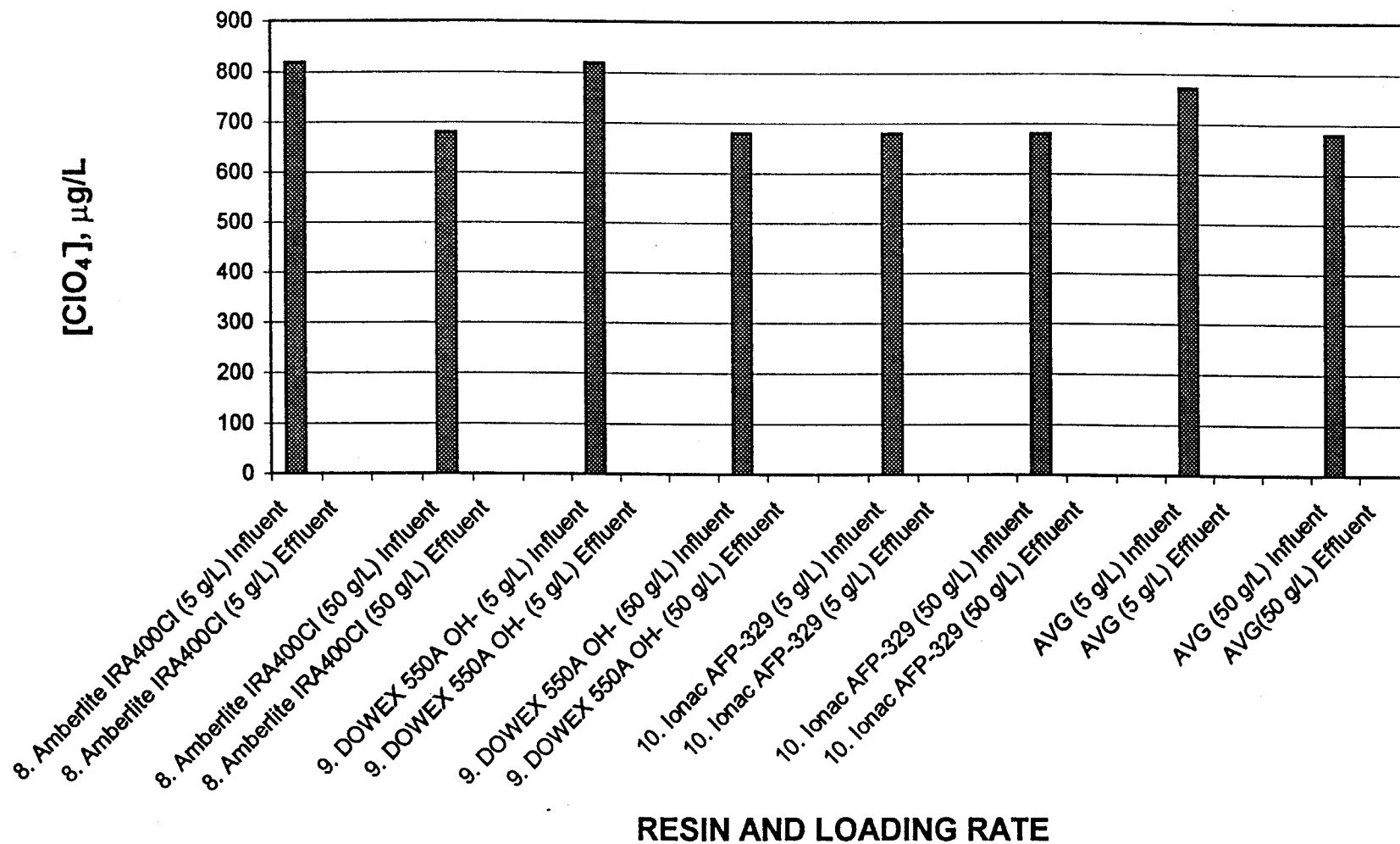
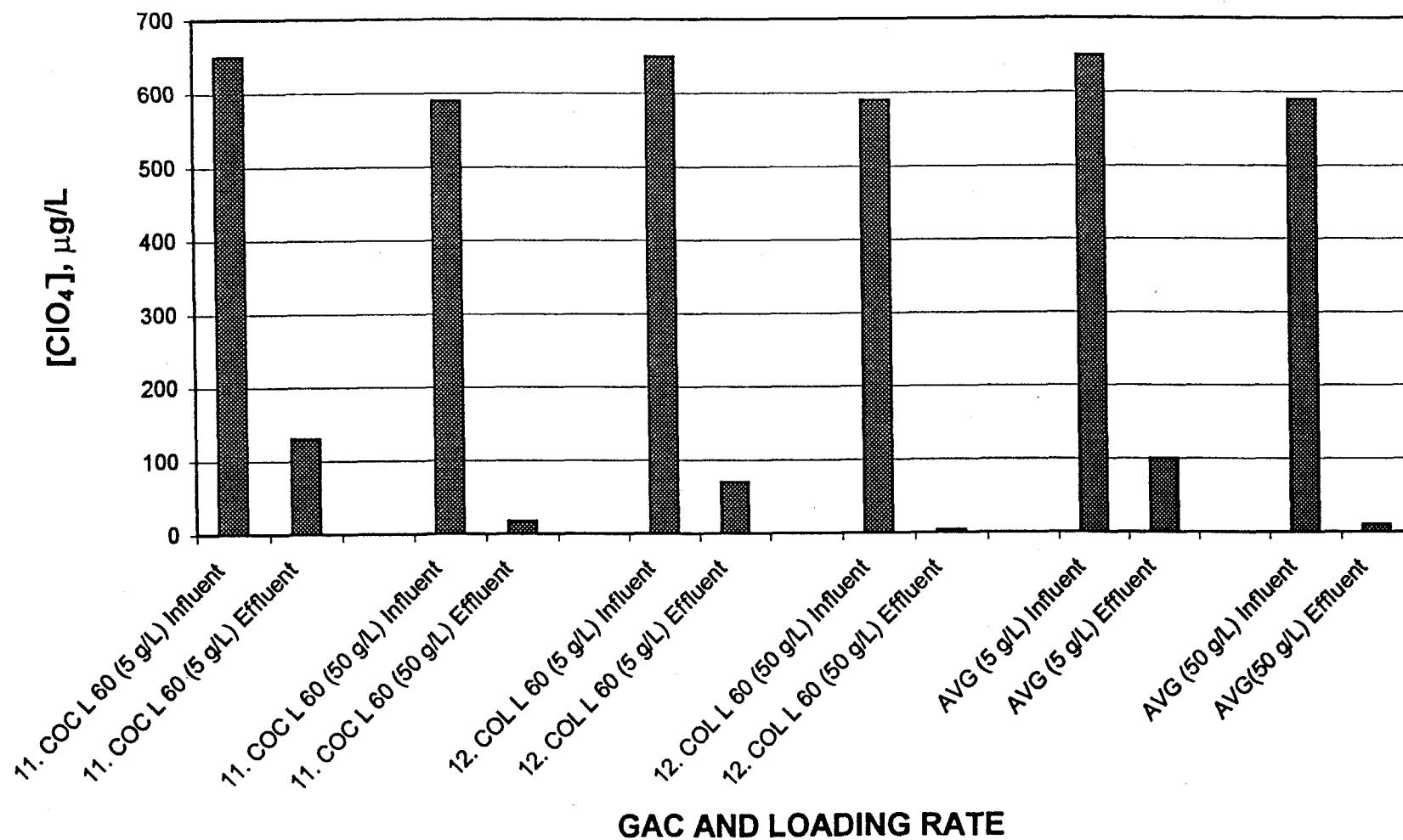


Figure 6. Removal of Perchlorate by Anion Exchange Resins (5 and 50 g/L) from Deionized Water

(Refer to Table 2 for details regarding anion exchange resins)



**Figure 7. Removal of Perchlorate by Granular Activated Carbon (5 and 50 g/L)
from JPL Groundwater**
(Refer to Table 2 for details regarding GACs)



**Figure 8. Removal of Perchlorate by Granular Activated Carbon (5 and 50 g/L)
from Deionized Water**
(Refer to Table 2 for details regarding GACs)

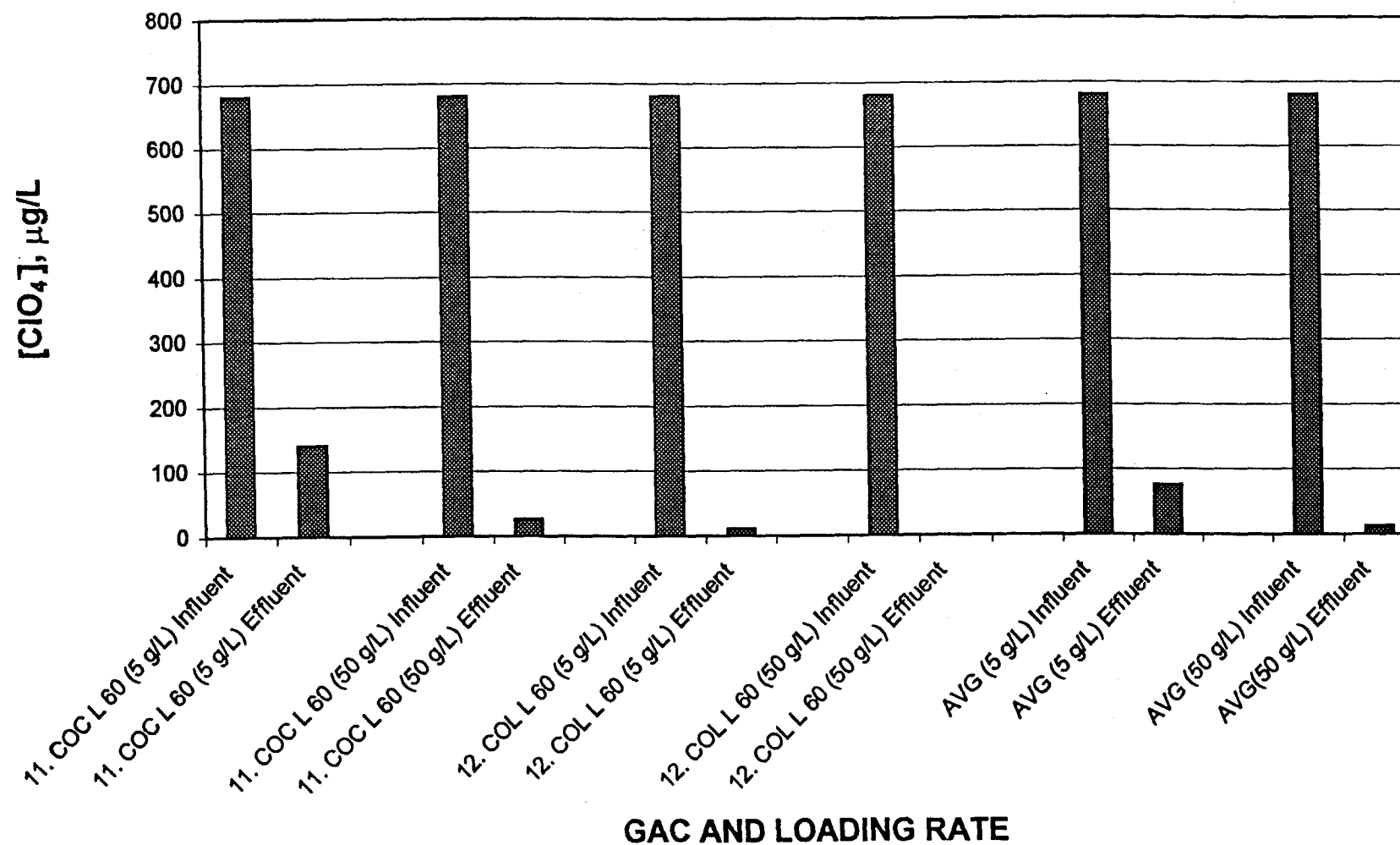


Figure 9. Removal of Perchlorate by Soluble Reducing Agents (1 g/L) from JPL Groundwater
(Refer to Table 2 for details regarding reducing agents)

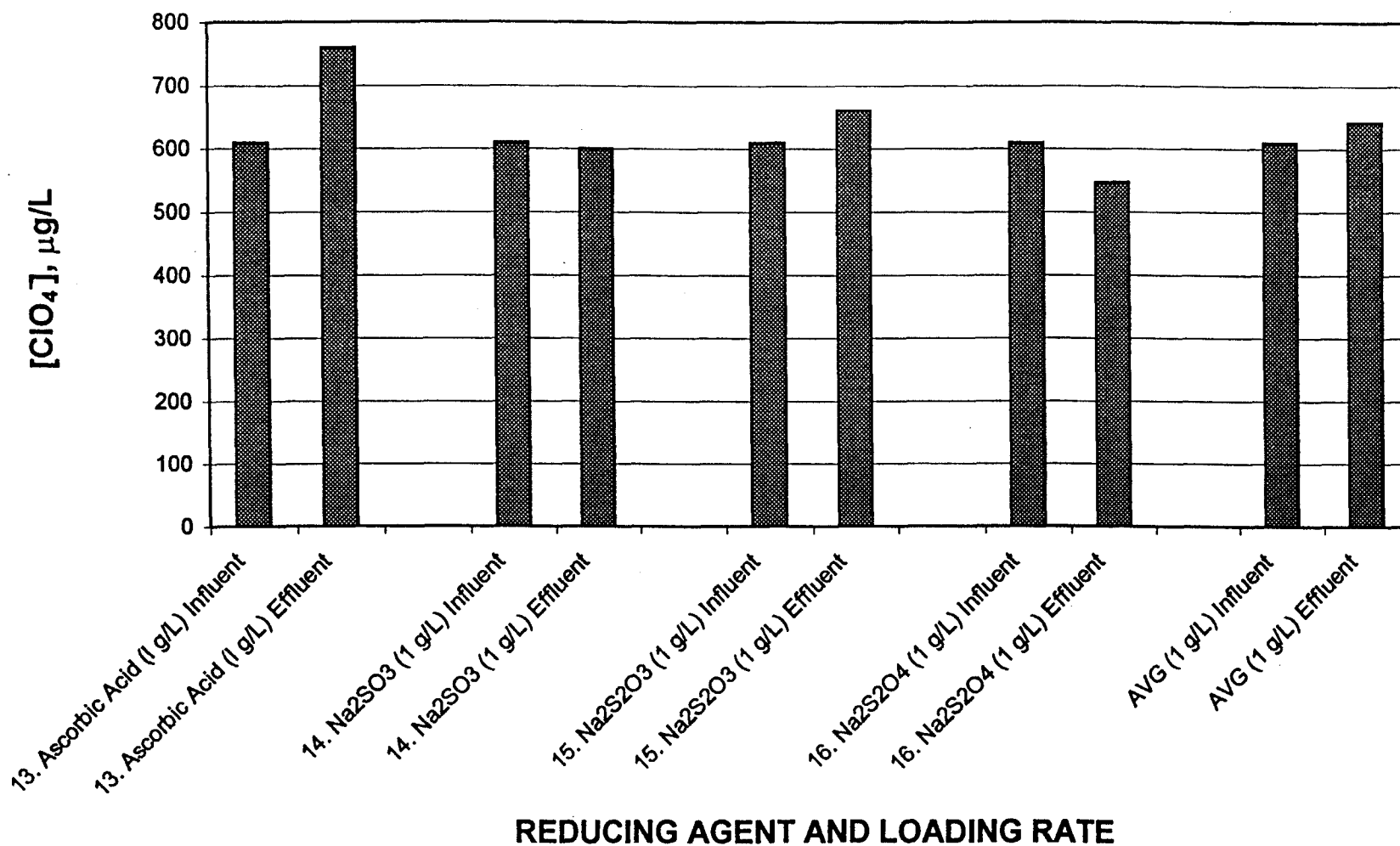


Figure 10. Removal of Perchlorate by Soluble Reducing Agents (1 g/L) from Deionized Water
(Refer to Table 2 for details regarding reducing agents)

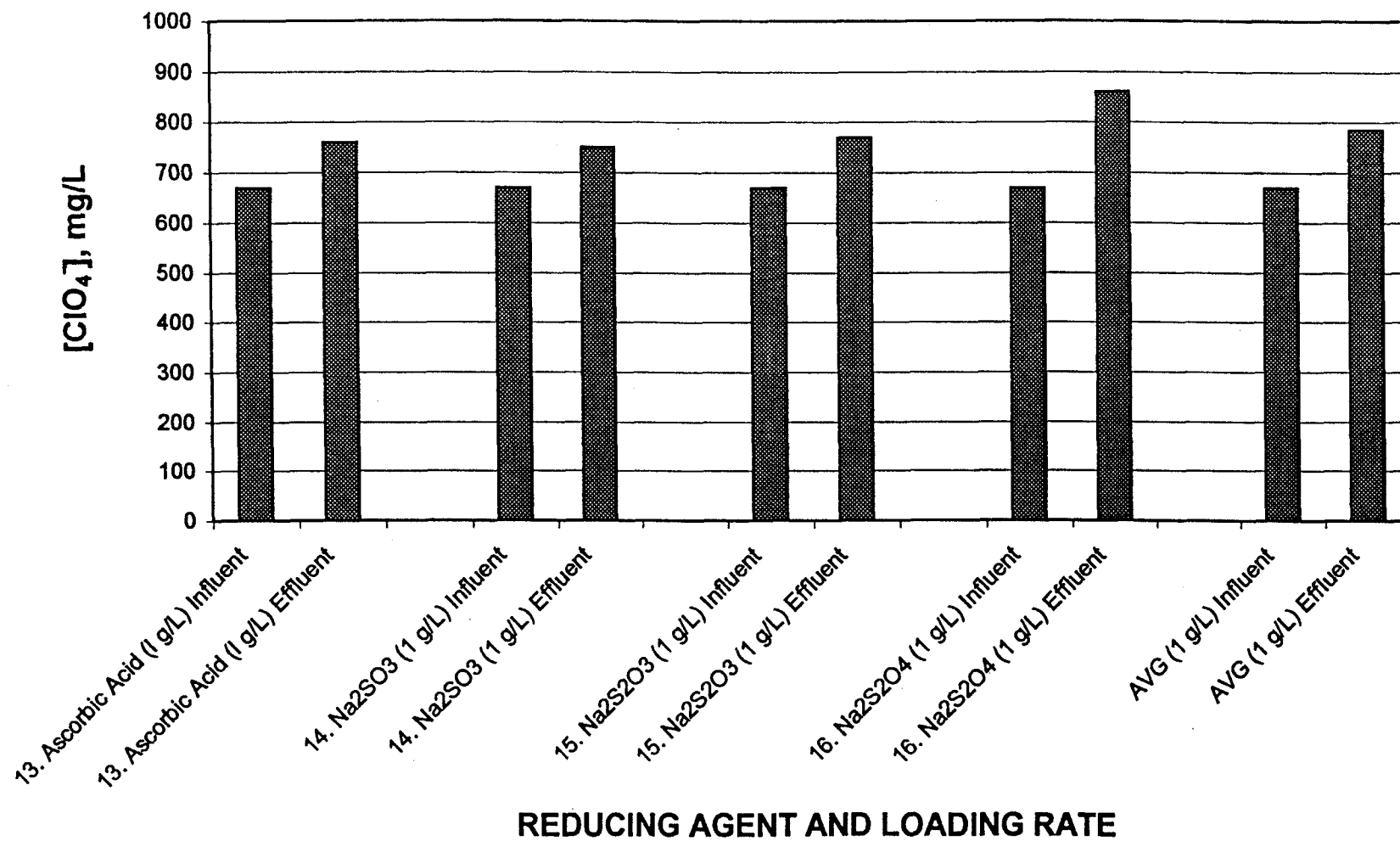


Figure 11. Resin Loading Ranges - Amberlite IRA400 Cl

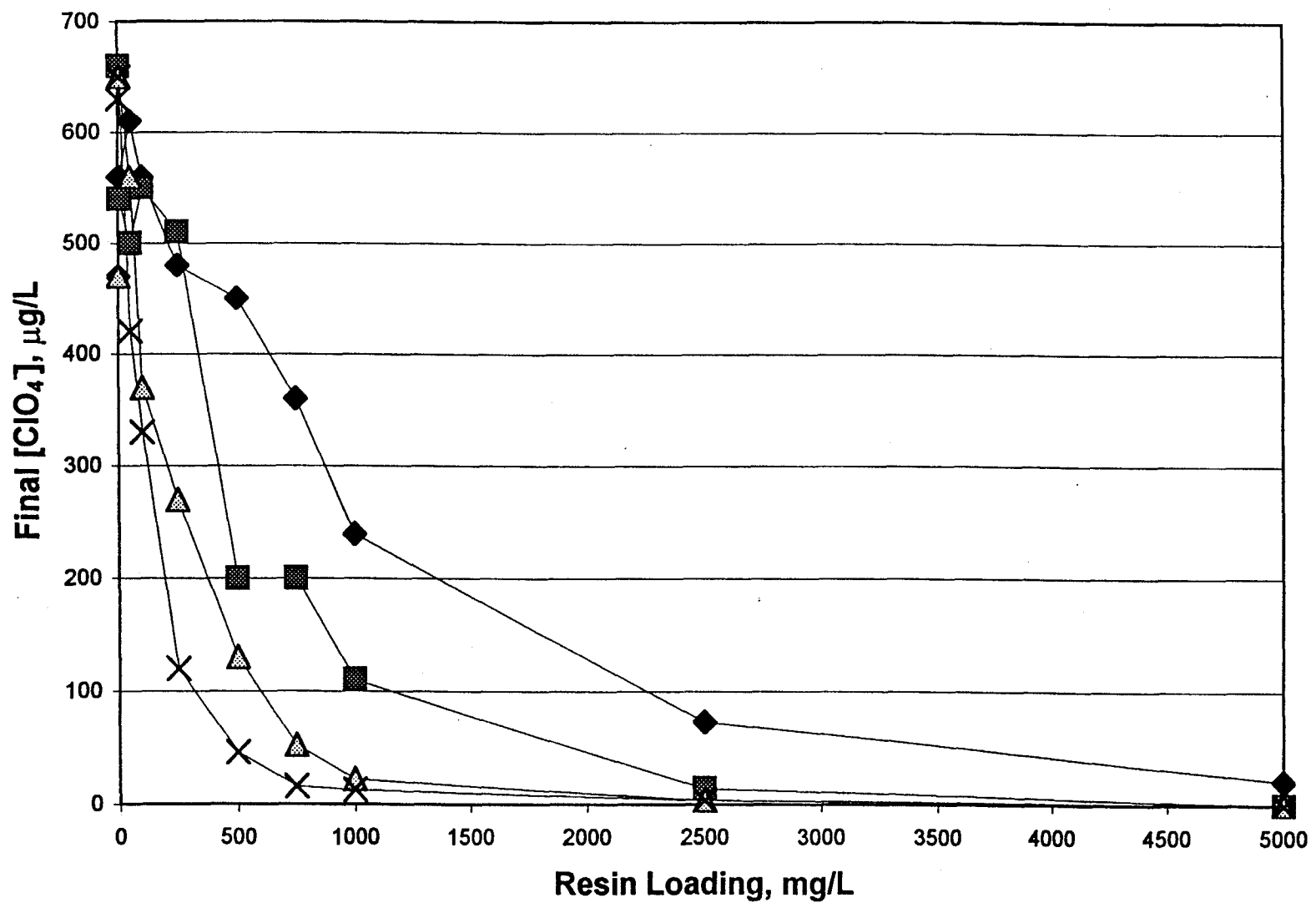


Figure 12. Contact Time Ranges - Amberlite IRA400 Cl

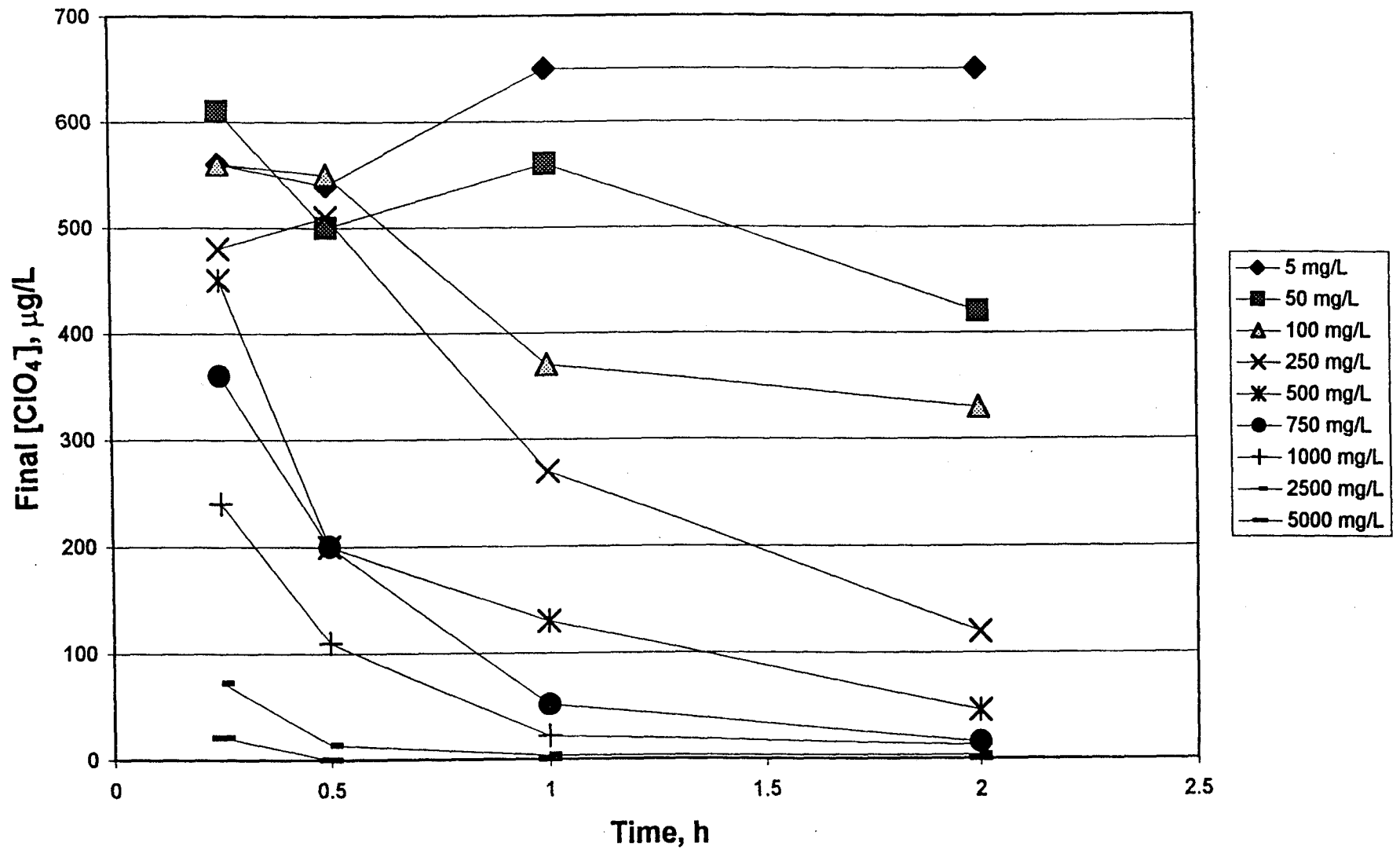


Figure 13. Perchlorate Removal from JPL Groundwater and DI Water by Amberlite IRA400 Cl for Different Resin Loadings - 2 hour Contact Time

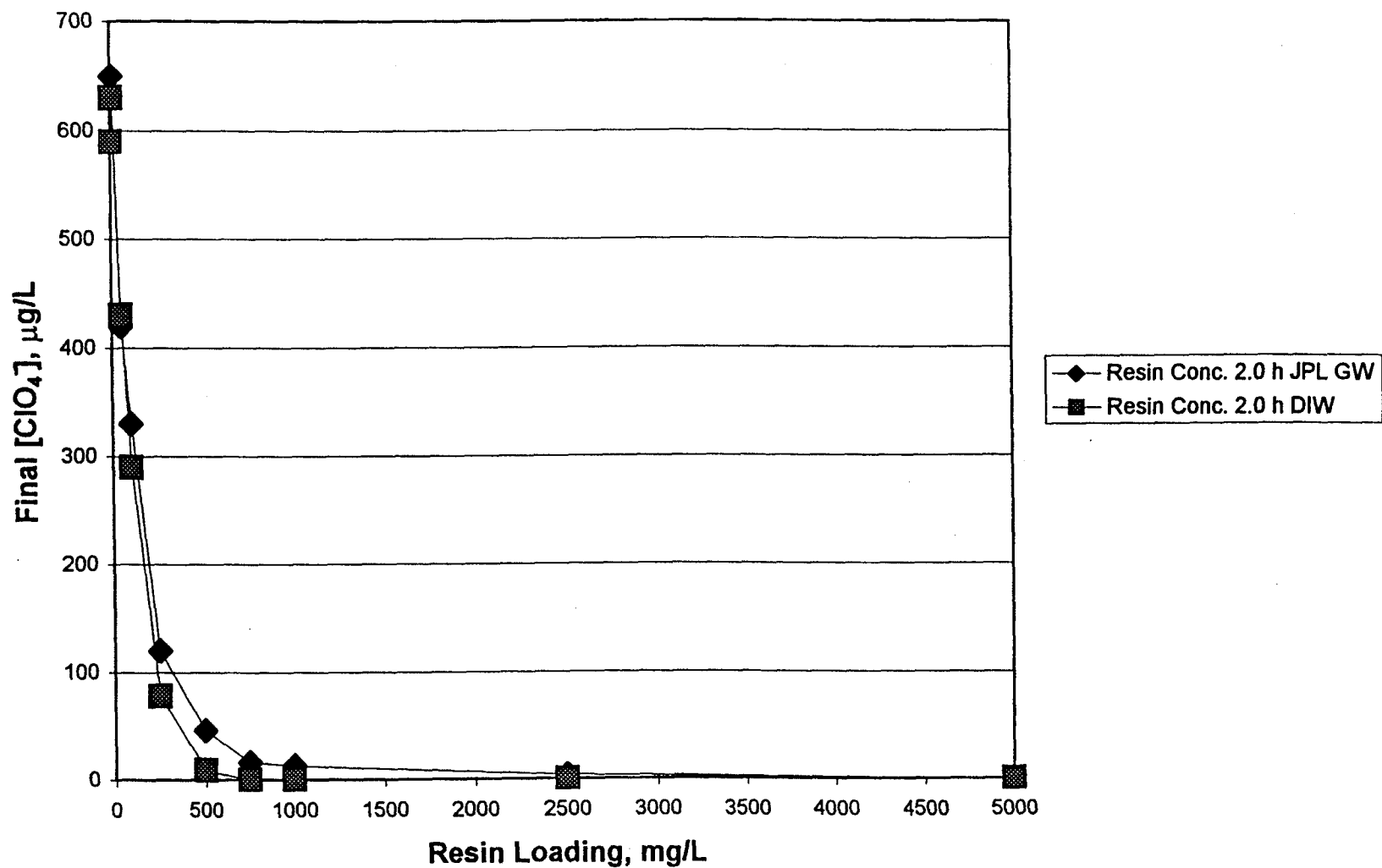
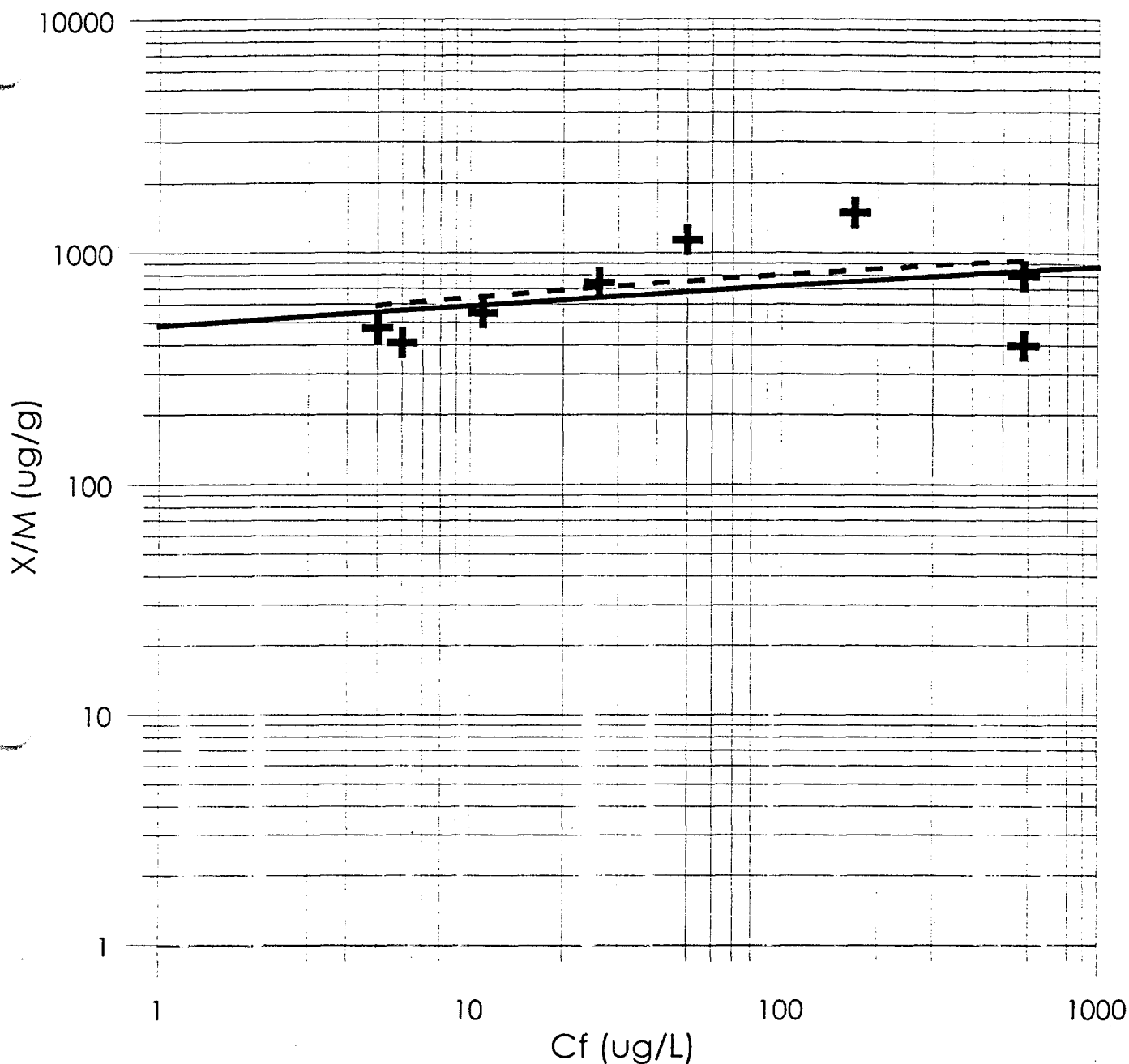


Figure 14. Freundlich Isotherm: Amberlite IRA400 CI (SBA)



Fit Results

Fit 1: Power, $\log(Y) = B \cdot \log(X) + A$

Equation:

$$\log(Y) = 0.0857023 \cdot \log(X) + 6.18576$$

Alternate equation:

$$Y = \text{pow}(X, 0.0857023) \cdot 485.784$$

Number of data points used = 8

Average $\log(X)$ = 3.85388

Average $\log(Y)$ = 6.51605

Regression sum of squares = 0.190989

Residual sum of squares = 1.44882

Coef of determination, R-squared = 0.116471

Residual mean square, $\sigma^2_{\text{hat}} = 0.241469$

Fit Results

Fit 3: Log, $Y = B \cdot \log(X) + A$

Equation:

$$Y = 70.983 \cdot \log(X) + 478.758$$

Number of data points used = 8

Average $\log(X)$ = 3.85388

Average Y = 752.318

Regression sum of squares = 131019

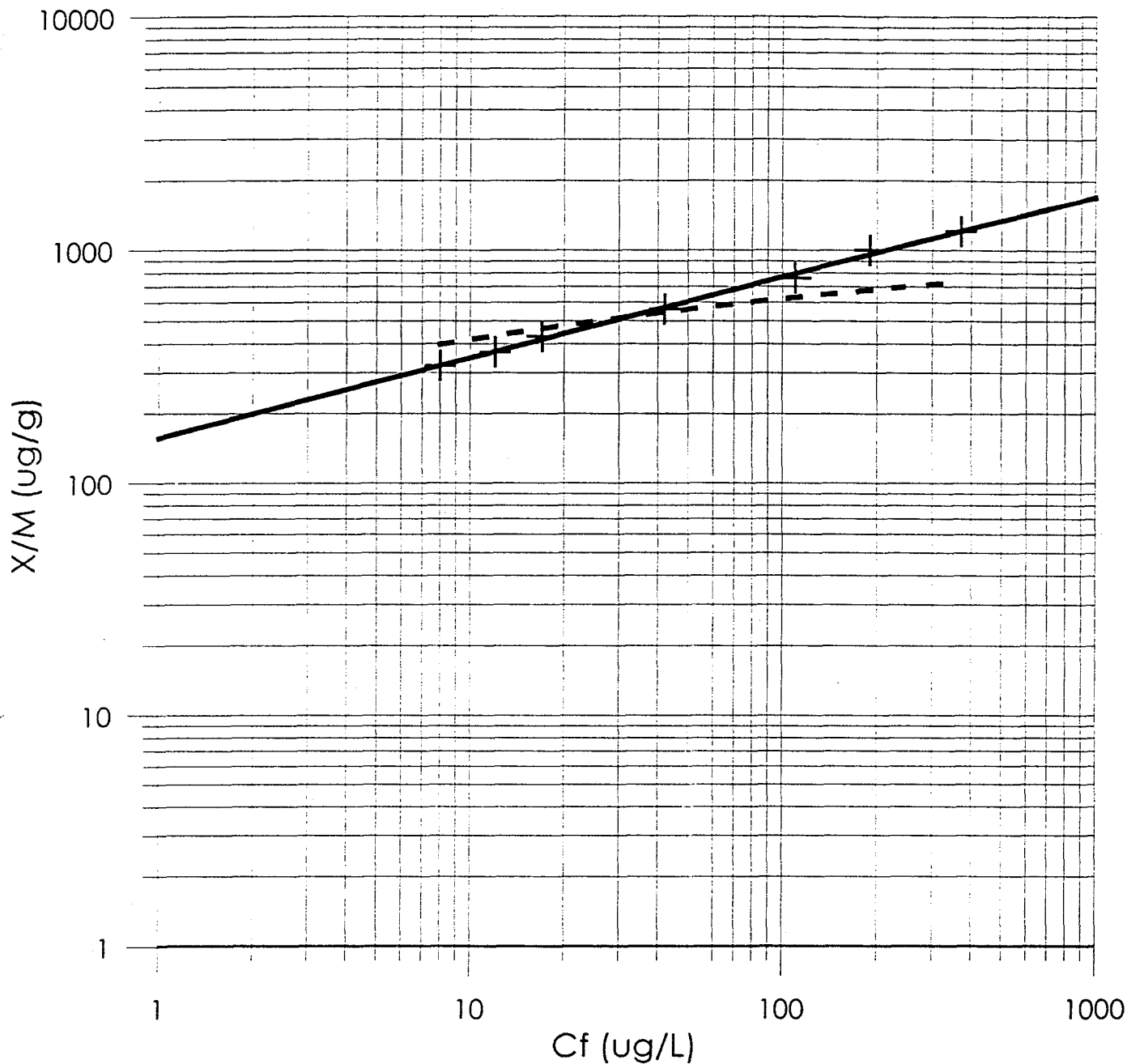
Residual sum of squares = 939894

Coef of determination, R-squared = 0.122343

Residual mean square, $\sigma^2_{\text{hat}} = 156649$

— Fit 1: Power $\log(Y) = B \cdot \log(X) + A$
 - - Fit 3: Log, $Y = B \cdot \log(X) + A$

Figure 15. Freundlich Isotherm: Dowex MSA-1 (SBA)



Fit Results

Fit 2: Power, $\log(Y)=B*\log(X)+A$

Equation:

$$\log(Y) = -2.07489 * \log(X) + 12.4721$$

Alternate equation:

$$Y = \text{pow}(X, -2.07489) * 260959$$

Number of data points used = 8

Average $\log(X)$ = 4.14883

Average $\log(Y)$ = 3.86373

Regression sum of squares = 76.4589

Residual sum of squares = 282.3

Coef of determination, R-squared = 0.213121

Residual mean square, $\sigma^2_{\text{hat-sq'd}}$ = 47.05

Fit Results

Fit 1: Log, $Y=B*\log(X)+A$

Equation:

$$Y = 88.9854 * \log(X) + 213.059$$

Number of data points used = 8

Average $\log(X)$ = 4.14883

Average Y = 582.244

Regression sum of squares = 140628

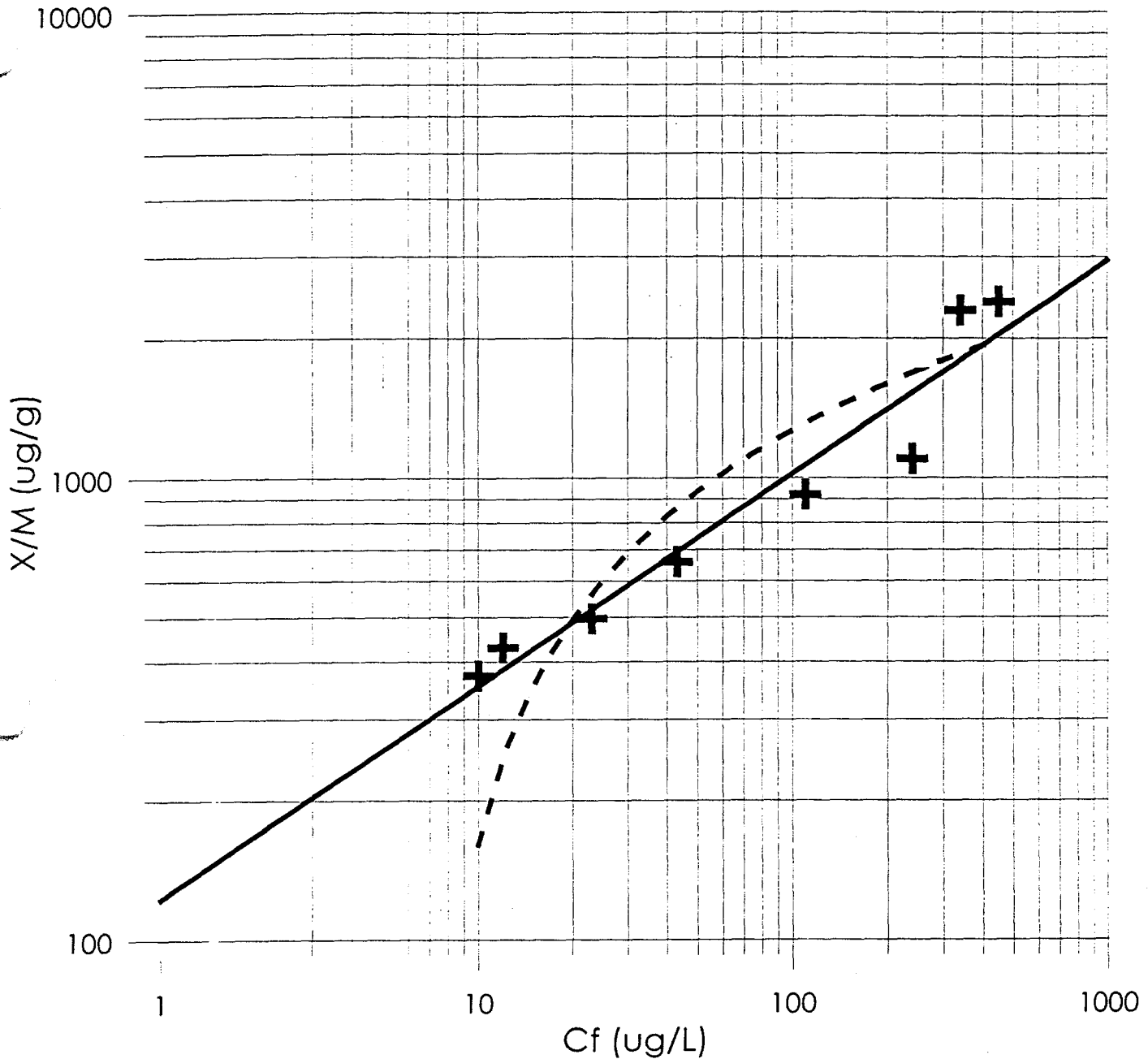
Residual sum of squares = 938858

Coef of determination, R-squared = 0.130273

Residual mean square, $\sigma^2_{\text{hat-sq'd}}$ = 156476

— Fit 2: Power, $\log(Y)=B*\log(X)+A$
 - - - Fit 1: Log, $Y=B*\log(X)+A$

Figure 16. Freundlich Isotherm: Dowex MS 500A (SBA)



Fit Results

Fit 1: Power, $\log(Y)=B*\log(X)+A$

Equation:

$$\log(Y) = 0.460187 * \log(X) + 4.80992$$

Alternate equation:

$$Y = \text{pow}(X, 0.460187) * 122.722$$

Number of data points used = 8

Average $\log(X)$ = 4.22544

Average $\log(Y)$ = 6.75441

Regression sum of squares = 3.39925

Residual sum of squares = 0.237244

Coef of determination, R-squared = 0.93476

Residual mean square, sigma-hat-sq'd = 0.0395406

Fit Results

Fit 2: Log, $Y=B*\log(X)+A$

Equation:

$$Y = 480.592 * \log(X) + -945.887$$

Number of data points used = 8

Average $\log(X)$ = 4.22544

Average Y = 1084.82

Regression sum of squares = 3.70738E+006

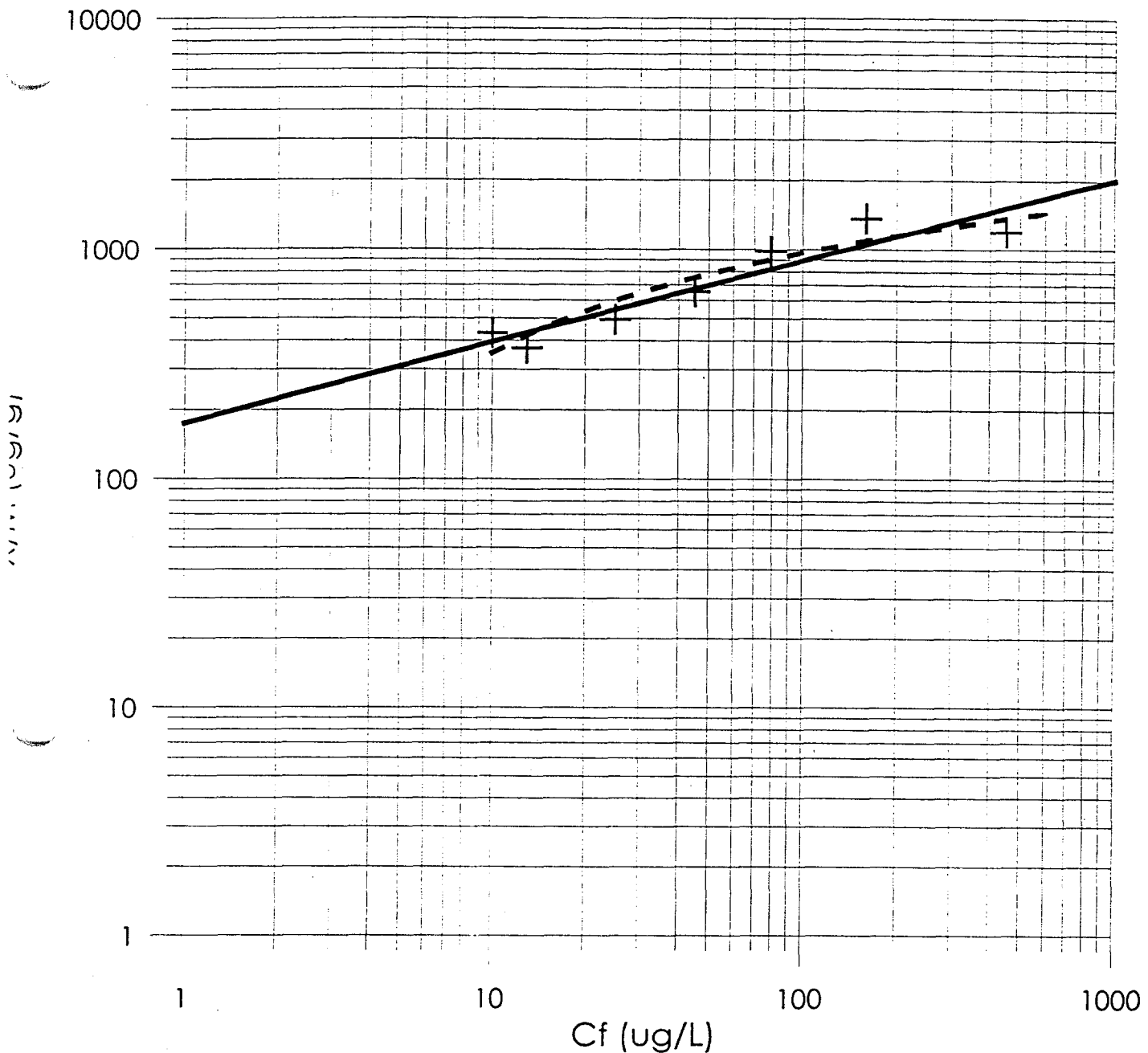
Residual sum of squares = 989132

Coef of determination, R-squared = 0.78939

Residual mean square, sigma-hat-sq'd = 164855

— Fit 1: Power, $\log(Y)=B*\log(X)+A$
 - - Fit 2: Log, $Y=B*\log(X)+A$

Figure 17. Freundlich Isotherm: Ionac AFP-329 (WBA)



Fit Results

Fit 1: Power, $\log(Y)=B*\log(X)+A$

Equation:

$$\log(Y) = -1.43916 * \log(X) + 11.0039$$

Alternate equation:

$$Y = \text{pow}(X, -1.43916) * 60105.9$$

Number of data points used = 9

Average $\log(X)$ = 4.4598

Average $\log(Y)$ = 4.58548

Regression sum of squares = 42.3161

Residual sum of squares = 81.3004

Coef of determination, R-squared = 0.342317

Residual mean square, sigma-hat-sq'd = 11.6143

Fit Results

Fit 2: Log, $Y=B*\log(X)+A$

Equation:

$$Y = 2.72454 * \log(X) + 599.257$$

Number of data points used = 9

Average $\log(X)$ = 4.4598

Average Y = 611.408

Regression sum of squares = 151.66

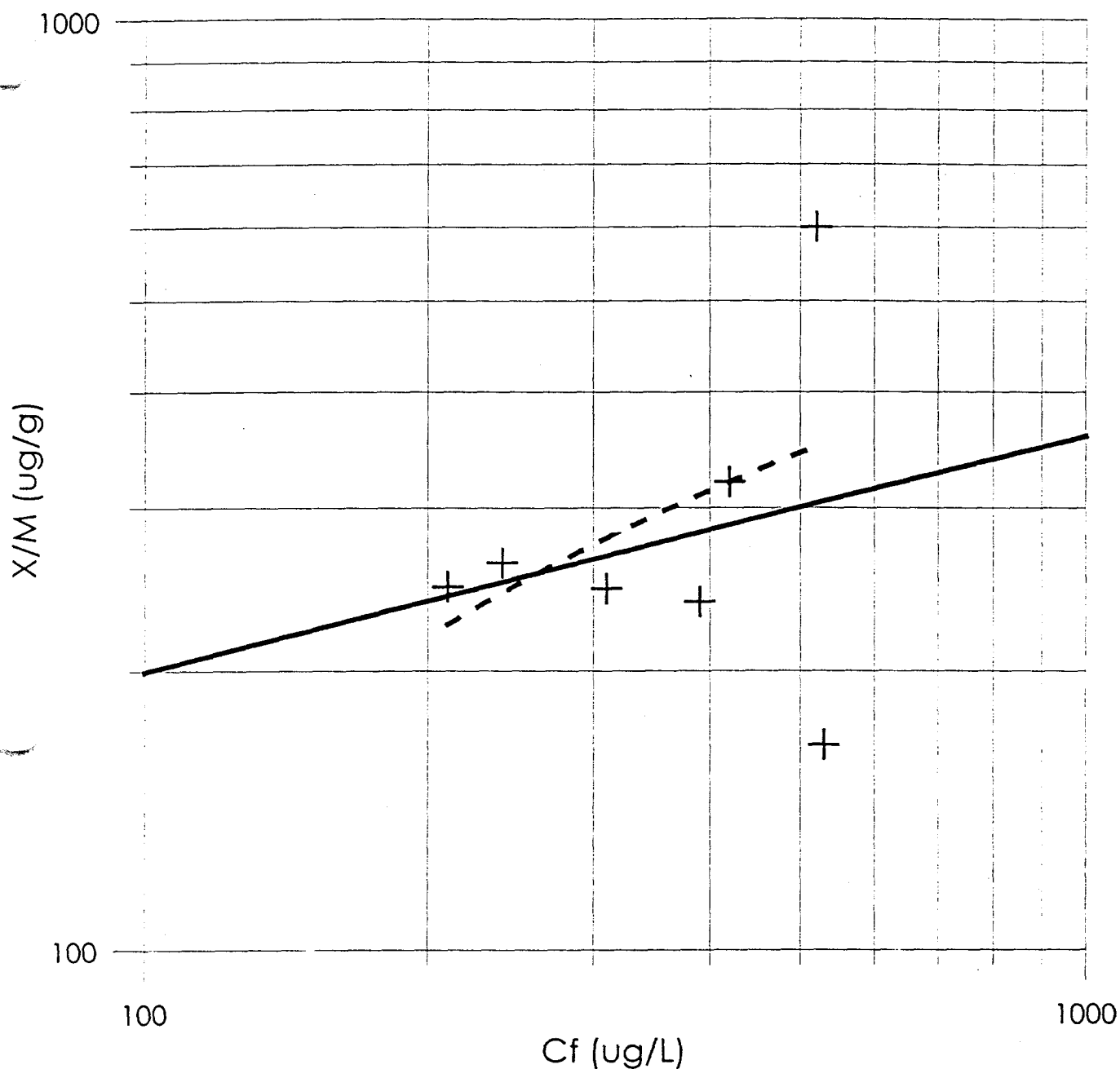
Residual sum of squares = 1.90716E+006

Coef of determination, R-squared = 7.95152E-005

Residual mean square, sigma-hat-sq'd = 272452

— Fit 3: Power, $\log(Y)=B*\log(X)+A$
 - - - Fit 4: Log, $Y=B*\log(X)+A$

Figure 18. Freundlich Isotherm: Ionac A-305B (WBA)



Fit Results

Fit 1: Power, $\log(Y)=B*\log(X)+A$

Equation:

$$\log(Y) = 0.254153 * \log(X) + 4.1263$$

Alternate equation:

$$Y = \text{pow}(X, 0.254153) * 61.9483$$

Number of data points used = 7

Average $\log(X)$ = 5.87106

Average $\log(Y)$ = 5.61845

Regression sum of squares = 0.051073

Residual sum of squares = 0.880051

Coef of determination, R-squared = 0.0548509

Residual mean square, sigma-hat-sq'd = 0.17601

Fit Results

Fit 2: Log, $Y=B*\log(X)+A$

Equation:

$$Y = 137.846 * \log(X) + -512.471$$

Number of data points used = 7

Average $\log(X)$ = 5.87106

Average Y = 296.832

Regression sum of squares = 15024.1

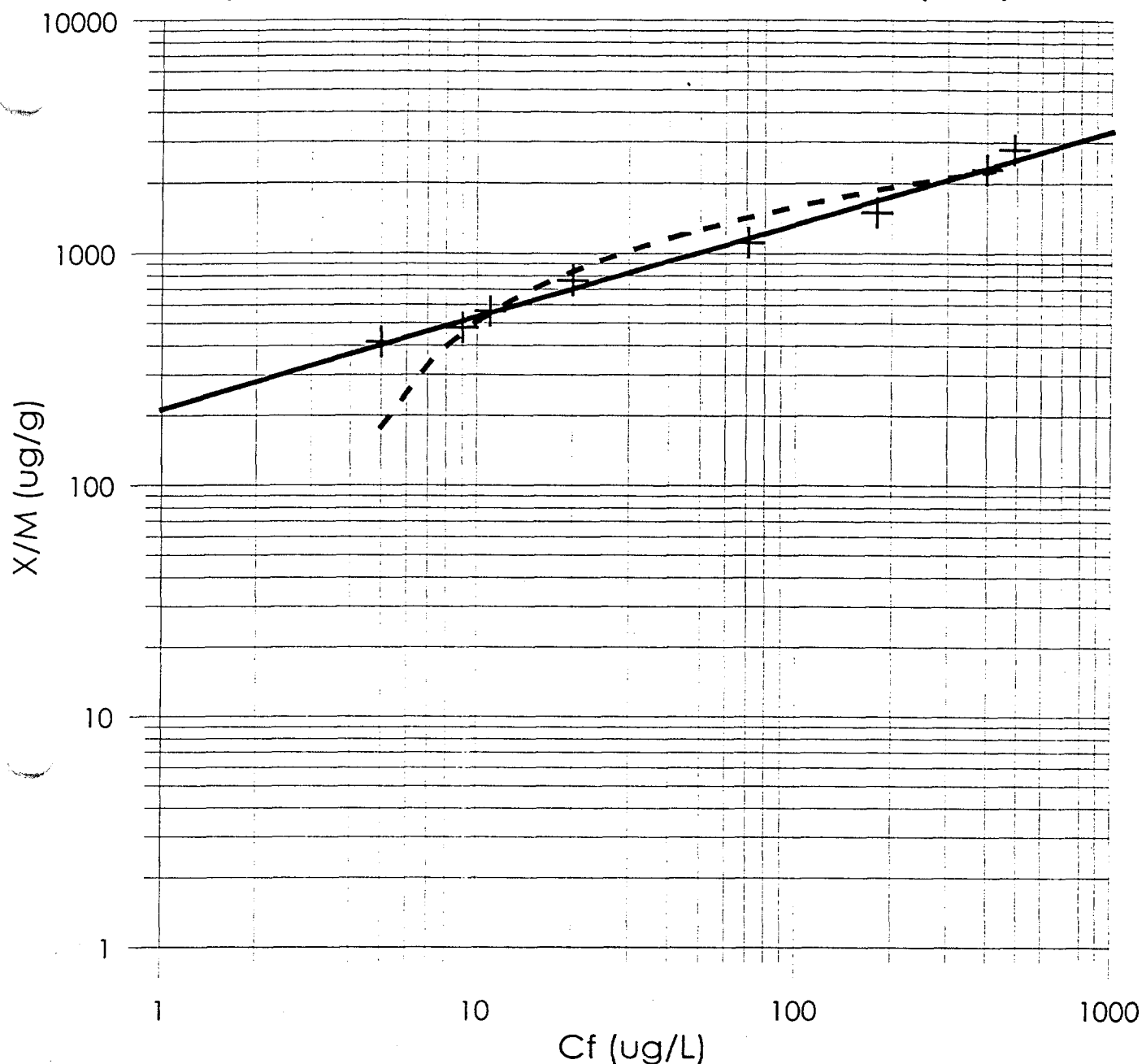
Residual sum of squares = 104289

Coef of determination, R-squared = 0.125922

Residual mean square, sigma-hat-sq'd = 20857.7

— Fit 1: Power, $\log(Y)=B*\log(X)+A$
 - - Fit 2: Log, $Y=B*\log(X)+A$

Figure 19. Freundlich Isotherm: Ionac A-641 (SBA)



Fit Results

Fit 1: Power, $\log(Y) = B \cdot \log(X) + A$

Equation:

$$\log(Y) = 0.399083 \cdot \log(X) + 5.35909$$

Alternate equation:

$$Y = \text{pow}(X, 0.399083) \cdot 212.533$$

Number of data points used = 8

Average $\log(X)$ = 3.85522

Average $\log(Y)$ = 6.89765

Regression sum of squares = 3.60676

Residual sum of squares = 0.039482

Coef of determination, R-squared = 0.989172

Residual mean square, sigma-hat-sq'd = 0.00658034

Fit Results

Fit 2: Log, $Y = B \cdot \log(X) + A$

Equation:

$$Y = 473.463 \cdot \log(X) + -583.108$$

Number of data points used = 8

Average $\log(X)$ = 3.85522

Average Y = 1242.2

Regression sum of squares = 5.07647E+006

Residual sum of squares = 508875

Coef of determination, R-squared = 0.908891

Residual mean square, sigma-hat-sq'd = 84812.5

— Fit 1: Power, $\log(Y) = B \cdot \log(X) + A$
 - - Fit 2: Log, $Y = B \cdot \log(X) + A$

APPENDIX C

**CALGON CARBON CORPORATION FINAL REPORT
ON A PILOT STUDY FOR REMOVAL OF PERCHLORATE
FROM JPL GROUNDWATER**

FINAL REPORT

**Removal of Perchlorate and Other
Contaminants from Groundwater at JPL**

A Pilot Study

By

Calgon Carbon Corporation
Pittsburgh, PA

Submitted to

Jet Propulsion Laboratory
Pasadena, CA

June 28, 1999

EXECUTIVE SUMMARY

A study funded by National Aeronautics and Space Administration (NASA) to demonstrate the removal of trichloroethylene (TCE), 1,2-dichloroethane (DCA), carbon tetrachloride (CCl_4) and perchlorate (ClO_4^-) from groundwater at Jet Propulsion Laboratory (JPL) has recently been completed by Calgon Carbon Corporation. Calgon Carbon successfully utilized its integrated granular activated carbon (GAC) and ISEP+™ treatment systems for the removal of the contaminants from ground water during the study conducted between September 15, 1998 - March 5, 1999. Results indicated that the organic contaminants were reduced to low levels and perchlorate in various inlet concentration levels (upto ~1200 ppb) was removed to non-detectable levels (<4 ppb) in treated water. In addition, the system was successful in removing other anionic species such as nitrate and sulfate from the groundwater to low levels in treated water, while producing minimal amounts of regeneration waste.

The integrated ISEP+™ system (comprising continuous ion exchange system (ISEP®) and perchlorate and nitrate destruction module (PNDM)) was successfully demonstrated for about 10 days. Perchlorate and nitrate present in regeneration waste from ISEP® were destroyed and substantial amounts of sulfate (exceeding 96%) was removed in the PNDM. The regenerant (brine), thus 'purified' in the PNDM, was recycled and was effective in regenerating the resin for the period of study. The overall process waste from the integrated ISEP+™ system for treating up to ~1200 ppb perchlorate was about 0.16%, based on the volume of feed water. Over one-half of a million gallons of ground water at the JPL site was successfully treated to produce a high quality water with non-detectable TCE, DCA and CCl_4 concentrations, non-detectable perchlorate (<4 ppb), low nitrate (<2 ppm) and sulfate (<2 ppm) concentrations.

Testing at various process conditions enabled Calgon Carbon to optimize each of the process units of the ISEP+™ system and confirm steady state operation. Sufficient operating data were obtained from this pilot study to design full-scale ISEP® system and to further develop the ISEP+™ integrated system for the complex treatment needs of JPL and other sites.

1.0 INTRODUCTION

Perchlorate and other anionic contaminants in ground water are effectively removed by ion-exchange, a process where contaminant anions are exchanged and replaced by an innocuous anion, typically chloride. Ion-exchange is one of the most effective methods for most ground water treatment applications due to its efficiency in removing contaminants present in varying concentrations at relatively low costs. Most of the ion-exchange resins manufactured are used for water treatment and ion-exchange resins have been treating drinking water for several years. Although ion-exchange technology is well-known, the effectiveness of an ion-exchange process depends, among other factors, on the operational configuration of the process. Key parameters that determine the efficiency and impact the economics of an ion-exchange process are treatment ratio and regeneration waste. Treatment ratio refers to the volume of feed water that can be treated before breakthrough of the contaminant(s) is obtained. Regeneration waste refers to the volume of waste generated by the ion-exchange process while regenerating the ion-exchange resin saturated with contaminants. An effective ion-exchange process is one that achieves high treatment ratios while producing low regeneration waste. Calgon Carbon's ISEP® system utilizes an effective ion-exchange process configuration that achieves high perchlorate treatment ratios while producing minimal waste.

Calgon Carbon utilized its patented multi-port ISEP® valve in developing an ion-exchange system for the removal of perchlorate and other anionic contaminants from ground water. The system bears similarity to Calgon Carbon's ISEP®-based system used commercially for the treatment of nitrate from drinking water. The two fundamental advantages of the ISEP® system are better utilization of the mass transfer zone* and continuous split-flow or counter-current* regeneration, which lead to high treatment ratios and low regeneration waste as compared to conventional ion-exchange processes using fixed bed systems. The ISEP® system involves sequential segmentation of the mass transfer zone where on a continuous basis, the loaded segment of the resin is removed from the 'top' of the mass transfer zone and regenerated

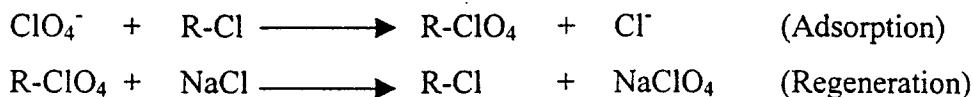
* The portion of the bed where ion exchange is taking place, sometimes called the "wavefront".

* 'Counter-current' in ISEP® refers to the fact that the direction of stream flow is opposite to the direction of rotation of the ISEP® columns.

resin is added back at the 'bottom' of the mass transfer zone, leading to better utilization of the ion-exchange resin during the adsorption cycle.

In the regeneration cycle, the technology utilizes a split-flow regeneration scheme where the regenerant flow is split equally and pumped into each column in the regeneration zone in parallel. This allows the fresh regenerant to be available to each column in the regeneration zone that results in efficient removal of perchlorate from the loaded resin compared to conventional fixed bed systems where split-flow regeneration is not feasible. This enables a highly efficient use of the regenerant thereby producing significantly lower wastes than the fixed-bed system. In another variation, regeneration of the resin in the ISEP® system may be accomplished by a staged counter-current mass transfer approach wherein the entire regeneration flow is passed through each column in series. In this configuration, the concentration of contaminants in the regenerant stream progressively increases as it traverses through each column in the regeneration zone. The resin columns, traveling in a direction counter-current (opposite) to the flow of regenerant, get progressively regenerated. This scheme can also result in an effective utilization of the regenerant, depending on the levels of contaminant loading on the resin. The ability to vary the configuration of adsorption and regeneration zones independently to operate at their optimum efficiencies on a continuous basis makes the ISEP®-based design effective, versatile and economical for ground water treatment applications involving ion-exchange.

Prior to the JPL pilot test program, Calgon Carbon had conducted extensive screening tests and identified an optimal anion exchange resin (Resorb+™) for the ISEP® system. The following scheme illustrates how perchlorate is removed by the ion exchange resin (R) in the ISEP® system:



The resin cycles through the above reaction steps in adsorption and regeneration zones of the ISEP® thus producing a continuous supply of treated water.

The ISEP+™ system piloted at JPL refers to ISEP® and a catalytic destruction and nanofiltration system together referred to as the perchlorate and nitrate destruction module

(PNDM). A granular activated carbon (GAC) system that serves to remove organic contaminants from the ground water prior to the ISEP® was also included in the pilot study. The PNDM serves to eliminate perchlorate, nitrate and sulfate from the spent brine stream from the ISEP®. The individual systems are further described in the following sections. For the purposes of this report, 'Integrated ISEP+™' refers to the fact that the individual components of the ISEP+™ (ISEP® and PNDM) are operationally integrated with each other.

2.0 ISEP+™ PILOT PROGRAM AT JPL

Calgon Carbon was retained by the Jet Propulsion Laboratory (JPL) to demonstrate the removal of organic contaminants (specifically, trichloroethylene (TCE), 1,2-dichloroethane (DCA) and carbon tetrachloride (CCl₄)) and inorganic anions (specifically, perchlorate) from the groundwater at its site. The pilot test program, conducted between September 15, 1998 and March 5, 1999, featured Calgon Carbon's ISEP+™ system, which was successful in removing all the target contaminants from the ground water. The program achieved major technological milestones in the removal and destruction of perchlorate from ground water, most notably the demonstration of an effective and efficient perchlorate and nitrate destruction system (PNDM).

2.1 Pilot Objectives

The original objectives for the program were revised by mutual agreement between Calgon Carbon and JPL. Revisions to the original objectives were necessitated by technological enhancements to the ISEP+™ system that rendered some of the original objectives obsolete or irrelevant to the main goals of the pilot study. The revised objectives for the JPL pilot study were:

- Determine the water chemistry of the source water at either the MW-7 or MW-16 site.
- Demonstrate treatment for the reduction of TCE, 1,2-DCA and CCl₄ to <5.0 ppb, <0.5 ppb and <0.5 ppb, respectively.
- Demonstrate removal of perchlorate to <4 ppb using the ISEP® unit.
- Demonstrate removal of nitrate in addition to removal of above contaminants.
- Optimize the individual process units of the ISEP+™ system and demonstrate continuous removal of the target contaminants in the integrated ISEP+™ system.
- Optimize the overall ISEP+™ system for the removal of all target contaminants while minimizing the volume of waste produced.

These objectives were achieved during the pilot program and salient results are presented in the report.

2.2 Technology Discussion

The conceptual diagram of the ISEP+™ system as implemented at JPL is shown in Figure 1. The ISEP+™ system is an integrated process system comprised of a granular activated carbon (GAC) system to remove the organic contaminants, a continuous countercurrent ion exchange system (ISEP®) for the removal of perchlorate, nitrate and other anions, and a PNDM system that contains a catalytic reactor system for destroying nitrate and perchlorate from brine plus a nanofiltration system to remove sulfate from brine. The PNDM system serves to purify the brine waste from ISEP®, thereby recycling the brine as regeneration feed for the ISEP® system.

In the process, the well water is passed through a granular activated carbon (GAC) system that serves to remove any organic contaminants in the water. Based on the data available from the JPL pilot study as well as an earlier pilot study, the GAC system has very limited perchlorate loading capacity in a ground water treatment system. Therefore, perchlorate breaks through rapidly from the GAC bed while the organics are retained. The organic-free well water is passed through the ISEP® system as indicated.

Depending upon pilot objectives, a perchlorate spiking system to spike the influent perchlorate concentration was used after the GAC system and prior to the ISEP® system. The ISEP® system contains thirty (30) columns attached to the rotating portion of the multi-port valve. Each of the columns is packed with the chloride form of the chosen anion-exchange resin. The ISEP® columns can be divided into three functional zones, namely, adsorption, regeneration and rinse. The perchlorate (as well as nitrate and sulfate) present in the feed water is exchanged with chloride on the resin in the adsorption zone. The water treated in this way by the columns in the adsorption zone can have non-detectable levels (< 4 ppb) of perchlorate. The resin containing adsorbed perchlorate is treated in the regeneration zone using a brine solution that exchanges the perchlorate, nitrate and sulfate ions on the resin with the chloride ions from brine. The regenerant for the JPL pilot study was designed to be a 7% NaCl solution (brine) prepared using softened city water. Even though the brine concentration in the regeneration zone was set at 7% NaCl, it was determined at the end of the study that the conductivity-based control in the brine feed tank intended to regulate the rich brine, fresh water and recycled brine flows to maintain 7%

NaCl did not function properly throughout the study. As a result, the actual concentrations of brine were lower and were between 2.5-4.5% NaCl throughout the pilot study. This does not affect the conclusions from the study and moreover, it has a positive impact on the performance of the ISEP® system. This is because regenerant consumption decreases with increasing concentration of brine. So, the waste percentages reported during the optimization of the ISEP® can be expected to be even lower when 7% NaCl is used.

The brine flow in the regeneration zone was initially operated in series flow counter current configuration* leading to sufficient concentration gradients between the brine phase and the resin phase in each column in the regeneration zone. For most of the treatment study, a split-flow regeneration configuration was implemented. This was accomplished by splitting the regenerant flow into each column of the regeneration zone. The advantage of this method, as mentioned in Section 1.0, is the availability of fresh brine to each column in the regeneration zone thereby achieving the highest regeneration efficiency in each column.

The spent brine effluent from the ISEP® regeneration zone understandably contains the perchlorate anions in a significantly higher concentration than the feed. The rinse zone serves to remove the entrained brine from the columns coming out of the regeneration zone before they enter the adsorption zone for the next cycle. The rinse flow effluent is a weak brine solution that is treated by the RO unit to produce a product and concentrate stream. The product stream is purified water which is used to make-up part of the rinse flow influent. The concentrate stream is a brine solution that is utilized to make-up fresh regenerant used in the regeneration zone. The columns cycle through adsorption, regeneration and rinse zones with controllable residence times in each zone. The residence time calculations for each zone is translated into step time, which indicates the time for which the columns (and the valve) stay in one position. The step time for the ISEP® system during the JPL pilot was set at 16.6 min. In other words, the 30-column ISEP® system took 8.3 hours to complete one rotation. The treated water from the ISEP® system was then sent to a GAC guard bed intended to capture any perchlorate leakage from the ISEP®, thereby discharging treated water with non-detectable levels of perchlorate. The treated

* See Section 1.0 for a description of the counter current staged mass transfer operation in the ISEP regeneration zone.

water from the GAC guard bed complied with regulatory requirements throughout the pilot study and showed non-detectable levels of perchlorate for most of the testing period.

The spent brine effluent from the ISEP® system is sent to a catalytic reactor system to which small amounts of a reductant (such as ethanol) is added. Perchlorate and nitrate present in the brine effluent are reduced to chloride and molecular nitrogen respectively, while the reductant is oxidized to carbon dioxide and water. This reduction-oxidation (*redox*) reaction occurs over a proprietary solid catalyst in the reactor at an elevated temperature and pressure. The effluent from the reactor is almost free of perchlorate and nitrate and is passed into a nanofiltration (NF) system where sulfate is removed from the brine into a small purge stream containing high concentrations of sulfate, but no perchlorate and nitrate. The purge stream from the NF system is the only waste stream from the entire process. This waste stream is expected to be in the range of 0.05-0.2% of the total feed water treated by the process. The product brine from the NF system is now 'purified' as it is free of perchlorate, nitrate and contains low levels of sulfate. This brine is recycled back into the regeneration zone of the ISEP® system along with a small fresh brine make-up stream. Thus, the entire brine treatment train is nearly a closed-loop process where more than 90% of the ISEP® brine effluent is recycled. Thus, the entire ISEP+™ process results in effective removal of contaminants while producing minimal waste for disposal.

2.3 Program Methodology

The ISEP+™ system described above was implemented in two phases. The first phase involved the demonstration and optimization of the GAC and ISEP® systems for removal of target organic and anionic contaminants. The second phase involved the demonstration and optimization of the PNDM system and the integration with ISEP® to demonstrate the integrated ISEP+™ treatment system.

2.3.1 Pilot Optimization Methodology

Phase I: A dual-GAC bed was designed based on the influent concentrations of the organics and operated in series. As mentioned earlier, GAC has a limited capacity for perchlorate removal. Nevertheless, to avoid the perchlorate breakthrough profile from the GAC system and its temporary reduction of the influent concentration to the ISEP®, the GAC was pre-treated

with a dilute solution of ammonium perchlorate to saturate the GAC system with perchlorate. This was done to achieve the steady state GAC performance right from start-up, and thus efficiently utilize the pilot testing time towards optimizing ISEP® and PNDM.

It should be emphasized that GAC pre-treatment is neither advantageous nor required for commercial scale operation as the GAC effluent perchlorate concentration will reach that of the influent after a relatively short breakthrough period (~3-5 days). A schedule for GAC change-out was developed and implemented based on the organic leakage observed from the first bed. This proved sufficient to ensure the continuous removal of organics from the GAC system. The sampling points in the GAC system (influent, after first bed and just prior to the ISEP® system) were chosen so as to monitor organics removal performance and change-out GAC at appropriate frequencies.

The ISEP® system was first operated at design conditions (6% waste) to demonstrate removal of perchlorate and other anions. Then, optimization of the ISEP® followed at different inlet concentrations. Perchlorate concentrations of 250 ppb and ~1200 ppb were chosen to conduct the optimizations. The optimization program involved minimizing the brine effluent (or regenerant use) in the ISEP® system. After each change in the brine flow rate, the system performance was monitored for at least 2 days (approximately 6 rotations of ISEP® system) to determine the impact of the process change. After the final optimized brine flow rate level was reached, the ISEP® system was maintained at the optimal process conditions for the remainder of pilot test. During Phase I of the pilot test period, the spent brine was stored in a large waste tank and was periodically removed from the site and properly disposed by Safety-Kleen Corporation. The samples in the ISEP® were taken at the inlet and outlet of adsorption zone and the brine samples were taken from the rinse and regeneration zones. In addition, treated water samples were taken at five different columns evenly distributed within the adsorption zone. Samples were also taken after the guard GAC bed just prior to discharge from the site.

Phase II: This phase consisted of continued operation of the ISEP® at the optimal conditions for ~1200 ppb ClO₄ and treating the spent brine effluent by the PNDM. The spent brine was passed through the catalytic reactor system, where the performance of perchlorate and nitrate

destruction was demonstrated and contact time optimization study was conducted. In addition, the performance of the nanofiltration system was evaluated and fine tuning adjustments to obtain desired performance were made. Since optimization of the ISEP® and PNDM were independently conducted, the final step was to integrate all the unit operations to evaluate the performance of the integrated ISEP+™ system. This was demonstrated towards the end of the pilot which marked the completion of the pilot program.

2.3.2 Sampling and Analytical Protocols

Sampling of various ISEP® and PNDM streams were conducted throughout the study. The ISEP® samples were taken over a period of one step time (16.6 min.) to remove the effect of intrastep concentration profiles thereby observing the true trends in the system. Samples taken from PNDM were typically grab samples and they were sufficient indicators of the true system performance. For anions analyses, the samples were collected in plastic bottles with solid screw cap covers. For organics analyses, the samples were collected in clear glass bottles with no headspace and covered by screw caps with teflon septa. In addition, samples collected for special analyses followed appropriate EPA protocols for sample collection, storage and analyses. Perchlorate and other anions were analyzed using two high-resolution ion chromatography systems, one customized to detect low-level perchlorate and the second for other anions. The analytical method used for perchlorate and other anions was the EPA method 300.0 (modified) for anions analyses. The samples containing high brine concentrations were pre-treated by a silver nitrate cartridge to minimize the interference of chloride on perchlorate analysis. Analyses of the organics were conducted using a gas chromatograph with an electrolytic conductivity detector.

3.0 RESULTS AND DISCUSSION

A representative profile of target organics and perchlorate observed in the groundwater from the MW-7 well site is shown in Figure 2. It is clear that perchlorate concentration from the well head fluctuated significantly and was in the range of 110-160 ppb for the majority of the test. Among the organics present in the well head, CCl_4 varied between 14-35 ppb and TCE between 6-15 ppb for the bulk of the test. Interestingly, the 1,2-DCA remained constant and at a very low level (< 0.5 ppb) throughout the test. The results obtained from performance evaluation and optimization studies of the individual process units of the ISEP+™ system are discussed below.

3.1 GAC System Performance

Representative steady state results showing removal of 1,2-DCA, CCl_4 , TCE and over the GAC system are shown in Figures 3, 4 and 5 respectively. The 1,2-DCA inlet and outlet concentrations were both less than 0.5 ppb indicating that the impact of GAC on the reduction in 1,2-DCA could not be detected. On the other hand, the GAC system consistently removed CCl_4 and TCE down to less than 0.5 ppb in the treated water. The period of operation between GAC change-outs were designed to ensure that all the target organics are continuously removed to less than 1 ppb in treated water. It was mentioned earlier that activated carbon has a limited capacity for perchlorate in ground water. The pilot data collected at JPL (shown in Appendix) as well as at an earlier field test site indicated that the perchlorate breakthrough profile from a GAC bed continuously increases till it reaches the influent concentration and remains at that level. There was no evidence of perchlorate displacement from GAC bed. In other words, the perchlorate concentration at the effluent of the GAC system never exceeded the influent concentration.

3.2 ISEP® Performance and Optimization

After initial optimization of the rinse flow to ensure effective and efficient rinse of the resin coming off the regeneration zone, the bulk of ISEP® demonstration and optimization focused on minimizing the regenerant consumption (i.e., spent brine flow rate). The continuous removal of perchlorate from the influent water by the ISEP® system for two different inlet concentrations is

shown in Figure 6. It is evident that the ISEP® system produced near-complete removal of perchlorate at both inlet concentrations. At ~250 ppb inlet ClO_4 , the system was optimized to produce treated water with non-detectable perchlorate (< 4 ppb) concentration and a regeneration brine effluent (waste) of 1.25%, based on the volume of feed water. At the ~250 ppb perchlorate influent concentration level, the regeneration was conducted in series flow configuration. To obtain even higher regeneration efficiencies, the regeneration configuration was changed to split-flow before conducting performance and optimization studies at ~1200 ppb ClO_4 . Even at ~1200 ppb ClO_4 inlet, the system was effective in producing less than 4 ppb perchlorate in treated water for an optimized regeneration effluent level of 1.75%, based on feed water. It is important to note that a nearly five-fold increase in feed perchlorate concentration (from 250 ppb to 1200 ppb) was easily accommodated by only a 40% change in regenerant consumption. The ISEP® system, in this pilot study as well as in earlier studies, proved capable of handling feed waters of widely varying perchlorate concentrations, after only a minor adjustment to regenerant consumption. In all cases, the treated water produced contained non-detectable level of perchlorate at optimized conditions.

Small portions of the curve in Figure 6 where treated water perchlorate concentration significantly exceeded non-detectable levels is attributed to an inadvertent loss of regenerant flow to the ISEP® caused by malfunction of the regeneration feed pump. Once the regenerant flow was restored, the ISEP® performance was restored thereby producing non-detectable perchlorate in treated water, as shown in Figure 6. Nitrate removal performance was also temporarily affected by the impact of inadvertent loss of regenerant flow as shown in Figure 7.

In addition to perchlorate removal, the ISEP® system was effective in concomitantly removing substantial amounts of nitrate and sulfate from the feed water, as shown in Figures 7 and 8. About 90% of influent nitrate (15-20 ppm down to < 2 ppm) and more than 95% of the influent sulfate (from 45-50 ppm down to < 2 ppm) were removed from the inlet water. The treated water produced by the ISEP® system was of superior quality with the representative characteristics shown in Table 1.

The treated water from the ISEP® was sent to another GAC system (guard bed) and discharged from the GAC guard bed. This was done as an additional precaution to ensure that the treated water discharged complies with all federal, state and local regulations. The discharged water was periodically monitored throughout the pilot study and results indicated that the perchlorate level in the discharged water always remained below the California PAL (< 18 ppb) and remained at non-detectable (< 4 ppb) levels, for the most of the pilot study. A representative analytical profile of discharged treated water is shown in Table 1.

Table 1. Representative treated water characteristics produced at the outlet of the ISEP® system during the JPL pilot trial.

<i>Target Contaminant</i>	<i>Concentration</i>
ORGANICS:	
1,2-DCA	< 0.5 ppb
CCl ₄	< 0.5 ppb
TCE	< 0.5 ppb
ANIONS:	
Perchlorate	< 4 ppb
Nitrate	< 2 ppm
Sulfate	< 2 ppm

3.3 PNDM Performance and Optimization

The perchlorate and nitrate destruction module (PNDM) was brought on-line after successful optimization of the ISEP® system in treating feed water at ~1200 ppb ClO₄ to produce non-detectable perchlorate in treated water at a spent brine level of 1.75%. A typical composition of the spent brine is shown in Table 2. This spent brine effluent from the ISEP® was stored and used for performance evaluation and optimization of the PNDM. The catalytic reactor system was operated at different temperatures, pressures and contact times during the optimization study and their impact on perchlorate and nitrate destruction kinetics was ascertained.

Table 2. Typical anion composition of spent brine effluent from the ISEP® system, influent to the PNDM.

<i>Anion</i>	<i>Concentration</i>
Perchlorate	~60,000 ppb
Nitrate	~1,000 ppm
Sulfate	~3,500 ppm

The catalytic reactor system in the **PNDM** is comprised of a fixed bed containing solid catalyst pellets, made from a proprietary composition. Although the exact mechanism of perchlorate and nitrate reduction is debatable, laboratory and pilot data indicated that both nitrate and perchlorate are reduced via intermediates that contain progressively lower oxidation states of nitrogen and chlorine respectively. The reaction occurring on the catalyst is reduction-oxidation (*redox*) where the slight stoichiometric excess of ethanol fed into the reactor is oxidized to carbon dioxide and water, concurrently reducing perchlorate and nitrate present in the brine stream to chloride and nitrogen, respectively.

Internal laboratory studies with the catalyst prior to the pilot study indicated that the reactions of perchlorate and nitrate reduction could each be categorized as first order* with respect to each of the reactants. In addition, nitrate destruction occurs more readily than perchlorate destruction over the catalyst. These results were borne out by pilot data as indicated below.

The steady state destruction of perchlorate achieved by the catalytic system during the pilot trial is shown in Figure 9. It is evident that perchlorate destruction exceeding 99.8% was achieved producing non-detectable (<125 ppb)[#] perchlorate concentration in brine. The kinetics of perchlorate destruction at the tested conditions followed first order with a reaction rate constant of 0.0013 sec⁻¹. Concurrently, nitrate present in the brine was also completely destroyed as shown in Figure 10. The treated brine from the reactor had a non-detectable (<20 ppm) nitrate concentration. Consistent with our laboratory studies, the rate constant for nitrate destruction in the pilot study was substantially higher than that for perchlorate destruction. Perchlorate and nitrate destruction are parallel reactions occurring on the catalyst surface.

The proprietary catalyst used for the pilot study, similar to many other catalysts, is subject to loss of activity (deactivation) under abnormal conditions. Deactivation can be either reversible or irreversible depending upon the phenomena causing it. Reversible deactivation in this treatment system is most commonly induced by loss of reductant flow in the treatment stream. In the

*Implies that the effluent concentration of the reactant decreases exponentially with reaction time.

[#] Due to interference by the high concentration of chloride ions in brine, the perchlorate detection limit in brine is 125 ppb as opposed to 4 ppb or less in water. Similarly, the nitrate detection limit in brine is 20 ppm as opposed to 0.2 ppm in water.

absence of the reductant (say, ethanol), the catalyst will be unable to reduce perchlorate and nitrate. Based on data obtained from the pilot study, such loss of activity is immediately restored when the reductant flow is re-established. In other words, the catalyst regains its original activity in the presence of reductant. Irreversible deactivation may occur by the deposition or interference of certain undesirable compounds (catalyst poisons) that may be present in the brine stream. Some compounds or elements that may poison the catalyst are iodine, organosulfur, organonitrogen, heavy metal (such as vanadium) compounds and to a lesser degree, iron. Poisoning of the catalyst to a level where the performance is substantially affected is known to occur primarily under sustained exposure to the poisons at significant concentration levels. Since these compounds are not normally present in most ground water streams, the catalyst is not likely to be poisoned under normal operating conditions. The reaction rate constant remained the same throughout the pilot study at JPL indicating that the catalyst was not poisoned and moreover, no potential catalyst poisons were detected in the water or brine streams.

The treated brine from the catalytic reactor was stored and used for evaluation of the nanofiltration (NF) system. The NF system consists of a membrane that separates divalent anions from monovalent anions. Thus, the divalent sulfate anions are selectively removed from the brine stream. Two parameters that describe the performance of the NF system are recovery and rejection rate. Recovery refers to the percent of feed that is recovered as permeate (or product) and rejection rate refers to the percent of target ion (sulfate) present in feed that is rejected to the waste (or concentrate) stream. Optimization of the nanofiltration system was conducted by varying the recovery of brine and studying its impact on sulfate rejection rate. Once an appropriate recovery was set, efforts to improve the quality of the recovered brine by varying the operating pressure were conducted. The impact of NF operating pressure on the quality (sulfate concentration) of permeate is shown in Figure 11. A slight improvement in permeate quality is obtained at increasing pressures which appeared to level off around 300 psig. The NF system was set to operate at 300 psig and produced a 91% brine recovery and a 96% sulfate rejection rate. This implies that only 9% of the inlet brine stream is discarded as the waste (concentrate) stream. This is the only waste stream produced in the ISEP+™ process. This waste stream corresponds to ~0.16% of the total feed water treated by the ISEP® system.

Moreover, this low waste stream primarily consists of sulfate in brine but non-detectable amounts of perchlorate or nitrate and so, can be easily disposed.

3.4 Overall Process (ISEP+™) Integration

Since the individual process units of the ISEP+™ system were independently validated and optimized, integration of the overall process was accomplished as the final requirement of the pilot study. The integration strategy followed is highlighted in Figure 12. First, the ISEP® system was continuously integrated with the catalytic reactor system. Next, the catalytic reactor system was integrated with the NF system. Finally, the permeate stream ('purified' brine) from the NF system was integrated with the ISEP® brine feed control tank. The automated level and conductivity controls in the brine feed tank instantaneously adjusted the rich brine and make-up water flows to ensure that the brine feed into the ISEP® remained at the design flow rate and concentration. The integrated ISEP+™ system operated continuously for about 10 days before the pilot was shutdown.

Results obtained from the integrated system indicated that the ISEP® continued to produce treated water below California PAL while using about 91% reclaimed or 'purified' brine. The overall process waste from the integrated ISEP+™ system was about 0.16%, based on the feed water influent to the system. Analysis of the process waste stream indicated that it had a sulfate concentration of about 2% in brine with no detectable amounts of perchlorate (<125 ppb) or nitrate (<20 ppm). While this performance is in line with the criteria for the successful integration of the entire system, it should be recognized that this performance is based on a relatively short duration (~10 days) of integrated operation. Calgon Carbon is presently conducting further developmental activities to better understand the potential issues that may arise in long term operation of the ISEP+™ system. It is anticipated that the developmental issues would be resolved and the integrated ISEP+™ system would be commercialized in the third quarter of 1999.

4.0 CONCLUSIONS

Calgon Carbon has successfully demonstrated its **GAC**, **ISEP®** and **PNDM** systems for the removal and/or destruction of organics, perchlorate, nitrate and sulfate present in the ground water at JPL. All of the revised pilot objectives, mentioned earlier, were accomplished during the pilot study. The results indicated effective removal of organics by the **GAC** system. The results clearly demonstrated that even at influent perchlorate levels of ~1200 ppb, the **ISEP®** system produced a treated water with non-detectable level of perchlorate at a relatively low regeneration (brine) effluent level of 1.75%. Concomitantly, substantial amounts of influent nitrate and sulfate were also removed. The **PNDM™** system was successful in achieving near-complete destruction of perchlorate and nitrate from the **ISEP®** spent brine effluent stream. The nanofiltration system was effective in producing substantial amounts of 'purified' brine, while maintaining a high sulfate rejection level. Based on the several performance evaluation and optimization studies conducted during the pilot study, it is evident that the main process units of the **ISEP+™** system performed each function effectively and efficiently. The integrated **ISEP+™** system was successful in maintaining acceptable performance level, although the period of continuous integrated operation was relatively short. A low overall brine waste stream, at ~0.16% of the feed water treated, has been obtained in the integrated **ISEP+™** system. This waste stream contains non-detectable levels of perchlorate (<125 ppb) and nitrate (<20 ppm) and so, can be easily disposed.

LIST OF FIGURES

- Figure 1. Schematic of the ISEP+™ process implemented at JPL site.
- Figure 2. Representative VOC and ClO₄ profile data for MW-7 well at JPL.
- Figure 3. cis-1,2-DCA concentration data from GAC system during JPL pilot trial.
- Figure 4. Representative CCl₄ removal data from GAC system during JPL pilot trial.
- Figure 5. Representative TCE removal data from GAC system during JPL pilot trial.
- Figure 6. Perchlorate removal performance of the ISEP® system at ~250 ppb and ~1200 ppb influent concentrations.
- Figure 7. Nitrate removal performance of the ISEP® system during JPL pilot trial.
- Figure 8. Sulfate removal performance of the ISEP® system during JPL pilot trial.
- Figure 9. Steady state destruction of Perchlorate in PNDM during JPL pilot trial.
- Figure 10. Steady state destruction of Nitrate in PNDM during JPL pilot trial.
- Figure 11. Impact of nanofiltration operation pressure on permeate sulfate concentration.
- Figure 12. ISEP+™ integration strategy at JPL.

Appendix. Perchlorate breakthrough profile over granular activated carbon (GAC) observed during JPL pilot study.

Figure 1. Conceptual Diagram of the ISEP+ system as implemented at JPL site.

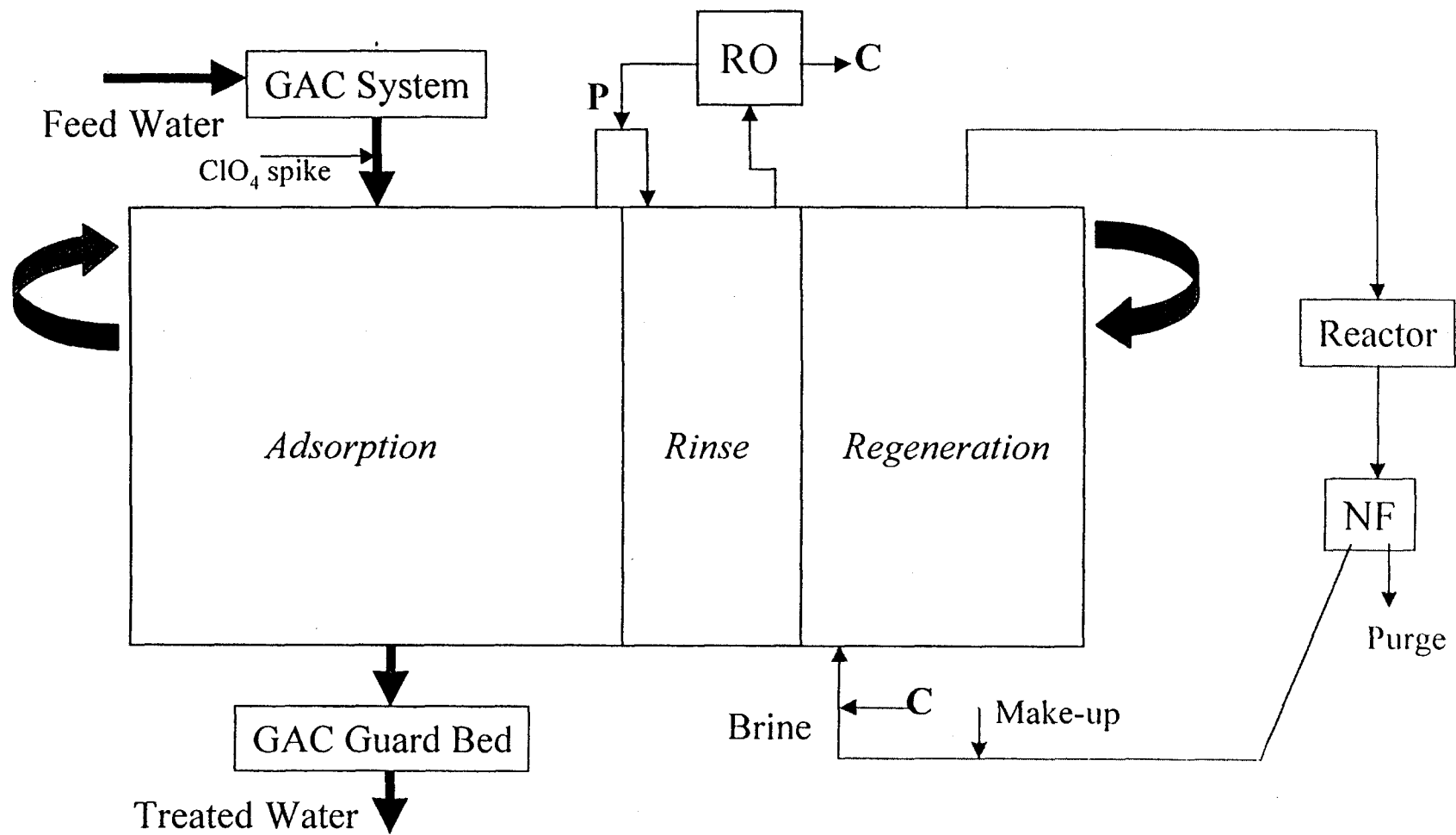


Figure 2. Representative VOC and CIO4 Profile Data for MW-7 well at JPL

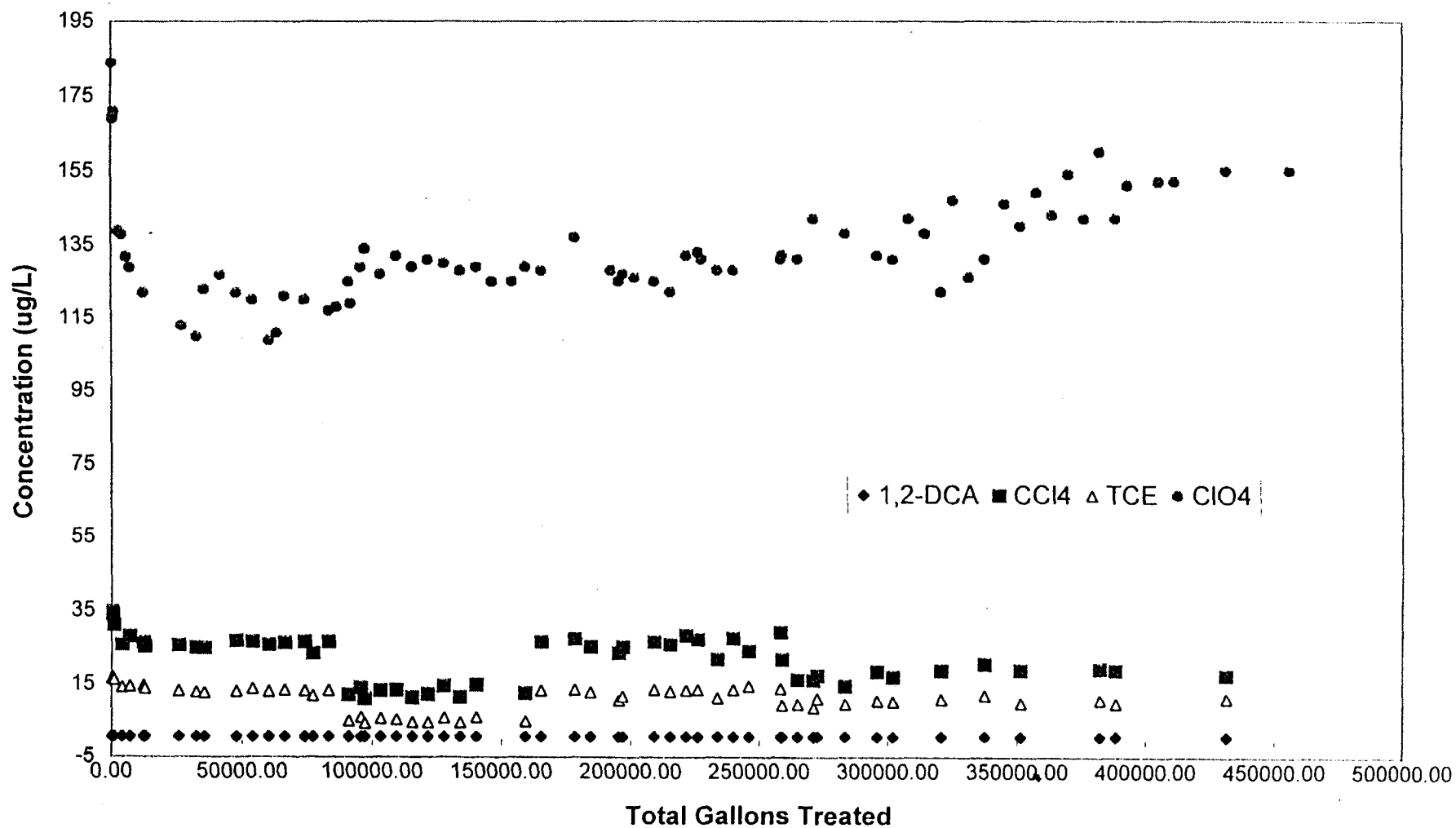


Figure 3. cis-1,2-DCA concentration data from GAC system during JPL pilot trial.

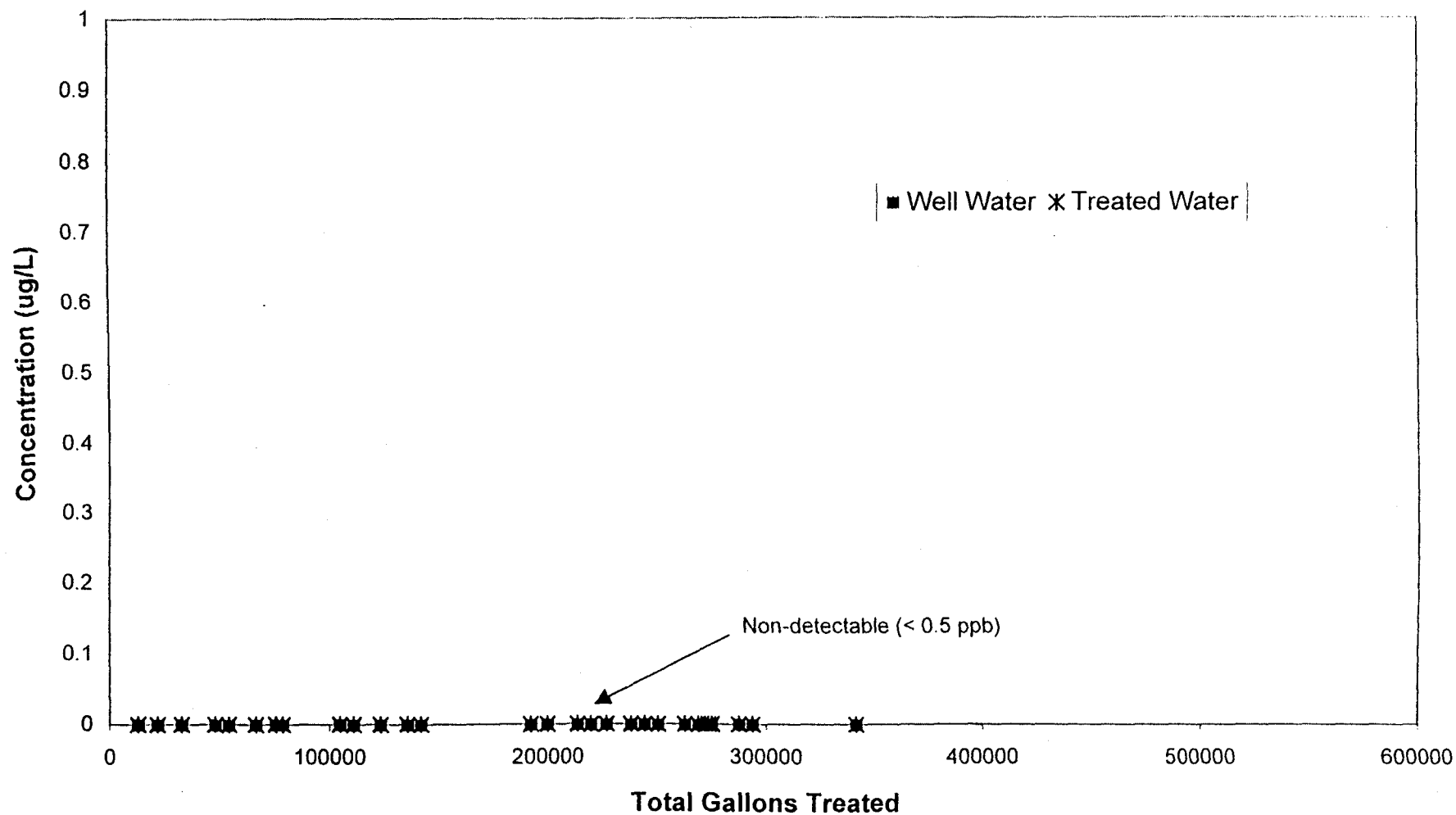


Figure 4. Representative CCl₄ removal data from GAC system during JPL pilot trial.

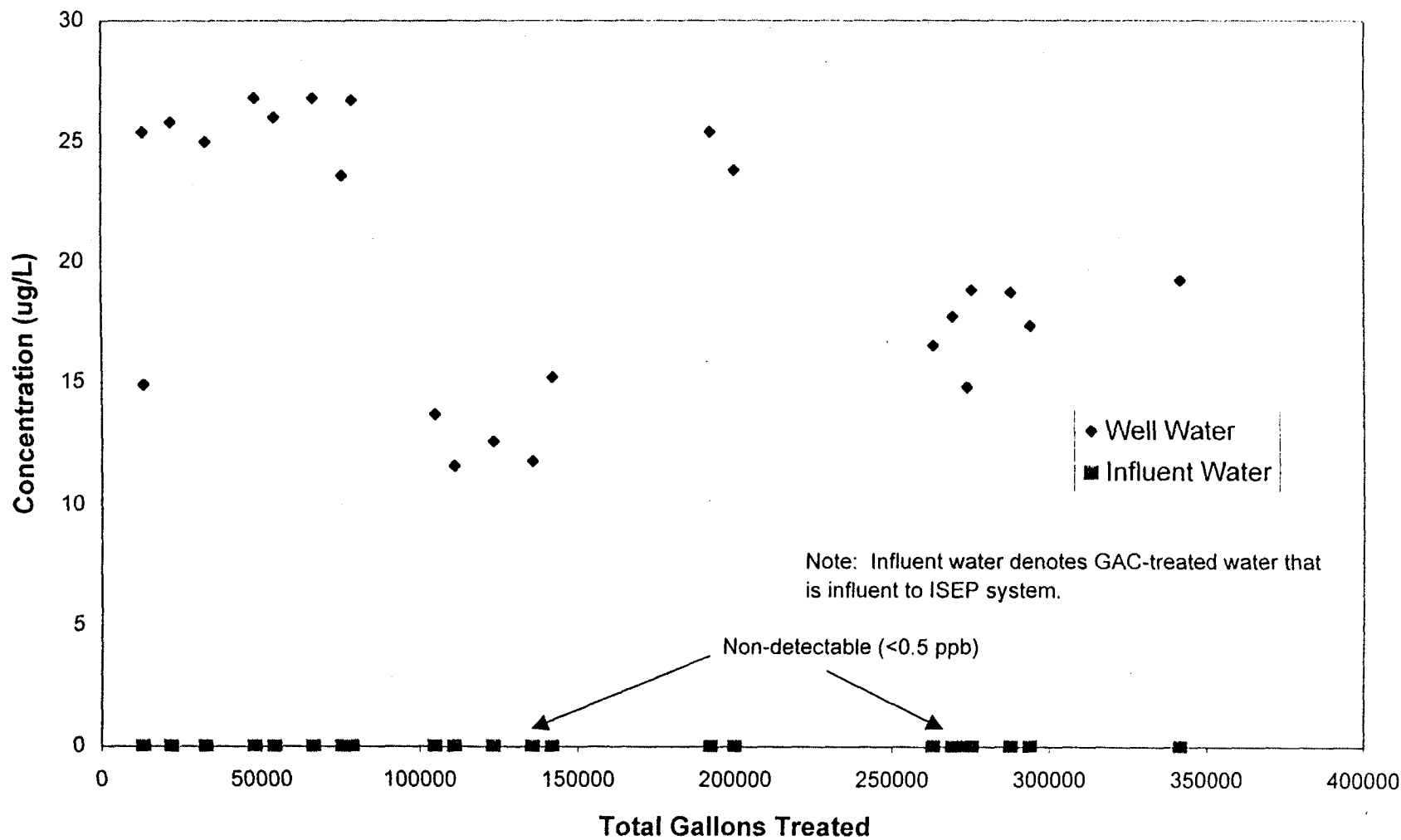


Figure 5. Representative TCE removal data from GAC system during JPL pilot trial

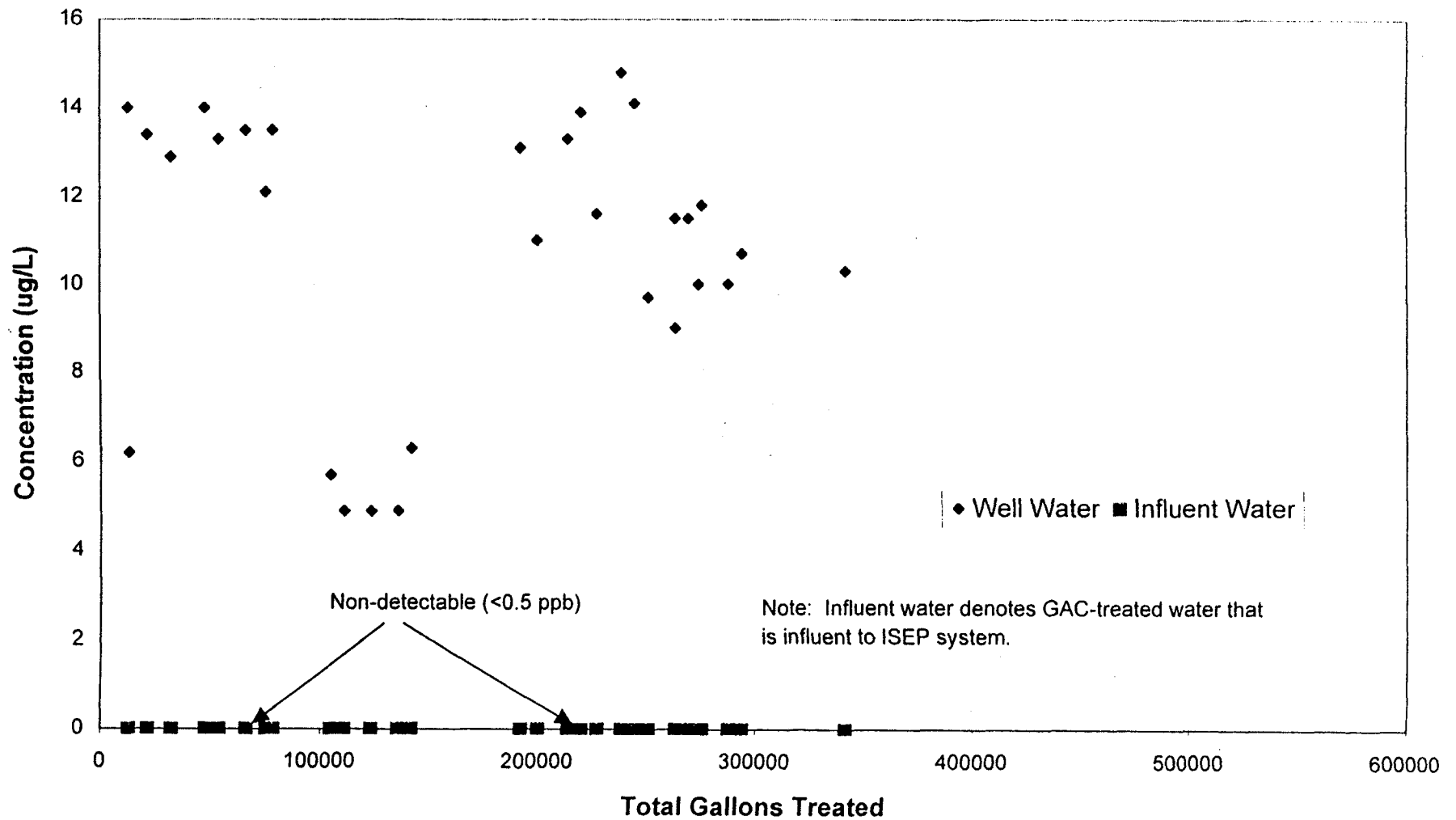


Figure 6. Perchlorate removal performance of the ISEP® system at ~250 ppb and ~1200 ppb influent concentrations.

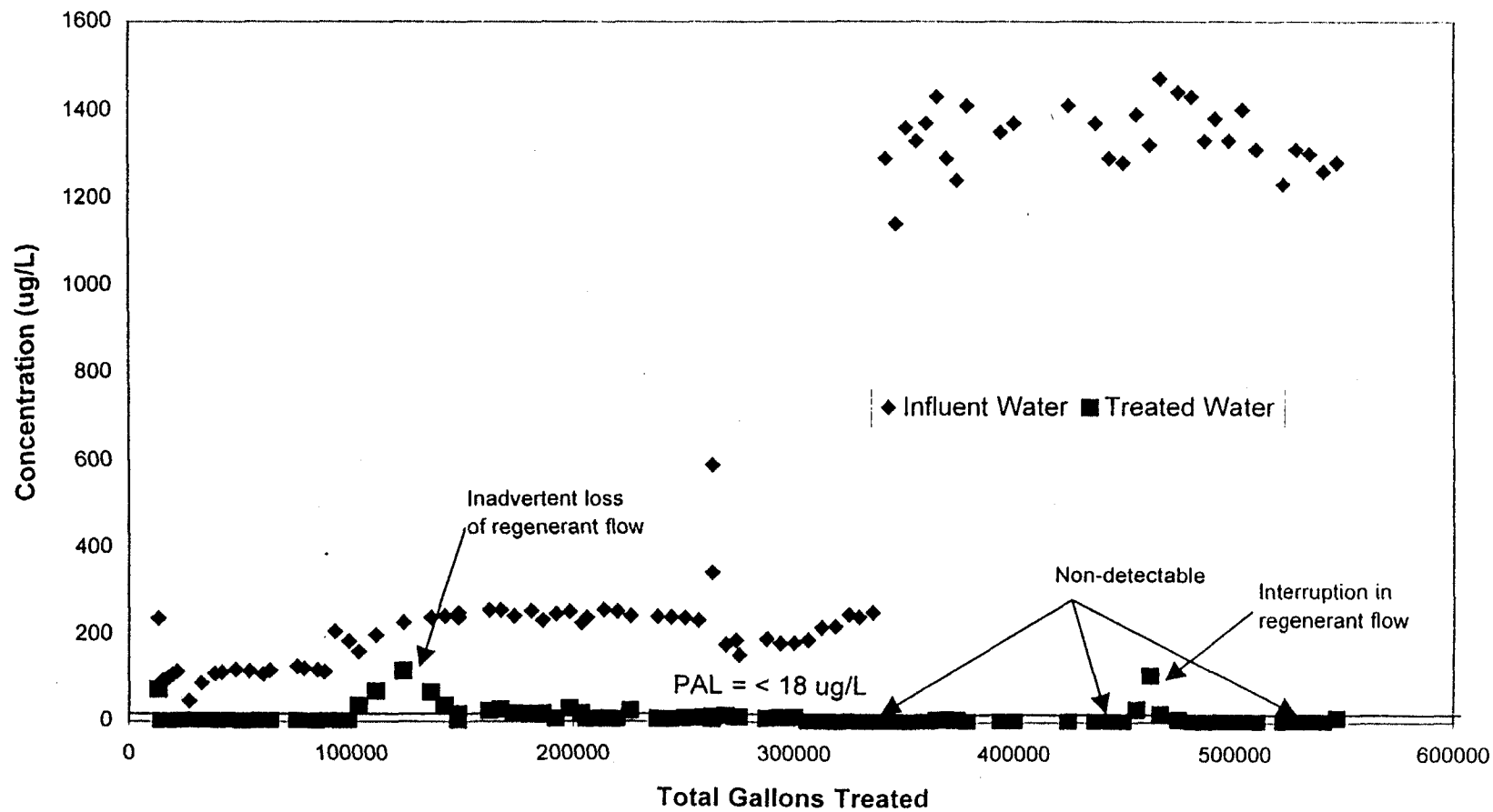


Figure 7. Nitrate removal performance of the ISEP® system during JPL pilot trial

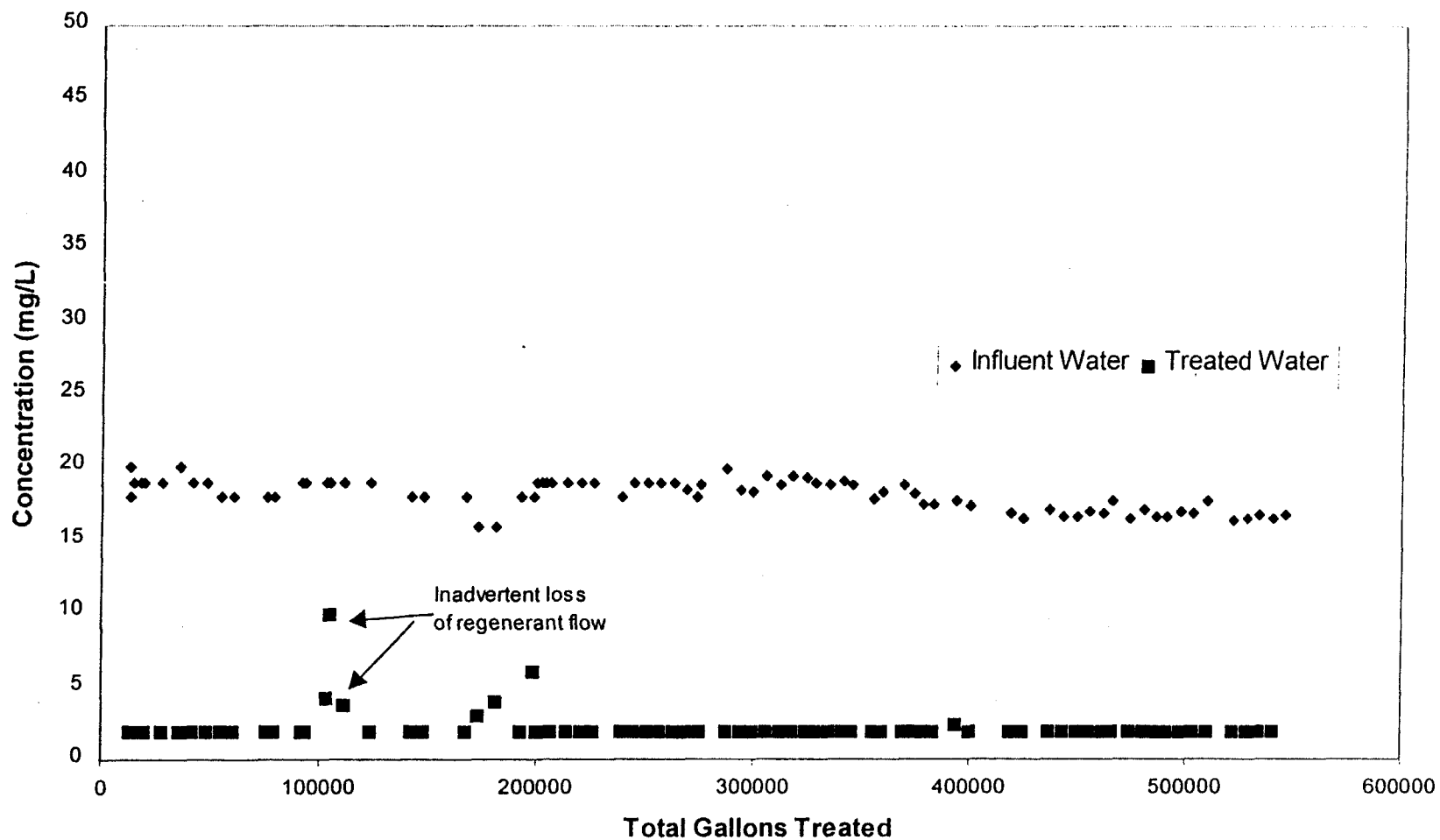


Figure 8. Sulfate removal performance of the ISEP® system during JPL pilot trial.

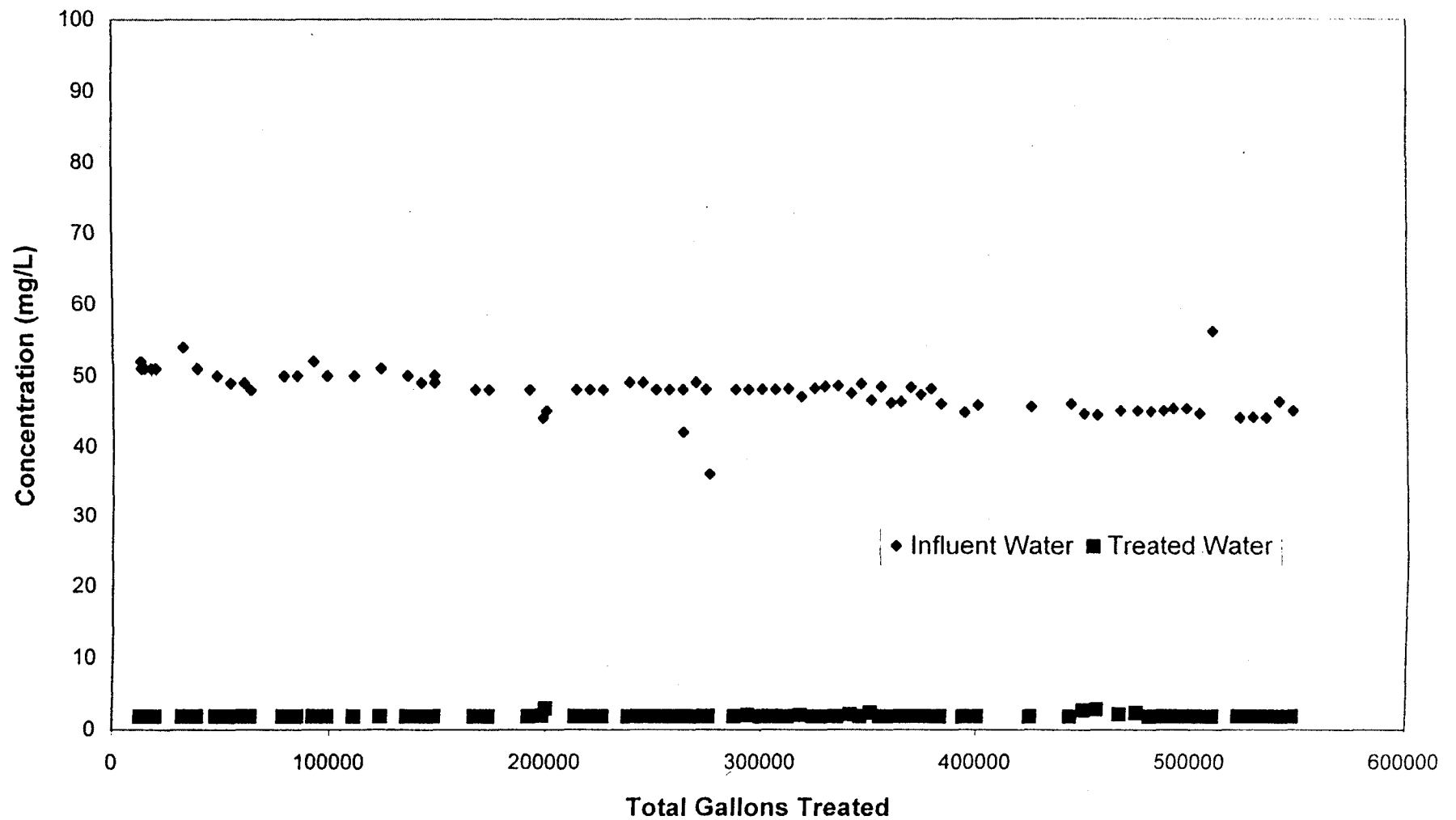


Figure 9. Steady state destruction of Perchlorate in PNDM during JPL pilot trial.

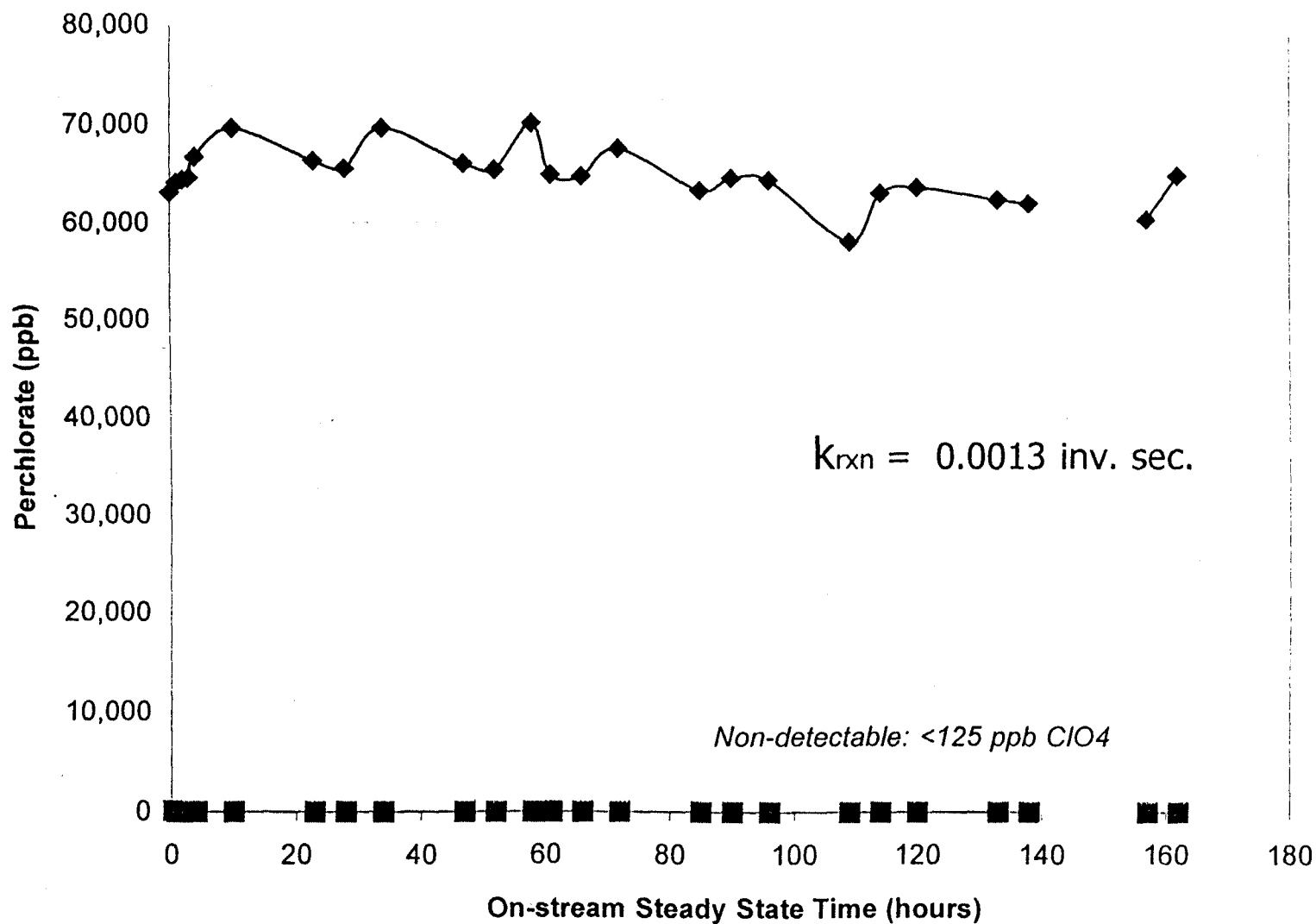


Figure 10. Steady state destruction of Nitrate in PNDM during JPL pilot trial.

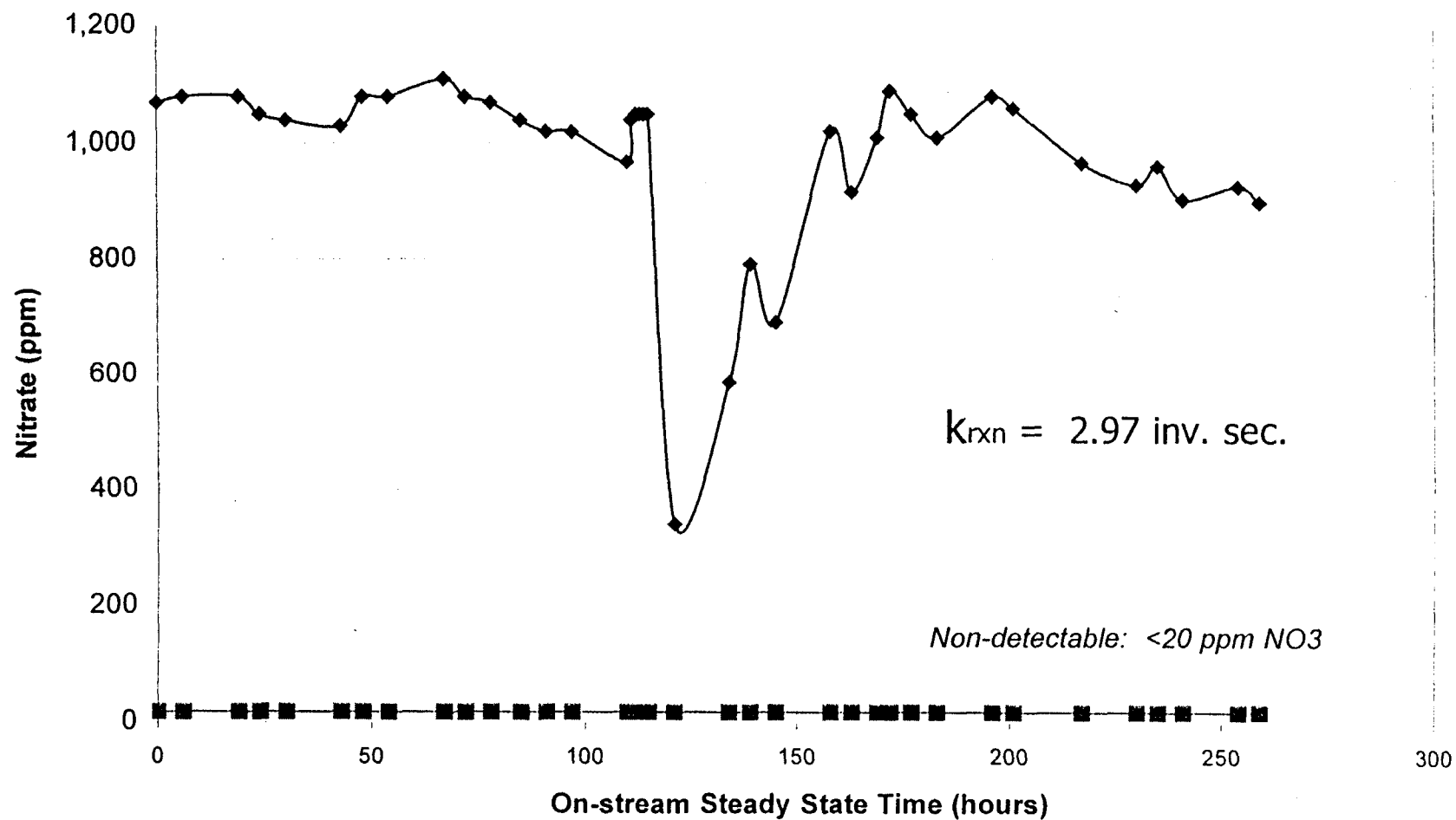


Figure 11. Impact of nanofiltration operating pressure on permeate sulfate concentration.

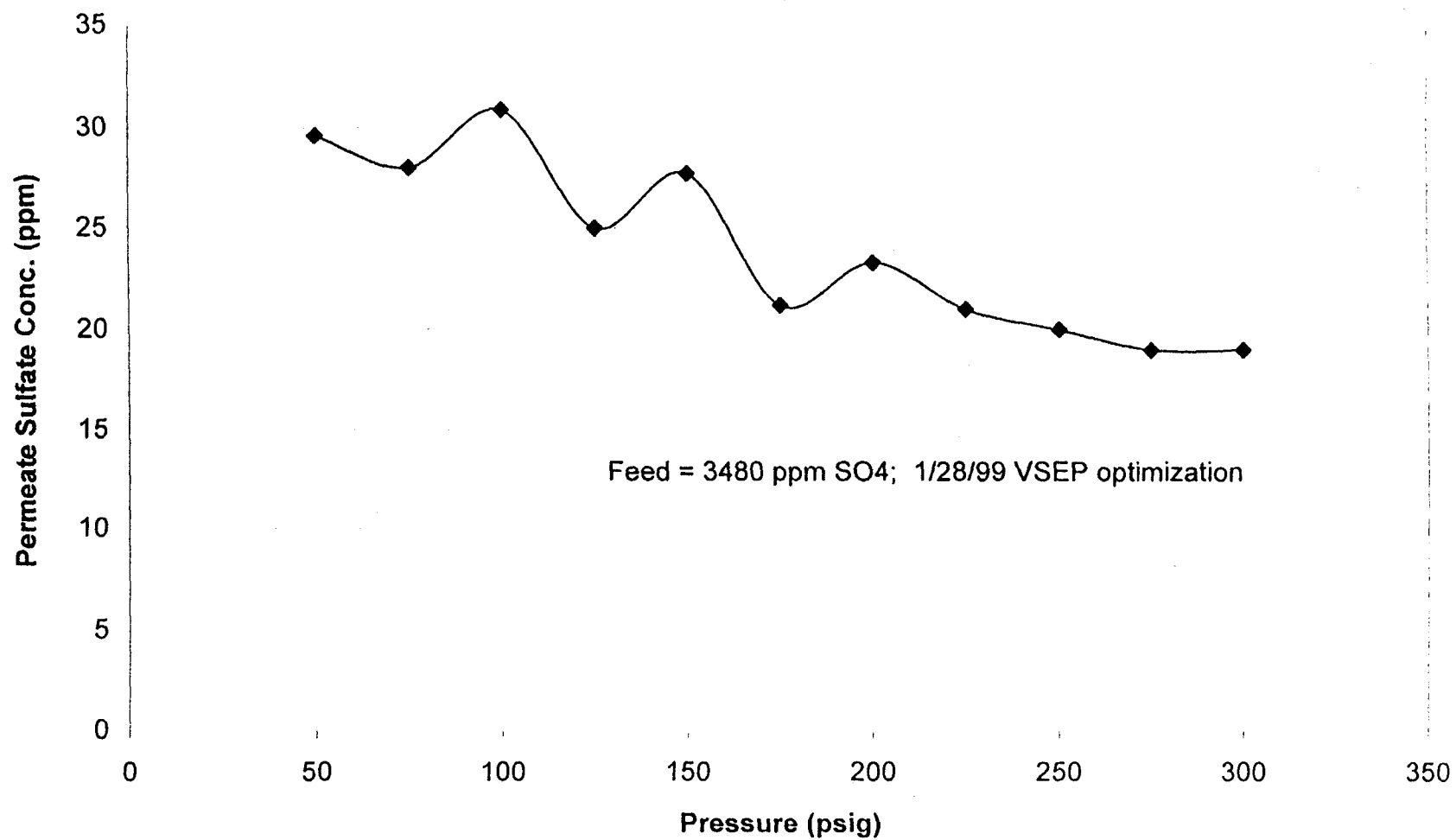
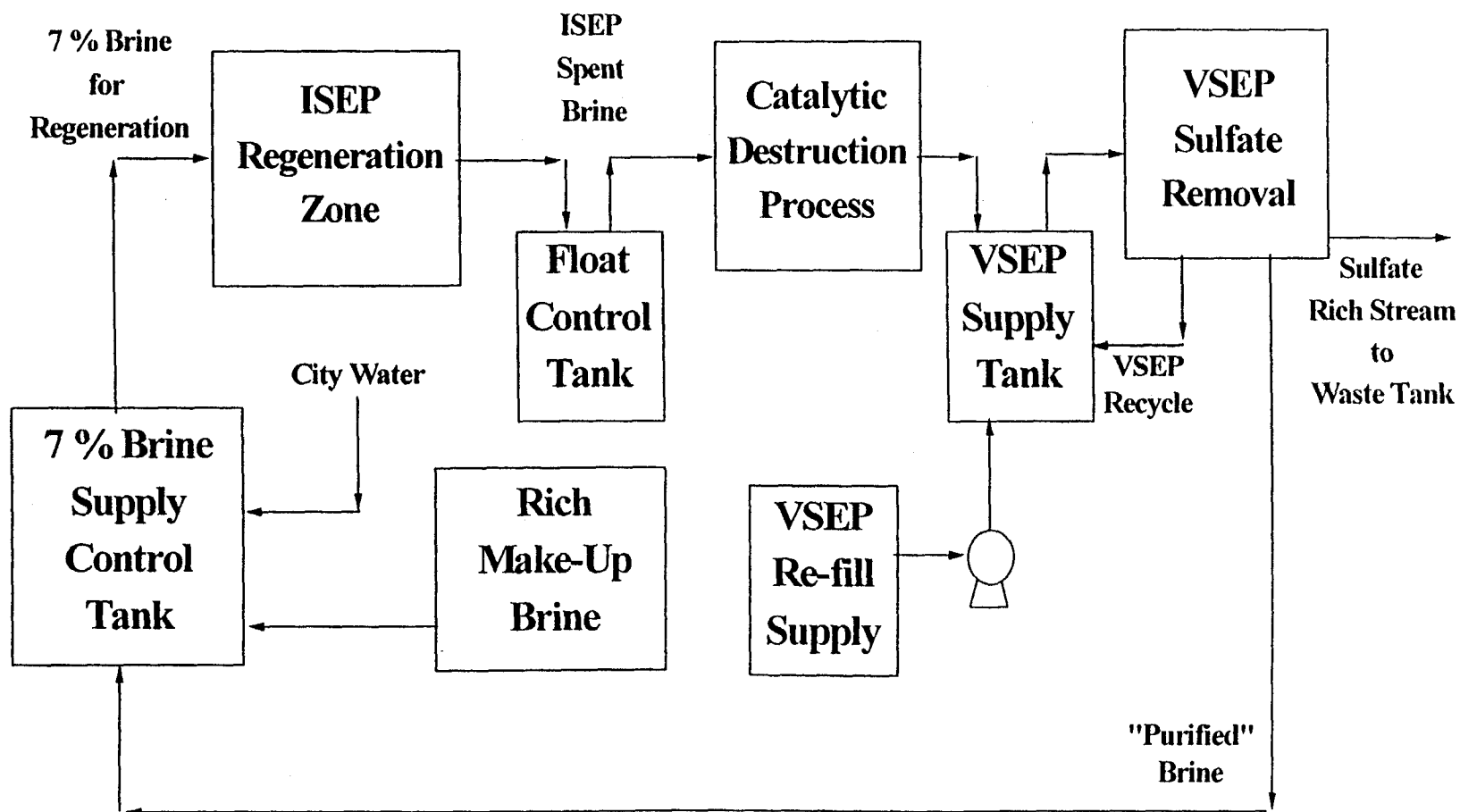
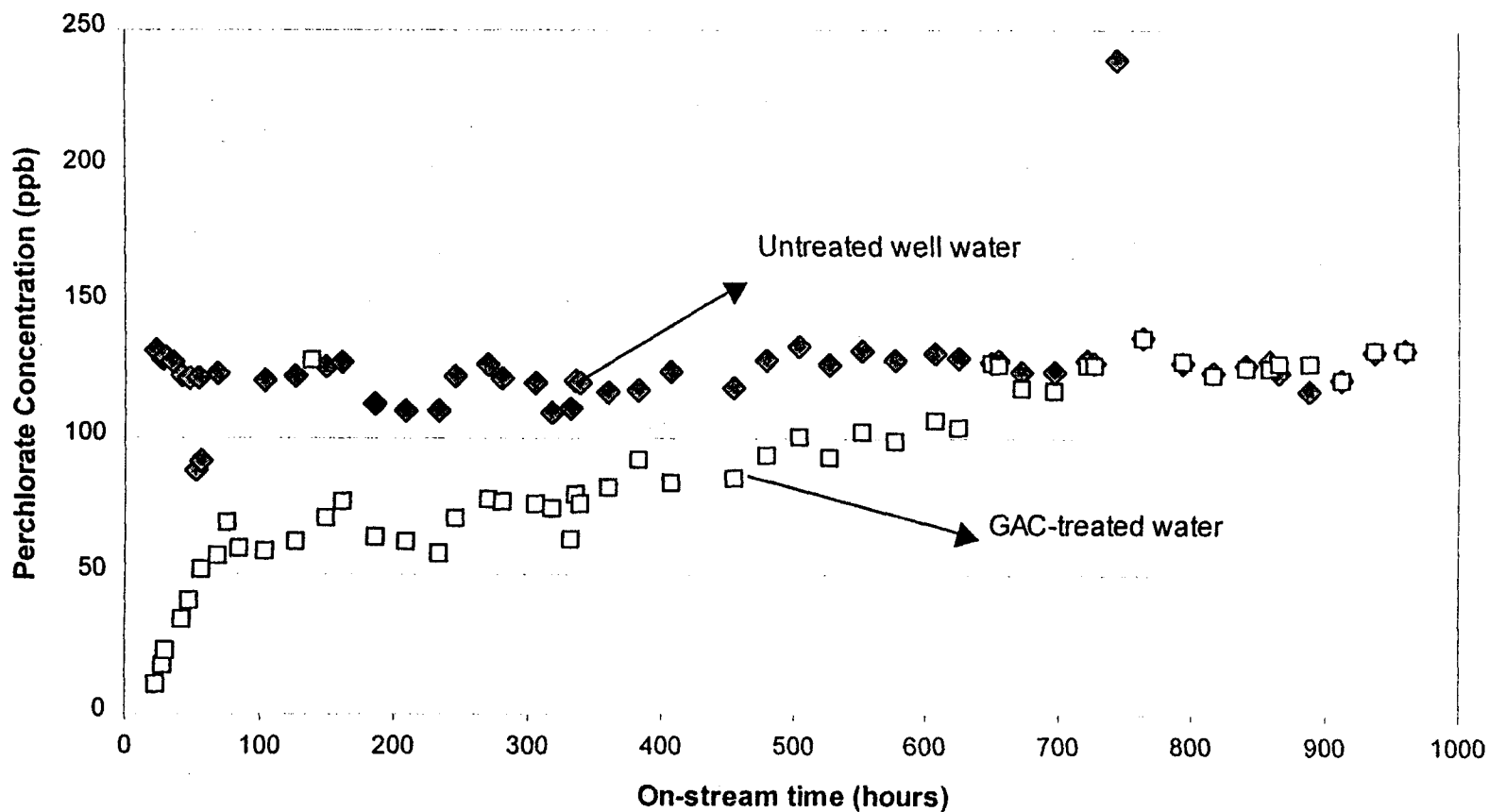


Figure 12. ISEP+ Integration Strategy at JPL



Appendix: Perchlorate breakthrough profile over granular activated carbon (GAC) observed during JPL Pilot Study.

Profile from GAC Bed 1 in ISEPTM system.



APPENDIX D

**REMOVAL OF PERCHLORATE FROM
GROUNDWATER USING REVERSE
OSMOSIS AND BIOLOGICAL TREATMENT**

U.S. FILTER WASTEWATER GROUP

**Treatability Study
Conducted For**

**Foster Wheeler Environmental Corporation
611 Anton Boulevard, Suite 800
Costa Mesa, CA 92626**

**(Removal of Perchlorate from Groundwater using
Reverse Osmosis and Biological Treatment)**

August 11, 1999
Revised October 29, 1999
Report No. 53016

Submitted by:

U.S. Filter
1100 East Willow Street
Signal Hill, CA 90806

1.0 Introduction

USFilter Corporation (USFilter) was contracted by Foster Wheeler Environmental Corporation (Foster Wheeler) to conduct a laboratory treatability study on a representative groundwater sample from the Jet Propulsion Laboratory (JPL) site located in Pasadena, CA. The purpose of the study was to evaluate the feasibility of reverse osmosis (RO) and fluidized bed reactor (FBR) technologies in reducing the perchlorate (ClO_4^-) concentration in the groundwater to less than 4 micrograms per liter (ug/l). Perchlorate contamination is generally the result of the dissociation of ammonium perchlorate (in water), which is an oxidizer used in rocket fuels. The scope of evaluation included treatment of the groundwater with RO alone, with FBR alone and a scenario whereby the RO reject was treated by the FBR. The treatment approach involved using an RO at 80% recovery and treating the reject with a seawater RO to achieve a total of 90% recovery. However, due to the silica concentration in the sample, the recovery was reduced to 75% in the design to avoid a softening pretreatment requirement. All tests were performed at USFilter's laboratory located in Warrendale, PA. In-house performance was tracked using an ion-specific probe. All reported analyses were performed by Del Mar Analytical of Irvine, CA using EPA method 300.

2.0 Technology Descriptions

This section provides descriptions of the technologies applied during the treatability study.

2.1 Reverse Osmosis

Reverse osmosis was selected for evaluation due to anticipated economic feasibility, simplicity of operation, modular design flexibility, and robustness in removing not just the perchlorate, but other potential contaminants. RO filtration typically removes constituents down to less than 0.0001 microns in size. This makes it highly applicable for the removal of perchlorate. The RO technology involves forcing water, under greater than osmotic pressure, through a semi-permeable membrane from a solution of greater concentration to a lower concentration solution. Both cellulose acetate (CA) and thin film composite (TFC) membranes were evaluated.

2.2 Fluidized Bed Reactor

USFilter's fluidized bed reactor technology is an anoxic biological treatment process, which consists of a columnar reactor that optimizes biological treatment by employment of a bed media such as sand or granular activated carbon (GAC). The bed media serves as support material for biological growth. Water flows upward through the reactor at a sufficient velocity to expand and fluidize the bed. The design allows a large inventory of biomass to be maintained within the reactor while maximizing the contact between the microorganisms and the target contaminants. For perchlorate treatment, a carbon substrate and nutrients are added to the influent of the reactor.

3.0 Sample Description

Four hundred (400) gallons of samples was received on March 10, 1999. The sample was clear, colorless, and contained a few suspended fines.

A complete analysis of the as received sample is presented in Table 1

Table 1- "As Received" Sample

<u>Parameter</u>	<u>Units</u>	<u>Results</u>
Aluminum	(mg/l)	<0.008
Barium	(mg/l)	0.071
Calcium	(mg/l)	57.1
Iron	(mg/l)	0.01
Magnesium	(mg/l)	21.4
Manganese	(mg/l)	0.002
Potassium	(mg/l)	1.61
Silica	(mg/l)	33.1
Sodium	(mg/l)	25.3
Strontium	(mg/l)	0.401
pH		6.97
Conductance	um/cm	567
Ammonia	(mg/l)	<0.08
COD	(mg/l)	<10
Solids - Dissolved	(mg/l)	375
TOC	(mg/l)	<1.3
Turbidity	NTU	1
Alkalinity	(mg/l)	149
Chloride	(mg/l)	25.6
Nitrogen - nitrate	(mg/l)	14.8
Phosphate -0	(mg/l)	0.052
Sulfate	(mg/l)	50.1

4.0 Test Procedures

4.1 Reverse Osmosis Testing

Two stages of RO testing were performed in the initial testing phase. The first stage RO received untreated sample as a feed source. The second stage RO treated the reject stream from the first stage RO. Two separate reverse osmosis membranes were evaluated. Cellulose acetate (CA) and thin film composite (TFC). The cellulose acetate membranes are generally more stable in oxidizing environments, while the thin film composite membranes generally allow for lower levels of contaminant leakage. However, consultation with membrane suppliers indicates that the oxidation reduction potential (ORP) of the JPL sample is not considered sufficient to create problems with the membranes.

4.1.1 First Stage RO Tests

A single element 2.5" spiral wound membrane was used for testing. The RO module was a 2.5" diameter x 40" long element, fed by a centrifugal pump. A schematic of the system used for testing is presented in Figure 1. The following conditions apply to both tests:

Permeate recovery.....	80%
Membrane flux.....	13 GFD (gallons/day/sq. ft.)
Pretreatment.....	none
Membrane surface area.....	23 ft ²

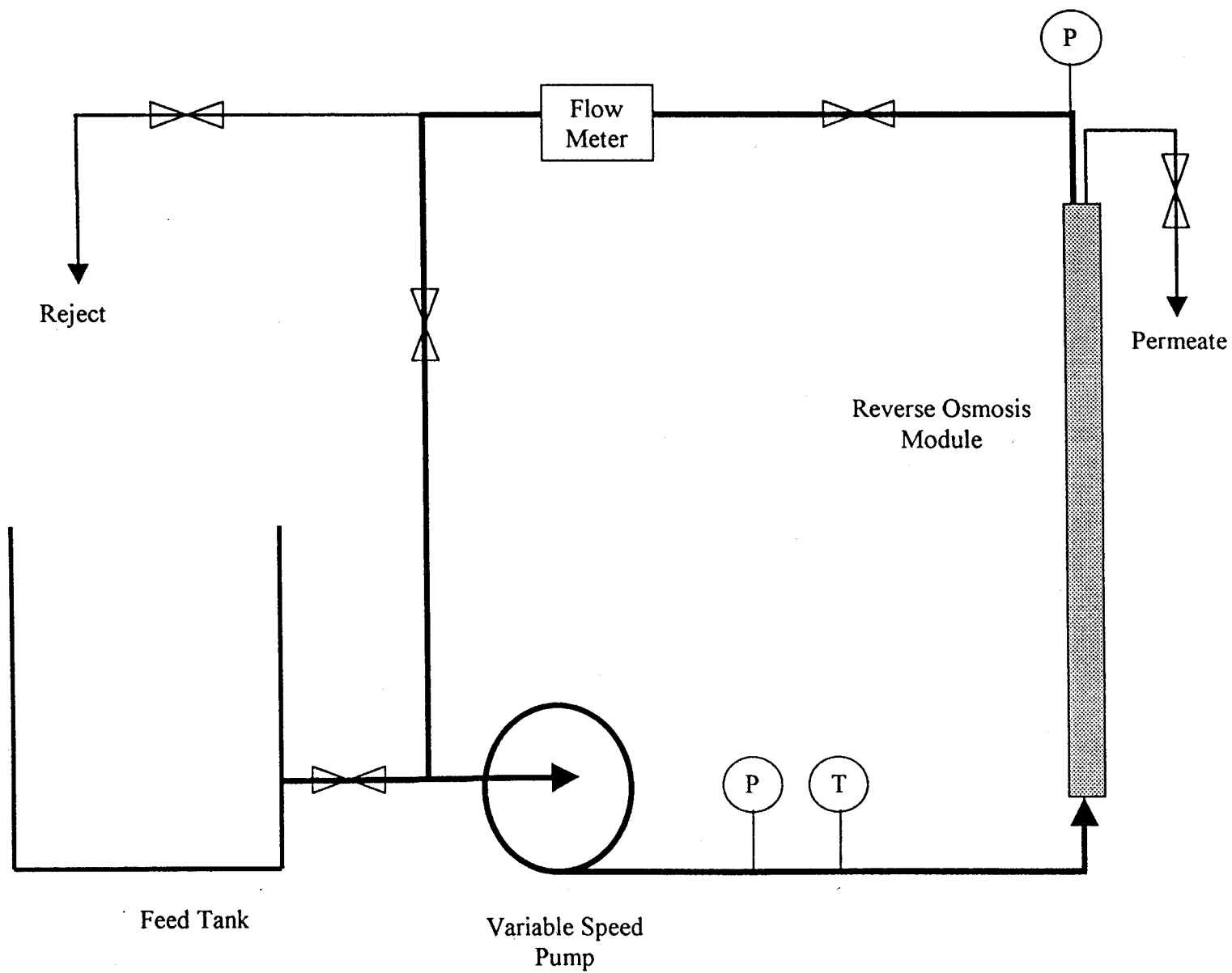
The permeate recovery and membrane flux were selected based upon historical experiences in treating similar wastewater samples. Both tests ran very well with respect to flux rates and pressure. Effluent quality from the TFC membrane was significantly superior to that obtained with the CA membrane. Data collected during these tests is presented in Table 2 (TFC) and Table 3 (CA).

4.1.2 Secondary Stage Tests (RO treatment of the First Stage Reject Stream)

The reject from each of the initial runs was further concentrated with a secondary stage RO. Because the samples were already concentrated once, a TFC seawater membrane was used for both tests. Both secondary concentration tests were conducted using the following conditions:

Membrane type	2.5 inch seawater
Permeate recovery.....	50%
Membrane flux.....	10 GFD (gallons/day/sq. ft.)
Pretreatment.....	none
Membrane surface area.....	23 ft ²

Figure 1
Reverse Osmosis Schematic



It should also be noted that the volume of sample available for this test was relatively small, therefore making for a short run time (20 minutes).

Once again, both tests ran very well with respect to flux rates and pressure. The effluent quality for both runs was good. Data collected during these tests is presented in Table 4 (TFC) and Table 5 (CA).

4.1.3 Permeate Polish Using 2nd Pass RO

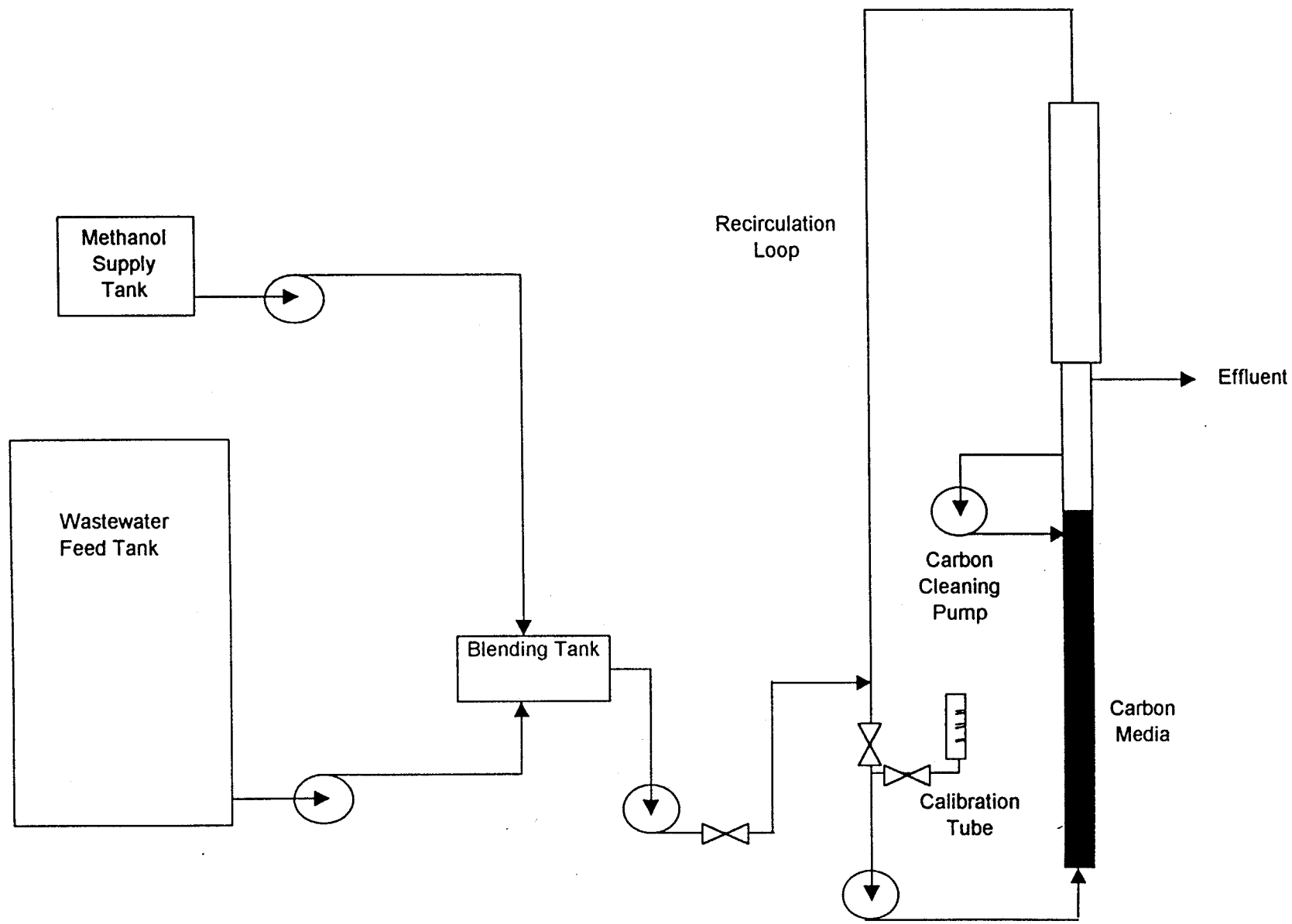
To assure that the perchlorate concentration could be reduced to below the detection limit of 4 ug/l, testing was performed using a second pass RO to treat the primary stage RO permeate. A RO permeate with perchlorate concentrations of 27 ug/l, 30 ug/l and 38 ug/l was fed to a TFC RO membrane in a 2.5" diameter x 40" long module. Three separate tests were performed with a 13 GFD flux rate and recovery rates of 80%, 85%, and 90% respectively.

4.2 Fluidized Bed Reactor Treatment

Biological studies require a relatively large volume of sample (20 gallons/day). To reduce shipping charges, the plan at the onset of the study was to prepare a synthetic waste stream having the same characteristics as the groundwater. This synthetic solution would be used to acclimate the fluidized bed reactor (FBR). Acclimation was expected to take several weeks. Once the system was fully acclimated and producing an acceptable quality effluent, actual feed would be used.

Unfortunately, due to test equipment malfunctions small-scale bench system, we were unable to produce the consistent high quality effluent (<4 ppb perchlorate) as has been demonstrated in other projects. These malfunctions are more an issue with small-bench scale biological systems than pilot plant or full-scale systems. However, it is important to note that treatment of perchlorate to the required levels using the FBR is easily achievable and well documented. This can easily be verified in a pilot test. Data is readily available that supports the applicability of the FBR system in reducing perchlorate in the groundwater sample.

Figure 2
Fluidized Bed Reactor Schematic



4.3 Ion Exchange Polish of RO Permeate

As part of the assurance that the perchlorate concentration could be consistently reduced to below detection, ion exchange was used to polish the RO permeate. Two separate tests were performed. The first test was performed by running 180 bed volumes (BV) through a weak base anion resin. The second test was performed by running 180 BV through a strong base anion resin. The permeate for these tests contained 30 ug/l of perchlorate.

5.0 Results

5.1 Reverse Osmosis Results

Results of both the primary RO system and secondary RO membrane tests indicate that the TFC membrane is highly effective in removing perchlorate from the JPL sample. At the high recovery rate of 80%, the perchlorate was reduced to 12-16 ug/l in the first stage RO. In the second stage RO, the recovery rate was 50% and the perchlorate leakage was only 17 – 18 ug/l. This was especially encouraging since the RO testing approach US Filter takes on this type of bench scale work is to focus on the last element in the last stage of the RO train. This gives the worst case conditions for scaling and rejection, since the feed leaving the last element will be the most concentrated. In full-scale design, the product results will almost always be better than our test results because the permeate from the last element will be diluted by the permeate from the preceding elements. For example, typically a single stage RO with 6 elements in series would concentrate a feed by 50 %. Therefore, the permeate from the first element is seeing a feed 1/2 the strength of the permeate from the 6th element. The actual combined permeate quality is sum of the 6 elements. This becomes clear with the RO projection. The TDS out of the 6th element in the first stage of one our projections for this project was projected at 11 ppm TDS. The TDS out of the first element was projected at 5ppm TDS. The composite for all 6 elements was 8 ppm TDS. The perchlorate projections for a full scale unit would be directly analogous to this. This of course is impacted by the RO configuration.

Leakage was unacceptably high in the test using cellulose acetate (CA) membranes (~600 ppb). While analytical results of the second RO permeate indicate that the perchlorate concentration was reduced to below the detection limit of 4 ppb, this result does not correlate with the reject and feed results. Therefore, it is likely that these results are analytical anomalies.

To assure that the objective 4 ug/l concentration could be consistently be achieved, analyses were performed using a second pass RO membrane and ion exchange (anion) resin system to polish the RO permeate. For this test, a higher concentration permeate was used (30 ug/l of perchlorate) than was detected in our RO testing. Analytical results indicate that at 80% recovery, the perchlorate concentration was reduced to

below the detection limit of 4 ug/l. At 85% recovery, 4.2 ug/l of perchlorate was detected. At 90% recovery, only 4.3 ug/l was detected. While this indicates that perchlorate can easily be reduced to below detection with RO membranes, polishing the permeate with ion exchange was also evaluated and results are provided in Section 5.3 of this report.

Table 2
Primary RO Test - Thin Film Composite Membrane

Time (min)	Influent Pressure (psi)	Effluent Pressure (psi)	Reject Flow (ml/min)	Permeate Flow (ml/min)	Temp (F)	Permeate pH	Reject pH	Permeate Conductivity (uS)	Reject Conductivity (uS)	Permeate TDS (mg/l)	Reject TDS (mg/l)	Permeate Perchlorate (ug/l)	Reject Perchlorate (ug/l)
0	190	170	197	786	82	---	---	0	---	---	---	---	---
30	190	170	204	782	82	6.59	---	18.44	---	13	---	12	---
60	190	170	238	790	82	6.41	7.78	19.51	2123	41	1574	12	3400
90	190	170	200	780	82	6.21	---	22.17	---	32	---	15	---
120	190	170	186	780	82	6.13	7.88	20.52	2231	22	1618	14	3200
150	190	170	188	780	82	6.13	---	21.45	---	7	---	15	---
180	190	170	195	780	82	6.2	7.85	21.67	2242	34	1668	14	3700
210	190	170	200	780	82	5.79	---	22	---	6	---	15	---
240	190	170	200	780	82	5.86	7.71	22.79	2304	16	1719	16	4000
270	190	170	194	780	82	5.73	---	23.35	---	---	---	16	---
280	190	170	192	780	82	---	---	---	---	---	---	---	---

Thin film composite membrane
Membrane surface area = 23 ft²
80% recovery
13 GFD (gallons / day / ft²)

Table 3
Primary RO Test - Cellulose Acetate Membrane

Time (min.)	Infuent Pressure (psi)	Effluent Pressure (psi)	Reject Flow (ml/min)	Permeate Flow (ml/min)	Temp (F)	Permeate pH	Reject pH	Permeate Conductivity (uS)	Reject Conductivity (uS)	Permeate TDS (mg/l)	Reject TDS (mg/l)	Permeate Perchlorate (ug/l)	Reject Perchlorate (ug/l)
0	210	180	198	790	80	---	---	---	---	---	---	---	---
30	200	175	250	800	82	5.64	---	104.3	---	92	---	650	---
60	200	175	197	790	82	5.73	7.29	114.4	1926	118	1424	670	1600
90	200	175	186	786	84	5.78	---	134	---	123	---	680	---
120	200	175	210	780	84	5.86	7.59	129	1990	109	1347	660	---
150	205	180	186	775	84	5.86	---	137	---	120	---	650	---
180	205	180	188	790	84	5.74	7.45	137.4	2084	109	1518	640	1600
210	205	180	188	790	84	5.7	---	137.5	---	117	---	650	---
240	205	180	190	788	84	5.91	7.41	137.2	2093	125	1526	650	1600
270	205	180	188	785	84	5.87	---	135.2	---	127	---	650	---

Cellulose acetate membrane
Membrane surface area = 23 ft²
80% recovery
13 GFD (gallons/day/ft²)

Table 4
Secondary RO Test - TFC Reject

Time (min)	Influent Pressure (psi)	Effluent Pressure (psi)	Reject Flow (ml/min)	Permeate Flow (ml/min)	Temp (F)	Permeate pH	Reject pH	Permeate Conductivity (uS)	Reject Conductivity (uS)	Permeate TDS (mg/l)	Reject TDS (mg/l)	Permeate Perchlorate (ug/l)	Reject Perchlorate (ug/l)
0	230	200	600	620	85	--	--	--	--	--	--	--	--
5	230	200	630	630	84	--	--	--	--	--	--	--	--
10	230	200	610	610	85	6.29	7.67	17.58	3,072	5	2,795	17	7,900
15	230	200	620	610	85	--	--	--	--	--	--	--	--
20	230	200	610	610	85	6.2	7.74	16.84	3,110	<5	2,901	18	7,800
25	230	200	610	620	85	6.14	6.14	18.08	--	37	--	17	--

Thin film composite membrane (seawater)

Membrane surface area = 23 ft²

50% recovery

10 GFD (gallons / day / ft²)

Table 5
Secondary RO Test - CA Reject

Time (min.)	Influent Pressure (psi)	Effluent Pressure (psi)	Reject Flow (ml/min)	Permeate Flow (ml/min)	Temp (F)	Permeate pH	Reject pH	Permeate Conductivity (uS)	Reject Conductivity (uS)	Permeate TDS (mg/l)	Reject TDS (mg/l)	Permeate Perchlorate (ug/l)	Reject Perchlorate (ug/l)
0	230	200	605	605	80	--	--	--	--	--	--	--	--
5	230	200	630	620	83	--	--	--	--	--	--	--	--
10	220	195	620	630	83	5.95	7.91	12.1	2303	29	1,897	<4	390
15	220	195	630	610	83	--	--	--	--	--	--	--	--
20	220	195	620	610	83	5.91	7.87	12.3	2345	21	1,885	<4	380
25	220	195	620	610	83	6.12	--	13.3	--	--	--	<4	--

Thin film composite membrane (seawater)
 Membrane surface area = 23 ft²
 50% recovery
 10 GFD (gallons / day / ft²)

5.2 Fluidized Bed Reactor Results

The FBR was able to produce an effluent containing less than 100 ppb of perchlorate for several days at a time. Unfortunately this high quality effluent was not sustainable for longer periods of time. This was due to mechanical and operational problems related to the scale of the laboratory study (pump failures, plumbing leaks, and accidental chemical overdose). This is not due to the applicability of the technology.

Documented historical data indicates that consistent effluent would be achieved using larger scale equipment and more continuous monitoring (the lab system was monitored only during the day shift).

A bench study currently underway is running on actual site water. The raw feed has between 300 and 400 mg/l of perchlorate, 25 mg/l of nitrate nitrogen, and a TDS of 11,000 mg/l. Two reactors are operating, FBR #1 is at a loading of 600 lbs COD/D/1000cu.ft. This is equivalent to 130 lbs NO₃-N/D/1000 cu.ft. FBR #2 is at a loading of 440 lbs COD/D/1000 cu. ft. COD and NO₃-N loading rates are on the design summaries. We operate denitrification systems at two to three times these loading rates. Additional IC data is pending, however, using a specific ion electrode, we are maintaining very low perchlorate levels out of the stage 1 reactor.

5.3 Permeate Polish

After initial testing, RO permeate samples containing perchlorate concentrations of 27 ug/l, 30 ug/l and 38 ug/l were treated with ion exchange. Each of these three samples were split and half was treated with a weak base resin and the other half with a strong base resin. Results indicate that for each sample, the perchlorate was reduced to below the detection limit of 4 ug/l for both the weak base and for the strong base resins.

Table 6
FBR - Influent and Effluent Analysis

Date	Influent Nitrate (mg/l)	Effluent Nitrate (mg/l)	Influent Nitrite (mg/l)	Effluent Nitrite (mg/l)	Influent P (mg/l)	Effluent P (mg/l)	Influent COD (mg/l)	Effluent COD (mg/l)	Influent ClO4 (mg/l)	Effluent ClO4 (mg/l)	Influent Sulfate (mg/l)	Effluent Sulfate (mg/l)	Comments (see last pg)
03/03/99	---	---	---	---	---	---	---	---	1.2	0.5	---	---	
03/05/99	---	---	---	---	---	---	62	26	1	0.4	---	---	
03/06/99	---	---	---	---	---	---	52	19	0.8	0.5	---	---	
03/07/99	---	---	---	---	---	---	47	15	0.9	0.35	---	---	
03/08/99	---	---	---	---	---	---	67	13	0.8	0.4	---	---	
03/09/99	---	---	---	---	---	---	44	14	---	---	---	---	
03/10/99	---	---	---	---	---	---	60	13	0.7	0.4	---	---	
03/11/99	---	---	---	---	---	---	49	12	0.6	0.3	---	---	
03/12/99	---	---	---	---	---	---	47	14	0.9	0.5	---	---	
03/13/99	---	---	---	---	---	---	52	8	1	0.5	---	---	
03/14/99	---	---	---	---	---	---	48	11	1.1	0.4	---	---	
03/15/99	22	0.22	0.9	0.3	0.62	0.48	---	---	1.1	0.45	---	---	
03/16/99	24	0.2	---	---	---	---	40	11	1	0.3	---	---	
03/17/99	27	0.2	0.9	0.2	0.7	0.4	37	8	1	0.3	---	---	
03/18/99	---	---	---	---	---	---	---	---	---	---	---	---	
03/19/99	25.0	0.2	0.3	0.1	0.5	0.3	42	9	1.1	0.25	---	---	
03/24/99	37.4	5.6	11	4	0.92	0.70	37	7	1.2	1.0	85	78	(1)
03/25/99	---	---	---	---	---	---	47	8	---	---	---	---	
03/26/99	26.5	0.4	6	< 1	0.75	0.35	42	6	1	0.4	80	68	
03/29/99	---	19.8	---	18	---	1.83	24	< 1	2.4	0.5	---	100	
03/30/99	---	---	---	---	---	---	---	< 1	---	---	---	---	
03/31/99	---	15.8	---	35	---	2.22	---	< 1	---	0.4	---	116	
04/01/99	---	---	---	---	---	---	---	< 1	---	---	---	---	
04/02/99	35.6	2.9	22	13	---	1.00	---	< 1	1.1	0.20	---	92	
04/03/99	---	---	---	---	---	---	---	< 1	1.1	0.19	---	---	
04/05/99	25.5	0.4	15	8	1.40	1.20	---	< 1	1.3	0.14	---	98	
04/06/99	---	---	---	---	---	---	---	---	---	---	---	---	
04/07/99	---	0.4	12	5	---	0.9	29	< 1	1.2	0.18	---	105	
04/09/99	22.0	< 0.2	12	10	1.2	0.4	39	< 1	1.2	0.1	118	96	
Del Mar Labs (4-9-99):										0.023			
04/10/99	---	---	---	---	---	---	---	---	---	---	---	---	
04/12/99	30.8	0.9	---	---	1	0.6	37	< 1	1.4	0.1	140	110	(2)
04/13/99	---	---	---	---	---	---	---	---	1.6	0.09	---	---	(3)

Table 6
FBR - Influent and Effluent Analysis

Date	Influent Nitrate (mg/l)	Effluent Nitrate (mg/l)	Influent Nitrite (mg/l)	Effluent Nitrite (mg/l)	Influent P (mg/l)	Effluent P (mg/l)	Influent COD (mg/l)	Effluent COD (mg/l)	Influent ClO4 (mg/l)	Effluent ClO4 (mg/l)	Influent Sulfate (mg/l)	Effluent Sulfate (mg/l)	Comments (see last pg)
04/14/99	18.5	0.9	---	---	0.8	0.55	52	12	1.2	0.1	122	108	
04/15/99	---	---	---	---	---	---	---	---	0.9	0.1	---	---	
04/16/99	21.1	1.3	---	---	0.87	0.55	58	10	1.1	0.11	140	128	
							Del Mar Labs (4-16-99):		1.8	0.17			
04/18/99	18.5	< 1	---	---	0.80	0.6	---	---	1.2	< 0.10	140	128	
04/19/99	19.3	< 1	---	---	0.87	0.55	59	12	1.2	< 0.10	140	136	
04/21/99	27.3	0.9	---	---	0.87	0.55	62	8	1.35	0.1	160	140	
04/22/99	---	---	---	---	---	---	---	---	1.3	0.2	---	---	
04/23/99	19.3	< 1	---	---	0.90	0.6	55	13	1	< 0.1	155	135	
							Del Mar Labs (4-23-99):			0.19			
04/24/99	---	---	---	---	---	---	---	---	0.9	< 0.1	---	---	
04/25/99	---	---	---	---	---	---	---	---	1.4	0.13	---	---	
04/26/99	18.9	1.2	---	---	0.75	0.5	60	18	0.9	< 0.1	130	120	
04/27/99	---	---	---	---	---	---	---	---	0.8	< 0.1	---	---	
04/28/99	18.9	0.2	---	---	0.80	0.65	62	12	0.9	< 0.1	130	120	
04/29/99	---	---	---	---	---	---	---	---	0.9	< 0.1	---	---	
							Del Mar Labs (4-29-99):			0.23			
04/30/99	18.5	0.9	---	---	0.80	0.6	63	14	1.1	0.1	130	110	
05/01/99	---	---	---	---	---	---	56	13	1.1	< 0.1	---	---	
05/02/99	---	---	---	---	---	---	58	12	1	< 0.1	---	---	
05/03/99	17.6	1.0	---	---	0.80	0.6	60	18	1.3	0.16	130	120	
05/04/99	---	---	---	---	---	---	65	14	1	< 0.1	---	---	
							Del Mar Labs 5-4-99):			<0.004			
05/05/99	--	0.9	--	13.0	--	1.1	62	9	1	0.5	--	< 0.1	
05/06/99	--	--	--	--	--	--	60	15	1.2	< 0.1	--	--	
05/07/99	--	0.6	--	14.0	--	0.96	60	6	--	< 0.1	--	< 0.1	
05/10/99	--	< 0.10	--	17.0	--	2.56	--	--	1.1	<0.1	--	70	
05/11/99	---	---	---	---	---	---	269	230	1.3	1.2	--	--	(4)
05/12/99	---	---	---	---	---	---	---	---	1.2	1.2	---	---	
05/13/99	---	---	---	---	---	---	---	---	1.2	1.2	---	---	
05/14/99	---	---	---	---	---	---	---	---	1.2	1.2	---	---	
05/15/99	---	---	---	---	---	---	---	---	1.2	1.2	---	---	
05/16/99	---	---	---	---	---	---	---	---	1.2	1.2	---	---	

Table 6
FBR - Influent and Effluent Analysis

Date	Influent Nitrate (mg/l)	Effluent Nitrate (mg/l)	Influent Nitrite (mg/l)	Effluent Nitrite (mg/l)	Influent P (mg/l)	Effluent P (mg/l)	Influent COD (mg/l)	Effluent COD (mg/l)	Influent ClO4 (mg/l)	Effluent ClO4 (mg/l)	Influent Sulfate (mg/l)	Effluent Sulfate (mg/l)	Comments (see last pg)
05/17/99	18.5	19.8	15	15	2.3	1.6	18	6	1.1	1.1	75	70	
05/18/99	18.5	2.6	15	14	1.7	1	24	6	1.1	0.9	---	---	
05/19/99	18.5	1.1	15	11	1.7	0.9	55	6	1.1	0.7	75	68	
05/20/99	---	---	---	---	---	---	---	---	---	---	---	---	
05/21/99	18.0	0.9	15	<1	1.7	0.8	63	9	1.2	0.2	70	70	
05/22/99	---	0.9	---	---	---	0.8	---	12	---	0.25	---	---	
05/23/99	---	0.9	---	---	---	0.7	180	24	---	0.3	---	---	
05/24/99	17.6	1.3	---	<1	---	0.8	40	10	1.1	0.2	---	42	
05/25/99	---	1.3	---	---	---	---	58	21	1.1	0.2	---	---	
05/26/99	18.9	0.9	---	<1	2.3	1.8	48	13	1.1	0.15	34	26	
05/27/99	---	---	---	---	---	---	40	10	1.1	0.1	---	---	
05/28/99	20.2	0.4	---	<1	1.6	1.2	42	10	1	0.1	62	60	
06/02/99	---	6.6	---	11	---	2.02	116	< 1.0	1.2	0.5	---	1	(5)
06/03/99	---	4.8	---	17	0.3	1	110	< 1	1.2	1.1	---	2	
06/04/99	17.6	12.8	18	14	---	---	110	< 1	1.2	1.1	36	3	
06/06/99	17.6	17.2	---	---	---	---	80	35	1.2	0.95	36	3	
06/07/99	18.2	13.2	3	6	1.6	1.58	90	44	1.2	0.88	44	40	
06/09/99	18.2	3.1	---	---	1.6	1.4	95	22	1.2	0.25	44	42	
06/10/99	18.2	1.32	---	---	1.6	1.2	80	18	1.2	< 0.1	44	25	
06/14/99	19.2	0.88	---	---	1.9	1.25	65	10	1	0.09	71	36	
06/15/99	---	0.88	---	---	---	---	60	10	1	< 0.1	---	---	
06/16/99	---	0.88	---	---	---	---	65	14	1	< 0.1	---	---	
06/17/99	---	0.66	---	---	---	---	60	18	1	< 0.1	---	---	
06/21/99	---	0.44	---	---	1.1	0.9	---	---	1.1	< 0.1	---	---	
06/22/99	---	0.44	---	---	1.1	1	---	---	1.1	< 0.1	---	---	
06/23/99	---	5.72	---	<1	---	0.22	---	---	---	0.15	---	1	(6)
06/24/99	---	---	---	---	---	---	---	---	---	0.24	---	---	
06/25/99	---	3.96	---	1	---	1.18	---	<1	---	0.38	---	<1	
06/28/99	---	9.24	---	---	---	---	---	<1	---	1	---	---	
06/29/99	---	13.2	---	---	---	---	---	8	---	1.2	---	---	
06/30/99	---	12	---	1	---	1.89	---	7	---	1.4	---	53	
07/06/99	0.1	4.1	1	0.1	0.1	2.2	111	<1	1.5	0.6	46	20	

Del Mar Labs 6-14-99:

0.69 0.033

Table 6
FBR - Influent and Effluent Analysis

Date	Influent Nitrate (mg/l)	Effluent Nitrate (mg/l)	Influent Nitrite (mg/l)	Effluent Nitrite (mg/l)	Influent P (mg/l)	Effluent P (mg/l)	Influent COD (mg/l)	Effluent COD (mg/l)	Influent ClO4 (mg/l)	Effluent ClO4 (mg/l)	Influent Sulfate (mg/l)	Effluent Sulfate (mg/l)	Comments (see last pg)
07/07/99	---	0.6	---	0.3	---	4.1	22	<1	1.5	1.1	---	---	
07/08/99	---	0.3	---	---	---	---	--	--	1.5	0.7	---	---	
07/09/99	6.1	0.2	---	0.2	---	2.9	--	--	1.3	0.5	---	10	
07/10/99	--	--	--	--	--	--	---	---	---	0.4	---	---	
07/11/99	--	--	---	---	---	3	---	---	---	0.4	---	---	
07/12/99	--	--	---	---	---	--	--	--	1.8	0.25	---	---	
07/13/99	---	---	---	---	---	---	69	<1	---	---	---	---	
07/15/99	4.9	1.8	---	---	---	2.8	94	<1	1.2	0.4	--	--	
07/16/99	4.8	1	---	---	---	2.8	56	<1	1.2	0.3	--	--	
07/18/99	--	--	---	---	---	---	55	4	1.4	0.2	--	--	
07/19/99	4.6	0.7	---	---	0.09	0.35	--	--	1.4	0.2	---	---	
07/20/99	--	1.8	--	--	--	--	--	--	--	1	--	--	
07/21/99	--	0.5	--	--	--	--	--	--	--	---	--	---	
07/23/99	--	1.3	--	--	--	0.53	--	<1	--	0.8	--	4	
07/26/99	--	4.2	--	--	--	0.4	--	<1	--	0.6	--	3.5	
07/28/99	--	2.9	--	--	--	0.45	--	<1	--	0.3	--	2.9	
07/29/99	--	3.3	--	--	--	---	--	---	--	0.2	--	---	
07/30/99	--	2.5	--	--	--	---	8	9	--	0.8	---	--	
08/02/99	2.6	2	--	--	0.45	0.41	8	2	1.05	1	<0.1	<0.1	

Notes

- (1) Overnight leak in tubing
- (2) Increase methanol dosage to increase COD by 5 mg/l
- (3) Begin nitrogen purge of feed tank to insure low DO in system
- (4) Feed was prepared using acidic water (anionic portion of mixed bed resin used to prepare feed was spent)
The cannister was changed and the reactor re-seeded.
- (5) Problems with MeOH feed pump. Redesigned system to ensure better blending and more consistent feed.
- (6) Accidentally added sodium carbonate instead of sodium bicarbonate for pH adjust

6.0 Conclusions and Recommendations

It is well known in the industry that biological treatment of perchlorates is the most economical approach. However, when the treated water is intended for drinking water supply, acceptance of biologically treated water is currently not approved by the regulatory agencies. Therefore, US Filter has devised with Foster Wheeler the conceptual design that utilizes RO to reduce the perchlorate and act as additional barrier to other unidentified species. The approach of the testing was to be aggressive as far as achieving a high rate of recovery. It is important to note that in a full-scale system design, lower recovery rates would be recommended to assure minimal maintenance. This is especially true should the silica concentrations in the groundwater be as high as detected in the sample. In any event, the results of the testing indicate that this approach provides treated water of such high quality that numerous options for reuse are possible. These options include cooling tower makeup, boiler feed water, and drinking water.

The test results indicate that 800 ug/l of perchlorate detected in the JPL groundwater can be reduced to below the detection limit of 4 ug/l using either a two-pass RO or a RO with an anion resin ion exchange polish. Further, the TFC membrane will produce quite low perchlorate leakage as a primary RO with a recovery rate of 80% and a flux rate of .13 GFD. When the reject from the first stage RO is treated by a second stage seawater TFC RO, 50% of the first stage reject can be recovered with negligible increase in permeate perchlorate concentration. This results in approximately 90% recovery of the total groundwater flow. However, the limiting factor in RO recovery is the influent silicon concentration. Typically elevated silicon concentrations can create scaling problems unless calcium and magnesium are essentially completely removed by ion exchange or dispersants (anion-scalants) are added. Based upon our influent silica concentration of 33.1 mg/l, the silica in the reject of the primary RO at 80% recovery is approximately 165 mg/l. This concentration is greater than the solubility and would result in scaling. While dispersant manufacturers such as Argo have developed anti-scalant chemicals that can prevent scaling with silica concentrations in excess of 300 mg/l, the reject from the secondary RO system would be 330 mg/l (based upon a 50% recovery). Certainly the desired recovery should be taken into consideration vs. pretreatment and maintenance requirements in the full-scale system design.

The final RO reject would then be treated by the FBR, which would reduce the perchlorate to below the sewer discharge limit. It is important to note that our approach to the overall treatment of the RO reject is anoxic and denitrification is required because of the 260 ppm of nitrate nitrogen detected and only 8 mg/l of perchlorate detected in the RO reject. This level of nitrate will create a significant design challenge should an anaerobic reactor be applied. The organic carbon addition required for treating 8 mg/l of perchlorate is highly insufficient to sustain the required anaerobic reaction, meaning that significant excesses will need to be wasted and later treated in order to sustain the reaction. The large levels of nitrate nitrogen actually drive the reactor ORP or reductive environment the wrong direction for true anaerobes.

USFilter has over 70,000,000 gallons of water being denitrified every day with FBR technology and our experience and reliability is unsurpassed on large scale. The two largest plants include Reno/Sparks NV (over ten years of continuous operation), and Stockholm Sweden. Both of these are good references and welcome visitors. There is also a very large system in a Dupont facility in Singapore.

USFilter's FBR system offers many significant advantages over alternative biological systems. These advantages are provided below:

- First, we have years of experience providing large-scale reliable systems. There is nothing in our conceptual design that does not exist on the denitrification process, thus the system we are offering has a proven track record of years of field operation with proven robustness.
- The biology is a consortium of microorganisms that want to grow in this type of environment. This is not a special seed or single organism that has to be pampered to perform.
- The FBR system operates at ambient temperatures, unlike alternative anaerobic systems that must heat reactors to 25° - 35°C.
- The excess organic feed necessary to drive the perchlorate to below detection with the FBR is not as excess as is typical of an anaerobic process. BOD exiting the FBR reactors can be reduced in a simple post aeration tank. Other systems can require complete activated sludge plants to eliminate excess BOD and results in large sludge disposal costs.

The FBR systems are high rate systems and result in the smallest footprint possible.

To assure consistent supply of treated water with a concentration less than 4 ug/l, an anion ion exchange system is recommended. This is an effective resin that has been proven in these tests to reduce concentrations (greater than those detected in the test RO permeate) to less than 4 ug/l. The resin can either be regenerated on-site or collected and regenerated off-site by US Filter. If treated on-site, the regenerant would be pumped to the FBR for perchlorate destruction.

Assuming 90% recovery (80% by the first stage and 50% by the second stage) and a permeate concentration of 17 ug/l, the ion exchange resin would only have to remove less than 0.13 lbs of perchlorate per day. If the design involves a single RO stage and a 75% recovery, the ion exchange resin would treat 0.107 lbs of perchlorate per day. With the high purity of the RO permeate, very little competing ions will contribute to the IX loading. This results in significantly high efficiency. A further benefit is the variety of uses the high purity water affords. For drinking water application, the water would flow to a calcite filter to add necessary minerals.

It is important to note that these are conceptual designs. While the results of the laboratory testing and historical data indicate both performance and economic feasibility of the RO system and Ion Exchange systems, it is recommended that a pilot study be performed to confirm the design of the FBR system. US Filter can provide the equipment and personnel to perform such a verification pilot testing and provide a full-scale system economical and performance guarantee.

7.0 Conceptual Full-Scale System Design Based Upon 700 GPM

Based upon the analytical results of the groundwater sample from JPL and the results of the treatability study, a 75% recovery system is recommended to easily control scaling and reduce cleaning and maintenance. This is not to say that a higher recovery can not be achieved. However, dispersant usage, cleaning frequency and membrane life should all be factored when considering higher recovery rates. The recovery of the permeate is highly dependent upon the effectiveness of the dispersants applied and the adjustment of the pH prior to treatment.

7.1 System Description

The 75% recovery system provides a more conservative maintenance, chemical and pretreatment regimen than the 90% recovery approach that was proven achievable in the laboratory. The groundwater would be pretreated with a multimedia filter. This consists of three vessels with a capacity of 150 cubic feet each. These vessels are arranged in parallel. A chemical anti-scalant system shall be provided which includes two 100% chemical metering pumps with appropriate piping and fittings. The metering pumps are controlled by a 4-20 mA signal from a digital flow meter to pace the injection rate with the groundwater flow.

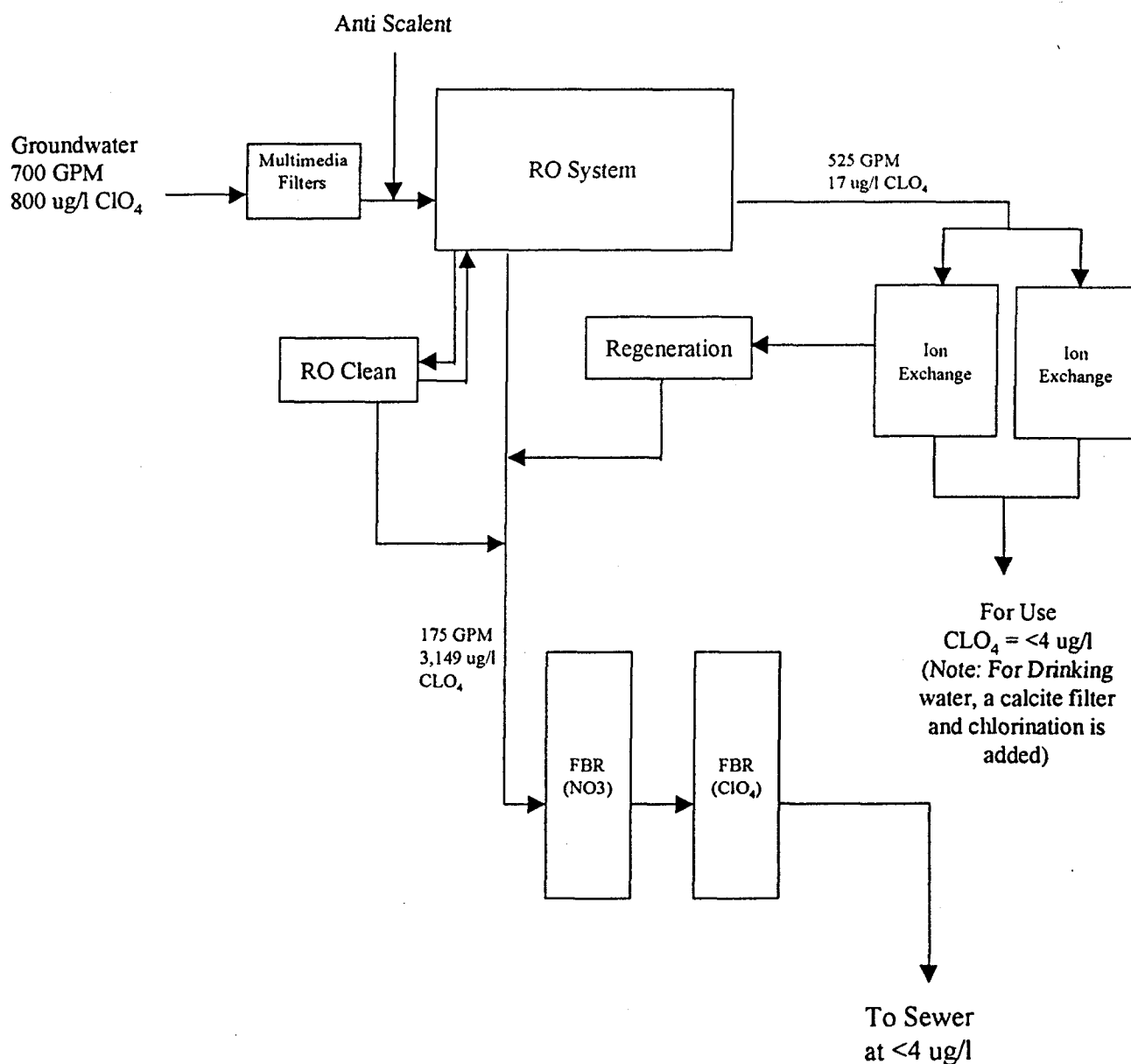
The RO system would be a single stage system consisting of two arrays. Each array shall consist of 14 pressure vessels, containing 6 membranes each for a total of 168 membranes. The permeate shall be pumped from the RO at a flow rate of 525 GPM and shall contain less than 20 ug/l of perchlorate. The permeate would then be pumped through a weak base anion resin to reduce any residual perchlorate to below the detection limit of 4 ug/l.

An RO membrane cleaning system is also included. This system includes a cleaning solution tank, pump, heater, and associated piping, valves and controls.

The ion exchange system would consist of 2 vessels (100%) with a capacity of 250 cubic feet each. The vessels would be arranged in a parallel configuration to allow for added assurance of perchlorate removal and to allow regeneration without cessation of operations. The system shall include a chemical regeneration system, pH neutralization system, and a pump skid to slowly bleed the regenerant to the reactor. Regeneration is expected to be required every 3-4 months based upon 24 hr/day operation.

The reject from the RO system shall flow at the rate of 175 gpm to the two-stage fluidized bed reactor system. As in the 90% recovery system, the FBR shall consist of a primary reactor designed to reduce the nitrates and a secondary reactor to reduce the perchlorates. It should be noted that the FBR design is based upon a Nitrate concentration of 26.7 mg/l as opposed to the concentration of 14.8 mg/l detected in the sample. The higher concentration was detected in earlier analyses by Foster Wheeler and is applied to make the design more conservative. The treated water shall contain less than 4 ug/l and flow to the sewer.

Figure 3
Jet Propulsion Laboratory
Conceptual Process Flow Diagram



8.0 Economics

This section provides a budgetary estimate of the costs of perchlorate treatment systems as described in Section 7.0 of this report. The costs are based upon a Build Own Operate Maintain (BOOM) contract whereby USFilter would install the treatment system, own the system and operate the system using USFilter employees. These cost estimates are based upon a 10 contract and assume that utilities, adequate space, any required shelter and civil engineering are provided by the client. Permits and sewer surcharges are not included.

The estimated contract price is \$83,800 per month plus the variable charge of \$0.24 per 1000 gallons treated.

APPENDIX E

PERCHLORATE BIOTREATABILITY STUDIES: USE OF THE BACTERIAL ISOLATE "*PERCIACE*" IN A PACKED BED BIOREACTOR TO TREAT JPL GROUNDWATER AND RO REJECTATES

TABLE OF CONTENTS

	PAGE
LIST OF TABLES	E-ii
LIST OF FIGURES	E-ii
1.0 INTRODUCTION	E-1
2.0 METHODOLOGY	E-3
2.1 Packed Bed Reactor Study-Treatment of Groundwater.....	E-3
2.2 Biotreatment Laboratory Screening Study-Treatment of RO Rejectates.....	E-4
2.3 Packed Bed Reactor Study-Treatment of RO Rejectates.....	E-5
2.4 Flask Study: Reduction of Cr(VI) by <i>Perclace</i>	E-6
3.0 Results and Discussion	E-6
3.1 Packed Bed Reactor Study-Treatment of Groundwater.....	E-6
3.2 Biotreatment Laboratory Screening Study-Treatment of RO Rejectates.....	E-8
3.3 Packed Bed Reactor Study-Treatment of RO Rejectates.....	E-8
3.4 Flask Study: Reduction of Cr(VI) by <i>Perclace</i>	E-11
4.0 CONCLUSIONS.....	E-11
5.0 REFERENCES	E-12

APPENDICES

Appendix E-1	Summary of All Data Collected in PBR Groundwater Treatment Study.
Appendix E-2	Formulation of RO Rejectates for PBR Experiments.
Appendix E-3	Summary of All Data Collected in PBR RO Rejectate Studies.
Appendix E-4	Experimental Design for Flask Study to Assess the Ability of <i>Perclace</i> to Reduce Cr(VI)

LIST OF TABLES

<u>TABLE NUMBER</u>	<u>FOLLOWING SECTION</u>
1	Removal of ClO_4^- by Various Inocula in Flask Study to Preliminarily E Assess Biological Reduction of ClO_4^- in Aqueous Saline Environments

LIST OF FIGURES

<u>FIGURE NUMBER</u>	<u>FOLLOWING SECTION</u>
1	Influent and Effluent Perchlorate and Acetate Concentrations, E Groundwater PBR Study
2	Influent and Effluent Nitrate Concentration and pH, Groundwater PBR E Study
3	Influent and Effluent Concentrations of Ammonium Nitrogen and E Sulfate, Groundwater PBR Study
4	Influent and Effluent Perchlorate and Acetate Concentrations, RO E Rejectate PBR Study (Days 1-12 constituted the start-up period)
5	Influent and Effluent Nitrate Concentration and pH, RO Rejectate PBR E Study (Days 1-12 constituted the start-up period)
6	Influent and Effluent Perchlorate and Acetate Concentrations, RO2 E Rejectate PBR Study
7	Influent and Effluent Nitrate Concentration (A) and pH (B), RO2 E Rejectate PBR Study
8	Results of Flask Study Showing Chromate $[\text{Cr(VI)}]$ removal by E <i>Perclace</i> in the Presence and Absence of Perchlorate

APPENDIX E

PERCHLORATE BIOTREATABILITY STUDIES: USE OF THE BACTERIAL ISOLATE "*Perc1ace*" IN A PACKED BED BIOREACTOR TO TREAT JPL GROUNDWATER AND RO REJECTATES

1.0 INTRODUCTION

Perchlorate (ClO_4^-) was detected in groundwater at the Jet Propulsion Laboratory (JPL) and in down-gradient municipal production wells during the OU-1/OU-3 Remedial Investigation (RI), and is a major factor with regard to the OU-1/OU-3 Feasibility Study (FS). The identification of ClO_4^- as an environmental contaminant has occurred relatively recently (due to refinements in analytical methodology) and although much progress has been made, reliable technologies for treating ClO_4^- -impacted water are still under investigation.

Because of the depth and extensiveness of impacted groundwater at JPL, it appears at this time that pump-and-treat technology may offer the only workable option for remediation of ClO_4^- -impacted groundwater at JPL. Unlike the volatile organic compounds (VOCs) detected in JPL groundwater (carbon tetrachloride, trichloroethene, etc.) ClO_4^- is not volatile, and therefore can not be removed by VOC treatment processes. However, several processes that are amenable to pump-and-treat systems have been identified for removing ClO_4^- from water, and/or converting it to less toxic forms.

There are three basic removal technologies that are currently considered to be applicable: ion exchange (IE), reverse osmosis (RO), and biological treatment (via biological reduction). Of these, IE and RO are capable of producing water that can be used for domestic consumption, whereas the California Department of Health Services (CA DHS) has indicated that biotreated water may not be used in this regard. However, IE and RO both produce waste streams containing concentrated ClO_4^- , which must be addressed via secondary treatment, or disposed of appropriately. If the treated water is not intended for domestic consumption, biotreatment may be the preferred option because it destroys ClO_4^- (converting it to chloride, which is innocuous) and because it is much less expensive than IE and RO.

There is a general lack of verifiable information regarding technical and economic aspects of ClO_4^- treatment technologies, which have only recently been developed. In addition, uncertainties exist at JPL regarding disposal of treated water, which is crucial in selecting an appropriate treatment technology. For these reasons, each of the three removal technologies mentioned above were tested (to varying degrees) for the JPL FS. IE has been tested at the bench- and pilot-scales at JPL (see Appendices B-2; C), and RO was tested at the bench-scale (see Appendix D).

Biotreatment (via biological reduction) was also assessed for removal of ClO_4^- from JPL groundwater. Because the feasibility of RO rests largely on treatment of waste streams (rejectates), biological removal of ClO_4^- from primary and secondary rejectates generated from RO was also assessed (see Section 3.4 of the FS for explanation of waste generation from RO; and Appendix B-1 for details of the biological reduction process).

This report summarizes results of experiments conducted using a packed bed reactor (PBR) inoculated with a ClO_4^- -reducing organism (*perclace*) isolated by W. T. Frankenberger Jr. of the University of California, Riverside. Other inocula/reactor configurations were also tested (see Appendices D and F). This study was conducted largely because this organism had previously demonstrated the ability to destroy ClO_4^- in JPL groundwater (see Appendix B-2), and as very few treatment systems of this nature were known, it was deemed prudent to test this system.

Finally, hexavalent chromium [Cr(VI)] has been detected in a limited number of groundwater samples collected on-site at JPL (see Section 3.1.1.2). Hexavalent Cr is similar to ClO_4^- in several respects, one of which is that, like ClO_4^- , Cr(VI) is subject to biological reduction reactions that reduce its toxicity (as well as its mobility). Although this constituent is not expected to be of major importance with regard to remediation at JPL, information regarding its propensity for bioreduction by the various ClO_4^- -reducing inocula may prove useful. A flask experiment was therefore conducted to preliminarily assess the ability of *perclace* to reduce Cr(VI) in the simulated RO rejectates.

Objectives

Experiments were conducted to address the following overall objectives:

1. Demonstrate process feasibility of the packed bed reactor/*perclace* for treatment of JPL groundwater and estimate initial scale-up parameters.
2. Screen inocula with potential for reducing ClO_4^- in RO rejectates. If salt-tolerant (halotolerant) microorganisms capable of carrying out reduction of ClO_4^- in saline environments can be isolated, this will provide a good indication that the RO rejectate is biologically treatable (IE regenerant from ClO_4^- applications is currently not considered biologically treatable).
3. Assuming Objective 2 is achieved, demonstrate process feasibility of the packed bed reactor for treatment of simulated RO rejectates formulated based on previous results of RO tests carried out using JPL groundwater.
4. Determine whether the *perclace* organism is capable of reducing Cr(VI) in RO rejectates.

The objectives were addressed in four separate experiments, as described below. All experiments were conducted in Dr. Frankenberger's facility, The Center for Environmental Microbiology.

2.0 METHODOLOGY

2.1 Packed Bed Reactor Study-Treatment of Groundwater

A bench-scale PBR was set up, with 200-gallon influent and effluent tanks. The PBR consisted of a cylindrical plexiglass column operated in an up-ward flow mode. The column specifications were as follows: total height: 21.4 cm; inside diameter: 13.5 cm; bed height: 12.5 cm; total volume: 3062 mL; total bed volume: 1789 mL; pore volume: 1236 mL. The reactor was contained in a controlled environment in which a temperature of 28°C was maintained (determined to be optimal for ClO_4^- reduction by *perclace* in previous studies). A number of support media are available for PBRs, such as Celite, activated carbon, and sand. Celite (World Minerals Corporation, Lompoc, CA) was used for this study, based in part on the fact that Celite was used in Dr. Frankenberger's previous study, as well as in a similar PBR for treating ClO_4^- wastewater at Tyndall Air Force Base. A Master Flex 4S (Cole Parmer, Vernon Hills, IL) peristaltic pump was used to deliver the influent feed to the reactor. The column was colonized with a perchlorate/nutrient/inoculum rich stream for approximately 3 weeks. The bacterial isolate previously identified by Dr. Frankenberger, *perclace* (Herman and Frankenberger 1999), was used.

Once the column was effectively colonized (substantial reduction in ClO_4^- concentration demonstrated by ion-selective probe measurements of ClO_4^- in influent and effluent samples), actual JPL groundwater, collected from JPL monitoring well MW-16, was amended with nitrogen and phosphorous (as NH_4Cl and KH_2PO_4 , respectively). The water was supplemented with sodium acetate (energy source) via an in-line feed pump [as determined in previous work-Herman and Frankenberger 1999)], and fed into the reactor. We attempted to maintain the influent acetate concentration between 500 and 1,000 mg/L. Influent samples were collected daily, and effluent samples were collected at intervals of from 2-5 days. Samples were immediately frozen (to stop the reaction), and subsequently analyzed for ClO_4^- in-house, in accordance with (EPA Method 300.0, modified), by ion chromatography (IC) using a Dionex DX 500 instrument with an ASII column, with 100 mM NaOH eluent.

The general approach was to begin with a residence time that yielded non-detectable effluent ClO_4^- concentrations (based on prior experimentation), and incrementally increase the flow rate, thereby decreasing the residence time until breakthrough occurred. Flow rates and corresponding residence times that were ultimately evaluated are listed below:

Flow Rate, (mL/min)	Residence Time, (hr)
10	2.1
25	0.8
50	0.4
75	0.3
100	0.2

Influent and effluent samples were also periodically evaluated for other parameters, including pH (Accumet, Fisher Scientific); nitrate, sulfate, and acetate (Dionex ASII, 10 mM NaOH eluent); and ammonium-nitrogen (Technicon Auto Analyzer). A complete list of samples, analyses performed, and analytical detection limits is provided in Appendix E-1.

2.2 Biotreatment Laboratory Screening Study-Treatment of RO Rejectates

A screening level experiment was conducted to identify inocula capable of reducing ClO_4^- in liquid medium approximating the salt content of RO rejectates. This experiment was designed to provide an indication of the feasibility of biologically reducing ClO_4^- in primary and secondary RO rejectates. This included testing the bacterium previously isolated by Dr. Frankenberger (*perclace*), and several new sources of inoculum from saline environments. Flasks containing 100 ml of simulated RO rejectates were inoculated, provided with a carbon source, and tested for a decrease in ClO_4^- concentrations as described below.

A total of twenty 250-ml Erlenmeyer flasks were set up (four different inocula, two feed concentrations, two carbon sources, plus four uninoculated control flasks) at Dr. Frankenberger's facility. Inocula included *perclace*, and sediments collected from saline environments including the Arroyo Seco, the Bolsa Chica Wetlands, and a water sample collected from salt evaporation ponds in Niger, Africa. The carbon sources included acetate and ethanol (0.5 g/L), and the two feed concentrations were formulated to simulate the electrical conductivity of a rejectate from RO of JPL water, and a rejectate from RO of rejectate, as described below.

It was initially estimated that the RO rejectate would contain salts elevated over the influent stream by a factor of five (20% rejection rate). Groundwater sampling results from JPL monitoring well MW-16, which is located in the contaminant source area, have shown total dissolved solids (TDS) of approximately 300 mg/L. Concentration of this water by a factor of five, would yield a rejectate with a TDS level of approximately 1500 mg/L. It was further estimated that this rejectate could be treated with RO to reject 50% of the original rejectate, yielding a secondary rejectate with a TDS concentration on the order of 3000 mg/L.

The following empirical relationship can be used to estimate the electrical conductivity (EC) of a solution for which the TDS is known:

$$\text{TDS (mg/L)} \sim \text{EC (dS/m)} \times 640 \text{ (Bohn et al., 1985).}$$

Using this relationship, solutions with TDS levels of 1500 and 3000 mg/L would have EC values of approximately 2.3 and 4.6 dS/m, respectively. To be conservative, minimal salts medium, which contains all of the major ions present in JPL groundwater in relatively similar concentrations, was formulated to EC levels of 3.1 and 6.25 dS/m. Following sterilization of the medium, the carbon sources were added, and ClO_4^- (as NaClO_4) was added at a standardized concentration of 100 mg/L. The flasks were flushed with dry N_2 , capped, and incubated anaerobically for 2 weeks. ClO_4^- concentrations were measured at 1 and 2 weeks using a ClO_4^- -selective probe.

It is noted that, although VOCs are present in JPL groundwater, they were not considered in this experiment (or subsequent experiments) because it is assumed that they will be removed prior to RO treatment. In addition, osmotic stress is assumed to be the major factor limiting cellular metabolism, and hence, ClO_4^- -reduction. Because this was a screening level experiment to preliminarily assess ClO_4^- reduction with respect to general salt tolerance, it was not necessary to attempt to duplicate all ion concentrations in the simulated rejectates.

2.3 Packed Bed Reactor Study-Treatment of RO Rejectates

Based on the successes of the laboratory screening study (described below) and the RO tests (see Appendix D), a reactor study was conducted to assess biotreatment of primary and secondary RO rejectates using the PBR described above. In this study, residence times of 0.8, and 0.4 hours were assessed. The RO rejectates were formulated based on results from the US Filter study, which tested the use of RO to treat JPL groundwater and primary RO rejectate (see Appendix D). The US Filter study showed that the treatment of groundwater yielded a rejectate with ion concentrations 5x the original groundwater levels, and treatment of the rejectate yielded a secondary rejectate with ion concentrations 10x the original groundwater levels. These factors were used to formulate primary and secondary rejectates to closely match actual samples (actual rejectate samples could not be used because a prohibitive volume of water would have had to be processed through an RO system).

The chemical compositions of the rejectate feeds are shown in Appendix E-2. In preliminary attempts to formulate the secondary rejectate, potentially significant precipitation was observed. In order to prevent this precipitation, the amounts of calcium (Ca^{2+}) and sulfate (SO_4^{2-}), which commonly form precipitates, were reduced by a factor of ten, and excesses of sodium (Na^+) and chloride (Cl^-), which typically do not form precipitates, were added to make up for the lost TDS.

This effectively reduced precipitation, while insuring that the osmotic effects of the simulated rejectates matched the results of the RO studies as closely as possible (replacing Ca^{2+} and SO_4^{2-} with Na^+ and Cl^- is not expected to have a significant effect on cellular metabolism). The primary rejectate feed was formulated to the ion concentrations based on the RO test results, as precipitation was not observed.

For this study, influent and effluent samples were periodically analyzed for pH, EC, NO_3^- , acetate and ClO_4^- as described in Section 2.1. A complete list of samples, analyses and results for the RO rejectate treatment studies are provided in Appendix E-3.

2.4 Flask Study: Reduction of Cr(VI) by *Perclace*

The ability of *perclace* to reduce Cr(VI) in simulated RO rejectates, was assessed in a flask study. In this study, the simulated primary and secondary RO rejectates formulated for the previously described reactor experiment (Section 2.3, Appendix E-2) were amended with Cr(VI) in the form of chromate (CrO_4^{2-}), which is the dominant form of Cr(VI) in environmental systems (Losi et al., 1994). The highest Cr(VI) concentration detected in JPL groundwater in recent sampling events is slightly below 0.050 mg/L. Assuming that this would be the worst-case concentration, and applying the concentration factors determined in the RO study (5x and 10x for primary and secondary rejectates, respectively), Cr(VI) concentrations of 0.25 and 0.5 mg/L were used for the study.

The simulated rejectates were sterilized by filter sterilization, and 100-ml aliquots were dispensed into 250-ml Erlenmeyer flasks. The flasks were inoculated with the *perclace* organism, and amended with acetate (0.5 g/L), and CrO_4^{2-} (as Na_2CrO_4) at the above-specified concentrations. For each rejectate, flasks were set up with and without ClO_4^- , and un-inoculated controls were also set up. The headspace was flushed with dry N_2 , and the flasks were capped and incubated at 20°C for 1 week. Following the incubation period, samples were filtered and analyzed for Cr(VI) using EPA method 7196. In this method, the absorbance of samples at 540 nm (measured using a Milton Roy Spectronic 1001) is compared with that of standards following reaction with diphenylcarbazide. The experimental design for this study is summarized in Appendix E-4.

3.0 RESULTS AND DISCUSSION

3.1 Packed Bed Reactor Study-Treatment of Groundwater

Influent and effluent ClO_4^- and acetate concentrations for the various residence times over the duration of the groundwater experiment are shown in Figure.1. Influent ClO_4^- concentrations were generally measured between 700 and 800 $\mu\text{g/L}$, which is consistent with recent results of

ClO_4^- analysis of water from MW-16, from which this water was extracted (Figure 1A). The first 15 days of the experiment evaluated residence times of 2.1 and 0.8 hours. Effluent ClO_4^- concentrations were non-detect over this period with the exception of days 10 and 11, where the ClO_4^- levels were 13.6 and 4.25 $\mu\text{g/L}$, respectively.

Based on these results, the flow rate was increased incrementally, to evaluate residence times of 0.4 and 0.3 hours. For the remainder of the experiment, effluent ClO_4^- concentrations were below (or in a few cases, slightly above) the detection limit, with two exceptions (as noted in the following paragraphs), due to upset conditions involving dispensation of acetate.

On Day 15, the flow rate was increased such that the residence time was lowered to 0.4 hr. This necessitated changing out the acetate feed pump to accommodate the higher flow rate. Problems were initially encountered with the new pump, which interrupted the acetate flow to the column for several days. The problem was not detected until Day 19, at which time it was corrected. From Day 16 through Day 20, there was very little acetate in the system, (Figure 1B) and as a result, significant ClO_4^- breakthrough occurred over this period (Figure 1A). However, when acetate was re-supplied to the system, ClO_4^- concentrations dropped to below the detection limit for 5 of the next 6 days for which it was sampled. Although inadvertent, this upset condition verified that the observed ClO_4^- -removal was coupled with utilization of acetate.

On Day 27, the flow rate was again increased, which decreased the residence time to 0.3 hr. This flow rate was maintained for only 3 days, due to the fact that the influent supply tank was nearly depleted. Over this period, ClO_4^- concentrations remained very low (non-detect or slightly above). Based on this result, a final flow rate increase was carried out on Day 31, which decreased the residence time to 0.2 hr. The ClO_4^- concentration was 18.6 $\mu\text{g/L}$, following one day at this flow rate, however, an acetate pump failure occurred on Day 32, and acetate was again absent from the system. It is therefore not clear whether the ClO_4^- breakthrough observed on Days 32, 33, and 34 would have occurred if acetate had been present in the system. At this point, the experiment was terminated due to exhaustion of the influent water supply.

Figure 2 depicts influent and effluent NO_3^- concentrations and pH values measured over the course of the experiment. Data presented in Figure 2A show that, as with ClO_4^- , removal of NO_3^- was generally complete, with the exception of the periods where the acetate pump failed (refer to Figure 1). Influent pH values were between 7.0 and 7.6, which can generally be considered optimal for biological processes. Effluent pH values were generally between 7.0 and 8.0, indicating that the process did not appreciably influence pH.

Influent and effluent concentrations of NH_4^+ and SO_4^{2-} are presented in Figure 3. NH_4^+ , which was added to the feed at a level of 20 mg/L , was consistently present in the effluent, and was

therefore provided in excess (PO_4^{3-} was also added at a level of 6 mg/L, based on preliminary experiments, but was not tracked analytically in this study). This indicates that the amount of NH_4^+ can probably be reduced in future applications. Influent and effluent SO_4^{2-} concentrations were essentially the same, indicating that SO_4^{2-} -reduction did not occur in the reactor during this experiment.

3.2 Biotreatment Laboratory Screening Study-Treatment of RO Rejectates

Results of the screening study are presented in Table 1. This study was intended to provide an indication of whether ClO_4^- -reduction in saline environments (approximating RO rejectates) would be feasible, with the secondary goal of obtaining a halotolerant, ClO_4^- -reducing inoculum (or isolate) for potential future work in treating RO rejectates, were the need to arise. The data shown in Table 1 indicate that ClO_4^- removal occurred in the saline solutions, to varying degrees, for all inocula tested. ClO_4^- concentrations in the control flasks remained virtually unchanged, and therefore observed removal can be attributed to the respective inoculum.

The inoculum/carbon source combination showing the most effective ClO_4^- -removal in the solution where the EC was adjusted to 3.1 dS/m (simulated primary RO rejectate) were the Arroyo Seco Sediment/acetate, and *perclace*/acetate. In the solution where the EC was adjusted to 6.25 (simulated secondary RO rejectate), the Bolsa Chica Sediment/acetate, and *perclace*/acetate were the most efficient. These results indicate that ClO_4^- -reducing bacteria that tolerate salinity in the range expected in RO rejectates are present in various environments, and inoculum is therefore obtainable. Importantly, this information does not allow for any conclusions regarding ClO_4^- -reduction efficiency or rates in saline environments.

The *perclace* organism was retained for further experimentation for the following reasons: (1) in this experiment, ClO_4^- -removal by *perclace* (growing on acetate) was equally or more efficient than the other inoculum/carbon source combinations, and (2) initial characterization, including (most importantly) efficacy for use in the PBR system, has been carried out for this organism. It is noted, however, that the other inocula could contain organisms potentially more efficient in ClO_4^- -reduction in saline environments than *perclace*, which could be determined in additional, shorter-term batch experiments.

3.3 Packed Bed Reactor Study-Treatment of RO Rejectates

Primary RO rejectate

Because salinity affects various biological processes in a number of ways, it was anticipated that ClO_4^- reduction in the simulated RO rejectates would be less efficient than in the groundwater. Accordingly, residence times of 0.8 and 0.4 hours were tested in this experiment. Figure 4 shows

the influent and effluent ClO_4^- and acetate concentrations for these two residence times for the duration of the RO rejectate experiment.

As shown in Figure 4A, influent ClO_4^- concentrations were reasonably constant, and results were within 20% of the 5000 $\mu\text{g/L}$ spike value (results if the RO testing showed a ClO_4^- concentration of 4000 $\mu\text{g/L}$ in the rejectate, however to be conservative, the simulated rejectate was spiked to 5000 $\mu\text{g/L}$). Data presented in Figure 4A show that the effluent ClO_4^- concentrations were consistently non-detect through day 34 (residence time 0.8 hours), with the exception of Days 13 (25.2 $\mu\text{g/L}$) and 21 (14.7 $\mu\text{g/L}$).

Data presented in Figure 4A show that, upon decreasing the residence time to 0.4 hours, breakthrough occurred (Day 34). It is possible that acetate was limiting, as concentrations in the effluent were very low (between 5 and 12 mg/L), and influent concentrations were not measured over this period. It is, therefore, not clear whether breakthrough occurred due to the reduction in residence time, or to a lack of acetate in the system. Although this experiment was terminated on Day 42 due to time limitations, the decrease in effluent ClO_4^- concentration from Day 41 to Day 42 may indicate that the column was becoming acclimated to the new flow rate, and that non-detect could possibly have been achieved. Additional studies would be needed to confirm this. Overall, the results preliminarily indicate that RO rejectate can be treated to non-detectable ClO_4^- levels in this system, with a residence time of 0.8 hr, and possibly less.

Shown in Figure 5 are the influent and effluent NO_3^- concentrations and pH values measured over the course of the primary RO rejectate experiment. The data presented in Figure 5A show that removal of NO_3^- was significant with the PBR operating at a residence time of 0.8 hr, and as with ClO_4^- , breakthrough was observed concurrent with residence time decrease. As mentioned above, effluent acetate levels were very low following the decrease in residence time and the duration of this experiment may not have allowed for sufficient acclimation to the more rapid flow rate. It therefore can not be determined whether breakthrough occurred due to the reduction in residence time, to a lack of acetate in the system or to insufficient acclimation period. As shown in Figure 5B, the majority of influent pH values were between 7.0 and 8.0, which is generally considered acceptable for biological processes. Effluent pH values were also generally between 7.0 and 8.0, indicating that the process did not appreciably influence pH.

Secondary RO rejectate

Figure 6 shows the influent and effluent ClO_4^- and acetate concentrations for the secondary RO rejectate experiment. As shown in Figure 6A, influent ClO_4^- concentrations were relatively constant, and although approximately 20% below the spiked value of 10,000 $\mu\text{g/L}$, they were

representative of measured concentrations in the secondary RO rejectate of approximately 8,000 $\mu\text{g/L}$ throughout the experiment (refer to Appendix D).

As with the previous experiment (primary RO rejectate), we initially planned to evaluate the residence times of 0.8 and 0.4 hours. As shown in Figure 6A, breakthrough was evident at the initial residence time of 0.8 hours, with effluent ClO_4^- levels ranging from 189 to 4814 $\mu\text{g/L}$. Low effluent acetate concentrations measured on Days 0, 1 and 2 (Figure 6B) suggest that acetate was limiting initially, and is reflected by the relatively high effluent ClO_4^- levels detected over this period (Figure 6A). During the following 13 days, however, acetate was detected in the effluent (and was therefore present throughout the reactor), and removal of up to 90% of the influent ClO_4^- was observed, although non-detect levels were not achieved.

When it appeared that non-detectable ClO_4^- levels were not attainable, the residence time was increased to 2.1 hr by lowering the flow rate to 10 mL/min thus increasing the contact time of the water with the biomass. A small corresponding decrease in effluent ClO_4^- concentrations was observed, however, concentrations remained in the 100-300 $\mu\text{g/L}$ range. The residence time was again increased to 4.2 hours by lowering the flow rate to 5 mL/min. Effluent ClO_4^- concentrations again reflected approximately 90% removal, and non-detect levels were not achieved. This can not be attributed to a lack of acetate in the reactor, since results show that acetate was present in effluent samples (following Days 0, 1, and 2), and therefore was not limiting. Due to problems encountered with clogging at the 2.1- and 4.2-hour residence times, the experiment was terminated.

Influent and effluent NO_3^- concentrations and pH values measured over the course of the secondary RO rejectate experiment are depicted in Figure 7. Data shown in Figure 7A indicate that removal of NO_3^- was significant with the PBR operating at a residence time of 0.8 hr and breakthrough was not observed following the first 3 days. As shown in Figure 7B, the majority of influent pH values were between 7.5 and 8.0, which is generally considered acceptable for biological processes. Effluent pH values were slightly elevated over influent levels, however, these levels generally fell between 8.0 and 8.5, indicating that the process did not have a major influence on pH.

Results of this experiment preliminarily indicate that the PBR system is capable of achieving non-detect effluent concentrations for NO_3^- , but not ClO_4^- in treatment of secondary RO rejectate. This may be due to metabolic limitations of the *perclace* organism in response to the salinity encountered in the secondary RO rejectate. However, because significant ClO_4^- removal was observed (approximately 90% in most cases), it may be possible with further work to optimize the system to achieve the goal of treating the secondary RO rejectate to non-detectable ClO_4^- levels.

3.4 Flask Study: Reduction of Cr(VI) by *Perclace*

Hexavalent Cr has been detected in on-site JPL groundwater at low concentrations, but is not expected to be a major issue in remedial action. Cr(VI), which is present as the chromate ion (CrO_4^{2-}), could possibly be encountered in an extraction stream during on-site treatment, and if RO is used as the primary treatment, CrO_4^{2-} would be present in the rejectates at elevated levels (it is noted here that CrO_4^{2-} would also sorb to anion exchange resins and would therefore also be present in ion exchange brines as well). Because CrO_4^{2-} is subject to biological reduction reactions which reduce its toxicity and mobility (bringing about precipitation above pH of 5.5), this flask experiment was carried out to preliminarily assess the potential of *perclace* to reduce CrO_4^{2-} in the presence and absence of ClO_4^- . Results of this experiment are presented in Figure 8. As shown, reduction of CrO_4^{2-} was observed to varying degrees in the inoculated flasks. No reduction was observed in control flasks, and therefore observed reduction can be attributed to *perclace*. This is consistent with other studies documenting bioreduction of CrO_4^{2-} (Losi, et al., 1994).

In this experiment, CrO_4^{2-} levels were reduced in the flasks, but CrO_4^{2-} was still detectable. It is important to note that although this demonstrates the metabolic capability of *perclace* to reduce CrO_4^{2-} , nothing is known regarding optimization of the reaction. However, given that CrO_4^{2-} is known to be subject to bioreduction by a wide variety of organisms (Losi, et al., 1994), and that reduction was demonstrated in this flask study, it is possible that CrO_4^{2-} in RO rejectates would be biologically treatable.

4.0 CONCLUSIONS

The major conclusions of the studies described here are as follows:

Treatment of Groundwater:

1. Results preliminarily suggest that JPL groundwater is treatable to non-detect ClO_4^- concentrations in the PBR/*perclace* system with a residence time as low as 0.4 hours.
2. Influent acetate (energy source) concentrations of less than 500 mg/L and potentially less than 250 mg/L yielded non-detect effluent ClO_4^- levels, and low acetate (in many cases less than 50 mg/L) were present in the effluent.
3. Nitrate is also removed in this system, and pH remains relatively constant during the process.
4. The need for addition of nitrogen as a nutrient is minimal.
5. Reduction of sulfate was not observed.

Treatment of RO Rejectates

1. Results preliminarily suggest that primary RO rejectate is treatable to non-detect ClO_4^- and non-detect nitrate concentrations in the PBR/*perclace* system with a residence time as low as 0.8 hours.
2. Results further suggest that secondary RO rejectate is treatable to non-detect nitrate but not non-detect ClO_4^- concentrations in the PBR/*perclace* system, although 90% ClO_4^- removal was observed.
3. *Perclace* is metabolically capable of reducing hexavalent chromium in simulated RO rejectates.

5.0 REFERENCES

- Bohn, H. L., B. L. McNeal, and G. A. O'Connor. 1985. Soil Chemistry. John Wiley and Sons. P. 241.
- Herman, D. C. and W. T. Frankenberger, Jr. 1999. Bacterial Reduction of Perchlorate and Nitrate in Water. J. Environ. Qual. 28:1018-1024.
- Losi, M. E., C. Amrhein, and W. T. Frankenberger. 1994. Environmental Biochemistry of Chromium. Reviews of Environmental Contamination and Toxicology. Vol. 36:91-121 Springer Verlag. NY, NY.
- Urbansky, E. T. 1998. Perchlorate Chemistry: Implications for Analysis and Remediation. Biorem. J. 2(2):81-95

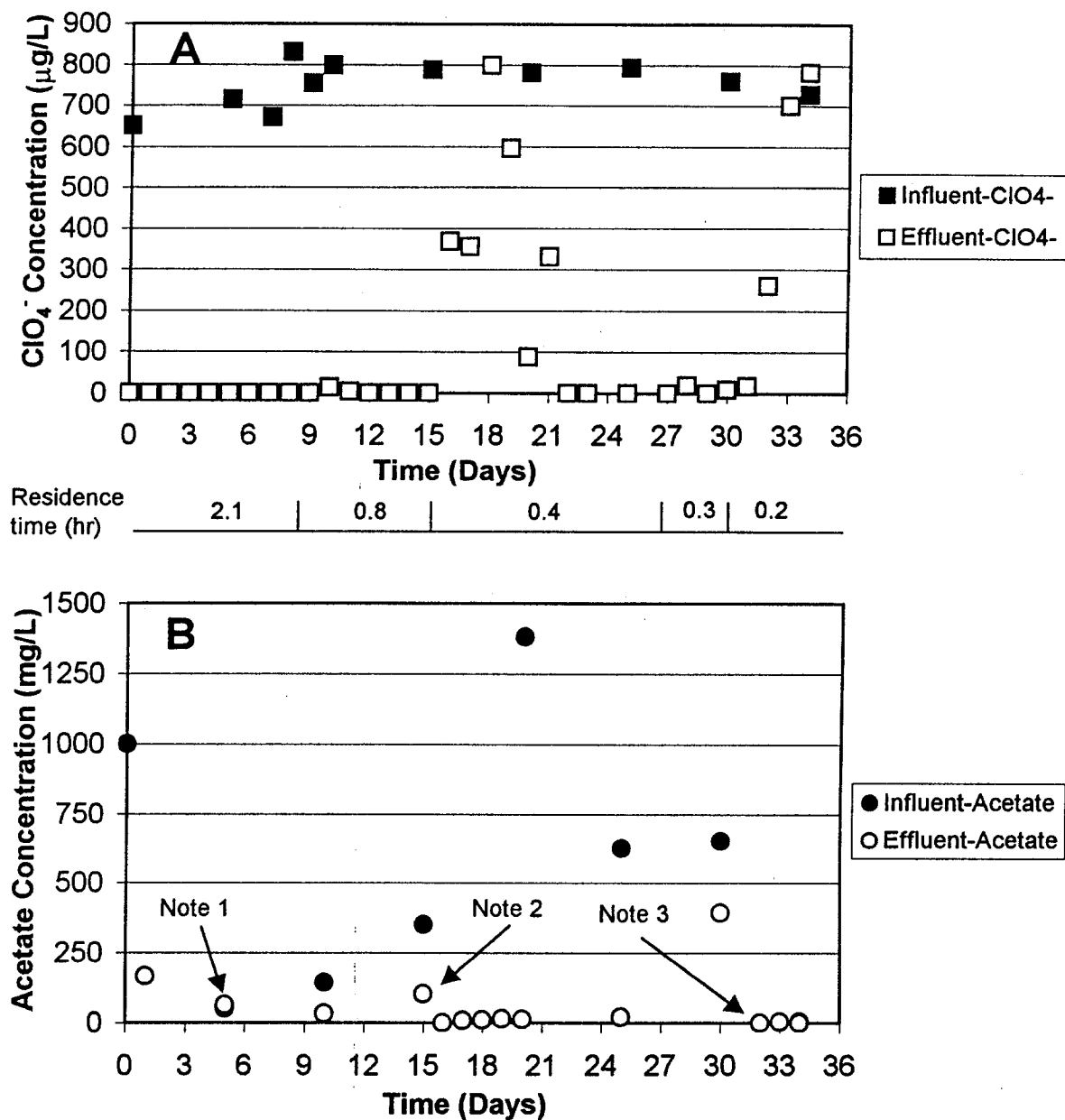
TABLES

Table 1. Removal of ClO_4^- by various inocula in flask study to preliminarily assess biological reduction of ClO_4^- in aqueous saline environments. Initial ClO_4^- concentration was 100 mg/L.

Inoculum	Electrical conductivity of medium (dS/M)	Carbon source	ClO_4^- Removal, Day 7 (%)	ClO_4^- Removal, Day 14 (%)
Control (uninoculated)	3.1	Acetate	0	0
Control (uninoculated)	3.1	Ethanol	0	1.7
Control (uninoculated)	6.25	Acetate	1.7	1.7
Control (uninoculated)	6.25	Ethanol	0	1.7
Arroyo Seco Sediment	3.1	Acetate	99.5	98.9
Arroyo Seco Sediment	3.1	Ethanol	1.7	13.9
Arroyo Seco Sediment	6.25	Acetate	0	97.9
Arroyo Seco Sediment	6.25	Ethanol	1.7	0
Bolsa Chica Sediment	3.1	Acetate	57.6	99.1
Bolsa Chica Sediment	3.1	Ethanol	17.6	99.2
Bolsa Chica Sediment	6.25	Acetate	99.6	98.2
Bolsa Chica Sediment	6.25	Ethanol	27.9	98.8
Water, African Evaporation Ponds	3.1	Acetate	27.9	31.0
Water, African Evaporation Ponds	3.1	Ethanol	27.9	95.3
Water, African Evaporation Ponds	6.25	Acetate	10.0	21.2
Water, African Evaporation Ponds	6.25	Ethanol	10.0	17.6
Perclace	3.1	Acetate	98.9	99.6
Perclace	3.1	Ethanol	53.6	99.1
Perclace	6.25	Acetate	99.6	99.7
Perclace	6.25	Ethanol	55.6	99.4

FIGURES

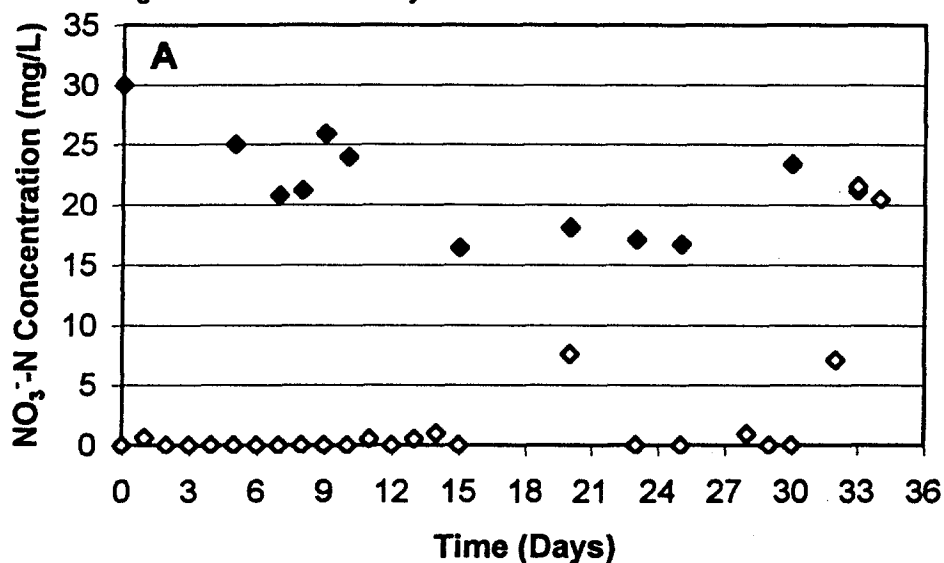
Figure 1. Influent and effluent perchlorate (A) and acetate (B) concentrations, groundwater PBR study.



NOTES

1. Day 5: acetate feed pump failure. This was corrected shortly after influent sample was collected. Because acetate was present in the effluent samples, process efficiency was assumed to have not been effected.
2. Day 15: acetate feed pump was changed to accommodate increased reactor flow rate, problems with pump were initially encountered (see text, Sec. 3.1)
3. Day 32: acetate feed pump failure (see text, Sec.3.1).

Figure 2. Influent and effluent nitrate concentration (A) and pH (B), groundwater PBR study.



Residence time (hr)	2.1	0.8	0.4	0.3	0.2
------------------------	-----	-----	-----	-----	-----

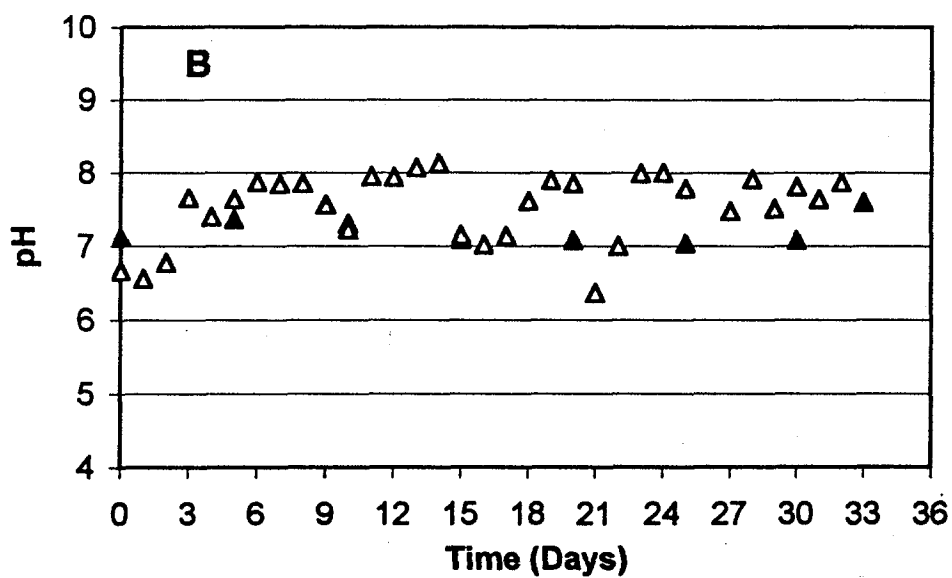
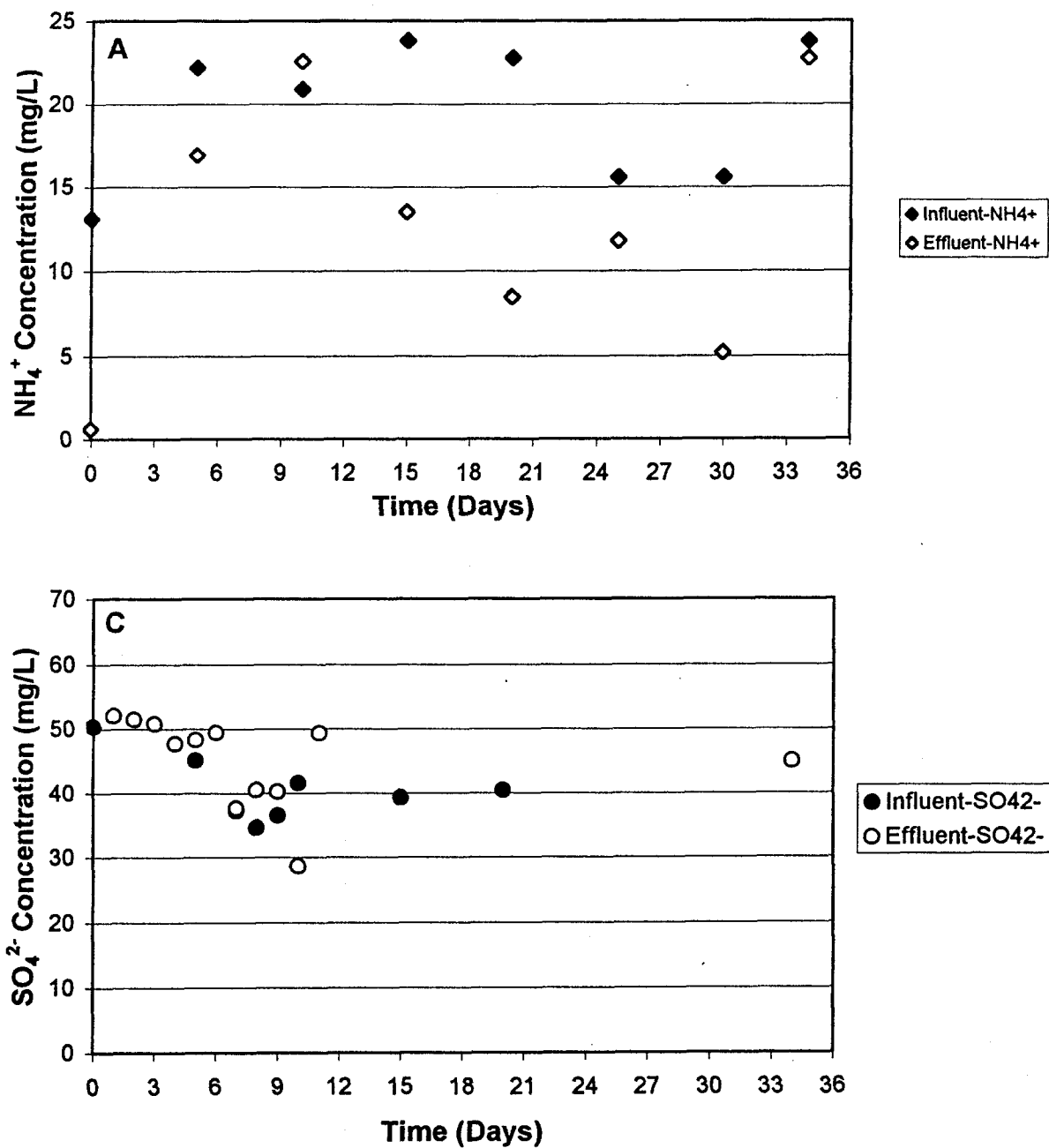


Figure 3. Influent and effluent concentrations of ammonium nitrogen (A) and sulfate (B), groundwater PBR study.



Notes:

- 1) Frequency of sulfate analyses was decreased after it had become apparent that sulfate reduction was not occurring to a measurable extent.

Figure 4. Influent And effluent perchlorate (A) and acetate (B) concentrations, RO rejectate PBR study (Days 1-12 constituted the start-up period).

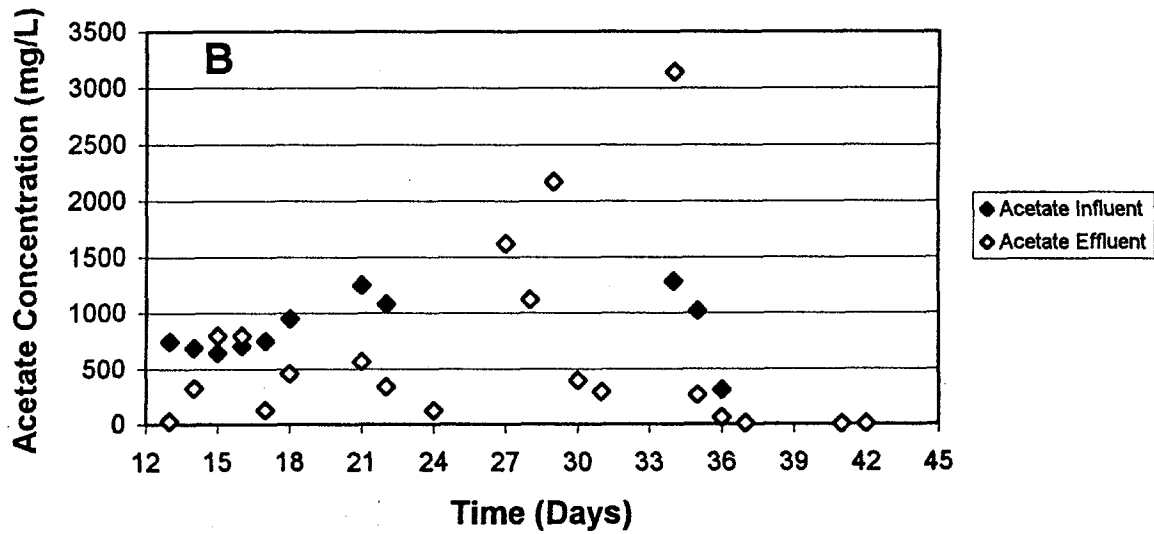
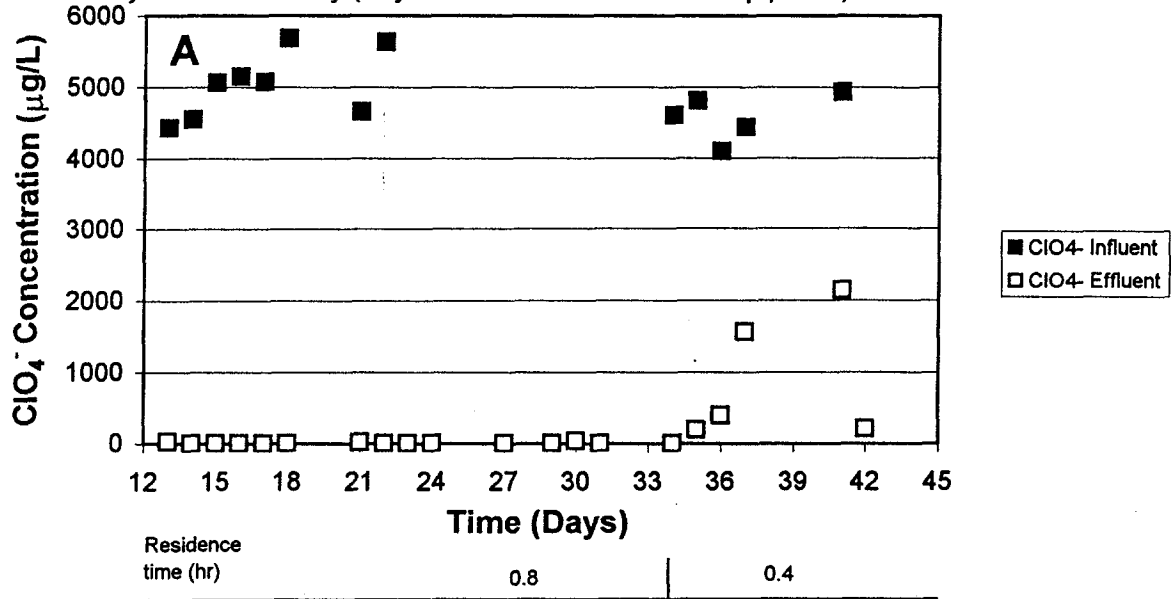


Figure 5. Influent and effluent nitrate concentration (A) and pH (B), RO rejectate PBR study (Days 1-12 constituted the start-up period).

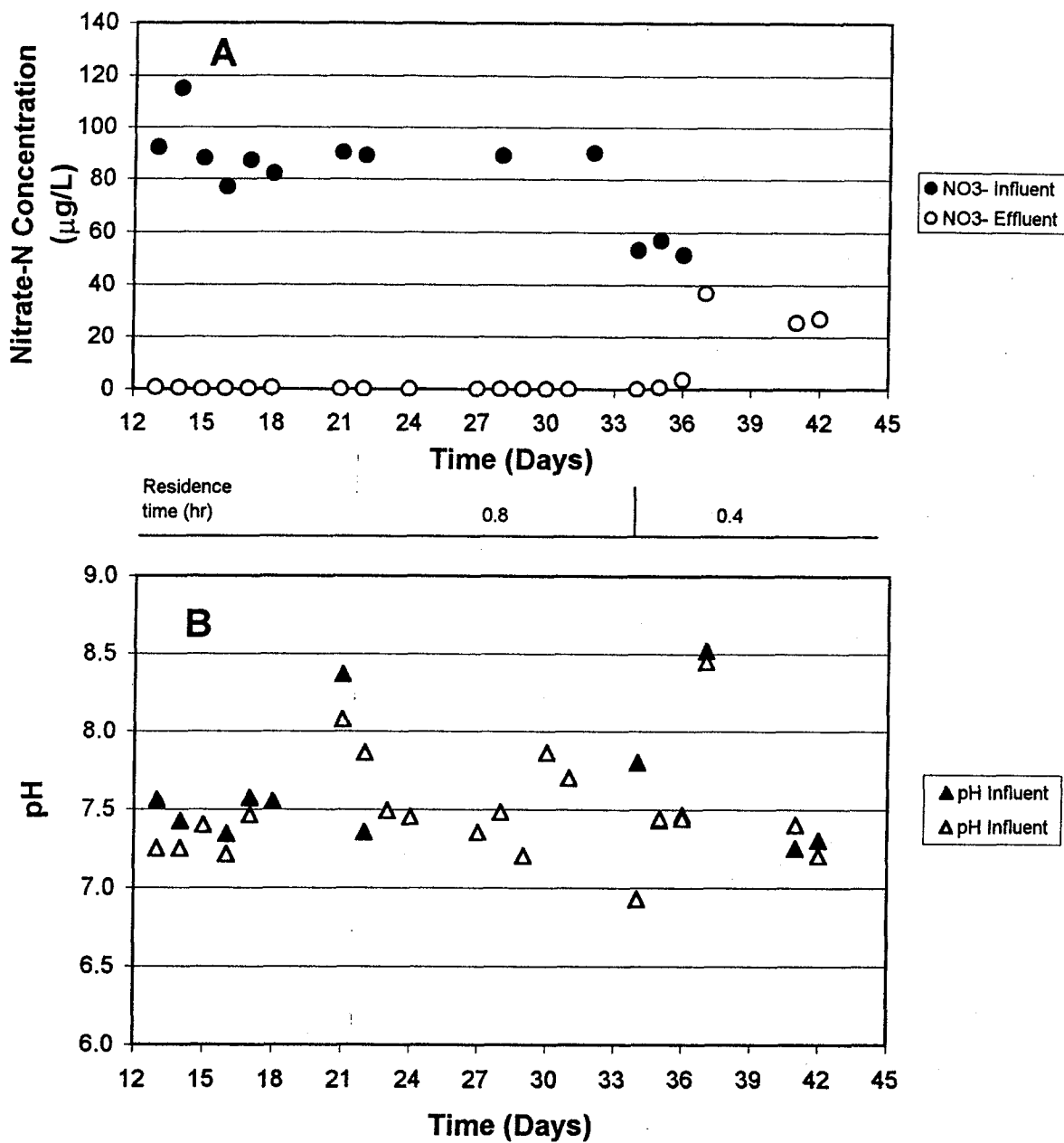


Figure 6. Influent and effluent perchlorate (A) and acetate (B) concentrations, RO² rejectate PBR study.

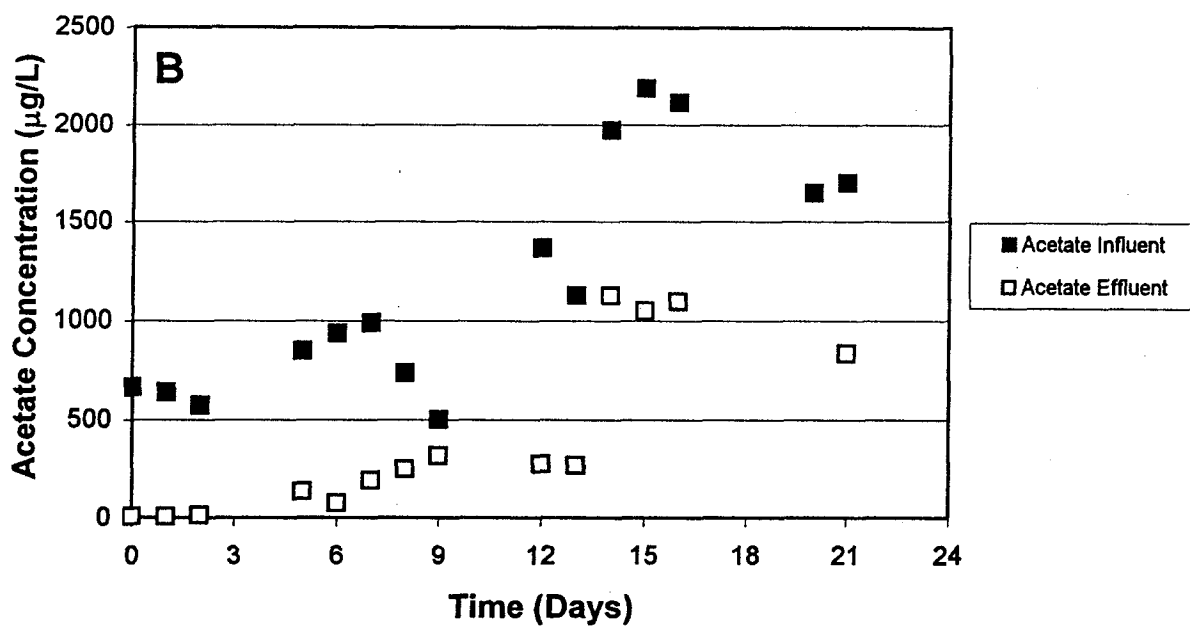
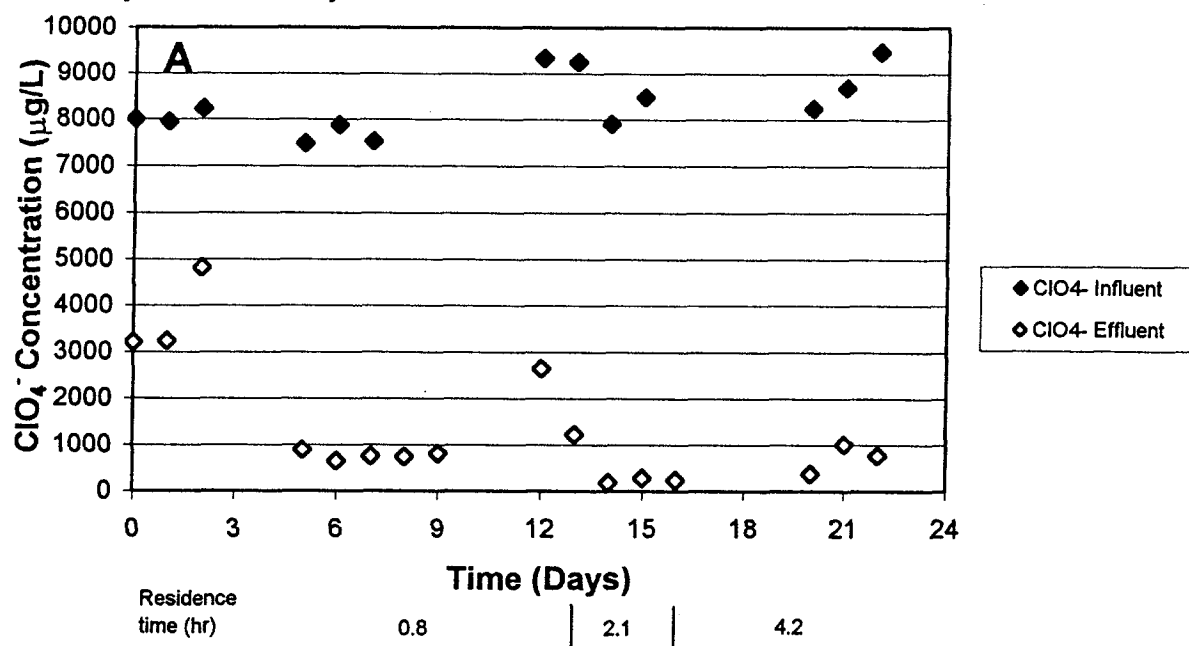


Figure 7. Influent and effluent nitrate concentration (A) and pH (B), RO² rejectate PBR study.

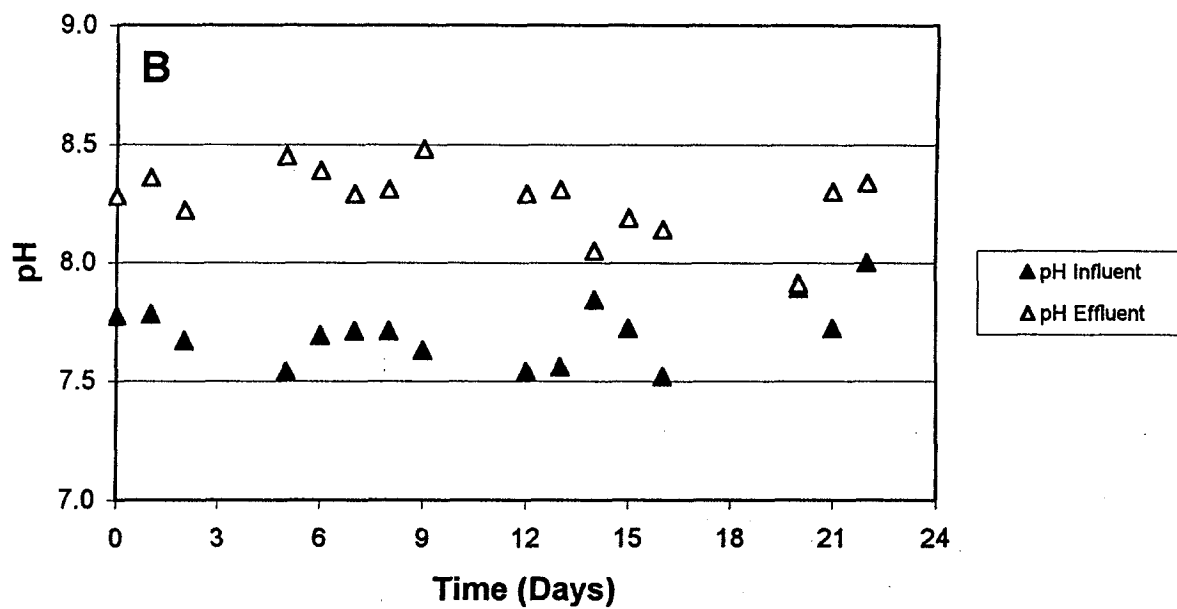
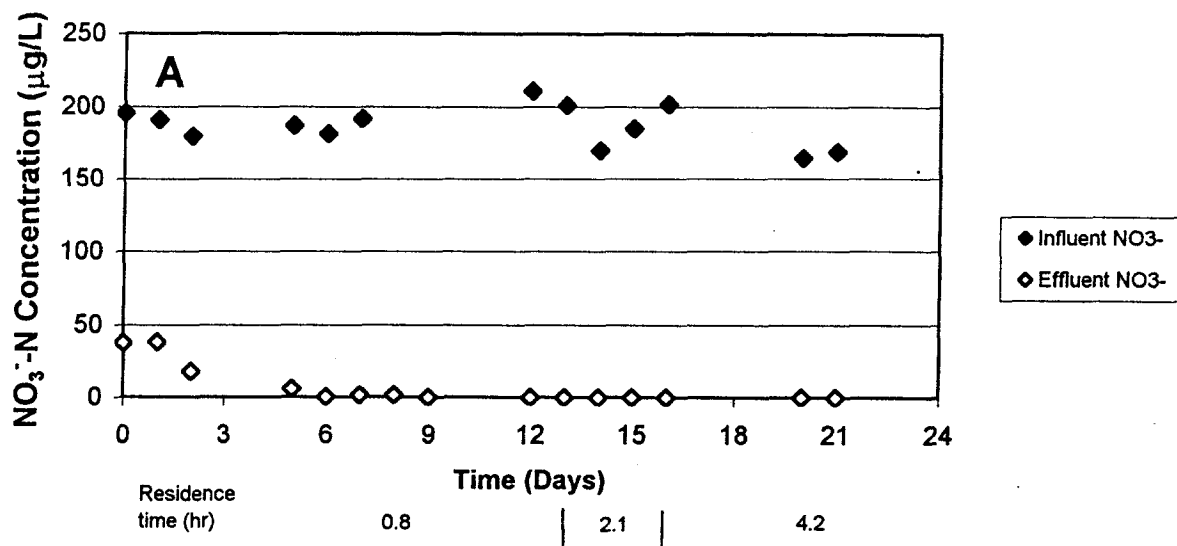
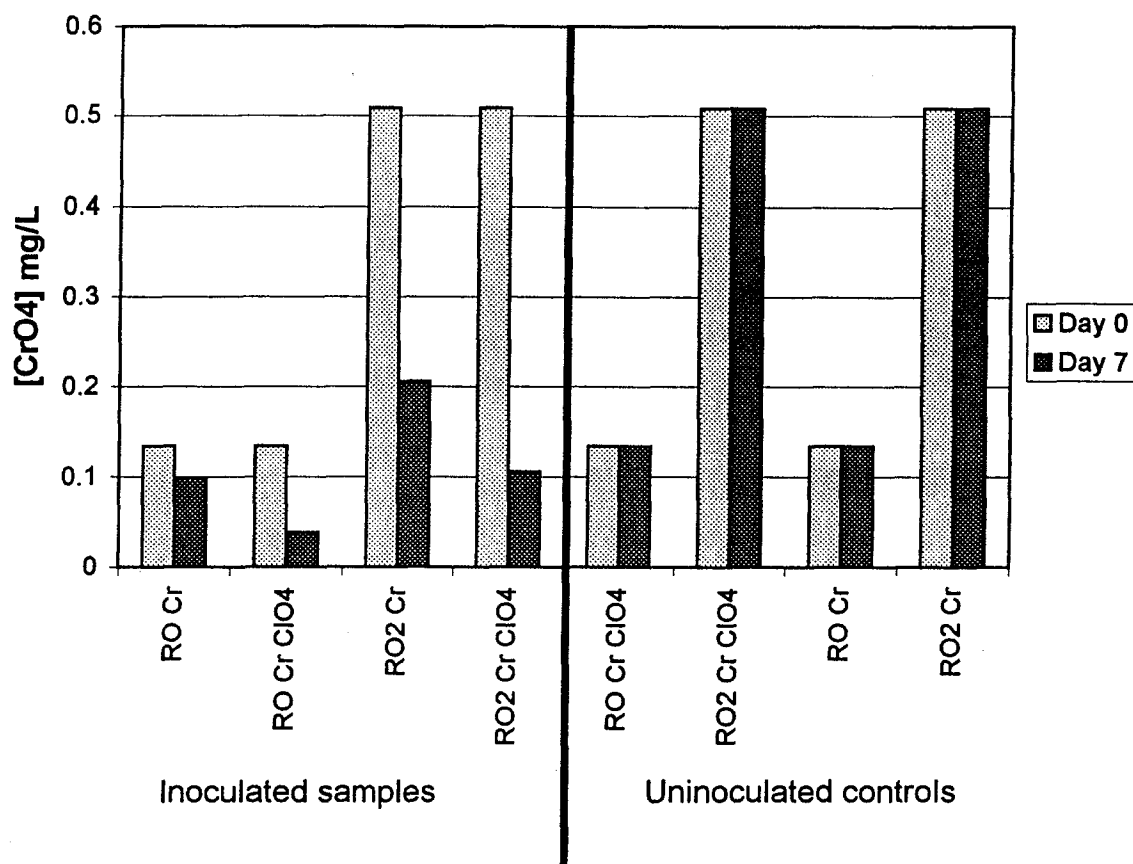


Figure 8. Results of flask study showing chromate [Cr(VI)] removal by *perc1ace* in the presence and absence of perchlorate*.



* On the x axis: RO refers to simulated RO rejectate, RO2 to simulated secondary rejectate (RO²), Cr to the presence of chromate only, and Cr ClO4 to the presence of chromate and perchlorate in the flasks. Results of inoculated treatments represent the mean of two replicates. Refer to Appendix E-4 for experimental design.

Note: This study was intended only to demonstrate the metabolic capability of *perc1ace* to reduce chromate and no inferences regarding kinetics can be drawn.

APPENDICES

Summary of All Data Collected in PBR Groundwater Treatment Study

Sample #	Sample	Date	pH	Acetate mg/L	NO ₃ ⁻ -N mg/L ⁻¹	SO ₄ ²⁻ mg/L	ClO ₄ ⁻ μg/L	NH ₄ ⁺ -N mg/L
R1-0I	Influent	27-Apr	7.11	1.00E+03	30	50.4	650.1	13.1
R1-0E	Effluent	27-Apr	6.66	NA	ND	203.9	ND	0.62
R1-1E	Effluent	28-Apr	6.55	165.25	0.65	52.1	ND	NA
R1-2E	Effluent	29-Apr	6.77	NA	ND	51.5	ND	NA
R1-3E	Effluent	30-Apr	7.65	NA	ND	50.8	ND	NA
R1-4E	Effluent	1-May	7.39	NA	ND	47.7	ND	NA
R1-5I	Influent	2-May	7.36	51.1	25	45.1	714	22.2
R1-5E	Effluent	2-May	7.64	63.05	ND	48.3	ND	16.9
R1-6E	Effluent	3-May	7.87	NA	ND	49.4	ND	NA
R1-7I	Influent	4-May	NA	NA	20.8	37.2	671	NA
R1-7E	Effluent	4-May	7.84	NA	ND	37.6	ND	NA
R1-8I	Influent	5-May	NA	NA	21.2	34.6	830	NA
R1-8E	Influent	5-May	7.85	NA	ND	40.5	ND	NA
R1-9I	Influent	6-May	NA	NA	25.9	36.5	754	NA
R1-9E	Effluent	6-May	7.56	NA	ND	40.25	ND	NA
R1-10I	Influent	7-May	7.3	143.5	24	41.5	798	20.9
R1-10E	Effluent	7-May	7.22	32.1	ND	28.6	13.6	22.6
R1-11E	Effluent	8-May	7.95	NA	0.5	49.3	4.25	NA
R1-12E	Effluent	9-May	7.94	NA	ND	NA	ND	NA
R1-13E	Effluent	10-May	8.07	NA	0.5	NA	ND	NA
R1-14E	Effluent	11-May	8.13	NA	1	NA	ND	NA
R1-15I	Influent	12-May	7.08	350.77	16.4	39.3	787.3	23.8
R1-15E	Effluent	12-May	7.14	101.7	ND	NA	ND	13.5
R1-16E	Effluent	14-May	7.01	ND	NA	NA	368.24	NA
R1-17E	Effluent	15-May	7.13	7.5	NA	NA	355.9	NA
R1-18E	Effluent	16-May	7.61	10	NA	NA	797.64	NA
R1-19E	Effluent	17-May	7.9	13.7	NA	NA	595.9	NA
R1-20I	Influent	18-May	7.07	1381	18.1	40.4	780.6	22.8
R1-20E	Effluent	18-May	7.85	11.85	7.6	NA	88.14	8.5
R1-21E	Effluent	19-May	6.36	NA	NA	NA	330.84	NA
R1-22I	Influent	20-May	NA	NA	NA	NA	NA	NA
R1-22E	Effluent	20-May	7	NA	NA	NA	ND	NA
R1-23I	Influent	21-May	NA	NA	17.1	NA	NA	NA
R1-23E	Effluent	21-May	7.99	NA	ND	NA	ND	NA
R1-24E	Effluent	22-May	8	NA	NA	NA	NA	NA
R1-25I	Influent	23-May	7.03	625	16.7	NA	792.9	15.6
R1-25E	Effluent	23-May	7.78	19.85	ND	NA	ND	11.8
R1-26E	Effluent	24-May	NA	NA	NA	NA	NA	NA
R1-27E	Effluent	25-May	7.47	NA	NA	NA	ND	NA
R1-28E	Effluent	26-May	7.91	NA	0.95	NA	18.9	NA
R1-29E	Effluent	27-May	7.51	NA	ND	NA	ND	NA
R1-30I	Influent	28-May	7.07	652	23.4	NA	760	15.6
R1-30E	Effluent	28-May	7.81	394	ND	NA	9.26	5.2
R1-31E	Effluent	29-May	7.64	NA	NA	NA	18.6	NA
R1-32E	Effluent	30-May	7.87	ND	7.1	NA	260.7	NA
R1-33I	Influent	31-May	7.59	NA	21.2	NA	NA	NA
R1-33E	Effluent	31-May	NA	4.55	21.6	NA	700.8	NA
R1-34I	Influent	1-Jun	NA	NA	20.5	NA	728	23.8
R1-34E	Effluent	1-Jun	NA	ND	20.5	44.95	781	22.8
Detection Limit				4.0	0.47	0.75	4.0	2

NOTES:

ND = Result below detection limit

NA: Not Analyzed

Salt	Ion	Molecular Weight	RO ² rejectate	RO rejectate	Ground water	ADDS	RO ² rejectate	RO rejectate	Ground water	
Concentration Factor			10	5						
			mg/L	mg/L	mg/L					
KCl		74.55	57.20							
	K	39.1	30	15	3.0	(mg/L)	57.2	28.6	5.7	
	Cl	35.45	27.20	13.6	2.7	(g/120 gal)	26.0	13.0	2.6	
NaClO ₄		122.44	12.3							
	Na	22.99	2.3	1.2	0.23	(mg/L)	12.3	6.2	1.2	
	ClO ₄	99.45	10	5	1.0	(g/120 gal)	5.6	2.8	0.6	
NaNO ₃		84.99								
	Na	22.99	234	117	23	(mg/L)	863.6	431.8	86.4	
	NO ₃	62.00	630	315	63	(g/120 gal)	392.4	196.2	39.2	
MgCl ₂ -6H ₂ O		203.21	1588							
	Mg	24.31	190	95	19	(mg/L)	1588.2	794.1	158.82	
	2Cl	70.9	554	277	55.4	(g/120 gal)	721.6	360.8	72.2	
Na ₂ SO ₄		142.04								
	2Na	45.98	26	13	3	(mg/L)	79.8	39.9	8.0	
	SO ₄	96.06	54	27	5.4	(g/120 gal)	36.3	18.1	3.6	
NaHCO ₃		84.01								
	Na	22.99	584	292	58	(mg/L)	2134.0	1067.0	213.4	
	HCO ₃	61.02	1,550	775	155	(g/120 gal)	969.5	484.8	97.0	
CaCl ₂ -2H ₂ O		147.02								
	Ca	40.08	50	25	5	(mg/L)	183.4	91.7	18.34	
	2Cl	70.9	88	44	9	(g/120 gal)	83.3	41.7	8.3	
Na ₂ CO ₃		105.99	18							
	2Na	45.99	8	4	0.8	(mg/L)	17.7	8.8	1.8	
	CO ₃	60.00	10	5	1.0	(g/120 gal)	8.0	4.0	0.8	
FeCl ₃ -6H ₂ O		270.2	4.8							
	Fe	55.85	1.0	0.5	0.1	(mg/L)	4.84	2.4	0.48	
	3Cl	106.35	1.90	1.0	0.2	(g/120 gal)	2.2	1.1	0.2	
Final compositions based on additions calculated above (groundwater not formulated)						Actual groundwater concentrations (based on historic data) and target rejectate concentrations				
			RO ²	RO	GW	RO ²			RO	GW
EC (est)			6.33	3.16	0.63		5.0	2.5		0.5
TDS, mg/l			4,050	2,025	405		3183.0	1591.5		318.3
Cl			672	336	67		242.0	121.0		24.2
Na			853	427	85		227.0	113.5		22.7
SO ₄			54	27	5		266.0	133.0		26.6
Ca			50	25	5		498.0	249.0		49.8
Mg			190	95	19		190.0	95.0		19.0
K			30	15	3		25.0	12.5		2.5
NO ₃			630	315	63		633.0	316.5		63.3
HCO ₃			1,550	775	155		1552.0	776.0		155.2
CO ₃			10	5	1		3.0	1.5		0.3
ClO ₄			10	5	1		8.0	4.0		0.8
Fe			1.0	0.5	0.1		1.0	0.5		0.1
NOTES:										
1) Boxed values are the basis for RO calculation										
2) : Concentration lowered to reduce precipitation (TDS not reduced due to addition of excess Na ⁺ and Cl ⁻)										
3) All concentrations in mg/L										

Page 1 of 3

Date	Day	[NO ₃ ⁻ -N] ^a Influent	[NO ₃ ⁻ -N] ^a Effluent	[Acetate] ^a Influent	[Acetate] ^a Effluent	pH Influent	pH Effluent	EC ^b Influent	EC ^b Effluent	[ClO ₄] ^c Influent	[ClO ₄] ^c Effluent	Babcock ^d	Feed	Notes*
Tues, 6/15	0	286.4	ND	607.2	129.6	6.9	7.2	7	1.1	ND	ND	NA	Start-up	1
Wed, 6/16	1	258	62.7	586.7	3.6	6.9	7.2	6.8	3.9	ND	ND	NA	Start-up	2
Thurs, 6/17	2	107.5	0.4	578.3	381.2	7	7.26	3.9	3.4	11990	25.72	NA	Start-up	
Fri, 6/18	3	107.3	0.45	510.1	255.6	7	7.16	3.3	3.1	12080	28.05	NA	Start-up	
Sat, 6/19	4	NA	NA	NA	NA	NA	NA	NA	NA	NA	NA	NA	Start-up	
Sun, 6/20	5	NA	NA	NA	NA	NA	NA	NA	NA	NA	NA	NA	Start-up	
Mon, 6/21	6	132	14.5	277	287.8	7.13	7.33	2.1	3.1	1200	ND	NA	Start-up	3
Tues, 6/22	7	98.7	55	145.9	12.05	7.1	7.4	2.9	2.6	12200	3762	NA	Start-up	
Wed, 6/23	8	123	45	454	11.06	8	8.3	3.1	2.6	NA	2547	NA	Start-up	
Thurs, 6/24	9	130	40.6	151	112	7.2	7.33	2.9	2.6	11568	2830	NA	Start-up	
Fri, 6/25	10	73	46.8	2844	17.5	7.54	7.5	6.4	2.8	12227	5300	NA	Start-up	4
Sat, 6/26	11	NA	NA	NA	NA	NA	NA	NA	NA	NA	NA	NA	Start-up	
Sun, 6/27	12	NA	NA	NA	NA	NA	NA	NA	NA	NA	NA	NA	Start-up	
Mon, 6/28	13	92	0.68	750	28	7.56	7.25	2.3	3	4430	25.23	42	Rejectate	5
Tues, 6/29	14	115	0.5	689	326	7.42	7.25	1.5	3.1	4555	ND	NA	Rejectate	
Wed, 6/30	15	88	ND	647	800	7.4	7.4	4.2	3.3	5059	ND	NA	Rejectate	
Thurs, 7/1	16	77	ND	707	800	7.34	7.21	3.6	3.3	5150	ND	ND	Rejectate	
Fri, 7/2	17	87	ND	754	129	7.57	7.46	3.1	2.8	5067	ND	NA	Rejectate	
Sat, 7/3	18	82.15	0.44	949.29	458.46	7.55	9.1	3.2	2.9	5685	ND	NA	Rejectate	
Sun, 7/4	19	NA	NA	NA	NA	NA	NA	NA	NA	NA	NA	NA	Rejectate	
Mon, 7/5	20	NA	NA	NA	NA	NA	NA	NA	NA	NA	NA	NA	Rejectate	
Tues, 7/6	21	90.15	ND	1251.94	564.06	8.37	8.08	3.3	3.1	4656	14.67	13	Rejectate	6
Wed, 7/7	22	89.04	ND	1082.73	338.89	7.35	7.86	3.3	3	5635	ND	ND	Rejectate	
Thurs, 7/8	23	NA	NA	NA	NA	NA	7.49	NA	2.8	NA	ND	NA	Rejectate	
Fri, 7/9	24	NA	ND	NA	127.26	NA	7.45	NA	2.8	NA	ND	NA	Rejectate	
Sat, 7/10	25	NA	NA	NA	NA	NA	NA	NA	NA	NA	NA	NA	Rejectate	
Sun, 7/11	26	NA	NA	NA	NA	NA	NA	NA	NA	NA	NA	NA	Rejectate	
Mon, 7/12	27	NA	ND	NA	1619.27	NA	7.35	NA	2.8	NA	ND	NA	Rejectate	
Tues, 7/13	28	89	ND	NA	1118.69	NA	7.48	NA	2.9	NA	NA	NA	Rejectate	
Wed, 7/14	29	NA	ND	NA	2171.54	NA	7.2	NA	2.8	NA	ND	ND	Rejectate	
Thurs, 7/15	30	NA	ND	NA	395.16	NA	7.86	NA	2.9	NA	33	34	Rejectate	
Fri, 7/16	31	NA	ND	NA	294.6	NA	7.7	NA	2.9	NA	ND	NA	Rejectate	
Sat, 7/17	32	90	NA	NA	NA	NA	NA	NA	NA	NA	NA	NA	Rejectate	
Sun, 7/18	33	NA	NA	NA	NA	NA	NA	NA	NA	NA	NA	NA	Rejectate	

APPENDIX E-3
Summary of All Data Collected in PBR RO Rejectate Studies.

Date	Day	[NO ₃ ⁻ -N] ^a Influent	[NO ₃ ⁻ -N] ^a Effluent	[Acetate] ^a Influent	[Acetate] ^a Effluent	pH Influent	pH Effluent	EC ^b Influent	EC ^b Effluent	[ClO ₄] ^c Influent	[ClO ₄] ^c Effluent	Babcock ^d	Feed	Notes*
Mon, 7/19	34	53.12	ND	1286.59	3144.77	7.8	6.93	4.5	9.1	4609	ND	NA	Rejectate	7
Tues, 7/20	35	56.94	0.7	1019.64	268.63	7.43	7.44	4.5	4.2	4804	197.3	NA	Rejectate	
Wed, 7/21	36	51.45	3.6	308.86	64.95	7.46	7.44	3.7	3.6	4098	394.27	NA	Rejectate	
Thurs, 7/22	37	NA	36.77	NA	11.19	8.52	8.45	3	2.9	4439.2	1563.85	NA	Rejectate	
Fri 7/23	38	NA	NA	NA	NA	NA	NA	NA	NA	NA	NA	NA	Rejectate	
Sat 7/24	39	NA	NA	NA	NA	NA	NA	NA	NA	NA	NA	NA	Rejectate	
Sun, 7/25	40	NA	NA	NA	NA	NA	NA	NA	NA	NA	NA	NA	Rejectate	
Mon, 7/26	41	NA	25.5	NA	5.96	7.25	7.4	3.7	3.5	4928	2141	NA	Rejectate	
Tues, 7/27	42	NA	26.83	NA	5.03	7.3	7.2	3.9	3.5	NA	208.4	NA	Rejectate ²	8
Wed, 7/28	0	195.6	37.78	661.7	6.04	7.77	8.28	4.9	4.3	8000	3225	NA	Rejectate ²	
Thurs, 7/29	1	191.02	38.3	638.5	5.74	7.78	8.36	5.66	5.15	7946	3242.6	NA	Rejectate ²	
Fri, 7/30	2	179.8	18.09	572	12.79	7.67	8.22	6.21	5.66	8233	4814	NA	Rejectate ²	
Sat, 7/31	3	NA	NA	NA	NA	NA	NA	NA	NA	NA	NA	NA	Rejectate ²	
Sun 8/1	4	NA	NA	NA	NA	NA	NA	NA	NA	NA	NA	NA	Rejectate ²	
Mon, 8/2	5	187.2	6.05	846.7	134.8	7.54	8.45	5.41	4.21	7479	898	NA	Rejectate ²	
Tues, 8/3	6	181.4	0.49	934.6	74.5	7.69	8.39	5.26	4.73	7880	652	NA	Rejectate ²	
Wed, 8/4	7	191.7	1.64	987	191.64	7.71	8.29	5.45	4.75	7523	762	NA	Rejectate ²	
Thurs, 8/5	8	NA	1.85	734	250	7.71	8.31	5.55	4.3	NA	750	NA	Rejectate ²	
Fri, 8/6	9	NA	ND	501	318	7.63	8.48	5.6	4.8	NA	809	NA	Rejectate ²	
Sat, 8/7	10	NA	NA	NA	NA	NA	NA	NA	NA	NA	NA	NA	Rejectate ²	
Sun, 8/8	11	NA	NA	NA	NA	NA	NA	NA	NA	NA	NA	NA	Rejectate ²	
Mon, 8/9	12	211	ND	1364	274	7.54	8.29	5.17	4.66	9339	2655	NA	Rejectate ²	
Tues, 8/10	13	201	ND	1125	270	7.56	8.31	6.29	5.5	9250	1231	NA	Rejectate ²	9
Wed, 8/11	14	170	ND	1968	1124	7.84	8.05	5.62	5.26	7907	189	NA	Rejectate ²	
Thurs, 8/12	15	185	ND	2185	1048	7.72	8.19	5.61	5.16	8488	279	NA	Rejectate ²	
Fri, 8/13	16	202	ND	2111	1097	7.52	8.14	6.01	5.31	NA	238	NA	Rejectate ²	10
Sat 8/14	17	NA	NA	NA	NA	NA	NA	NA	NA	NA	NA	NA	Rejectate ²	
Sun, 8/15	18	NA	NA	NA	NA	NA	NA	NA	NA	NA	NA	NA	Rejectate ²	
Mon, 8/16	19	NA	NA	NA	NA	NA	NA	NA	NA	NA	NA	NA	Rejectate ²	
Tues, 8/17	20	165	ND	1647	NA	7.89	7.91	4.3	4.4	8235	373	NA	Rejectate ²	
Wed, 8/18	21	169	ND	1699	834	7.72	8.3	5.36	4.73	8688	1018	NA	Rejectate ²	
Thurs, 8/19	22	NA	NA	NA	NA	8	8.34	4.55	4.45	9474	776	NA	Rejectate ²	
Low Standard		0.4	0.4	4.0	4.0					4.0	4.0			

***Notes**

NA Not Analyzed

ND Not detected above limit of detection (Low Standard)

a Concentrations in mg/L

b Values expressed in deciseimens/meter (dS/m)

c Concentrations in $\mu\text{g/L}$

d Results of confirmatory ClO_4^- analyses (in $\mu\text{g/L}$) conducted by Babcock Laboratories

1 Filled tank with simulated RO rejectate, start flow 4pm, used 2x ClO_4^- for column conditioning

2 No ClO_4^- in influent, stir tank by bubbling with nitrogen gas

3 Switch to syringe pump for acetate

4 Flow set at 25 ml/minute (0.8 hr residence time).

5 Column plugged over weekend, agitated Monday morning, flow restored, return to 25 ml/min.

6 Backflushed column

7 Speed up to 50 ml/minute after this sample (0.4 hr residence time).

8 Initiated flow with simulated secondary rejectate (RO^2) begin 4pm, 25 ml/min (0.8 hr residence time).

9 After sample, slow to 10 ml/min (2.1 hr residence time).

10 After sample, slow to 5 ml/min (4.2 hr residence time).

APPENDIX E-4
Experimental Design for Flask Study to Assess the Ability of Perc1ace to Reduce Cr(VI)

Flask	Feed	Innoculated	Feed Volumes	[CrO ₄ ²⁻], mg/L	[ClO ₄ ⁻], mg/L	[Acetate], g/L
1	Rejectate	Yes	100 ml	0.125	0	0.5
2	Rejectate	Yes	100 ml	0.125	0	0.5
3	Rejectate	Yes	100 ml	0.125	4	0.5
4	Rejectate	Yes	100 ml	0.125	4	0.5
5	Rejectate ²	Yes	100 ml	0.5	0	0.5
6	Rejectate ²	Yes	100 ml	0.5	0	0.5
7	Rejectate ²	Yes	100 ml	0.5	8	0.5
8	Rejectate ²	Yes	100 ml	0.5	8	0.5
9	Rejectate	No (control)	100 ml	0.125	0	0.5
10	Rejectate	No (control)	100 ml	0.125	4	0.5
11	Rejectate ²	No (control)	100 ml	0.5	0	0.5
12	Rejectate ²	No (control)	100 ml	0.5	8	0.5

1) Add filter-sterilized electron donor and acceptor(s) following autoclaving of feeds

2) Inoculate with stock culture

3) Flush headspace with filter sterilized N₂, cap tightly

4) Sample and analyze initially (Day 0) and at 7 days

APPENDIX F

BIODEGRADATION OF PERCHLORATE IN REJECTATE FROM REVERSE OSMOSIS (RO) OF GROUNDWATER (APPLIED RESEARCH ASSOCIATES, INC.)

**BIODEGRADATION OF PERCHLORATE IN REVERSE OSMOSIS (RO)
REJECTATES FROM TREATMENT OF GROUNDWATER**

Applied Research Associates, Inc.

Prepared for

FOSTER WHEELER ENVIRONMENTAL CORPORATION

**611 Anton Boulevard, Suite 800
Costa Mesa, CA 92626
(714) 444-5535**

***Final Report
January 6, 2000***

Technical Point of Contact:

**Edward N. Coppola
Ecoppola@ara.com
(850) 914-3188 (voice)
(850) 914-3189 (fax)**

**Applied Research Associates, Inc.
215 Harrison Avenue
Panama City, FL 32401**

Applied Research Associates, Inc.

Biodegradation of Perchlorate in Reverse Osmosis (RO) Rejectates from Treatment of Groundwater

1. Executive Summary

The purpose of this study was to evaluate the biodegradation of perchlorate in rejectate from the treatment of contaminated groundwater by reverse osmosis (RO). Because of the large volumes of water required for this study, surrogate RO rejectate water was prepared based on actual groundwater analysis. Appropriate salts were used to prepare RO rejectates that represented a 5x (RO) and a 10x (RO²) concentration of the groundwater constituents. These concentrations were considered representative of rejectate from initial treatment of groundwater and rejectate (RO²) of further RO treatment of the initial rejectate. A bench-scale version of a full-scale, patented reactor system was employed in this study. This reactor system was operated as a fixed-film process and as a suspended-growth, continuous-stirred-tank-reactor (CSTR) process. Over three months of testing was conducted to evaluate the affects of reactor configuration, residence time, feed water (RO & RO²), and nutrient.

Perchlorate reduction was evaluated by ion chromatography. Due to the high concentration of dissolved solids in this water, the detection limit using this method was limited to approximately 20 parts-per-billion. During steady-state operation, perchlorate was routinely reduced from approximately 10 parts-per-million (ppm) in the feed to below the detection limit for ion chromatography. In addition to complete perchlorate reduction, nitrate was also completely reduced by the ARA process. Some perchlorate excursions were observed; however, they were always the result of startup transients, condition changes, or equipment problems (flow interruptions, loss of sensors, etc.). There was no indication that anything in the RO water would inhibit complete perchlorate reduction. Reduction of a potential co-contaminant, chromium (VI), was also evaluated. 120 ppb of chromium was added to RO rejectate feed water as chromate (CrO₄²⁻). This limited test showed that this process simultaneously reduced chromium (VI), measured at 80 ppb in the feed, to below the detection limit of 10 ppb.

Operating costs for the ARA process are projected to be \$60,000 per year for a system that can treat a 100 gallon-per-minute (gpm) RO rejectate stream containing 10-100 ppm of perchlorate. Operating cost estimate includes the carbon source (a nutrient that is a commercially available food byproduct), other micro-nutrients, and sodium hydroxide required for pH control. The nutrient added to the feed water increases the biological oxygen demand (BOD) of the effluent water to 500-1000 mg/L. In many cases, it may be permissible to discharge this effluent directly to a sewage treatment plant or reduce the BOD in a post treatment step before discharge. At Thiokol Corporation, near Brigham City, Utah, ARA's operational prototype has been destroying 500-5,000 ppm of perchlorate in a process continuously since December 1997. This effluent is treated at the local sewage treatment plant and discharged under a NPDES permit. On October 4, 1999, ARA was awarded a design and engineering contract by Kerr-McGee Chemical LLC to build a 825 gpm turnkey treatment plant designed to destroy over 2 tons per day of perchlorate in highly contaminated groundwater. The effluent from this process will be treated before discharge under a NPDES permit. The ARA process is uniquely designed to completely reduce perchlorate in highly contaminated water with low operating and maintenance costs.

2. Introduction

2.1 Objectives

This report describes the results of perchlorate biodegradation treatability studies focused on the treatment of rejectate from a reverse osmosis (RO) process for removing and concentrating perchlorate that has contaminated ground water. ARA applied their licensed and patented process and perchlorate-reducing cultures in a patented, bench-scale reactor system for this evaluation. The primary objectives of this study were to:

- Demonstrate the biodegradation of perchlorate in a surrogate RO rejectate
- Evaluate RO rejectate that represents 5x and 10x concentrations groundwater contaminants. These concentrations were considered representative of rejectate from initial treatment of groundwater and rejectate (RO²) of further RO treatment of the initial rejectate.
- Establish the performance characteristics using a low-cost nutrient
- Establish preliminary nutrient and residence time requirements to achieve complete perchlorate destruction (below the IC detection limit)
- Determine performance benefits (if any) for patented, fixed-film (fixed-bed) reactor process compared to a suspended-growth, CSTR process for perchlorate biodegradation

2.2 Approach

The patented, fixed-film process used in this study was developed by Tri-Bio, Inc. This process offers the advantage of the Aerojet/Envirogen fluidized-bed process (short residence time) without the disadvantages (high pumping rates, media attrition, maintenance of bed dynamics, affect of flow or process upsets, high nutrient cost, bioaccumulation of toxic co-contaminants, etc.). Compared to a suspended growth process, a fixed-film process may offer a smaller footprint due to the potential for shorter hydraulic residence time (HRT). Another advantage of the Tri-Bio system is that a multi-stage configuration may be optimal for achieving very low or non-detectable perchlorate concentrations. Some ARA studies have shown that perchlorate biodegradation proceeds as a zero order reaction until a low concentration is obtained (~1 ppm) and then reduction rate appears to become concentration dependent (greater than zero order). The Tri-Bio system is configured as a series of back-mixed reactors (up to 4 or 5) and, therefore, is a pseudo plug-flow reactor. This multiple-stage configuration is optimal for achieving high conversion with reaction orders greater than zero. ARA studies have demonstrated that suspended growth and fixed film, multiple-stage systems very effectively reduce perchlorate to non-detectable concentrations in the downstream stages.

The Tri-bio reactor system was inoculated with a microbial consortium that contains the HAP-1 perchlorate-reducing organism. This same culture has performed successfully since 1997 in ARA's full-scale operational prototype at Thiokol. The primary nutrient (carbon source) evaluated in this study is a liquid, commercially available, food byproduct. The Thiokol process has been converted to this nutrient, which is very inexpensive (\$25/ton) for such a high nutrient value material. This study evaluated the reduction of perchlorate in a surrogate RO rejectate (5x concentration) and a more concentrated (10x) rejectate(RO²). The RO² rejectate should represent a worst case situation with respect to nutrient and hydraulic residence time (HRT)

requirements. The less concentrated RO rejectate was evaluated for the potential to reduce HRT and nutrient requirements.

2.3 Background

Applied Research Associates, Inc. (ARA) has been developing perchlorate biodegradation processes for the United States Air Force for over nine years. ARA designed and managed the engineering and start-up of a 3000 gallons-per-day perchlorate biodegradation prototype process that has been in operation since December 1997 at Thiokol's production facility near Brigham City, Utah. This prototype treats a complex brine from ion exchange and potassium precipitation processes that contains high concentrations of perchlorate and nitrate.

In addition to having experience with biodegrading perchlorate in industrial wastewater, ARA has conducted over 25,000 reactor hours of testing on several different groundwater sources from near Henderson, Nevada, using various reactors, reactor configurations, and nutrients. These studies showed that nitrate (NO_3^-), chlorate (ClO_3^-), and chromium (VI), are also reduced by the ARA perchlorate reduction process. In order to drive the reduction reactions, organic nutrient must be added to the reactors to provide a carbon source. Recent nutrient research has enabled ARA to use very low-cost food process byproducts for nutrients. This has resulted in very low operating cost for nutrients and chemicals. On October 4, 1999, ARA was awarded a design and engineering contract by Kerr-McGee Chemical LLC to build a 825 gpm turnkey treatment plant designed to destroy over 2 tons per day of perchlorate in highly contaminated groundwater. The ARA process was selected over competing technologies as the lowest-risk, most cost-effective process. Engineering began October 4, 1999, and startup is projected for the summer of 2000.

Fixed-film reactor systems (fixed and fluid-bed) offer the potential to reduce residence time, reduce process size, and reduce nutrient consumption compared to suspended growth processes. In this study ARA evaluated perchlorate reduction performance in a rejectate from reverse osmosis (RO) in a patented, four-stage, fixed-film process. This process used a fixed plastic support media and has been employed in at least eleven full-scale applications for treating groundwater.

3. Experimental

3.1 The Tri-bio process

A patented reactor system manufactured by Tri-Bio, Inc., was the reactor system used for this study (*U.S. Patents 4,818,404 and 4,940,540*). The laboratory version of this system exactly mimics full-scale, fielded systems. The reactor component consists of four rectangular cells configured adjacent to one another to enable continuous flow from one cell to the next. Each cell is 5 liters in volume and is fitted with fixed plastic media that provides increased surface area for microbial growth. Figure 1 is a schematic of a single reactor cell configuration operating in the aerobic mode. The anaerobic/anoxic configuration is the same with the exception that fresh air is not supplied to the cell, and impeller speed is reduced so headspace gases are not entrained. Figure 2 is a schematic of the 4-cell, laboratory configuration used in this study. RO water and

nutrient were introduced to the first cell only and not to cells 2, 3, or 4. Effluent water proceeds through the system by gravity.

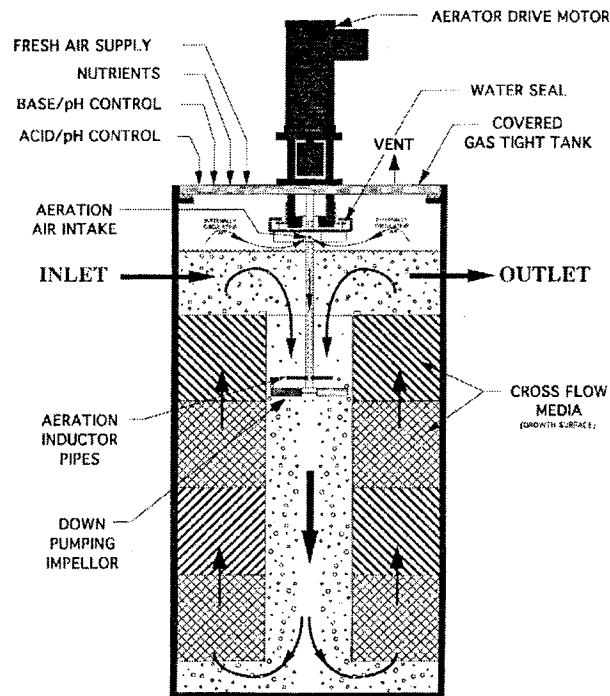


Figure 1. Tri-Bio Reactor Cell Configuration – Aerobic Operation

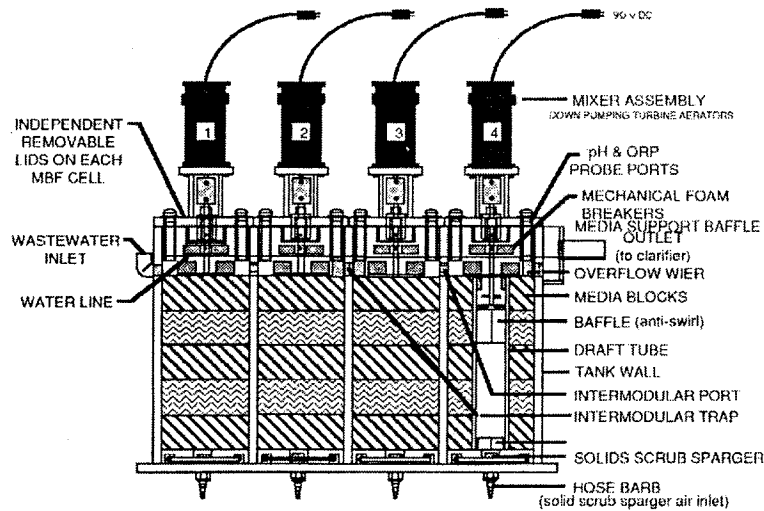


Figure 2. Tri-Bio Multi-Cell Reactor Configuration

The subsystem components consists of pH monitoring and control for each cell, oxidation-reduction potential monitoring, headspace purge (air or nitrogen), reactor gas sparge, primary and secondary clarifiers, and heat exchangers for temperature control. A programmable logic controller (PLC), which controls parameters such as feed rates, sparging cycles, and recycle/wasting rates, operates the entire system. Reactor sparge is designed as a scrubbing cycle that prevents the fixed media from becoming plugged. One of the patented aspects of this process is the impeller/air induction tube configuration shown in Figure 1 that entrains and distributes headspace gas rapidly and uniformly throughout the reactor. Figure 3 shows photographs of the Tri-Bio system at ARA's Panama City Research Facility.

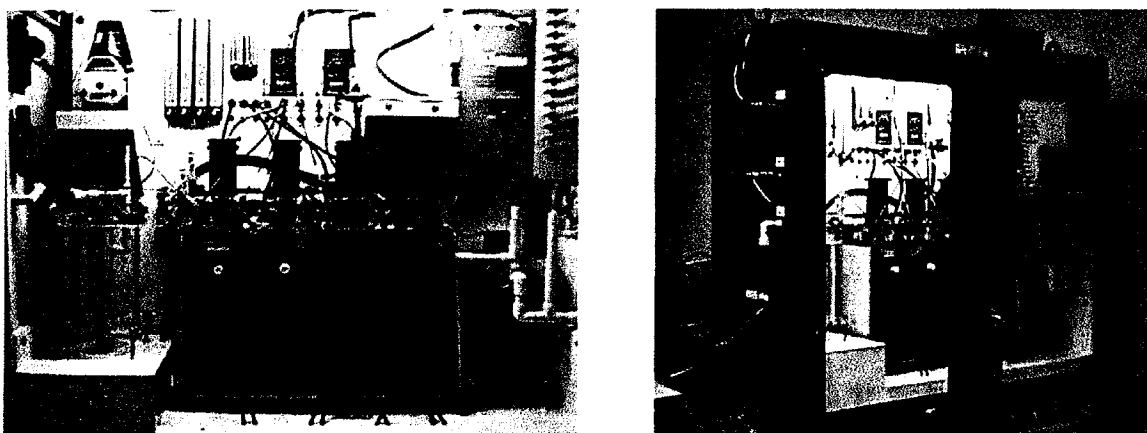


Figure 3. Photographs of the Tri-Bio Reactor System at the ARA Research Facility

For the purpose of this study, the reactor system was operated in an anoxic mode. Therefore, impeller speed was maintained at a low velocity to minimize entrained headspace gas. Temperature control was not provided. The system operated at ambient conditions in a semi-controlled environment between 22 and 28°C. The pH was maintained in each cell between 6.7 and 7.5. Typically, only caustic (NaOH) addition was necessary to maintain pH. Phosphoric acid was also used when necessary. The RO rejectate feed and a concentrated nutrient (carbon source) were delivered separately to the first cell of the reactor system. Effluent from the first cell would gravity flow to cells two, three, and four in turn. Neither clarification nor recycle of biomass were conducted.

5.2 Surrogate RO Rejectate

Because of the large quantity of water required for this study, a surrogate rejectate was prepared. Foster Wheeler Environmental based the composition of surrogate on the analysis of water from wells at the JPL site near Pasadena, California, and RO testing they conducted. The study concluded that perchlorate could be removed by the process when operated with as little as 20% rejectate, i.e., a 5:1 concentration factor. Also, this rejectate could be further concentrated by a factor of two (RO²). Table 1 shows the composition of the groundwater and two surrogate rejectates (RO & RO²) prepared for this study. Particular salts were selected for high solubility,

however, high concentrations of calcium, carbonate, bicarbonate, and sulfate resulted in some precipitation of salts in the feed tank and transfer lines. To mitigate this problem, the amount of sodium sulfate and calcium chloride were reduced to 20 and 10 percent of the predicted amount based on the groundwater concentration in Table 1. ARA has demonstrated in other studies that high concentrations of Ca^{+2} (800 mg/L), and $\text{SO}_4=$ (2000 mg/L) do not inhibit perchlorate reduction performance. In an operational environment, if this particular combination of ions results in precipitation, the salts would likely be removed before further processing.

Table 1. Composition of Groundwater and Surrogate RO Rejectates

Salt Used in Surrogate Prep	Ion of Interest	Concentration, mg/liter		
		Groundwater	RO Surrogate	RO ² Surrogate
KCl	K ⁺	3	15	30
NaClO ₄	ClO ₄ ⁻	1	5	10
NaNO ₃	NO ₃ ⁻	63	315	630
MgCl ₂ ·6H ₂ O	Mg ⁺²	19	95	190
Na ₂ SO ₄	SO ₄ =	27	135	270
NaHCO ₃	HCO ₃ ⁻	155	775	1550
CaCl ₂ ·2H ₂ O	Ca ⁺²	50	250	500
Na ₂ CO ₃	CO ₃ =	1	5	10
Calculated TDS		400	2000	4000

The surrogate rejectate waters were prepared by weighing and adding the required amount of each salt, with the exception of sodium bicarbonate, to a 2 liter flask containing tap water. Sodium bicarbonate was weighed and added to a separate 2 liter flask containing tap water. These flasks were then agitated on stir plates until most of the salts went into solution. Agitation was shut off, precipitate allowed to settle, and then the supernatant was decanted into a 55-gallon drum. Tap water was added to any precipitate left in either flask and agitation/decanting was repeated until all salts had dissolved. Tap water was then added to the 55-gallon drum until the level was approximately 200 liters. Perchlorate, and later chromate, was added to the drum giving the approximate concentration desired and the drum was mixed for 15-30 minutes by recirculating with a centrifugal pump.

5.3 Analytical

Daily and weekly analyses were performed throughout the operation of the Tri-Bio system. These analyses included perchlorate, anions, chemical oxygen demand (COD), and solids. The RO groundwater feed and all four reactor cells were sample points for perchlorate and anion analyses. Perchlorate analysis was conducted daily while anion analysis was conducted every two to three days. Low concentration perchlorate analysis was accomplished using the Dionex method on a Dionex model DX500 ion chromatograph configured with the IonPac AS11 4mm column. The anions were also analyzed using the same Dionex system and the IonPac AS11 HC 4mm column. Nitrite, nitrate, sulfate, phosphate and chloride anions were analyzed. Solids and COD analyses were performed twice a week starting August 19. The solids and COD analyses

were conducted immediately after samples were extracted from cell #4 of the reactor. The solids data includes total solids (TS), total volatile solids (TVS), total suspended solids (TSS), volatile suspended solids (VSS), and total dissolved solids (TDS). COD analysis was performed using HACH COD digestion tubes (0-1500 ppm range) and the HACH COD reactor and method. Total chromium and hexavalent chromium were analyzed by HACH methods 8024 and 8023 respectively on a HACH model DR 2010 spectrophotometer.

5.4 Test Conditions

Test conditions for this study have been divided into two test matrices. Test Matrix I shows conditions during startup. These first six test conditions were plagued by mechanical difficulties experienced during startup caused by prolonged storage of the Tri-Bio reactor system. Because of the startup difficulties, data during this period are not representative and will not be discussed in detail. A more complete summary of the data from Test Matrix I is in Appendix 1.

Table 2. Test Matrix I
Conditions during Inoculation and Start Up

Cond. #	Start Date	Period Days	Hydraulic Residence Time, hr	Nutrient Flow ml/hr	Water Type	Comments/Condition Changes
1	6/8/99	6	24	5.13	RO ²	Inoculation of Tri-bio reactor
2	6/14/99	3	8	5.13	RO ²	Decreased HRT
3	6/17/99	1	8	2.6	RO ²	Decreased nutrient flow rate
4	6/18/99	19	8	7.8	RO ²	Increased nutrient flow rate
5	7/6/99	1	8	7.8	RO ²	Nitrogen sparge programmed to sparge cells throughout day. Continued until 7/28/99
6	7/7/99	7	8	3.9	RO ²	Decreased nutrient flow rate

The second test matrix is provided in Table 3 and summarizes the test conditions following startup. Some operational difficulties were still experienced, however, the data is more reflective of responses to changes in process variables. A more complete summary of data from Test matrix II is provided in Appendix 2.

**Table 3. Test Matrix II
Conditions after Start Up**

Cond. #	Start Date	Period days	Hydraulic Residence Time, hr	Nutrient Flow ml/hr	Water Type	Comments/Condition Changes
7	7/14/99	2	8	3.9	RO ²	Drained, cleaned out biomass and permanently removed plastic media from Cell 1.
8	7/16/99	12	8	3.9	RO ²	Began adding micro-nutrients and H ₃ PO ₄ to the nutrient versus the RO water. Continued throughout study.
9	7/28/99	1	8	3.9	RO ²	Stopped nitrogen sparge permanently as a result of overflow problems in all Cells.
10	7/29/99	5	8	7.7	RO ²	Increased nutrient flow rate.
11	8/3/99	7	4	10.3	RO ²	Decreased HRT and increased nutrient flow rate.
12	8/10/99	2	8	7.7	RO ²	Increased HRT and decreased nutrient flow rate.
13	8/12/99	6	4	10.3	RO ²	Decreased HRT and increased nutrient flow rate.
14	8/18/99	3	4	10.3	RO	Changed feed from RO ² water to RO water. RO water used during remainder of study.
15	8/21/99	3	8	7.7	RO	Increased HRT and decreased nutrient flow rate.
16	8/24/99	3	8	7.7	RO	Increased H ₃ PO ₄ in nutrient. Removed plastic media from cell's 2,3 and 4. Plastic media was never returned to any cell.
17	8/27/99	5	8	7.7	RO	Started nitrogen purge. Purged cells throughout remainder of study.
18	9/1/99	7	8	7.7	RO	Began adding 250 ppb CrO ₄ to RO water.
19	9/8/99	10	4	10.3	RO	Decreased HRT and increased nutrient flow rate.

6. Results and Discussion

6.1 Startup – Test Matrix I

Figure 4 is a summary of feed and effluent (Cell 4) perchlorate concentrations during the startup period. Some condition numbers are labeled along the effluent perchlorate data line. The condition change can be referenced from Table 2. All other details can be found in Appendix 1.

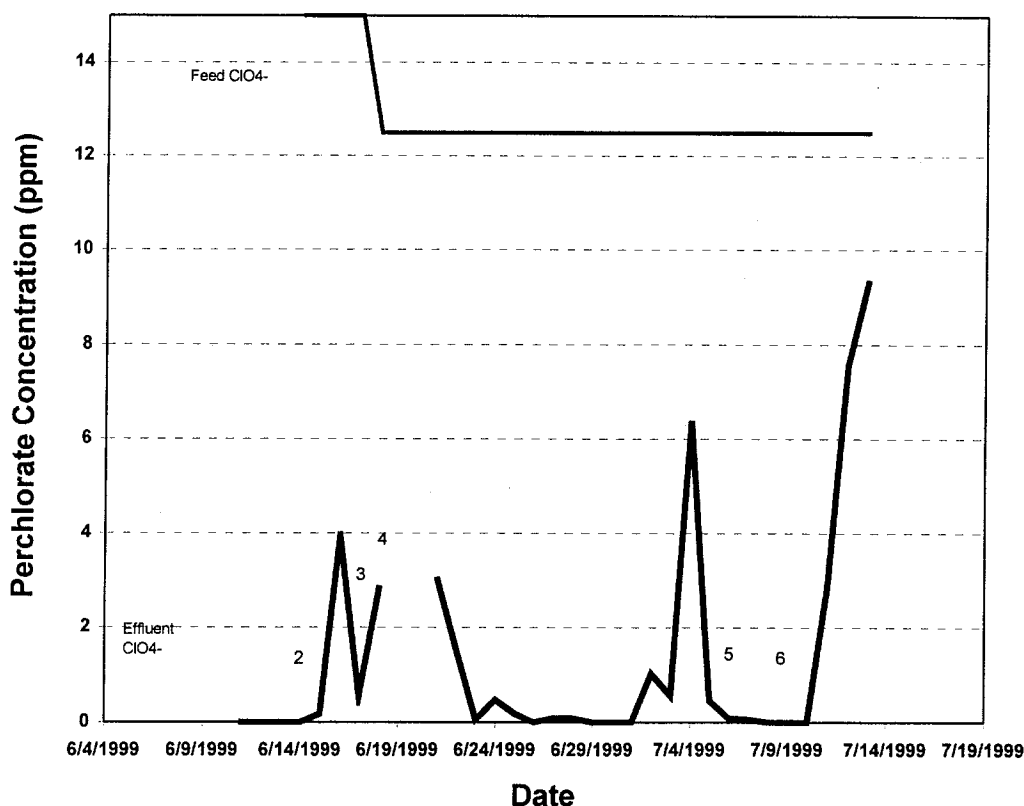


Figure 4. Feed and Effluent Perchlorate Concentrations During Startup Conditions

The Tri-Bio reactor system was inoculated using a mixed culture that ARA maintains in an anaerobic chamber. This culture contains the perchlorate-reducing organism HAP-1. Initial perchlorate concentration was elevated to approximately 40-50 ppm to make inoculation process easier to characterize using an ion selective probe for perchlorate analysis. As seen in Figure 4, the system was readily inoculated as evidenced by nearly complete perchlorate reduction. Perchlorate in the feed was reduced to approximately 12 ppm for the rest of startup. Perchlorate was completely reduced during several periods, however, performance in general was erratic due to many equipment and operational problems related to recommissioning this system that had been in storage for an extended period of time. Problems included:

- Malfunction of the gas scrubbing cycle
- pH control problems
- PLC keypad malfunction
- Loss of nutrient and water flow

The PLC keypad malfunction prevented control of feed rates and scrubbing cycles. This, coupled with the other problems led to excessive biomass accumulation, plugging and

channeling in the fixed media, and unsteady-state conditions in the reactor cells. By the time test Condition 7 was initiated, most of these conditions had been addressed.

6.2 Post Startup – Test Matrix II

Figure 5 summarizes the feed and effluent perchlorate concentrations during the remainder of the test plan, Conditions 7-19. The numbers shown in the figure identifies the start of corresponding test condition changes.

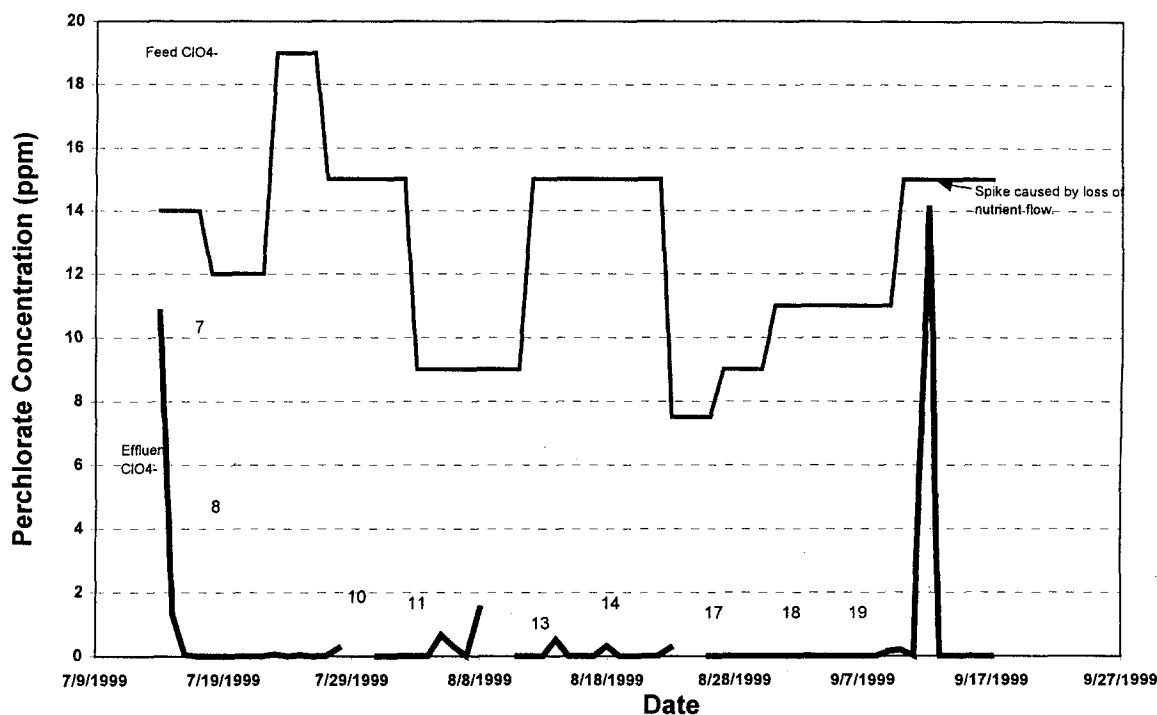


Figure 5. Feed and Effluent Perchlorate Concentrations During Test Matrix II

6.2.1 Discussion of Condition Changes

Figure 5 shows consistent, high perchlorate removal rates were achieved throughout most of the test matrix with the exception of the transition to Condition 7 and one perchlorate spike when nutrient flow was interrupted. Additional details of each condition are provided in the following text.

- Condition 7:** Cell 1 had accumulated large quantities of biomass because of failure of the nitrogen sparge-and-scrub cycle which is designed to reduce biomass accumulation by periodically dislodging it from the plastic media. This problem was compounded by addition of the entire nutrient directly into Cell 1. The cell was so dense with bio-mass that agitation

was severely impaired resulting in poor pH control, limited nutrient mixing, and interference with nutrient transferal into Cells 2, 3, and 4. Therefore, perchlorate performance was adversely affected. In order to overcome this situation, Cell 1 was drained and the plastic media and excess biomass was removed. The plastic media was never returned to Cell 1 which, in effect, converted Cell 1 to a suspended-growth, continuous-stirred-tank-reactor (CSTR).

- **Condition 8:** Initially, micro-nutrients and phosphoric acid were added directly to the surrogate RO² water. However, possible precipitation of nutrients with salts in the RO² water caused a concern that proper nutrients were not getting to the reactor. In order to mitigate this possibility, the micro-nutrients and phosphoric acid were added to the macro-nutrient for the remainder of the study.
- **Condition 9:** The nitrogen sparge-and-scrub cycle appeared limited in preventing excess biomass buildup in Cells 2, 3, and 4. In addition, the sparge would periodically cause all of the cells to overflow. As a result, the nitrogen sparge was discontinued and agitation was increased to help dislodge excess biomass and prevent flow obstruction in the fixed media.
- **Condition 10:** The nutrient flow rate was increased from 3.9 ml/hr to 7.7 ml/hr.
- **Condition 11:** The hydraulic residence time (HRT) was decreased from 8 hours to 4 hours and the nutrient flow rate was increased from 7.7 ml/hr to 10.3ml/hr. During this test, foaming in the reactors caused the system to overflow. Feeds to the reactors were temporarily suspended.
- **Condition 12:** This was a recovery condition from the upset caused in condition 11. The HRT was increased from 4 hours to 8 hours and the nutrient flow rate was decreased from 10.3 ml/hr to 7.7 ml/hr during this 2-day recovery time.
- **Condition 13:** The HRT was decreased from 8 hours to 4 hours and the nutrient flow rate was increased from 7.7 ml/hr to 10.3 ml/hr.
- **Condition 14:** The HRT and nutrient flow rate remained the same as condition 13, but the surrogate water formulation was changed from RO² to RO surrogate water. The RO surrogate water was used throughout the remainder of the study.
- **Condition 15:** Excess biomass was accumulating in cells 2, 3, and 4. The HRT was increased from 4 hours to 8 hours and the nutrient flow rate was decreased from 10.3 ml/hr to 7.7 ml/hr.
- **Condition 16:** The biomass build-up in cells 2, 3, and 4 became excessive. The cells were drained and the plastic media removed. For the remainder of this test matrix, the reactor system functioned as a series of CSTRs. Also, the phosphoric acid concentration in the nutrient was increased to ensure adequate phosphorus addition.

- **Condition 17:** Initiated a nitrogen purge in the headspace of each reactor cell. The reactor top closure has ports for pH and ORP probe measurements. These ports had previously allowed oxygen to enter into all reactor cells. When impeller speed was increased to prevent excess biomass accumulation (Condition 9), headspace air was entrained into the reactors causing atmospheric oxygen to compete with perchlorate as the terminal electron acceptor. In addition to the nitrogen sparge, probe ports were covered with parafilm to minimize air infiltration.
- **Condition 18:** Began adding approximately 250 ppb CrO_4 to the RO water. Actual measurements of chromium in the feed water were 120 ppb total chromium (137 calculated) and 80 ppb as chromium (VI).
- **Condition 19:** Decreased HRT and increased nutrient flow for a final study at 4 HRT.

6.2.2 Discussion of Perchlorate Results

Figure 6 shows the perchlorate analysis in Cell 4 during test Condition 8. These analyses were obtained by the Dionex ion chromatography method.

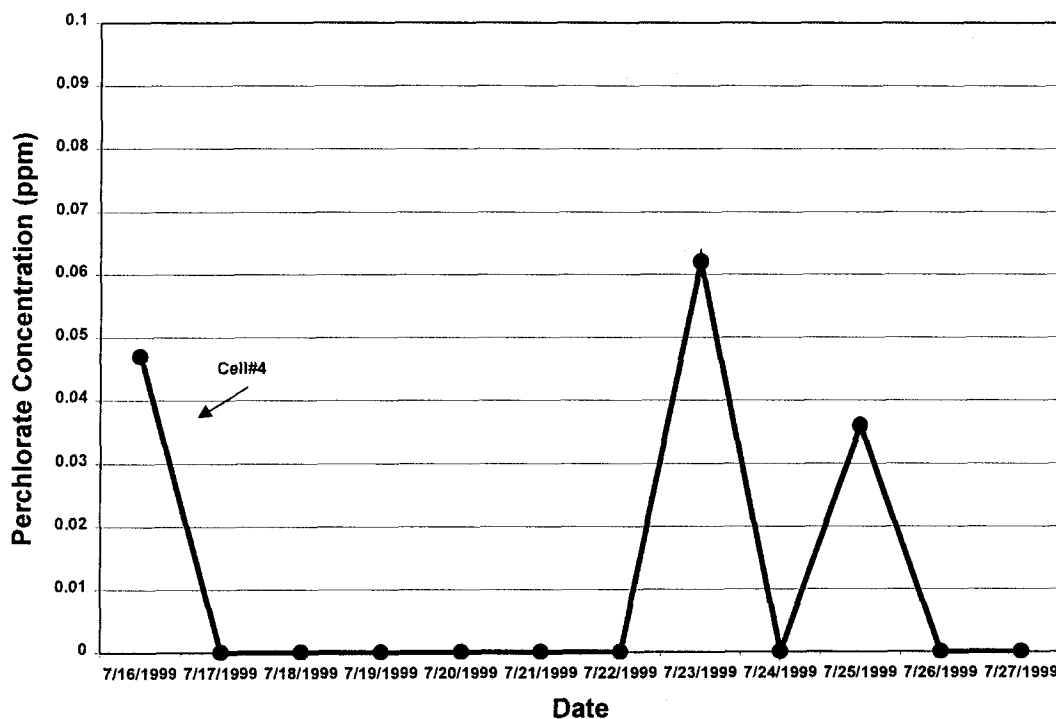


Figure 6. Perchlorate Analysis from Cell 4 During Test Condition 8

The slight perchlorate excursion on the 23rd could have been the result of the process adapting to a freshly prepared batch of RO water with higher perchlorate concentration (19 ppm). However, even these excursions were very low (40-60 ppb). Nine of the 12 days of analyses plotted in Figure 6 were below the detection limit (plotted as zero).

Figure 7 shows that there was a perchlorate excursion after reducing residence time to 4 hours from 8 hours. However, plugging and gas sparging problems caused some reactor overflows and spills. Also, nutrient feed problems were still being experienced so the excursion cannot be fully attributed to the reduced residence time.

Figure 8 shows the results of a second attempt to operate a 4-hour HRT (Conditions 13 & 14). Condition 14 shows the transition to RO water from the more concentrated RO² water. Restarting RO feed water after a mechanical problem had interrupted flow for several hours could have caused the excursion on the 14th. One other excursion occurred on the 18th that could have been the result of channeling and plugging of the media with biomass.

Figure 9 shows perchlorate results for the last four conditions tested (16-19). This period represents suspended-growth (CSTR) operation with RO water feed. A nitrogen headspace purge began with Condition 17 and very stable performance was observed for 14 days of operation. Figure 9 shows that perchlorate was below the detection limit in Cell 4. Chromium addition began with Condition 18. Condition 19 was a 4-hour HTR. The slight increase in perchlorate on September 9 and 10 was attributed to a temporary nutrient feed disruption. On September 12th almost no perchlorate reduction was observed when nutrient flow was interrupted for an extended period. The reactor was re-inoculated due to fear that too much of the active culture had been washed out of the system. Feed to the reactor was continued at the 4-hour residence time and the system dramatically recovered in one day.

Figure 10 shows the same time period that was shown in Figure 9. In Figure 10 the perchlorate in all four cell was plotted. As one would expect there was periods of time when some perchlorate could be detected in the first or second cell, however, cells three and four were almost always below the detection limit. Condition 19 demonstrated that a two-stage process, operated at a hydraulic residence time as short as 1-hour in each stage, could achieve acceptable performance.

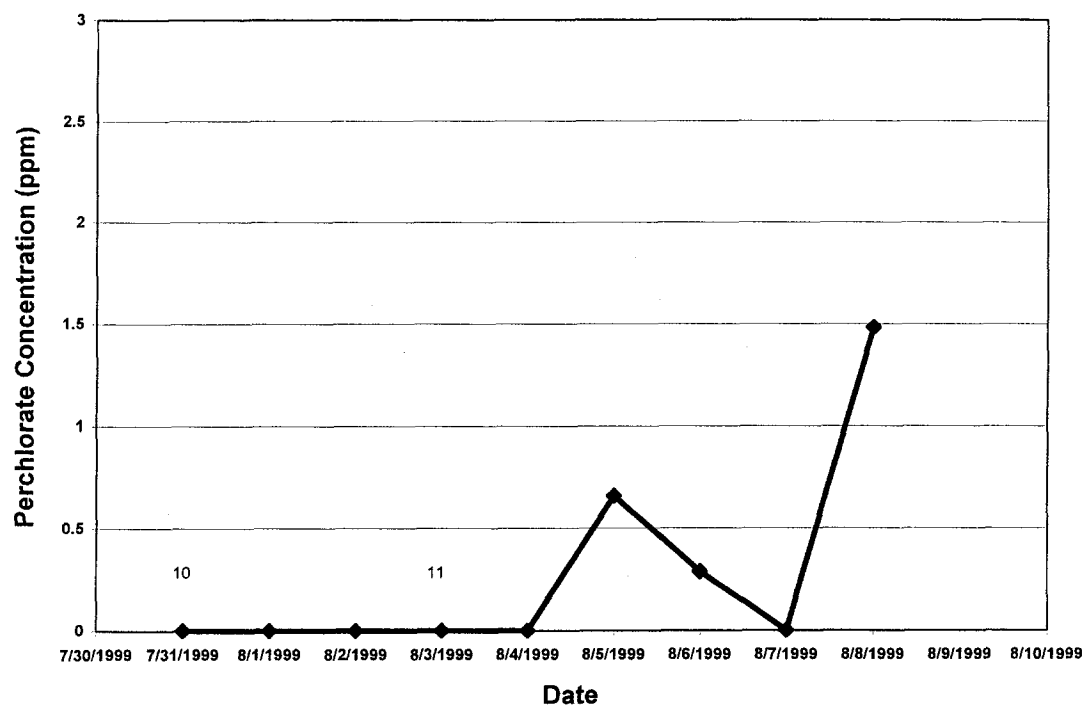


Figure 7. Perchlorate Analysis from Cell 4 During Conditions 10 & 11

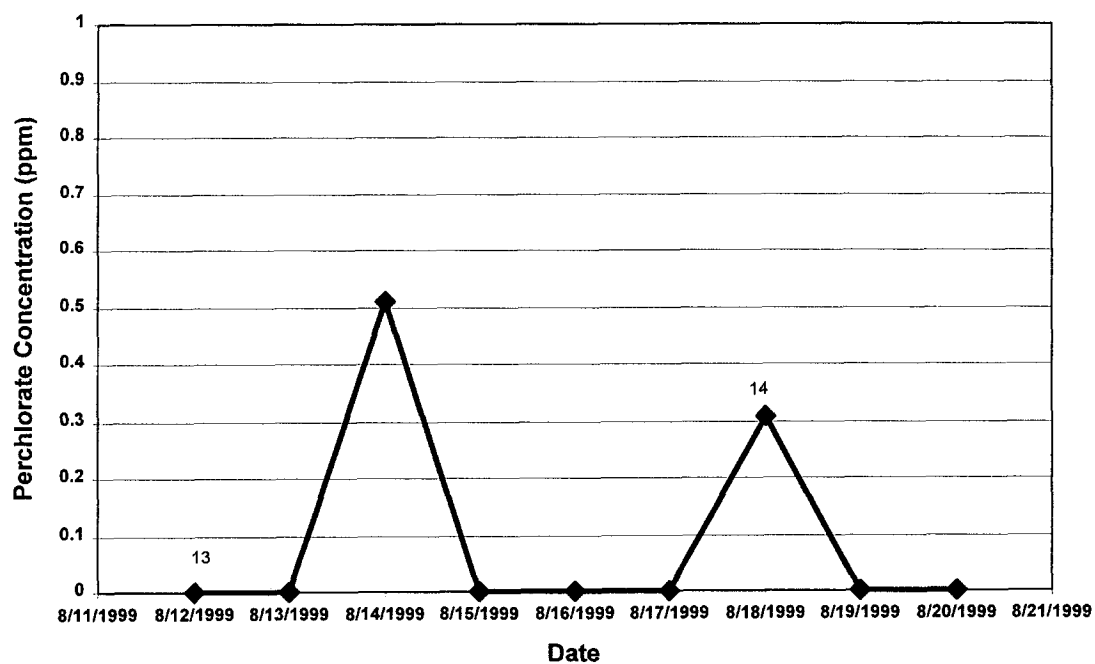


Figure 8. Perchlorate Analysis from Cell 4 During Conditions 13 & 14

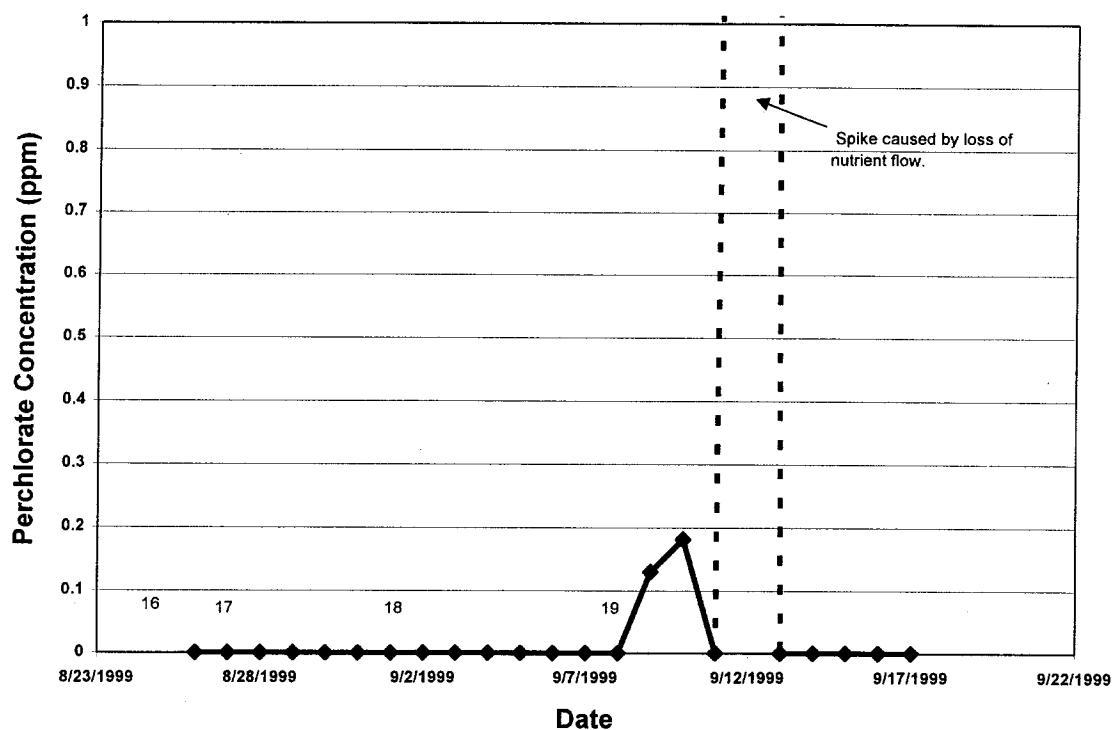


Figure 9. Perchlorate Analysis from Cell 4 During Conditions 16-19

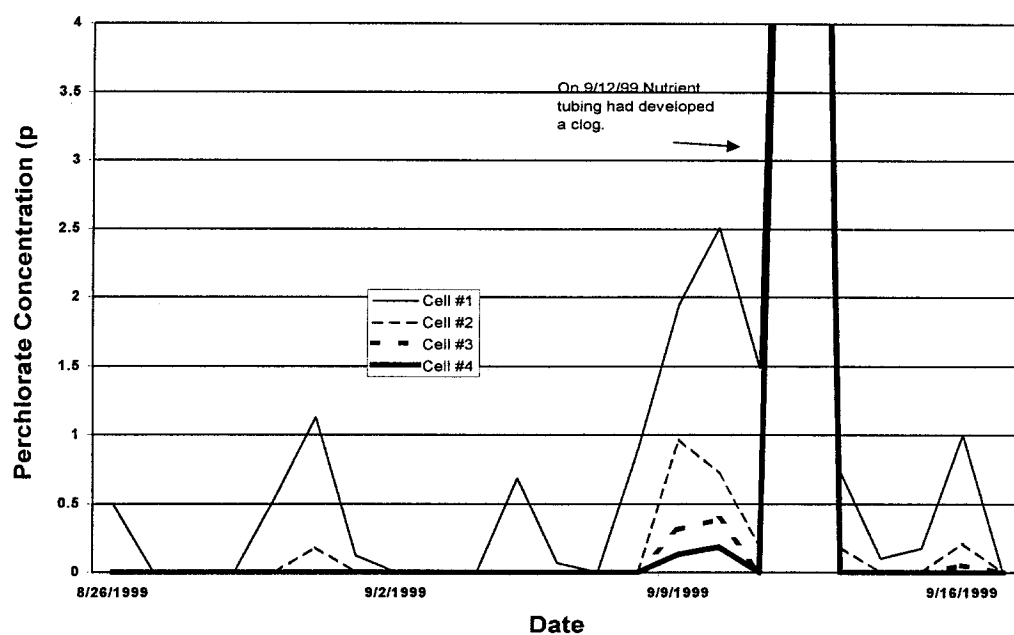


Figure 10. Perchlorate Analyses from All Cells During Conditions 16-19

6.2.3 Discussion of Anions Results

Samples for anions were analyzed every two to three days. The anions analyzed for were nitrite, nitrate, sulfate, phosphate and chloride. The complete anion data is provided in Appendix 3. Figure 11 shows nitrate reduction performance in all four cells over the entire test matrix II period (Conditions 7 – 19). Nitrate reduction is an important indicator because mimics perchlorate reduction. Other studies have shown that nitrate is typically reduced completely before perchlorate can be totally reduced. Nitrite is formed as an intermediate reduction product and is detectable in low concentrations especially during startup and during periods when nitrate is not completely reduced. After the culture has fully adapted to the nitrogen level of the feed, and complete nitrate reduction was observed, complete denitrification was achieved with no nitrite detected.

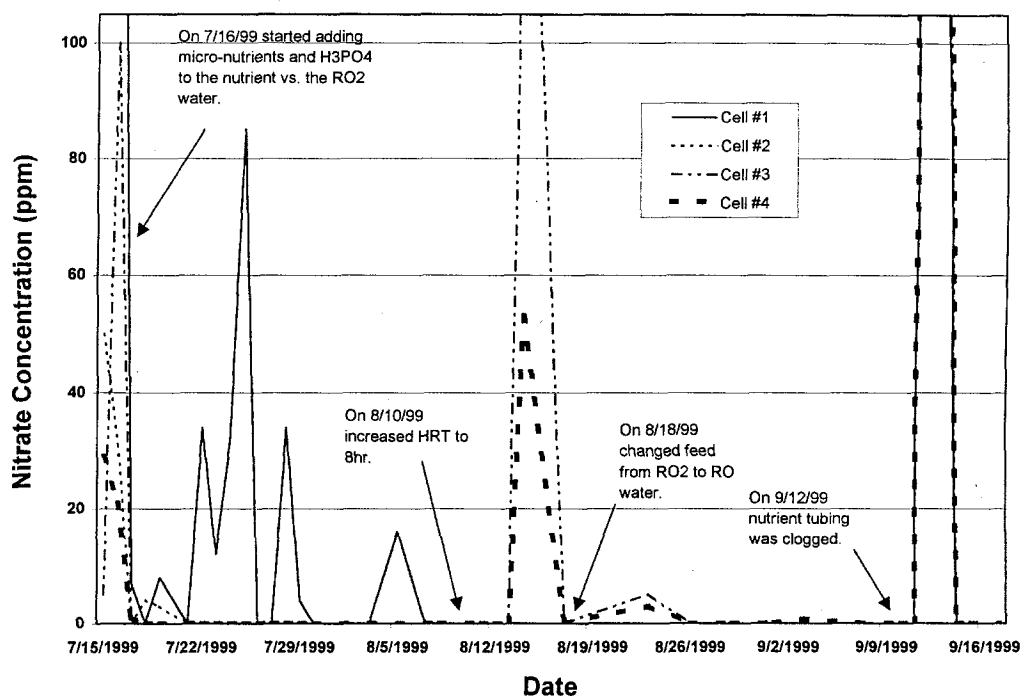


Figure 11. Nitrate Reduction Performance

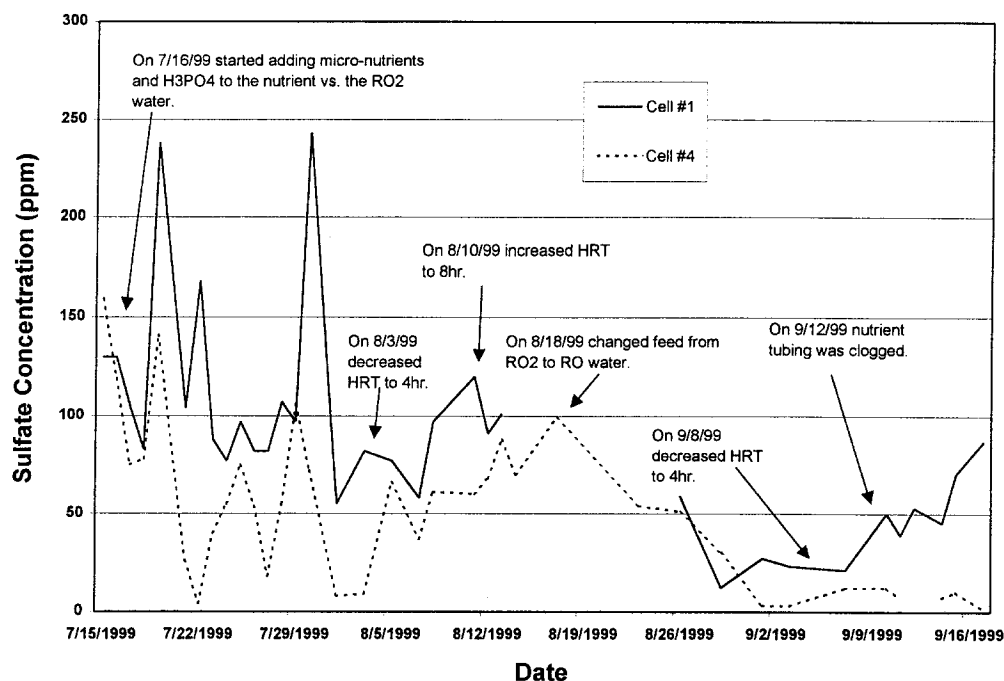


Figure 12. Sulfate Analysis

Figure 12 shows sulfate analysis for Cells 1 and 4. Some sulfate reduction was evident. Sulfate reduction was even more evident at the end of the study when a nitrogen purge was initiated due to the strict anaerobic environment that was created. Sulfate reduction can be almost completely prevented by controlling the oxidation-reduction potential or by maintaining an anoxic environment. Perchlorate reduction without sulfate reduction has been demonstrated in theory and practice. The sulfate data is presented with the anion analyses in Appendix 3.

6.2.4 Discussion of Solids Analysis

Figure 13 shows the total suspended solids (TSS) analyses. Samples for solids were mainly pulled from Cells 1 and 4. Analyses were conducted immediately after taking the sample. In addition to TSS, the following were also determined: TVS, TS, TSS, VSS, and TDS. All of these parameters vary proportionally to TSS. The TSS is representative of the biomass suspended in the process water. The low TSS observed near the end of the study is an important indicator for the magnitude of post treatment necessary for BOD and TSS reduction if necessary. Post treatment may be required before discharge under a NPDES Permit. All of the solids data is presented in Appendix 4.

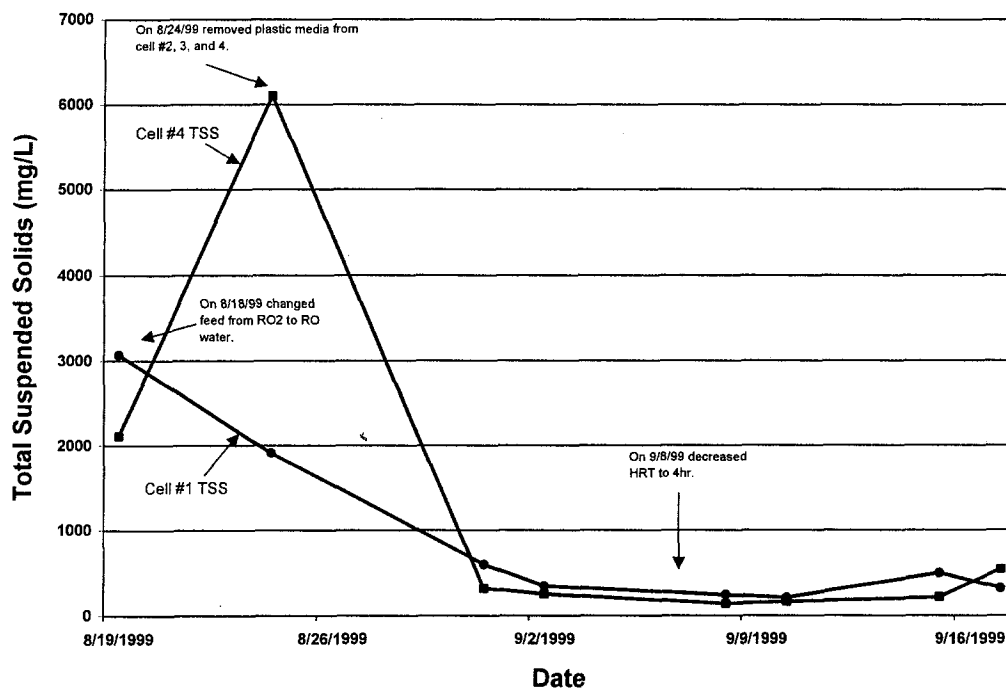


Figure 13. Total Suspended Solids (TSS) Analysis

6.2.5 Discussion of Chemical Oxygen Demand (COD) Results

Figure 14 shows the chemical oxygen demand for samples taken from Cell 4. The estimated biological oxygen demand (BOD) was consistently below 1000 mg/L. Other optimization studies have measured BOD under similar conditions in a CSTR process and have shown that much lower BODs (<300 mg/L) can be obtained. This may permit direct discharge of this effluent to a conventional sanitary sewage treatment process without post treatment for BOD reduction. The actual COD data is presented in Appendix 5.

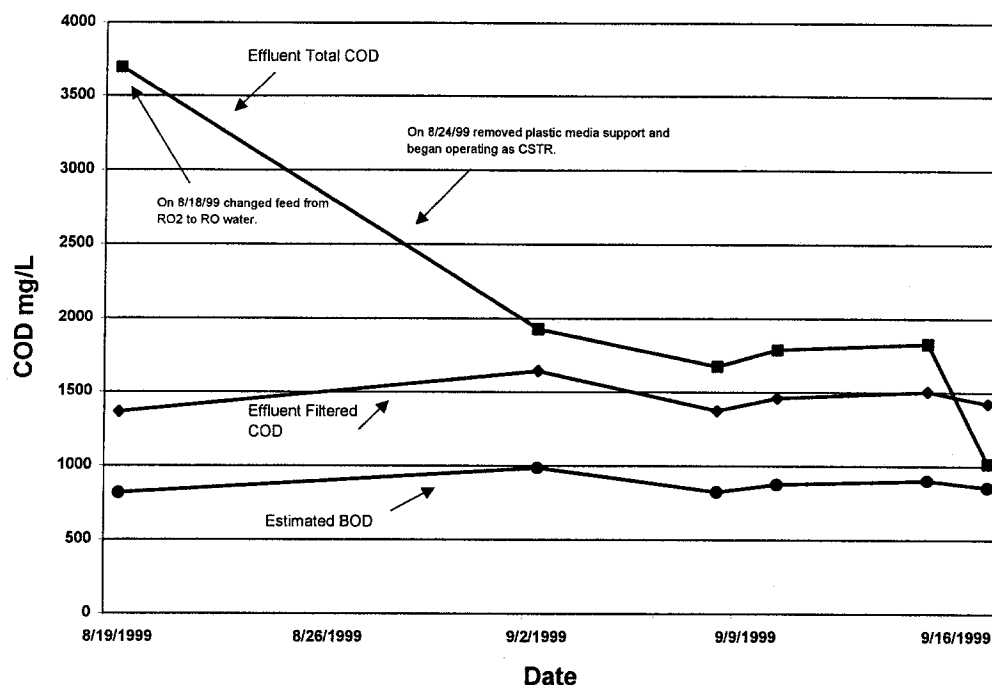


Figure 14. COD and BOD Data for Conditions 14 - 19

6.2.6 Chromium Reduction Test

Reduction of a potential co-contaminant, chromium (VI), was also evaluated. 120 ppb of chromium was added to RO rejectate feed water as chromate ($\text{CrO}_4^{=}$). This limited test showed that this process simultaneously reduced chromium (VI), measured at 80 ppb in the feed, to below the detection limit of 10 ppb.

7 Conclusion

7.1 Perchlorate Reduction Performance

During steady-state operation, perchlorate was routinely reduced from approximately 10 parts-per-million (ppm) in the feed to below the detection limit for ion chromatography. In addition to complete perchlorate reduction, nitrate and chromium (VI) were also completely reduced by the ARA process. Some perchlorate excursions were observed; however, they were always the result of startup transients, condition changes or equipment problems (flow interruptions, loss of

sensors, etc.). There was no indication that anything in the RO water would inhibit complete perchlorate reduction. The low-cost, commercially available nutrient used in these studies performed very well. The same nutrient has been used operationally in the Thiokol prototype system since May 1999. The Thiokol system performance with this nutrient has met or exceeded the performance demonstrated by previous nutrients, i.e., brewer's yeast and cheese whey.

7.2 Reactor Operation – Fixed-Film vs Suspended-Growth

One of the objectives of this study was to determine the benefits of a fixed-film process compared to a suspended growth process for perchlorate reduction. The premise that a fixed-film process could achieve significant reductions in residence time was not borne out by this short study. There may be several reasons for this result:

- The ARA process (microbial culture and nutrients used) may not be as well adapted for perchlorate reduction in a fixed-film environment.
- The particular reactor system used in this study may not be the optimal fixed-film configuration.
- The Tri-Bio process may not have been operated in an optimal manner, i.e., the quantity and type of nutrient addition, proper operation of the gas scrubbing cycle, proper temperature and pH, proper agitation, and anoxic maintenance of an environment.
- The Tri-Bio system was not designed for high BOD streams. Since high BOD is used to drive the perchlorate reduction reaction, too much nutrient may have resulted in excessive film growth leading to plugging and channeling.

Two factors that contributed to the difficulty of operation experienced and the variability in the data were the competing variables of agitation (impeller speed) and maintenance of an anaerobic or anoxic environment. Because of the rapid film growth, impeller speed was increased to help prevent plugging. However, the very nature of the Tri-Bio design is to provide an efficient way to introduce and mix the headspace gas (air) throughout the reactor for aerobic BOD reduction. Since the reactor cells were not well sealed, some air was intermittently, if not continually, introduced to the process. This air competed with and prevented efficient perchlorate reduction. When a small nitrogen purge was initiated (conditions 17-19) performance became very stable and consistent. The only instances of elevated perchlorate during this time were caused by loss or reduction of nutrient flow.

On the other hand, when the system was operated as a suspended growth process, very short residence times were achieved. When the process was operated at a 4-hour residence time overall, the residence time for each individual cell was only one hour. During steady-state operation for conditions 17-19, the perchlorate was always completely reduced in the first two cells. This is significant for several reasons:

- Demonstrates that the perchlorate-reducing culture will reproduce rapidly under proper conditions in a suspended-growth process and will not "wash out" of the reactor.
- A suspended-growth (CSTR) process will effectively reduce perchlorate with a residence time as short as 1-2 hours.

- Suspended-growth operation in the growth phase of a microbial culture may be the preferred mechanism perchlorate reduction. It is possible that this is also the mechanism for perchlorate reduction in other, short residence time, fixed-film processes.

7.3 Operational Considerations

Full-scale application of a suspended growth process for the destruction of perchlorate in rejectate from the reverse osmosis of groundwater is practical from operational and cost considerations. The very short residence times obtainable in suspended-growth processes will result in equipment size and space requirements comparable to fixed-film processes. In addition, the suspended-growth CSTR process is very easy to operate and maintain. Multiple-stage configuration can ensure perchlorate reduction to below the analytical detection limit. When feed perchlorate concentrations are measurable by ion selective electrodes (>5 ppm), a multiple-stage, fail-safe process can be configured that would mitigate against any perchlorate discharge.

Operating costs for the ARA process are projected to be \$60,000 per year for a system that can treat a 100 gallon-per-minute (gpm) RO rejectate stream containing 10-100 ppm of perchlorate. Operating cost estimate includes the carbon source (a nutrient that is a commercially available food byproduct costing \$25 per ton), other micro-nutrients, and sodium hydroxide required for pH control. The nutrient added to the feed water increases the biological oxygen demand (BOD) of the effluent water to approximately 300 mg/L. In many cases, it may be permissible to discharge this effluent directly to a sewage treatment plant or reduce the BOD in a post treatment step before discharge. At Thiokol Corporation, near Brigham City, Utah, ARA's operational prototype has been destroying 500-5,000 ppm of perchlorate in a process continuously since December 1997. This effluent is treated at the local sewage treatment plant and discharged under a NPDES permit. On October 4, 1999, ARA was awarded a design and engineering contract by Kerr-McGee Chemical LLC to build a 825 gpm turnkey treatment plant designed to destroy over 2 tons per day of perchlorate in highly contaminated groundwater. The effluent from this process will be treated before discharge under a NPDES permit. The ARA process is uniquely designed to completely reduce perchlorate in highly contaminated water. This process is inherently stable which affords significant flexibility in operation. In addition, very low operating and maintenance costs have been demonstrated because of the process design is not complex and low-cost nutrients perform very well.

8 Appendices

Appendix 1

Conditions during Inoculation and Start Up

Date	Condition	HRT	Flow Rates		Perchlorate, mg/L					Comments
	Number	hours	RO2 mL/min	nutrient mL/hr	Feed	Cell 1	Cell 2	Cell 3	Cell 4	
6/8/1999	1									Added initial inoculum to reactors (5 liters) and batched
6/9/1999	1									Added additional inoculum (at ~1000) and began flowing nutrient and RO2 water at ~1700
6/10/1999	1	24	13.9	5.13	50					RO2 water contained 50 mg/L ClO4 as AP
6/11/1999	1	24	13.9	5.13	50		5.835		ND	
6/12/1999	1	24	13.9	5.13	50				ND	
6/13/1999	1	24	13.9	5.13	50				ND	
6/14/1999	2	8	41.7	5.13	15	0.651	ND		ND	made up 200 L in 55 gal drum (~10ppm), changed HRT to 8 hrs
6/15/1999	2	8	41.7	5.13	15	2.06	1.65	1.26	0.177	
6/16/1999	2	8	41.7	5.13	15	2.209	4.102	4.391	3.947	* nutrient feed line out of container, reprimed and pumped some in, power off for about 2 hrs (11-1)
6/17/1999	3	8	41.7	2.6	15	1.595	0.979	0.873	0.542	Reduced nutrient feed to 2.6 ml/hr (logic was on for 69 sec changed to 35 sec)
6/18/1999	4	8	41.7	7.8	12.5	4.313	3.749	3.013	2.811	changed nutrient flow back up (logic set to on for 105 sec) ~ 7.8 ml/hr
6/19/1999	4	8	41.7	7.8	12.5					
6/20/1999	4	8	41.7	7.8	12.5					
6/21/1999	4	8	41.7	7.8	12.5	6	4	3	3	
6/22/1999	4	8	41.7	7.8	12.5	2.6			1.5	
6/23/1999	4	8	41.7	7.8	12.5	1.8	0.09	0.05	0.05	Dionex data using high ClO4 method. Setup to sparge throughout the day
6/24/1999	4	8	41.7	7.8	12.5		1.782	0.962	0.473	let sparge overnight and had spill..
6/25/1999	4	8	41.7	7.8	12.5	3.115	0.352	0.193	0.186	
6/26/1999	4	8	41.7	7.8	12.5	0.903	ND	ND	ND	Fluctuated speed of agitator attempting to loosen solids, will replace solenoids for N2 sparge
6/27/1999	4	8	41.7	7.8	12.5	4.274	0.395	0.095	0.086	
6/28/1999	4	8	41.7	7.8	12.5	5.129	2.667	0.064	0.079	cell 1 is basically clogged due to biomass build-up. Mixing limited.
6/29/1999	4	8	41.7	7.8	12.5	0.909	0.372	0.084	ND	
6/30/1999	4	8	41.7	7.8	12.5	1.27	0.123	ND	ND	Drained system, repaired sparge system and cleaned cell 1, put larger media in cell 1 & 2. Started back flowing @2:30
7/1/1999	4	8	41.7	7.8	12.5	2.292	0.314	ND	ND	
7/2/1999	4	8	41.7	7.8	12.5	7.353	4.101	1.765	1.021	In attempt to curb biomass growth diluted NUTRIENT to 50% in order to reduce NUTRIENT concentration. (Keypad not responding.)
7/3/1999	4	8	41.7	7.8	12.5	1.941	1.179	0.539	0.559	
7/4/1999	4	8	41.7	7.8	12.5	7.156	6.664	6.583	6.392	Tube feeding system nutrient had come out of NUTRIENT nutrient flask.
7/5/1999	4	8	41.7	7.8	12.5	1.724	1.009	0.535	0.457	N2 tank turned off overnight!
7/6/1999	5	8	41.7	7.8	12.5	1.339	0.294	0.128	0.085	N2 sparge on.
7/7/1999	6	8	41.7	3.9	12.5	1.621	0.208	0.174	0.059	
7/8/1999	6	8	41.7	3.9	12.5	1.815	0.207	ND	ND	
7/9/1999	6	8	41.7	3.9	12.5	1.43	0.123	ND	ND	Keypad repaired
7/10/1999	6	8	41.7	3.9	12.5	1.704	0.064	ND	ND	
7/11/1999	6	8	41.7	3.9	12.5	3.591	3.361	3.476	2.851	
7/12/1999	6	8	41.7	3.9	12.5	9.069	8.563	7.947	7.549	NUTRIENT feed rate low
7/13/1999	6	8	41.7	3.9	12.5	ND	8.5	8.5	9.3	Began feeding concentrated NUTRIENT again; 47 sec on, 528 off

Appendix 2. Test Matrix II Perchlorate Data

	Condition	Oxidation/	HRT	Flow Rates		Perchlorate, mg/L					Comments
Date	Number	Reduction	hours	RO2	Nutrient	Feed	Cell 1	Cell 2	Cell 3	Cell 4	
		mV		mL/min	mL/hr						
7/14/1999	7		8	41.7	3.9	14	10.89	11.1	10.46	10.81	Nutrient feed rate low - change to #14 tubing. Drained, cleaned out biomass and removed plastic media from cell #1.
7/15/1999	7	-29	8	41.7	3.9	14	7.29	5.45	1.74	1.3	
7/16/1999	8	-12	8	41.7	3.9	14	8.326	2.244	0.146	0.047	Turned on acid and base pumps ~ 3:30pm
7/17/1999	8	-13	8	41.7	3.9	14	5.92	0.819	0.048	ND	Changed nutrient to 10% trace metals and 1% H3PO4 ~ 3:00pm
7/18/1999	8	-12	8	41.7	3.9	12	1.832	0.708		ND	Started new drum of RO water ClO4 = 12ppm Tubing in the RO water was found floating, had not pumped any water
7/19/1999	8	-35	8	41.7	3.9	12	0.027	ND	ND	ND	
7/20/1999	8	-19	8	41.7	3.9	12	1.957	0.127	ND	ND	
7/21/1999	8	-13	8	41.7	3.9	12	9.047	1.889	0.144	ND	
7/22/1999	8		8	41.7	3.9	12	ND	ND	ND	ND	RO feed water stopped pumping - pump broken. Started back up with a new pump and set flow rate to 41.5ml/min (8hrt) N2 set not working properly and turned off.
7/23/1999	8	-11	8	41.7	3.9	19	10.014	5.279	0.792	0.062	
7/24/1999	8	-9	8	41.7	3.9	19	9.88	4.393	0.862	ND	New RO water ClO4 = 19ppm
7/25/1999	8	-8	8	41.7	3.9	19	11.588	6.056	1.27	0.036	Repaired N2 set and turned back on ~ 2:30pm. Set to come on every 1320 sec. Redox down to -49
7/26/1999	8	-6	8	41.7	3.9	19	9.402	5.637	1.374	ND	
7/27/1999	8	-19	8	41.7	3.9	15	4.928	2.321	0.301	ND	New RO water ClO4 = 15ppm
7/28/1999	9	-6	8	41.7	3.9	15	9.734	7.85	2.696	0.252	Turned the N2 sparge off at 10:15am - sparge causing cells to overflow.
7/29/1999	10	-3	8	41.7	7.7	15					Changed the Nutrient influent flow from 3.9ml/hr\ to 7.7 mL/hr
7/30/1999	10	-51	8	41.7	7.7	15					
7/31/1999	10	-50	8	41.7	7.7	15	0.337	nd	ND	ND	Cell 4 pH above the high set point. Re-filled acid container with 5N HCl.
8/1/1999	10	-54	8	41.7	7.7	15	1.548	0.036	ND	ND	
8/2/1999	10	-50	8	41.7	7.7	15	ND	ND	ND	ND	Flow rate increased to ~83ml/min giving a 4hrt
8/3/1999	11	-50	4	83.4	10.3	9	0.812	0.493	0.0562	ND	
8/4/1999	11	-49	4	83.4	10.3	9	1.009	0.509	0.08774	ND	Overflow coming out of cell #4
8/5/1999	11	-20	4	83.4	10.3	9	5.319	2.6	1.725	0.659	Increased nutrient flow by 1/3 (15 sec on, 149 sec off)
8/6/1999	11	-34	4	83.4	10.3	9	5.355	2.993	1.399	0.286	
8/7/1999	11	-31	4	83.4	10.3	9	1.013	0.131	0.499	nd	Foamy overflow - added antifoam to Cells 2 & 3 and nutrient nut.
8/8/1999	11	-43	4	83.4	10.3	9	4.347	0.743	1.149	1.482	
8/9/1999	11	-23	4	83.4	10.3	9					Spill - Shut off pumps for the day.
8/10/1999	12	-34	8	41.7	7.7	9					
8/11/1999	12	-43	8	41.7	7.7	9	0.150	ND	ND	ND	Did not pull samples because pumps were off. Started pumps at 4 PM.
8/12/1999	13	-48	4	83.4	10.3	15	ND	ND	ND	ND	7 AM Foamy overflow and pH of all cells ~9. Turned off agitation and pumps 230 PM Turned agitators on. 330 PM Started pumps at longer HRT and nutrient flow15 sec on, 225 sec off
8/13/1999	13	-49	4	83.4	10.3	15	ND	ND	0.065	ND	
8/14/1999	13	-43	4	83.4	10.3	15	ND	ND	1.632	0.510	Tubing out of RO water. Adjusted tubing.
8/15/1999	13	-36	4	83.4	10.3	15	ND	ND	2.267	ND	230 PM rotated tubing and adjusted flow rate to ~83 mL/min nutrient 15 sec on, 149 off
8/16/1999	13	-43	4	83.4	10.3	15	ND	ND	ND	ND	Cleaned out acid tank and refilled with 8.5% H3PO4
8/17/1999	13	-32	4	83.4	10.3	15	ND	ND	ND	ND	RO Water tubing came out of drum - taped down.
8/18/1999	14	-44	4	83.4	10.3	15	ND	ND	0.453	0.306	Changed RO Water tubing
8/19/1999	14		4	83.4	10.3	15	ND	ND	0.152	ND	
8/20/1999	14	-52	4	83.4	10.3	15	0.368	ND	0.246	nd	Started new RO water. Instead of RO2 it is now just RO.
8/21/1999	15	-36	8	41.7	7.7	15	nd	ND	ND	ND	
8/22/1999	15	-44	8	41.7	7.7	15	ND	ND	0.171	ND	Overflow. Shut off pumps for a few hours. Cleaned out RO Water drum.
8/23/1999	15	-46	8	41.7	7.7	7.5	ND	ND	0.345	0.241	Changed to 8 hrt - set flowrate to ~41ml/min. Set nutrient timer = on 15sec and off 225sec.
8/24/1999	16	-49	8	41.7	7.7	7.5		ND			Slight spill, leak from ground effluent port on cell #4, needs caulk. Solids look very high in samples (biomass high). Solids (biomass) are very high. Need to remove some solids and or take out plastic media.
8/25/1999	16	-30	8	41.7	7.7	7.5					

Appendix 2. Test Matrix II Perchlorate Data

Date	Condition	Oxidation/	HRT	Flow Rates		Perchlorate, mg/L				
	Number	Reduction	hours	RO2	Nutrient	Feed	Cell 1	Cell 2	Cell 3	Cell 4
		mV		mL/min	mL/hr					
8/26/1999	16	-28	8	41.7	7.7	7.5	0.496	nd	nd	nd
8/27/1999	17	-27	8	41.7	7.7	9	nd	nd	nd	nd
8/28/1999	17	-26	8	41.7	7.7	9	ND	ND	ND	ND
8/29/1999	17	-40	8	41.7	7.7	9	ND	ND	ND	ND
8/30/1999	17	-29	8	41.7	7.7	9	0.546	nd	nd	nd
8/31/1999	17	-28	8	41.7	7.7	11	1.127	0.181	nd	nd
9/1/1999	18	-27	8	41.7	7.7	11	0.119	ND	ND	ND
9/2/1999	18	-28	8	41.7	7.7	11	ND	ND	ND	ND
9/3/1999	18	-28	8	41.7	7.7	11	ND	ND	ND	ND
9/4/1999	18	-31	8	41.7	7.7	11	ND	ND	ND	ND
9/5/1999	18	-31	8	41.7	7.7	11	0.685	ND	ND	ND
9/6/1999	18	-32	8	41.7	7.7	11	0.066	ND	ND	ND
9/7/1999	18	-36	8	41.7	7.7	11	ND	ND	ND	ND
9/8/1999	19	-29	4	83.4	10.3	11	0.901	ND	ND	ND
9/9/1999	19	-29	4	83.4	10.3	11	1.945	0.966	0.31	0.13
9/10/1999	19	-44	4	83.4	10.3	15	2.507	0.724	0.387	0.182
9/11/1999	19	-25	4	83.4	10.3	15	1.487	0.19	nd	ND
9/12/1999	19	-15	4	83.4	10.3	15	15.12	14.946	14.509	14.168
9/13/1999	19	-26	4	83.4	10.3	15	0.725	0.182	nd	ND
9/14/1999	19	-29	4	83.4	10.3	15	109.61	nd	nd	nd
9/15/1999	19	-28	4	83.4	10.3	15	0.172	nd	nd	nd
9/16/1999	19	-28	4	83.4	10.3	15	1773.39	205.89	48.49	nd
9/17/1999	19	-32	4	83.4	10.3	15	nd	nd	nd	nd

Nutrient changed to 100ml macronutrient/10ml micronutrients/2ml H3PO4. **Cells were drained and media remaining in Cell #'s 2,3, and 4 was removed.** Reactor batched overnight.

0900 Started flowing the RO water. Did not pull samples, it had been batching overnight.

Covered all holes and started a N2 purge on all 4 cells. 2:00pm turned the N2 purge in Cell #4 because N2 line seemed to be leaking.

2:45pm RO feed tank empty, changed over to new tank.

1457 Started flow of RO water including 250 ppb CrO4

3:00pm changed to a 4 hr. Adjusted nutrient timer to 15s ON and 149 s OFF.

Nutrient pump clogged. Adjusted tubing and verified NUTRIENT flow.

Nutrient tubing was clogged. It looks like the cells have been completely washed out. The samples pulled looked clear as RO water. Added a total of 500ml inoculum to all 4 cells(most to cell #1) and 25ml nutrient to cell #1 and 10ml to each of the other cells.

Appendix 3. Summary of Anion Data

Date	Condition Number	SO4 mg/L				Cl, mg/L				NO2, mg/L				NO3, mg/L				PO4, mg/L			
		1	2	3	4	1	2	3	4	1	2	3	4	1	2	3	4	1	2	3	4
6/25/1999	4	101	74	66	76	1021	1060	1124	984	46	ND	ND	ND	3	ND	ND	ND	ND	ND	ND	ND
6/26/1999	4	100	84	91	86	866	838	869	827	19	3	6	3	3	ND	ND	ND	ND	ND	ND	ND
7/1/1999	4	256	133	46		749	533	640		86	32	8		12	ND	ND		ND	ND	ND	
7/2/1999	4	132	122	101	81	834	830	850	926	523	46	ND	ND	2	ND	ND	ND	ND	ND	ND	ND
7/8/1999	6	76	22	5	5	685	681	697	786	6	5	5	ND	1	ND	ND	ND	ND	ND	ND	ND
7/9/1999	6	88	48	39	24	1064	1072	1064	1147	ND	32	ND	11	1	ND	ND	ND	ND	ND	ND	ND
7/10/1999	6	186	73	43	38	1003	922	894	895	44	ND	ND	ND	12	ND	6	9	ND	ND	ND	ND
7/11/1999	6	97	97	103	110	891	893	899	978	173	135	101	53	40	29	24	19	ND	ND	ND	ND
7/12/1999	6	114	124	126	123	867	853	847	862	53	ND	ND	ND	170	114	97	112	ND	ND	ND	ND
7/13/1999	6	122	131	162	156	893	816	845	865	ND	ND	ND	ND	15	136	311	135	ND	ND	ND	ND
7/14/1999	7	116	136	150	164	828	826	818	832	ND	ND	ND	ND	900	946	905	864	ND	ND	ND	ND
7/15/1999	7	130	139	141	159	890	894	873	892	160	ND	ND	ND	334	50	5	29	ND	ND	ND	ND
7/16/1999	8	130	136	127	119	963	987	974	967	166	ND	ND	ND	224	31	100	21	ND	ND	ND	ND
7/17/1999	8	105	85	76	75	990	964	987	999	101	ND	ND	ND	7	0	0	1	ND	ND	ND	ND
7/18/1999	8	83	106	80	78	995	1042	997	1089	9	ND	ND	ND	ND	4	0	0	ND	ND	ND	ND
7/19/1999	8	238	43	129	141	1228	1060	1019	1008	41	7	ND	ND	8	3	0	0	16	ND	ND	ND
7/21/1999	8	104	76	37	26	892	905	910	919	222	11	ND	ND	0	0	0	0	ND	ND	ND	ND
7/22/1999	8	168	6	4	4	939	910	948	950	16	ND	ND	ND	34	0		0	ND	17	ND	ND
7/23/1999	8	88	87	63	40	866	881	896	945	307	88	10	ND	12	0	0	0	ND	ND	ND	ND
7/24/1999	8	77	82	70	55	803	814	838	866	244	49	10	ND	32	0	0	0	ND	ND	ND	ND
7/25/1999	8	97	105	95	75	798	805	848	911	258	73	8	ND	85	0	0	0	ND	ND	ND	ND
7/26/1999	8	82	89	74	54	817	816	853	942	176	ND	ND	ND	0	0	0	0	ND	ND	ND	ND
7/27/1999	8	82	91	53	18	967	1006	969	1061	24	ND	ND	ND	0	0	0	0	ND	ND	ND	ND
7/28/1999	9	107	105	85	55	107	803	849	1193	233	152	ND	ND	34	0	0	0	ND	ND	ND	ND
7/29/1999	10	97	111	113	106	97	740	739	755	196	97	13	ND	4	0	0	0	ND	ND	44	ND
7/30/1999	10	243	108	102	72	827	836	857	999	ND	ND	ND	ND	0	0	0	0	ND	ND	ND	ND
8/1/1999	10	55	42	25	8	642	612	626	623	ND	ND	ND	ND	0	0	0	0	ND	ND	ND	ND
8/3/1999	11	82	74	41	9	189	183	207	254	ND	3	ND	ND	0	0	0	0	ND	ND	ND	ND
8/5/1999	11	77	74	43	66	757	772	808	802	197	61	ND	ND	16	0	0	0	ND	ND	ND	ND
8/7/1999	11	58	54	68	37	1197	1156	1085	1261	4	ND	ND	ND	0	0	0	0	ND	ND	ND	ND
8/8/1999	11	97	65	63	61	794	767	5	565	27	ND	ND	ND	0	0	0	0	ND	ND	ND	ND
8/11/1999	12	120	42	97	60	641	583	819	1424	ND	ND	ND	ND	0	0	0	0	ND	ND	ND	ND
8/12/1999	13	91	45	88	68	635	612	601	804	ND	ND	ND	ND	0	0	0	0	ND	ND	ND	ND
8/13/1999	13	101	42	106	88	726	673	682	671	ND	ND	ND	ND	0	0	0	0	ND	ND	ND	ND
8/14/1999	13	4.87	17.52	101	70	1419	690	937	931	17.75	4	25	17	0	0	167	53	211	17648	11043	18717
8/17/1999	13	nd	3.16	121	99	1340	810	853	788	nd	ND	ND	ND	0	0	0	0	402	182	64	48
8/23/1999	15		109	50	54		739	380	405	nd	2	6	4	0	0	5	3		198	102	134
8/26/1999	16	59	56	45	51	395	356	346	351	nd	ND	ND	ND	0	0	0	0	72	63	ND	52
8/29/1999	17	12	10	14	30	483	414	415	416	nd	ND	ND	ND	0	0	0	0	96	56	40	ND
9/1/1999	18	27	11	7	3	400	403	418	406	nd	ND	ND	ND	0	0	0	0	ND	ND	ND	ND
9/3/1999	18	23	28	3	3	411	416	401	401	nd	ND	ND	ND	0	0	0	0.72	ND	ND	34	ND
9/7/1999	18	21	10	5	12	455	429	423	410	nd	ND	ND	ND	0	0	0	0	35	ND	ND	ND
9/10/1999	19	50	36	17	12	400	415	410	404	nd	ND	ND	ND	0	0	0	0	nd	ND	ND	ND

RO Water					
Date	SO4	Cl	NO2	NO3	PO4
7/16/1999	93	853	ND	1120	ND

Appendix 4. Solids Data

Solids Data in mg/L

Cell #1					
Date	TS	TVS	TSS	VSS	TDS
8/19/1999	31360	15410	3070	2320	28290
8/24/1999	12650	5750	1910	1480	10740
8/31/1999	3780	1640	596	516	3184
9/2/1999	3390	1360	342	303	3048
9/8/1999	3170	1200	238	220	2932
9/10/1999	3640	1580	207	187	3433
9/15/1999	3880	1640	494	448	3386
9/17/1999	8850	4050	316	348	8534

Cell #2					
Date	TS	TVS	TSS	VSS	TDS
8/19/1999	6600	2750	2100	1680	4500
8/24/1999	4900	2020	1620	1080	3280
8/31/1999	3780	1640	308	264	3472
9/2/1999	3430	1350	194	174	3236
9/8/1999	3620	1520	219	197	3401
9/10/1999	3820	1630	263	228	3557
9/15/1999	3900	1570	533	480	3376
9/17/1999	5340	1620	500	348	4840

Cell #3					
Date	TS	TVS	TSS	VSS	TDS
8/19/1999	11820	5800	6920	4320	4900
8/24/1999	5380	2350	1360	900	4020
8/31/1999	3570	1310	332	284	3238
9/2/1999	3390	1370	223	187	1183
9/8/1999	3400	1310	190	171	3210
9/10/1999	3540	1410	104	100	3440
9/15/1999	3630	1370	273	273	3357
9/17/1999	4970	1470	365	274	4605

Cell #4					
Date	TS	TVS	TSS	VSS	TDS
8/19/1999	7390	3270	2113	1675	5277
8/24/1999	7930	4230	6100	4200	1830
8/31/1999	3520	1250	316	272	3204
9/2/1999	3470	1400	250	220	3220
9/8/1999	3790	1560	136	132	3654
9/10/1999	3590	1470	159	145	3431
9/15/1999	3460	1320	212	200	3248
9/17/1999	4960	1500	540	370	4420

Appendix 5. COD Data

Chemical Oxygen Demand		
Date	Sample Description	mg/l
8/19/1999	Cell #4	3694
	Cell #4 filtered	1363
8/24/1999	Cell #1	13225
	Cell #2	2708
	Cell #3	2708
	Cell #4	5958
9/2/1999	Cell #4	1928
	Cell #4 filtered	1643
9/8/1999	Cell #4	1675
	Cell #4 filtered	1372
9/10/1999	Cell #4	1788
	Cell #4 filtered	1458
9/15/1999	Cell #4	1829
	Cell #4 filtered	1503
9/17/1999	Cell #4	1015
	Cell #4 filtered	1422

APPENDIX G

REPORT ON THE JPL GROUNDWATER MODEL

**REPORT
ON THE
JPL GROUNDWATER MODEL**

**FOR THE
NATIONAL AERONAUTICS AND SPACE ADMINISTRATION
JET PROPULSION LABORATORY**
4800 Oak Grove Drive
Pasadena, California 91109

Prepared by:

Multimedia Environmental Technology, Inc.
9232 Red Twig Drive
Las Vegas, Nevada 89134

October 1999

TABLE OF CONTENTS

	PAGE
LIST OF TABLES.....	iii
LIST OF FIGURES	iv
1.0 INTRODUCTION.....	1-1
1.1 PURPOSE AND SCOPE.....	1-2
1.2 BACKGROUND INFORMATION	1-2
1.3 GROUNDWATER MODEL DEVELOPMENT.....	1-2
1.3.1 Initial Two-Dimensional Model.....	1-2
1.3.2 Three-Dimensional Model.....	1-3
1.3.3 Refinement of the Three-Dimensional Model Calibration.....	1-4
1.4 REPORT ORGANIZATION.....	1-5
2.0 AVAILABLE DATA	2-1
2.1 RAYMOND BASIN DATABASE.....	2-1
2.2 JPL RI DATA	2-2
2.3 OTHER SOURCES OF INFORMATION.....	2-2
3.0 CONCEPTUAL AND NUMERICAL MODEL DEVELOPMENT AND INPUT PARAMETER SELECTION	3-1
3.1 CONCEPTUAL HYDROGEOLOGIC MODEL	3-1
3.1.1 Grid/Layer Development.....	3-1
3.1.2 Areal (Horizontal) Extent.....	3-2
3.1.3 Stratigraphy (Vertical Extent)	3-2
3.2 BOUNDARY CONDITIONS	3-4
3.3 AQUIFER PROPERTIES.....	3-5
3.3.1 Hydraulic Conductivity and Transmissivity.....	3-6
3.3.2 Storage Properties.....	3-6
3.4 PIEZOMETRIC LEVEL DATA	3-7
3.4.1 Two-Dimensional Model Piezometric Data.....	3-7
3.4.2 Three-Dimensional Model Piezometric Data.....	3-8
3.5 AQUIFER STRESSES	3-8
3.5.1 Pumping Withdrawal.....	3-8
3.5.2 Spreading Ground Recharge.....	3-8
3.5.3 Recharge from Precipitation and Other Sources	3-9
3.6 SUMMARY	3-10

TABLE OF CONTENTS (Continued)

	PAGE
4.0 MODEL SETUP.....	4-1
4.1 MODEL LAYER DEVELOPMENT (SPATIAL DISCRETIZATION).....	4-1
4.2 TEMPORAL DISCRETIZATION	4-1
4.3 MODEL REFINEMENTS.....	4-2
4.4 SUMMARY	4-2
5.0 MODEL CALIBRATION.....	5-1
5.1 TWO-DIMENSIONAL MODEL CALIBRATION	5-1
5.2 THREE-DIMENSIONAL MODEL CALIBRATION	5-1
5.3 REFINED MODEL CALIBRATION	5-4
5.4 SUMMARY	5-4
6.0 CALIBRATION RESULTS.....	6-1
6.1 TWO-DIMENSIONAL CALIBRATION RESULTS	6-1
6.2 THREE-DIMENSIONAL CALIBRATION RESULTS	6-2
6.3 REFINED MODEL CALIBRATION RESULTS	6-3
6.4 VERIFICATION OF CALIBRATION RESULTS	6-4
6.5 SUMMARY	6-5
7.0 RESULTS OF SIMULATION OF POTENTIALLY EXTREME SCENARIOS	7-1
7.1 SIMULATION OF DRAUGHT	7-1
7.2 SIMULATION OF EXTREME RECHARGE	7-1
8.0 CONCLUSIONS	8-1
9.0 REFERENCES	9-1

APPENDICES

- Appendix A - Observed Piezometric Elevations in Multi-Port
and Shallow JPL Wells for Three-Dimensional Modeling Time Period
- Appendix B - Observed vs. Simulated Piezometric Elevations in Multi-Port
and Shallow JPL Wells for Initial Three-Dimensional Calibration
- Appendix C - Observed vs. Simulated Piezometric Elevations in Deep and Shallow JPL
Wells and Residual Plot for Refined Three-Dimensional Calibration
- Appendix D - Observed vs. Simulated Piezometric Elevations in Deep and Shallow JPL
Wells and Residual Plot for Verification of the Refined Three-Dimensional
Calibration

LIST OF TABLES

Table 3-1	Results of Aquifer Tests in Shallow JPL Wells
Table 3-2	Results of Aquifer Tests in Deep JPL Multi-Port Wells
Table 3-3	Groundwater Elevation Data in JPL and City of Pasadena Wells
Table 3-4	Groundwater Extraction Data from Municipal Wells
Table 4-1	Screen Elevations and Their Layer Locations in the 3-D Model
Table 4-2	Screen Locations by Node and Layer Number for All Monitoring Wells
Table 4-3	Monitoring Well Port (Screen) Designations in 3-D Model
Table 4-4	Screen Elevations and Layer Designations in Refined Three Layer Model
Table 6-1	Summary of Correlation Coefficients of Observed vs. Simulated Data for Individual Wells and Overall Simulation
Table 6-2	Summary of Verified Correlation Coefficients of Observed vs. Simulated Data with a New Data Set for Individual Wells and Overall Simulation

LIST OF FIGURES

Figure 1-1	Location of the JPL Modeled Area in Raymond Basin
Figure 1-2	Topographic Map of JPL Vicinity with Approximate Boundary of the Modeled Area Shown
Figure 3-1	Municipal Well Locations with Model Grid
Figure 3-2	Elevation of Top of Bedrock used for Model Input
Figure 3-3	JPL Multi-Port Monitoring Well Locations
Figure 3-4	No-Flow Boundaries for JPL Model
Figure 3-5	Pumping Rates for City of Pasadena Wells for Time Period of Three-Dimensional Model
Figure 3-6	Pumping Rates for Nearby Municipal Wells for Time Period of Three-Dimensional Model
Figure 3-7	Recharge Volumes for Nearby Spreading Basins
Figure 3-8	Precipitation in the City of Pasadena
Figure 3-9	Recharge Values for Variable Recharge Nodes - Three-Dimensional Model
Figure 3-10	Recharge Areas in Three-Dimensional Model
Figure 4-1	Locations of Cross Sections in JPL Modeled Area
Figure 4-2a	Cross Section A-A'
Figure 4-2b	Cross Section AA-AA'
Figure 4-2c	Cross Section BB-BB'
Figure 4-2d	Cross Section CC-CC'
Figure 6-1	Observed vs. Simulated Piezometric Levels in Refined Model-Layer One
Figure 6-2	Observed vs. Simulated Piezometric Levels in Multi-Port Wells – Refined Three-Dimensional Model
Figure 6-3a	Horizontal Hydraulic Conductivity: Model Layer 1, Part 1 of 2
Figure 6-3b	Horizontal Hydraulic Conductivity: Model Layer 1, Part 2 of 2
Figure 6-3c	Horizontal Hydraulic Conductivity: Model Layer 2
Figure 6-3d	Horizontal Hydraulic Conductivity: Model Layer 3
Figure 6-3e	Horizontal Hydraulic Conductivity: Model Layer 4
Figure 6-3f	Horizontal Hydraulic Conductivity: Model Layer 5
Figure 6-3g	Horizontal Hydraulic Conductivity: Model Layer 6

LIST OF FIGURES

(Continued)

Figure 6-4a	Vertical Hydraulic Conductivity: Between Model Layers 1 and 2
Figure 6-4b	Vertical Hydraulic Conductivity: Between Model Layers 2 and 3
Figure 6-4c	Vertical Hydraulic Conductivity: Between Model Layers 3 and 4
Figure 6-4d	Vertical Hydraulic Conductivity: Between Model Layers 4 and 5
Figure 6-4e	Vertical Hydraulic Conductivity: Between Model Layers 5 and 6
Figure 6-5a	Primary Storage: Model Layer 1
Figure 6-5b	Primary Storage: Model Layer 2
Figure 6-5c	Primary Storage: Model Layer 3
Figure 6-5d	Primary Storage: Model Layer 4
Figure 6-5e	Primary Storage: Model Layer 5
Figure 6-5f	Primary Storage: Model Layer 6
Figure 6-6a	Secondary Storage: Model Layer 1
Figure 6-6b	Secondary Storage: Model Layer 2
Figure 6-6c	Secondary Storage: Model Layers 3 and 4
Figure 6-6d	Secondary Storage: Model Layers 5 and 6
Figure 6-7a	Recharge: Stress Period 1
Figure 6-7b	Recharge: Stress Period 2
Figure 6-7c	Recharge: Stress Period 3
Figure 6-7d	Recharge: Stress Period 4
Figure 6-7e	Recharge: Stress Period 5
Figure 6-7f	Recharge: Stress Period 6
Figure 6-7g	Recharge: Stress Period 7
Figure 6-7h	Recharge: Stress Period 8
Figure 6-8a	Simulated Piezometric Levels for Stress Period 1: Layer 1: September 1, 1995
Figure 6-8b	Simulated Piezometric Levels for Stress Period 1: Layer 2: September 1, 1995
Figure 6-8c	Simulated Piezometric Levels for Stress Period 1: Layer 3: September 1, 1995
Figure 6-9a	Simulated Piezometric Levels for Stress Period 2: Layer 1: October 1, 1995

LIST OF FIGURES

(Continued)

Figure 6-9b	Simulated Piezometric Levels for Stress Period 2: Layer 2: October 1, 1995
Figure 6-9c	Simulated Piezometric Levels for Stress Period 2: Layer 3: October 1, 1995
Figure 6-10a	Simulated Piezometric Levels for Stress Period 3: Layer 1: November 1, 1995
Figure 6-10b	Simulated Piezometric Levels for Stress Period 3: Layer 2: November 1, 1995
Figure 6-10c	Simulated Piezometric Levels for Stress Period 3: Layer 3: November 1, 1995
Figure 6-11a	Simulated Piezometric Levels for Stress Period 4: Layer 1: December 1, 1995
Figure 6-11b	Simulated Piezometric Levels for Stress Period 4: Layer 2: December 1, 1995
Figure 6-11c	Simulated Piezometric Levels for Stress Period 4: Layer 3: December 1, 1995
Figure 6-12a	Simulated Piezometric Levels for Stress Period 5: Layer 1: January 1, 1996
Figure 6-12b	Simulated Piezometric Levels for Stress Period 5: Layer 2: January 1, 1996
Figure 6-12c	Simulated Piezometric Levels for Stress Period 5: Layer 3: January 1, 1996
Figure 6-13a	Simulated Piezometric Levels for Stress Period 6: Layer 1: February 1, 1996
Figure 6-13b	Simulated Piezometric Levels for Stress Period 6: Layer 2: February 1, 1996
Figure 6-13c	Simulated Piezometric Levels for Stress Period 6: Layer 3: February 1, 1996
Figure 6-14a	Simulated Piezometric Levels for Stress Period 7: Layer 1: March 1, 1996
Figure 6-14b	Simulated Piezometric Levels for Stress Period 7: Layer 2: March 1, 1996
Figure 6-14c	Simulated Piezometric Levels for Stress Period 7: Layer 3: March 1, 1996
Figure 6-15a	Simulated Piezometric Levels for Stress Period 8: Layer 1: April 1, 1996

LIST OF FIGURES

(Continued)

- Figure 6-15b Simulated Piezometric Levels for Stress Period 8:
Layer 2: April 1, 1996
- Figure 6-15c Simulated Piezometric Levels for Stress Period 8:
Layer 3: April 1, 1996
- Figure 7-1a Simulated Piezometric Levels in Draught Case for Stress Period 1:
September 1, 1995
- Figure 7-1b Simulated Piezometric Levels in Draught Case for Stress Period 3:
November 1, 1995
- Figure 7-1c Simulated Piezometric Levels in Draught Case for Stress Period 5:
January 1, 1996
- Figure 7-1d Simulated Piezometric Levels in Draught Case for Stress Period 8:
April 1, 1996
- Figure 7-1e Simulated Piezometric Levels in Draught Case for Stress Period 10:
June 1, 1996
- Figure 7-1f Simulated Piezometric Levels in Draught Case for Stress Period 12:
August 1, 1996
- Figure 7-1g Simulated Piezometric Levels in Draught Case for Stress Period 14:
October 1, 1996
- Figure 7-1h Simulated Piezometric Levels in Draught Case for Stress Period 16:
December 1, 1996
- Figure 7-2a Simulated Piezometric Levels in Extreme Recharge Case for Stress Period 1:
September 1, 1995
- Figure 7-2b Simulated Piezometric Levels in Extreme Recharge Case for Stress Period 3:
November 1, 1995
- Figure 7-2c Simulated Piezometric Levels in Extreme Recharge Case for Stress Period 5:
January 1, 1996
- Figure 7-2d Simulated Piezometric Levels in Extreme Recharge Case for Stress Period 8:
April 1, 1996
- Figure 7-2e Simulated Piezometric Levels in Extreme Recharge Case for Stress Period 10:
June 1, 1996
- Figure 7-2f Simulated Piezometric Levels in Extreme Recharge Case for Stress Period 12:
August 1, 1996
- Figure 7-2g Simulated Piezometric Levels in Extreme Recharge Case for Stress Period 14:
October 1, 1996
- Figure 7-2h Simulated Piezometric Levels in Extreme Recharge Case for Stress Period 16:
December 1, 1996

1.0 INTRODUCTION

A groundwater Remedial Investigation (RI) was recently completed at the National Aeronautics and Space Administration (NASA), Jet Propulsion Laboratory (JPL). The primary objectives of the RI were to identify the spatial extent of contaminants in the groundwater beneath and around the site and to estimate risks to potential receptors. The results of the RI are used in the Feasibility Study (FS) to develop cost-effective remedial strategies. The FS uses this numerical groundwater model to simulate groundwater flow beneath and around the site during various pump and treat scenarios to help evaluate remedial alternatives.

Multimedia Environmental Technology, Inc. (MET) developed the numerical model for the JPL site. Figures 1-1 and 1-2 show the modeled area. The area is relatively large, and it is located in the northwestern portion of the Raymond Basin. A conceptual model of the hydrologic system in the area was developed using pertinent hydrogeologic data, both from the JPL RI and from previous larger-scale basin-wide studies. The numerical model was setup using MODFLOW, a three-dimensional finite-difference groundwater flow computer program (McDonald and Harbaugh, 1988).

In developing the numerical model, hydraulic test (slug and bail) and piezometric level data were compiled. Initial model code parameters were set using hydraulic test data, and the parameters were refined using piezometric level data. Observed piezometric levels at JPL monitoring wells with single or multiple ports (screens) placed at various depths were available over several time periods. A well with a single port had the port placed at a relatively shallow depth, while a well with multiple ports had only the uppermost port placed at a shallow depth. In this report, a well with a single port (screen) at the water table will be referred to as a shallow well, while a well with multiple ports will be referred to as a deep well.

Initially, a two-dimensional model was setup, and attempts were made to calibrate the model. The piezometric levels in some shallow wells could not be simulated with acceptable accuracy. Also, an examination of piezometric levels observed at multiple ports of the deep wells revealed the layering in the geologic deposits could not be simulated with a two-dimensional model. The model was upgraded to a three-dimensional model to incorporate the geologic layering. Most of the two-dimensional features were retained, and the resulting three-dimensional model was calibrated and verified to simulate the piezometric levels at deep ports with acceptable accuracy.

1.1 PURPOSE AND SCOPE

The purpose of this report is to describe the development of the three-dimensional numerical model used to simulate groundwater flow in the aquifer beneath and around the JPL site. The basic objectives of this study were:

- To calibrate the three-dimensional model to simulate observed piezometric levels.
- To verify the model.
- To simulate a series of pumping and recharge scenarios for the FS.

1.2 BACKGROUND INFORMATION

Two sets of data were used to develop a site conceptual model and to setup the numerical model for simulating groundwater flow beneath the JPL site. The two data sets include:

- The database developed by CH2MHill as part of the Raymond Basin Project for the City of Pasadena (CH2MHill, 1990, 1992).
- The data developed during completion of the RI for the JPL site.

The Raymond Basin Project was designed to assess the water storage capacity of the aquifer in the entire Raymond Basin, to estimate the potential impact using this storage could have on water quality, and to develop conjunctive-use scenarios to exploit the water resources available in the basin (CH2MHill, 1990, 1992). The Raymond Basin Model, a three-dimensional groundwater flow model of the basin, was developed as part of the project. However, the model covered a very large area, was calibrated for the 1955 to 1989 period, and it lacked detailed information needed for the JPL site. As such, the conceptual model and the database support developed for the basin-wide model were taken as a starting point to develop the conceptual and the numerical model for the JPL site. The resulting model was refined using hydraulic test and water-level data observed in and around the JPL site obtained during the RI.

1.3 GROUNDWATER MODEL DEVELOPMENT

1.3.1 Initial Two-Dimensional Model

Initially, a two-dimensional approach was used to develop the numerical model for the JPL site. It was expected to facilitate the eventual three-dimensional modeling of the site by improving the definition of the boundary conditions around the site. The following tasks were performed to develop and to calibrate the two-dimensional model:

- Reviewed the Raymond Basin Project database and the JPL RI data.
- Developed a conceptual model of the hydrologic system in and around the JPL site.
- Estimated a spatial distribution of the aquifer system based on the site-specific data.
- Developed spatial distributions for the hydraulic parameters of the aquifer system based on the site-specific data.

- Developed a model grid (mesh) considering available pumping- and monitoring-well data.
- Evaluated initial conditions based on the Raymond Basin Model.
- Established boundary conditions based on the Raymond Basin Model and the JPL site-specific investigation.
- Developed a steady state (static) two-dimensional numerical model using MODFLOW. Focused on integrating MODFLOW to a series of pre- and post-processing codes to speed-up input/output manipulation.
- Simulated the model under a steady state condition to evaluate the applicability of the parameter distributions.
- Selected a time period for calibration. Calibrated for a period over which site-specific data for piezometric levels and pumping schedules were available.
- Developed a transient (dynamic) model with 26 stress periods, corresponding to the most recent JPL site data available at the time (26 months between August 1992 and September 1994).
- Calibrated the transient model adjusting model parameters and boundary conditions. Performed simulations to attain an acceptable accuracy based on statistical analysis of the calibration results.
- Assessed local areas where the calibrated model performed with unacceptable accuracy.

1.3.2 Three-Dimensional Model

The two-dimensional model facilitated developing a three-dimensional model of a relatively large area in the northwest portion of the Raymond Basin, but could not be calibrated to simulate piezometric levels observed at all the JPL monitoring wells with acceptable accuracy. The model was subsequently upgraded to a three-dimensional model to attain acceptable accuracy at the JPL monitoring wells. In upgrading the two-dimensional model, its grid was examined to determine its suitability for the three-dimensional model. The grid appeared to be adequately detailed in the JPL site. The two-dimensional grid was adopted for the three-dimensional model without any change; the plan views of the two- and the three-dimensional grids were left exactly the same.

The following tasks were performed to develop and to calibrate the three-dimensional model:

- Upgraded the two-dimensional conceptual model to a three-dimensional one by developing layers in the conceptual model using site-specific data from geologic and geophysical logs, well screen elevations, and pumping well screens.
- Reviewed the spatial distributions of the hydraulic parameters of the two-dimensional model and revised these distributions for the three-dimensional model.
- Developed a correlation between recharge and precipitation for the two-dimensional calibration period (August 1992 to September 1994) and revised the correlation for

the three-dimensional calibration period to include the most recent JPL site data available at the time (August 1995 to December 1996).

- Modified MODFLOW to accommodate 60,000 nodes for the three-dimensional model and developed new codes for pre- and post-processing input/output files. Did not use existing pre- and post-processing codes such as Visual MODFLOW (Waterloo Hydrogeologic), GMS (BOSS International), and EVS (C-TECH) due to grid and other limitations.
- Developed a quasi-steady state model and calibrated it for a period of time with the least amount of water table elevation changes. Selected the period as February 1995, when nearby municipal pumping wells were shut down.
- Developed a transient model for 16 stress periods, corresponding to 16 months between August 1995 and December 1996 (most recent JPL site data available at the time).
- Selected a calibration period. Selected the period for which the maximum amount of site-specific piezometric level data at the JPL deep wells was available (August 1995 to December 1996).
- Calibrated the transient model adjusting model parameters and boundary conditions. Performed numerous simulations to attain acceptable accuracy based on statistical analysis of the calibration results.
- Assessed local areas where the calibrated model performed with less than desired accuracy.

1.3.3 Refinement of the Three-Dimensional Model Calibration

After the initial calibration of the three-dimensional model, it was believed calibration could be improved in some areas. The following tasks were performed to improve the initial work of calibration of the three-dimensional model for the JPL site:

- Developed an approach to refine calibration of the three-dimensional model using MODFLOWP (Hill, 1993), a code to parameterize MODFLOW.
- Subjected the model to a sensitivity analysis.
- Calibrated the model for parameter estimation.
- MODFLOWP failed, therefore, performed calibration refinement with an iterative technique. Developed pre- and post-processing codes to facilitate changing parameters and running simulations.
- At an appropriate calibration stage, refined the correlation between recharge and precipitation for the three-dimensional calibration period (August 1995 to December 1996).
- Improved calibration adjusting model parameters and boundary conditions. Performed numerous simulations to attain a calibration with acceptable accuracy based on statistical analysis of the calibration results.

- Attempted to refine the calibration using optimization technique. Focused on genetic algorithm (GA) to solve the optimization problem.
- GA failed, therefore, continued to refine the calibration using the iterative technique.

All development and calibration tasks are described in more detail in the remainder of this report. All these tasks were conducted according to the Quality Assurance/Quality Control (QA/QC) procedures for groundwater modeling described in the U.S. EPA guidance (OSWER, 1994). In developing the numerical model for the JPL site, the specific QA/QC procedures conducted have been summarized (Enserch, 1995a), and the specific MODFLOW version used has been verified (Enserch, 1995b).

1.4 REPORT ORGANIZATION

The remainder of this report has been organized into eight sections numbered from 2 to 9. The first six sections are related to model calibration, while the last three sections are related to results, conclusions and references. First, Section 2.0 provides references to sources and types of data considered in the model development. Section 3.0 provides references to the two- and three-dimensional conceptual models developed using Section 2.0 information. Section 4.0 provides a description of the model setup. Section 5.0 provides a discussion on the calibration procedures. Section 6.0 provides the calibration results obtained using Section 5.0 procedures. Section 7.0 presents some simulation results and Section 8.0 provides conclusions. Section 9.0 lists pertinent references used. For convenience, tables, figures, and appendices referred to in the text are included at the end of the report.

2.0 AVAILABLE DATA

In this section, the data used in the development of the two- and three-dimensional numerical models to simulate groundwater flow beneath the JPL site are briefly described. The two major data sources used were the Raymond Basin Model database and the JPL site-specific investigation data.

2.1 RAYMOND BASIN DATABASE

The Geographical Information System (GIS) database for the Raymond Basin Model from CH2MHill was loaded into ARC-INFO, a computer software to process GIS databases. Several coverages over the Monk Hill sub-basin, surrounding the JPL site were plotted. Each coverage was associated with a file group, and it was designated using the name of the group. The coverages plotted were:

- CF-Node — CFEST model nodes
- Geology — geologic unit areas
- GeoFaults — geologic fault-line locations
- LandSurf — land surface elevation contours
- AqBot — aquifer system bed (bottom) elevation contours
- SpGrnds — spreading ground locations
- Alluvium — alluvium thickness contours
- Alluv-Range — alluvium thickness zones in 400 ft. increments
- Sat86s — saturated thickness based on Spring 1986 piezometric heads
- HC — hydraulic conductivity contours
- Trmiss — transmissivity contours
- Spyield — specific yield contours
- AllGoodPump — pumping well locations

The CH2MHill database did not include any results from the Raymond Basin Model simulations. It included only the data collected from other agencies and compiled by CH2MHill. Its documentation was limited to a very brief data glossary and provided only one line of text to describe each file. In most cases, it was possible to determine the data represented by a file, either from the name of the file or by comparison to data presented in reports prepared by CH2MHill (1990, 1992).

Pertinent data were extracted from the CH2MHill database and supplemented with JPL site-specific data, when available, and converted to MODFLOW input file formats as discussed below.

2.2 JPL RI DATA

Over the past several years, the investigation at the JPL site has included borehole drilling, monitoring well installation, water-level measurements, and groundwater sampling and analysis. The results of this investigation have been summarized in the OU-1/OU-3 Remedial Investigation Report (Foster Wheeler, 1999). Data were reviewed to identify specific information pertinent to the development of the numerical model for the JPL site.

2.3 OTHER SOURCES OF INFORMATION

Other sources of data, such as reports on general hydrologic conditions in the Raymond Basin, including the annual Raymond Basin Watermaster Reports, especially from 1992 to 1994 (Watermaster, 1992, 1993, 1994), and on several previous investigations of the Raymond Basin from as far back as the 1960s, were also reviewed. However, since most of these data had already been included in the Raymond Basin Model database, a re-evaluation of these data was not required in this report.

3.0 CONCEPTUAL AND NUMERICAL MODEL DEVELOPMENT AND INPUT PARAMETER SELECTION

Both the development of the preliminary hydrologic conceptual model and the selection of numerical model input parameters for the JPL model were based on existing relevant hydrologic data. Because the conceptual model was interactively developed based on the results of preliminary numerical modeling, this section describes development of both models. The hydrologic data were obtained through a review of available reports and documents from both basin-wide and JPL site-specific investigations. In reviewing the existing data, efforts were focused on identifying and evaluating input parameters required for the development of the numerical model. Components of the conceptual model and inputs for the numerical model are both discussed under different data categories in the following sections. It should be noted that these categories are often interrelated.

The data for the Raymond Basin Model was primarily compiled by CH2MHill. This model covered a very large area, and it discretized the area with a grid coarser than that required for the JPL site. The basin-wide database of CH2MHill contained some gaps at the more detailed scale required for the JPL site. Whenever feasible, the JPL site-specific data were used to fill the gaps in the basin-wide database and to refine the JPL conceptual model.

For the most part, actual measurements of hydrologic parameters were available only from slug and bail-type aquifer tests at the JPL monitoring well locations. These parameter values were subsequently applied to model development.

3.1 CONCEPTUAL HYDROGEOLOGIC MODEL

3.1.1 Grid/Layer Development

The model grid, to the extent possible, was developed based on the physical and hydrogeologic features of the hydrologic system in the study area. The horizontal extent covered the JPL site, and was expanded to include hydrogeologic features and boundaries controlling the groundwater flow around the site (i.e. municipal production wells).

The study area was divided into a 101 by 96 grid. Figure 3-1 shows the grid with nearby municipal production well locations. The grid cell sizes around JPL are smaller to emphasize the features in the JPL site.

3.1.2 Areal (Horizontal) Extent

The study area, in the areal extent, is an approximate square with about 3 miles on each side rotated 23 degrees to the east of true north. The modeled area extends beyond nearby municipal production (water supply) wells affecting the aquifer system beneath and around the JPL site. It includes the City of Pasadena's Arroyo, Well #52, Ventura, and Windsor production wells.

These wells are located just east of the Arroyo Seco Spreading Grounds, and they were shown in the RI to have the most influence on the groundwater flow conditions beneath the JPL site. In addition, the study area includes the Arroyo Seco Spreading Grounds, Lincoln Avenue Water Company wells, Valley Water Company wells, La Canada Irrigation District wells, and the Rubio and Las Flores wells. The Valley Wells to the west and the Rubio and Las Flores wells to the east were included to assess their potential influence on the aquifer system beneath the JPL site. Both the two- and three-dimensional models used the same areal extent.

3.1.3 Stratigraphy (Vertical Extent)

Development of the conceptual model of the site in the vertical direction evolved over time as more data became available and as a result of modeling improvements. At first, a single, isotropic layer was assumed in the two-dimensional numerical model for the JPL site because of the absence at the time of direct physical data supporting the presence of significant aquifer layering. The Raymond Basin Model was the basis for this assumption. Also, when groundwater modeling began, it was desired to develop an initial simple model to better understand boundary conditions.

The two-dimensional model required knowing the aquifer system thickness. The thickness was determined from differences in elevations between the land surface and the top of the underlying bedrock. To determine bedrock elevations, three sources were reviewed: (1) the Raymond Basin Model (CH2MHill; 1990), (2) a State of California, Division of Mines and Geology report by Smith and Sprotte (1986); and (3) data from recent RI drilling on JPL. The different sources varied in their extent, detail, scale, and configuration of the bedrock. The RI data was from recently drilled JPL monitoring wells that encountered bedrock (MW-3, MW-4, MW-12, MW-14, MW-17, MW-19, and MW-21).

Outside the immediate vicinity of the JPL site, the RI data agree closely with the Smith and Sprotte (1986) data. On the other hand, the Raymond Basin Model data showed geologic faults in various locations and a very different geometry for the top surface of the bedrock. The JPL RI data and the Smith and Sprotte data showed the bedrock dipping to the north beneath the JPL site, while the Raymond Basin Model data showed the bedrock dipping to the south beneath the site.

The RI data and the Smith and Sprotte (1986) data were digitized into GIS files. Then, the RI, Smith, and Raymond Basin data were combined according to the following rules: the RI data had precedence where available; the Smith and Sprotte data were used where RI data were unavailable; and the Raymond Basin data were used outside the coverage of the other two data sets. Transitions between the domains of the data sets were manually smoothed, taking into account borehole locations used to create these data sets.

The resulting bedrock elevation data set was interpolated using a two-dimensional kriging method available in SPYGLASS, a graphical software. The resulting contour map (Figure 3-2)

was imported into the input file system of the MODFLOW for the two-dimensional model. The results of calibration of this model indicated that the hydraulics in the eastern portion of the modeled area could not be explained by a simple two-dimensional system.

Evaluation of multiple-port monitoring wells revealed that the stratigraphy of the alluvium filled Raymond Basin is very complex. Both the basin-wide and the JPL site-specific data sets indicate little evidence of widespread consistent layering within the aquifer system overlying the crystalline bedrock. The cross sections in the Raymond Basin study, depicting stratigraphy closest to the JPL site (CH2MHill, 1990), show no correlation of lithologies from one borehole to the next. Also, the boring logs for the monitoring wells installed on the JPL site indicate little correlation of specific lithologies from one borehole to the next. Examination of the geologic and geophysical logs from JPL borings located east and southeast of the JPL site, show the alluvium to consist of an intermingled system of sand and gravel layers with occasional silt-rich layers. This is not the case west of the JPL site, where the alluvium does not appear to contain abundant silt-rich layers (Foster Wheeler, 1999). One can conclude that the silt-rich layers (aquitards) are discontinuous across the study area. Based on this geologic information and the response of the hydraulic head measurement in multi-port monitoring wells to pumping of nearby municipal wells, three general aquifer layers, with two general silt-rich intervals (aquitards) separating them, was conceptualized (see RI Report, Foster Wheeler, 1999). These aquitards dip slightly to the east and south. These two prominent aquitards appear to be present beneath and to the east of the JPL site. The shallowest one is at an approximate elevation of 900 ft., and the deepest one is at an approximate elevation of 600 ft. These aquitards are not present to the west and southwest of JPL, where the three layers form a single thick aquifer.

The three-dimensional model was discretized into six conductive horizontal layers (referred to model layers 1 to 6). The reason for selecting six layers was to provide flexibility in evaluation of the response of the piezometric heads recorded in each of the multi-port monitoring wells. All multi-port monitoring wells have five monitoring ports placed at various elevations in the aquifer. The presence or absence of aquitards in the model and their confining effectiveness was simulated by varying the vertical hydraulic conductivity between adjacent model layers.

Figure 3-3 shows the multi-port monitoring wells that were installed at the JPL site in 1990 (MW-3 and MW-4), 1992 (MW-11), 1994 (MW-12 and MW-14), and 1995 (MW-17 through MW-21). Data from these wells exhibited differences in piezometric levels between ports, vertically separated by distances of 80 to 200 ft. These differences are often in the range of 5 ft, but occasionally are as much as 25 ft. The overall piezometric differences between the top and bottom ports for some wells was much greater, and they varied over time. For example, MW-12 had a piezometric difference of approximately 74 ft between the top and bottom ports in August 1994; the top and bottom ports were at depths of 243 and 548 ft, respectively.

These piezometric differences were observed only during periods of pumping of nearby production wells. In some months, such as January and February 1996, when all the municipal production wells were shut down, piezometric levels in all ports rose to approximately the same

level. This indicated, despite the existence of horizontal barriers, all the layers were connected through a complex intermingled system. Two of the deep wells located to the west and south of the JPL site (MW-14 and MW-21) do not show any appreciable vertical separation in piezometric levels during pumping, suggesting the lack of any significant aquitards in the areas to the west and south of the JPL site. Based on these observations and the calibration results, the shallower, or first main aquitard, seems to be primarily limited in extent to the area directly beneath the center of the JPL site extending to the east across the study area. The deeper, or second main aquitard, seems to cover the same area but extend farther to the west across JPL.

3.2 BOUNDARY CONDITIONS

The physical boundaries of the model and some of the factors considered in their delineation were described above in Section 3.1. The following describes rationale for assigning head and flux to these boundaries.

Because piezometric levels in the basin are very dynamic and the boundaries experience seasonal fluctuations, the northwestern and southeastern boundaries of the model were defined as varying flux boundaries controlled by recharge at the surface. One of the features of the northwest portion of the model area is the La Cañada Country Club. In this area, lawn irrigation and pond water appear to have noticeable effect on recharge. The flux from the western area of the Raymond Basin into the western boundary of the model cannot be separated from the recharge from the La Cañada Country Club. As such, these two fluxes are lumped into a variable recharge rate along the top boundary nodes along the north western side of the numerical model.

No-flow boundaries were imposed along crystalline rock comprising the valley walls to the north-northeast and to the south-southwest of the JPL site (Figure 3-4). However, the northeastern corner of the study area receives flow from the north resulting from surface water recharge in the Las Flores Canyon area. Therefore, the northeastern corner of the model area was also considered as a variable flux boundary.

The boundary conditions are summarized as follows:

- NW = variable inflow from La Cañada area
- SE = no flow since this boundary falls on a flow line and the bedrock is exposed in some zones except for the southeastern zone where groundwater leaves the study area and the boundary is set to constant head. The constant head is applied to the deepest aquifer only. The shallower aquifers exchange water with this layer through vertical connections.
- NE = no flow along the crystalline valley walls except for the northeastern corner where variable flow into the study area occurs.
- SW = no flow along the crystalline valley walls.

- Bottom = the bottom of the model was assumed to be a no-flow boundary since flux from and into crystalline rocks is relatively low.

3.3 AQUIFER PROPERTIES

In preparation of the two-dimensional model, every grid cell of the model was assigned initial values for hydraulic conductivity and specific storage based on the Raymond Basin Model study. Hydraulic conductivity values were varied on a cell by cell basis; and constant primary and secondary storage coefficient values were assigned to all cells. The Raymond Basin values for hydraulic conductivity were then refined based on the slug and bail test results observed at JPL monitoring wells. These values did not appear to be as accurate as desired around the City of Pasadena wells. For this reason, water-level observations over a two-month period were used to estimate the hydraulic properties in the vicinity of the City of Pasadena wells. Both the hydraulic conductivity and storage coefficient values were adjusted by calibrating to match the simulated piezometric levels to those observed at MH-01 and MW-5, which are close to the city wells. These observation wells showed distinct responses to pumping in the nearby Pasadena Well Field. This calibration of aquifer properties to observed piezometric levels is described in more detail in Sections 5.0 and 6.0.

In preparation of the three-dimensional model, horizontal distributions of the hydraulic conductivity for the six layers of the model were assumed to be the same as that for the single layer of the two-dimensional model. This was due to the initial effort spent on the development and calibration of the hydraulic conductivity for the two-dimensional model. The applicability of the horizontal distribution was verified by running the three-dimensional model with the pumping data from the calibration period of the two-dimensional model. Primary storage coefficient values were varied on a cell-by-cell basis in all layers. The secondary storage coefficient was also varied for all six layers. By varying vertical hydraulic conductivity, areal distribution of the aquitards was estimated.

3.3.1 Hydraulic Conductivity and Transmissivity

As part of the JPL site-specific investigation, hydraulic tests were conducted in the shallow and deep monitoring wells. The results of the estimated hydraulic conductivity values for the shallow monitoring wells are summarized in Table 3-1. It may be noted that multiple estimates have been provided for the wells due to repeated tests and that these estimated values are, in general, representative of the permeability values in the locality of the well screens. The hydraulic conductivity values estimated from the slug-test data range from 1.77 ft/day (13 gallons per day per square foot, gpd/ft²) for MW-9 to 41.27 ft/day (309 gpd/ft²) for MW-7. The hydraulic conductivity values estimated from the bail-test data range from 1.92 ft/day (14 gpd/ft²) for MW-9 to 26.4 ft/day (197 gpd/ft²) for MW-7. The estimated values indicate moderate-to-high soil permeability values, and they are consistent with the typical values for medium-grained silty-to-clean sand.

The results of the estimated hydraulic conductivity values for the deep monitoring wells are summarized in Table 3-2. Up to five conductivity values have been estimated for these wells, representing the formation characteristics at different depths of the ports. The hydraulic conductivity values range up to 15.5 ft/day (MW-14, port 4). In general, no trend (increase or decrease) in conductivity values with depth was observed.

The hydraulic conductivity values from the Raymond Basin Model data were adjusted to incorporate JPL site-specific investigation data. The transmissivity values were calculated internally in the MODFLOW code from the hydraulic conductivity and saturated thickness values.

3.3.2 Storage Properties

The average specific yield for the undifferentiated alluvial aquifer, calibrated in the Raymond Basin Model (CH2MHill, 1990), ranges approximately from 0.05 to 0.07 in the vicinity of the JPL site. Hydraulic tests performed in the JPL monitoring wells do not permit the calculation of site-specific storativity values. However, the response of on-site monitoring wells to the Pasadena Well Field was used to calibrate storage coefficients. The primary storage coefficient is applicable to an unconfined aquifer during the early stages of pumping, when it is still 100 percent water saturated and behaves similar to a confined aquifer. The secondary storage coefficient is applicable to an unconfined aquifer during pumping, after its pore space begins to desaturate.

These storage coefficients calculated for aquifer materials in the vicinity of the JPL site are considered more representative than the Raymond Basin data mentioned above because of the abundance of site-specific data in this area.

3.4 PIEZOMETRIC LEVEL DATA

3.4.1 Two-Dimensional Model Piezometric Data

Piezometric surface data in the form of groundwater levels were required in the numerical model to provide initial conditions to start a run and to serve as a target data set for the calibration process. The calibration period was selected to span over a 26-month period from August 1992 to September 1994, the most recent JPL site data available at the time.

The Raymond Basin Model database contains data on piezometric levels, mainly covering the period from 1955 to 1989, with contoured potentiometric surface maps at 100 to 200 ft. contour intervals for 1960, 1970, 1980, 1985, and 1989 (CH2MHill, 1990). In the database, there are also coverages for 1902, 1946, 1950, 1954, 1962, 1968, 1977, 1978, 1979, 1980, 1981, 1982, 1983, 1984, 1985, and 1986, mainly digitized from Los Angeles Flood Control District (LAFCD) maps and mainly for fall-season conditions (except map for Spring 1986). In general, these maps show flow entering the aquifer system from the west and from the northeast.

Groundwater levels were measured periodically in the JPL monitoring wells between February 1990 and August 1992. Continuous water level measurements with pressure transducers and computer data loggers have been conducted at the shallow JPL wells since August 1992 (Foster Wheeler, 1999). Water level data show that two general groundwater flow regimes occur beneath the JPL site.

- During a majority of the year, groundwater flow is from west to east across the site. This flow pattern is the natural flow direction from the northwest to the southeast through the valley.
- After the rainy season of the year (typically early spring), groundwater flow has occasionally been from the northeast to the west across the site for a relatively short period of time. This flow "reversal" is related to high levels of recharge to the Arroyo Seco Spreading Grounds just to the east of the JPL site.

There is no overlap between the Raymond Basin Model groundwater level data (ending in 1989) and the JPL RI water-level data (beginning in 1990). The Raymond Basin Project spring 1986 data show groundwater elevations in the range of about 970 to 1,030 ft. above mean sea level (msl) near the JPL site. Similarly, the fall data show groundwater elevations in the range of about 960 to 1,000 feet above msl near the JPL site. These seasonal values agree reasonably well with normal seasonal groundwater elevations observed in the JPL monitoring wells. However, the groundwater levels near the mouth of the Arroyo Seco measured in the JPL wells are relatively high in comparison to the Raymond Basin Project data.

It was necessary to develop a potentiometric surface map for use as initial conditions in the model that more closely agreed with the conditions observed in the JPL monitoring wells. The initial conditions were established by using the August 1992 groundwater level data from the JPL monitoring wells and by running the model to steady state without any recharge. The rationale for this was that the August 1992 data set represents groundwater levels under minimum recharge. An initial west-to-east gradient, believed to be representative of the conditions in August 1992, was established. The gradient was similar to gradients in previous years as determined from water-level data in Raymond Basin Water Master Reports.

Groundwater elevations in the JPL monitoring wells measured over the 26 months between July 1992 and September 1994 were used as the target potentiometric surface data set for the two-dimensional model calibration discussed in Section 5.0.

3.4.2 Three-Dimensional Model Piezometric Data

The calibration period for the three-dimensional model was selected to span over a 16-month period from August 1995 to December 1996. This was based on the most recent available water level data at the time for the shallow and deep monitoring wells at the JPL site.

Table 3-3 presents groundwater elevation data for the period from August 1995 to December 1996. Appendix A presents a graphical presentation of this data. These data show the same

general groundwater flow regimes beneath the JPL site that the 1992 to 1994 data used for the two-dimensional model displayed. That is, that groundwater flow across the site is generally from west to east, except during brief periods in the spring, when the groundwater flow direction can locally reverse.

The piezometric level data measured at the JPL monitoring wells over the 16 months between August 1995 and December 1996 were used as the target data set for the three-dimensional model calibration as discussed in Section 5.0.

3.5 AQUIFER STRESSES

Groundwater levels at the JPL site are predominantly influenced by the withdrawals from the City of Pasadena's production wells, the recharge from the Arroyo Seco Spreading Grounds, and the natural recharge from precipitation. These stresses are discussed in the following sections.

3.5.1 Pumping Withdrawal

In order to conduct preliminary modeling of fluctuations in piezometric levels during the modeled time periods, it was necessary to accurately input the pumping rates for the production wells and the recharge rate for the spreading grounds in the area. Such data have been obtained from the City of Pasadena. Figures 3-5 and 3-6 show the pumping rates of nearby production wells used over the calibration period of the three-dimensional model for the City of Pasadena wells and other nearby municipal production wells, respectively.

3.5.2 Spreading Ground Recharge

Volumetric discharge of water to the Arroyo Seco Spreading Grounds is shown in Figure 3-7 for the time period of the three-dimensional model. However, all water discharged to spreading ground does not percolate and reach the aquifer as recharge. Additionally, the amount of spreading reported cannot be equally distributed among the cells in the model beneath the spreading grounds for two reasons: 1) the depth to the water-table beneath the spreading grounds is over 100 ft and as the water infiltrates in the unsaturated zone, it spreads laterally; and 2) water in the spreading grounds is unevenly distributed due to the presence of natural and artificial grading and barriers. A simple cross-sectional, two-dimensional simulation with T2VOC, a multiphase flow and transport code developed by the Lawrence Berkeley National Laboratory for the U. S. Department of Energy, indicated the width of spreading at the water table could be as broad as four times the width of the spreading grounds. This result was used to distribute the recharge horizontally among the cells beneath the spreading grounds.

3.5.3 Recharge from Precipitation and Other Sources

Annual precipitation over the Altadena Golf Course, Highland Park, La Cañada, Sierra Madre, Arroyo Seco and Pasadena City Hall monitoring stations were used. Precipitation data are available in the Raymond Basin Water Master reports and from the National Weather Service for

nearby monitoring stations. Figure 3-8 presents a graph of precipitation in the City of Pasadena for the time period of the three-dimensional model.

The Raymond Basin Model (CH2MHill, 1992) presents relationships between average annual precipitation and average areal recharge, developed by the California Department of Water Resources (using data for the last 35 years) separately for four different land-use conditions (undeveloped, residential, industrial/commercial, and floodplain). These relationships may be found satisfactory for long term simulations with stress periods of one year or longer. However, they were not found satisfactory for the short term stress periods used in the calibration of the numerical model for the JPL site. This was because there is a relatively long time lag between precipitation and recharge in areas where the water table is 100 ft. deep or more. For example, comparison of Figures 3-8 and the graphs in Appendix A indicates the lag between precipitation and recharge to be in the order of up to two months. It should be emphasized that the groundwater level rise in the model area is not entirely due to the infiltration recharge at the land surface. Inflow from the northwestern boundary of the area also contributes to the water level rise.

Furthermore, undeveloped areas, such as Devil's Gate Reservoir area, sporadically contribute to groundwater recharge as a result of precipitation and/or surface runoff during rainy seasons. Also, it has been observed that in some areas, such as around MW-4, localized infiltration (storm drain discharge) contributes to recharge to groundwater (M. Cutler, pers. comm., 1995).

The recharge from all surface sources was calculated by developing a correlation between the recharge and precipitation for the model area. The variability of recharge in the vicinity of the modeled area (Figure 3-7) allowed to reach a correlation between the measured precipitation and the recharge applied to each individual node in the two-dimensional model. This correlation was then applied to the three-dimensional model with new recharge values (Figure 3-9) calculated from the rainfall measured in the City of Pasadena (Figure 3-8) for the 16-month modeled period. The regions where this variable relationship applies in this model are shown in Figure 3-10.

Recharge was applied to the top layer of the model in all cases, except where the water table fell below the bottom of the top layer. Recharge was also applied at a constant rate in the areas where precipitation and surface runoff were not contributing factors. This was the case where the inflow into the study area was combined with the recharge from the land surface. For example, both recharge from the La Cañada Country Club area and inflow through the northwestern model boundary were lumped into recharge in the northwestern boundary of the site. These areas are shown in Figure 3-10. In these cases, a calibrated recharge was applied to the appropriate nodes along the western boundary. Once these knowledge-based recharge distributions were assigned an initial value, the values were systematically changed to calibrate the top water levels in the shallow aquifer. Because the change in the rate of recharge affected deeper aquifers in simulation, numerous iterations had to be performed to calibrate both recharge and water levels.

3.6 SUMMARY

A two-dimensional grid consisting of 96 by 101 grid cells was initially setup for the JPL site. Hydrogeologic information from the Raymond Basin modeling effort and JPL site-specific investigation were compiled and transferred to the grid. The information from the two-dimensional model was later used to develop a three-dimensional model consisting of 6 horizontal layers. Initial hydraulic conductivity values were assumed to range from 2 to 80 ft/day. Primary storage coefficient was assumed to have a uniform value of 0.001. Specific yield was assigned a uniform value of 0.003. Water level data for the 26-month period from August 1992 to September 1994 were selected for the two-dimensional calibration, and data for the 16-month period from August 1995 to December 1996 were selected for the three-dimensional calibration. Monthly recharge data from Arroyo Seco Spreading Grounds were used for initial calibration, but they were modified based on analysis made using a two-dimensional variably saturated model. A relationship between rainfall and recharge for the calibrated two-dimensional model was used to predict the recharge values for the three-dimensional model.

4.0 MODEL SETUP

As previously discussed, the preliminary two-dimensional model was upgraded to a three-dimensional model. The following sections discuss horizontal discretization, which refers to using columns and rows, vertical discretization, which refers using layers, and temporal discretization.

4.1 MODEL LAYER DEVELOPMENT (SPATIAL DISCRETIZATION)

In the three dimensional model, the aquifer was divided into six layers with five intervening interfaces. The five interfaces simulated aquitards by adjusting the vertical hydraulic conductivity between the adjacent layers. The storage properties of the interfaces were ignored because the thicknesses of the aquitards is much smaller than the aquifer layer thicknesses.

In designing the layers, the location of the monitoring well ports and the pumping well screens were taken into consideration. Each deep well has five ports located at various depths. Each port falls within a single layer for most wells (Table 4-1). In some cases, two ports fall within the same layer. For example, the bottom two ports of MW-20 fall in model layer 6. Table 4-2 shows the port locations by row, column, and layer for both shallow and deep wells. Figures 4-1 and 4-2a through 4-2d show the locations of cross sections and cross-sectional views, respectively, of the wells with labeled ports, model layers, and low permeability interfaces.

4.2 TEMPORAL DISCRETIZATION

The transient period of calibration for the three-dimensional model was divided into 16 stress periods from the end of August 1995 to the end of December 1996. Each stress period corresponded approximately to a calendar month. According to the time interval between the monthly monitoring of water levels at the deep wells, an appropriate number of days was set in each stress period. For example, if water levels were measured on September 1, 1996, and then again on October 9, 1996, 39 days would be set for that time period. In presenting the observed and simulated data in the following sections, a particular month will refer to the water level monitoring day in the month, not necessarily its beginning or end. Each stress period consisted of 10 time steps for computational purposes.

Both pumping and recharge stresses were applied to the model at the beginning of each stress period, and they were kept constant throughout that stress period. This was necessary because both pumping and recharge were reported as a single value for an entire month.

4.3 MODEL REFINEMENTS

After initial calibration of the three-dimensional model, numerous refinements and recalibrations were performed based on availability of more up-to-date site-specific data.

A barrier system of unknown nature (possibly a fault zone) had to be implemented south of MW-1, MW-9, and MW-15 to effectively simulate the significant mound at the mouth of the Arroyo Seco. Also, the extent of the bottom layer (crystalline bedrock) was modified around MW-21 to correspond with data obtained from MW-21. This well encountered bedrock deeper than originally conceptualized from previous reports.

4.4 SUMMARY

Initially, a two-dimensional model with a grid consisting of 96 by 101 cells was setup for the JPL site. Later, the model was upgraded to a three-dimensional model with six layers. The three-dimensional model covered the same area as the two-dimensional model. The simulation time was discretized into 26 stress periods for the two-dimensional model and 16 stress periods for the three-dimensional model.

5.0 MODEL CALIBRATION

5.1 TWO-DIMENSIONAL MODEL CALIBRATION

The primary purpose of the two-dimensional calibration was to evaluate average hydraulic parameters for a one layer alluvial aquifer. Also, it was an attempt to test the two-dimensional conceptual model. Two phases of calibration were performed. The first phase involved calibration to estimate hydraulic parameters of the model. The calibration was performed over the period from May 1993 to July 1993. Over this period, MH-01 and MW-5 showed a distinct response to a sudden increase in pumping rates in the Pasadena Well Field located immediately east of the Arroyo Seco Spreading Grounds. Because the change in pumping stress was large, the recharge stress from the Arroyo Seco Spreading Grounds and other sources, discussed in Section 3.5.1, most likely had a minimal effect on the wells during this period. Therefore, calibration to this period provided good estimates of the hydraulic parameters between these monitoring wells and the Pasadena Well Field.

The second phase involved calibration to adjust recharge of the model. The calibration was performed over the entire 26-month period from August 1992 to September 1994. It involved no adjustment to hydraulic parameters. It began by establishing an initial potentiometric surface for the study area. As discussed in the previous sections, this surface was constructed considering water-level data from both the Raymond Basin Model and the JPL site-specific investigation. Emphasis was placed on water-level data from the JPL monitoring wells.

For calibration purposes, an automated pre- and post-processing system was devised to facilitate review of the model results and adjustment of the recharge parameters. The recharge file, an input to MODFLOW, was relatively large; it consisted of 9,696 entries for each stress period or 252,096 entries for the 26 stress periods. The pre-processor allowed changing recharge for specific cells and, thereby, eliminating editing of the recharge file.

5.2 THREE-DIMENSIONAL MODEL CALIBRATION

Two phases of calibration were again performed. The first phase involved calibration to estimate hydraulic parameters and initial piezometric levels for the model. The calibration was performed over the period from February 1996 to December 1996. Selection of the first phase was mainly for modeling convenience. The beginning time was chosen because all pumps were shut down in February 1996 and piezometric levels in the deep well ports had recovered approximately to the same level in each well. Although significant recharge occurred during this month, the monitoring wells showed very little vertical flow of groundwater during February 1996.

In the first simulation of the first phase of the preliminary calibration, the piezometric levels at the observation wells were fixed, and a three-year period was simulated to achieve a quasi-steady state condition. This provided smooth piezometric surfaces for the entire study, which were then used as the initial condition for the first phase of the calibration. This method of estimating the initial condition was more representative than the conventional method of kriging observed data to estimate the initial condition. The method used here could impose the influence of the hydraulic boundary conditions on the model more accurately and base the interpolation of the piezometric levels on flow equations rather than statistical parameters. The method used here was also selected for modeling convenience. The final initial condition was estimated using an iterative procedure based on the following considerations:

- In a complex transient model, such as the model for the JPL site, the number of unknowns greatly exceed the available known information, and the initial conditions for only 50 out of 58,176 cells were known.
- Recharge for the study area was unknown; no reliable method of accurately predicting recharge from precipitation or from flow into the spreading area ponds existed.
- The pumping wells were screened at various intervals straddling many model layers. No layer-specific pumping rates were available.

Pumping well screens, which overlapped several model layers, complicated the simulation. One complication involved the unknown allocation of the total flow of a pumping well to individual model layers. Only the total flow from a well was known, and the allocation of this flow to various layers was unknown. To overcome this uncertainty, the total flow of a well was assigned to model layer 4, and large vertical hydraulic conductivity values were assigned to the layer interfaces penetrated by the screens of the well. Model layer 4 was selected because most of the production wells end in this layer. The large conductivities of the interfaces at the screens made the model results rather insensitive to the assignment of the total flow to a specific layer. For example, if a well were to be screened from model layers 2, 3, and 4, large values would be assigned to $Kv_{2,3}$ and $Kv_{3,4}$, where $Kv_{i,j}$ = vertical conductivity at the interface between layers i and j . By assigning large values to $Kv_{2,3}$ and $Kv_{3,4}$, the uncertainty in allocating the total flow to the three model layers would be circumvented.

Another complication involved the model sensitivity, as determined by an analysis using MODFLOWP and MODFLOW. The analysis indicated the model to be strongly sensitive to:

- Recharge and the secondary storage coefficient (specific yield) of the first two model layers and to some extent the third layer.
- Primary storage coefficient of all layers.
- Vertical hydraulic conductivity of all layer interfaces.
- Horizontal hydraulic conductivity of all layers.

The sensitivity to secondary storage coefficient of the top layers was due to the intermittent development of unconfined conditions in these layers due to pumping. The secondary storage coefficient becomes important when the layer experiences dewatering. Because the wet and dry option of MODFLOW was used in all simulations, the secondary storage also affected the run time and conveyance of the specific run. The model is not very sensitive to recharge and boundary conditions on the northeast and northwest corners. Recharge from the Arroyo Seco can readily compensate the flow shortage from the west or east of the JPL site in the three-dimensional model, whereas attempts to provide such compensation would significantly affect the water levels at the site in the two-dimensional model.

Because the calibrated recharge was dependent on the vertical hydraulic conductivity of the two main interfaces (aquitards), many iterations were required to adjust the recharge values and obtain reasonable vertical hydraulic conductivity values. This interdependency also existed between the recharge and the primary storage coefficient and, to some extent, the horizontal hydraulic conductivity of the aquifers. Because of these uncertainties, the calibration results presented here are based on expert judgment.

During calibration refinement, the results of the piezometric head calculations in February 1996 were iteratively used as initial conditions in several occasions. This exercise was performed because the initial conditions affect the results of simulations. Interpolation of sparse data does not always result in appropriate initial conditions. However, if two similar water level conditions are used as the beginning and ending conditions, iteration and calibration will result in an improved initial condition because the interpolation of the water levels are forced by hydraulic factors rather than geostatistical factors.

Once the initial conditions for the first phase of the preliminary calibration were established, hydraulic parameters were adjusted to match the piezometric levels in the monitoring wells. Again, in the second phase, because of lack of reliable initial conditions, the simulated piezometric levels for May 1996 were used as initial conditions. The conditions in May 1996 were similar to those observed in August 1995. Therefore, the simulated piezometric levels in May 1996 were selected as initial conditions for the second phase of the preliminary calibration. This phase involved adjusting the recharge for the entire 16-month period of simulation, from August 1995 to December 1996.

For calibration purposes, an automated pre- and post-processing system was devised to facilitate review of the model results and adjustment of recharge parameters. The recharge file, an input to MODFLOW, was relatively large, consisting of 9,696 entries for each stress period or a total of 155,136 entries for the 16 stress periods. The pre-processor allowed changing recharge for specific cells and, hence, eliminated editing of the recharge file. Several pre-processors for changing hydraulic parameters in selected zones were also developed.

5.3 REFINED MODEL CALIBRATION

In this phase of the calibration, parameter estimation techniques of MODFLOWP (Hill, 1993) were first attempted. Many problems were encountered. First, MODFLOWP does not handle the convertible confined/unconfined aquifer very well; attempts to use this solution were not successful, resulting in large residuals in numerous runs performed. Second, the runs were unreasonably long, about 20 to 30 hours each, for the 16 stress periods. Third, some programming errors were found in the latest release of the MODFLOWP. These were communicated with the author, but no resolution has been achieved as of the date of this report. Thus, after several weeks of calibration effort with MODFLOWP, no improvement in the residuals were noticed over the preliminary calibration performed using the iterative technique.

An optimization model was also setup to perform the calibration, or the inverse analysis. The model was developed using Genetic Algorithm (GA) and MODFLOW. GA evaluated objective values using MODFLOW simulations. The model provided sufficient flexibility in designing numerical experiments to search near-optimal inverse solutions. Several experiments were performed. The best solution from earlier analysis was selected, and its perturbations (variations) were considered in designing the experiments.

The flow domain was divided into zones, and flow parameters within a zone were assumed to be constant. A range of S-, K-, and V-values (S = storativity, K = horizontal hydraulic conductivity, and V = vertical conductivity) for each zone were assumed to define the decision space, and GA was employed to search the best solution. A series of zone architectures was considered to find an acceptable solution. However, GA failed to find an acceptable solution.

Therefore, it was concluded that it would be more effective to continue refining the calibration with the iterative technique. Expert judgment was applied to estimate parameters and reduce their uncertainty bounds. The solution consisted of 11 zones, and attempts were made to refine the calibration with this zone architecture. Significant improvement was achieved with this architecture. Also, recharge was modified to match the overall observations at shallow wells.

5.4 SUMMARY

For both the two-dimensional and three-dimensional models, two phases of calibration were performed. The beginning simulation time period of the first calibration was selected from May 1993 to July 1993 for the two-dimensional model and from February 1996 to December 1996 for the three-dimensional model. The first phase of each provided preliminary estimates of the hydraulic properties and initial conditions for the second, main phase. The main phase of calibration was performed for the entire simulation period. Following the two phases of preliminary calibration, parameter estimation with MODFLOWP and inverse analysis with GA proved unsuccessful. The calibration was refined further using the iterative technique.

6.0 CALIBRATION RESULTS

6.1 TWO-DIMENSIONAL CALIBRATION RESULTS

The results of the first phase of the two-dimensional model calibration indicated the shallow monitoring wells were simulated with reasonable accuracy. A relatively good match between the simulated and observed water levels for both MH-01 and MW-5 monitoring wells were achieved; resulting from the emphasis placed on the calibration of hydraulic properties (hydraulic conductivities and storage coefficients) to groundwater level trends at these monitoring wells during the first phase of calibration.

The results of the second phase of the two-dimensional model calibration improved across the site with water levels generally simulated to within 15 feet of the observed values. Considering that groundwater level fluctuations are in excess of 100 feet during the calibration period, this represented a good fit of the data.

Regression analysis between the observed and simulated data was performed. A perfect simulation of the observed values would yield a slope "m" of 1.0, an intercept "b" of zero, and a regression coefficient (R^2) of 1.0 for the linear equation:

$$y = mx + b$$

where "y" and "x" are the observed and simulated potentiometric levels, respectively. If the intercept is forced to be zero, and allowing the intercept to be calculated, the lower and upper 95 percent confidence limit for the slope were 0.7908 and 0.8664, respectively. Similarly, the result of regression between observed and simulated potentiometric levels for monitoring well MW-5, with the intercept forced to zero, and allowing the intercept to be calculated, the lower and upper 95 percent confidence limit for the slope were 0.8666 and 0.9847, respectively.

Calibration near MW-1, however, was not as satisfactory. As was noted in earlier sections, the shallow aquifer in this part of the study area has low hydraulic conductivity values inhibiting vertical flow. This low conductivity together with the recharge from the mouth of the Arroyo Seco results in significant groundwater mounding in this part of the study area. This condition is best simulated with a multi-layered setup of the model. Although low hydraulic conductivity values may be assigned to the nodes in this part of the study area to simulate the response of the wells, this conductivity must be assigned to the entire thickness of the aquifer in the two-dimensional model. Such an assignment is not representative of the entire thickness of the aquifer, and it was not implemented in this phase of modeling.

It is interesting to note that short-term flow reversals near the eastern part of the JPL site, as shown in the groundwater contour maps, were weakly simulated with the model. It is probable that this reversal only occurs in the shallow part of the aquifer.

6.2 THREE-DIMENSIONAL CALIBRATION RESULTS

The results of the initial phase of the three-dimensional model calibration are shown in Appendix B. The general water levels of all the shallow monitoring wells are simulated with reasonable accuracy. The simulated water levels in MW-1, MW-9, and MW-15 are particularly of interest because the piezometric levels in these wells could not be calibrated in the two-dimensional model. A phase lag of about one month between the simulated and observed piezometric level fluctuations was evident in the monitoring wells on the western side of the JPL site (Appendix B). This is due to a discrepancy in the reported pumping schedule of nearby production wells, which was corrected in later simulations.

Most of the simulated piezometric levels for the shallow monitoring wells are within 10 ft. of the observed values with a few exceptions. Some have deviation of as much as 25 ft. from the observed values. These deviations are mostly due to the phase lag between the simulated and observed trends. Considering the actual water level fluctuations to be in excess of 150 ft. during the calibration period, the results of model calibration represent a reasonable fit of the data.

The trends of piezometric levels at the deep wells are simulated with reasonable accuracy except for MW-21 and MW-14. Model results from these two wells also have a phase lag of about one month (Appendix B). Data from these wells do not show much of any vertical piezometric water level separation. In calibrating the wells in the western zone of the study area, the vertical hydraulic conductivity of all the layer interfaces (aquitards) were increased to values in the same order of magnitude as those of the aquifer layers. In effect, the interfaces were removed in the western portion of the site. However, aside from the lag, the match in piezometric levels is very good.

At MW-20, the well located farthest east of all JPL wells, the piezometric levels were probably the most difficult to calibrate. The piezometric levels recorded at screens 1, 2, and 5, located approximately at depths of 230, 390, and 900 ft., respectively, were all at about the same elevation at all times. However, piezometric water levels at screens 3 and 4 were as much as 20 and 50 ft., respectively, lower than the other screens. It appears the layer represented by screen 5 is hydraulically isolated from affects of pumping from nearby municipal wells. Examination of the geological and geophysical logs of this well shows numerous layers of silt and silty sand throughout the entire length of the borehole. The screens of this well were installed in relatively isolated layers of sand and gravel material. Other JPL deep wells were simulated with reasonable accuracy.

Groundwater mounding appears to occur in three different spots at various times in the vicinity of the JPL site. The first and most persistent mounding occurs at the mouth of the Arroyo Seco. This mounding appears independent of the pumping rates in the Pasadena Well Field. As noted before, it appears to occur due to the interface between model layers 1 and 2. The interface has a low vertical conductivity in this area; it decreases the vertical water flow rate between the two layers, and any recharge in model layer 1 over this area results in mounding. A second more subtle mounding appears to occur south of JPL in the Devil's Gate Reservoir area. Interpreted from the aerial photographs, the reservoir remains empty most of the time, but the vegetation over the area suggests ponding during some parts of the year. The mounding disappears during heavy pumping periods. This is probably due to the slightly higher vertical permeability of the interface between model layers 1 and 2 in this area. The third mound appears to occur southeast of the Pasadena Well field. The source of this mound is not clear. However, it appears to occur midway between the Lincoln Avenue and the Rubio Canyon Well Fields. As discussed in the previous section, this area is underlain by interlayered fine and coarse aquifer material. Pumping in the Lincoln Avenue Well Field is mostly from model layers 3 and 4. Therefore, this mound could be an artifact of the delay in dewatering of model layers 1 and 2 in response to pumping. Model layer 6 appears to be more or less isolated and responds mainly to the overall piezometric level changes in the entire study area, not to local responses to pumping and recharge.

6.3 REFINED MODEL CALIBRATION RESULTS

The results of refinements made to the calibration of the three-dimensional model are shown in Appendix C and in Figure 6-1 for the upper layer of the model and in Figure 6-2 for the deeper layers. The general water levels of all the monitoring wells are simulated with reasonable accuracy. Figures 6-3a-g, 6-4a-e, 6-5a-f, 6-6a-d, and 6-7a-h show the final distribution of horizontal hydraulic conductivity (K_h), vertical hydraulic conductivity (K_v), primary storage (Sc_1), secondary storage (Sc_2), and recharge values over the model domain.

Most of the simulated piezometric levels for the shallow monitoring wells are within 10 ft. of the observed values with a few exceptions. Some have deviations of as much as 20 ft. from the observed values. Considering the actual water level fluctuations to be in excess of 150 ft. during the calibration period, the results of model calibration represents a reasonable fit of the data. The observed trends of MW-9 are underestimated by about 20 ft. Attempts to raise the water level in this well by increasing recharge was not successful. Such an increase affected more wells down-gradient. A significant increase in the water levels at MW-9 was observed when a fault with very low horizontal hydraulic conductivity was artificially placed just south of the well. The fault serves as a barrier to water movement. Simulation of the fault also improved the results for MW-15 and MW-11, which are nearby at the mouth of the Arroyo.

The trends of piezometric levels at the deep wells are also simulated with reasonable accuracy. MW-21 and MW-14 do not show a significant vertical piezometric head gradient. In calibrating for the wells in the western portion of the study area, the vertical hydraulic conductivity of all the

interfaces between layers was increased to values in the same order of magnitude as those of the layers. In effect, the interfaces do not exist in the western zone of the site. The match in piezometric levels is very good.

To statistically evaluate the "goodness of fit" of calibration, regression analysis between the observed and simulated water-level data was performed. Regression coefficients for the entire calibration period for all periods are provided in Table 6-1. Observation vs. simulation data with correlation factor (R) for each well and an overall residual plot of the final refined calibration are provided in Appendix C. It should be noted that a high correlation coefficient in regression analysis of a simulation is not necessarily indicative of a better calibration. Many other factors must be considered before judging the calibration of a groundwater flow simulation. A high correlation coefficient is indicative only of goodness of fit of the simulated trend.

The correlation coefficients between the observed and simulated piezometric levels for most of the shallow wells indicate a relatively good match in trends. Some of the deeper ports in some of the deep wells do not show as good of a match. Table 6-1 shows that the overall coefficient for the final calibration (R^2) to be 0.93

Piezometric contour maps for three simulated layers during selected months of simulation are presented for the study area in Figures 6-8a-c to 6-15a-c as an example of the results of calibration. These piezometric level maps closely resemble the observed water-level contour maps presented in the RI Report (Foster Wheeler, 1999). In these figures, there is a contrast in the piezometric levels between the wet (colored) and dry (black) regions at the boundaries, and kriging produces a hatched strip to be ignored. The change in shape of the plots for different layers is due to the boundary changes with depth of each layer and due to the sloping nature of the crystalline bedrock.

The mass balance error reported by MODFLOW was generally less than 0.4 percent. The relatively small error emphasizes the appropriateness of the grid size and the stress period lengths.

6.4 VERIFICATION OF CALIBRATION RESULTS

Verification of the refined calibration results was performed using piezometric heads observed over the period from August 1997 to April 1998, the most recent water-level data available at the time. Heads simulated over the period from August 1995 to April 1996 were compared to heads observed over the new period. Appendix D shows verification (generalization) results and the regression coefficient (R^2) between observed and simulated heads for the shallow wells, and the comparison between the same for the deep wells at specified ports as wells as an overall residual plot of these data. Table 6-2 shows R^2 for all the ports individually and collectively. The table shows the overall $R^2 = 0.85$, which compares with the refined calibration, $R^2 = 0.93$.

6.5 SUMMARY

The results of the refined calibration of the three-dimensional model have provided a much-improved prediction of the piezometric level fluctuations at MW-1, MW-9, and MW-15. The piezometric levels at most of the shallow well ports are calibrated within 10 ft. of the observed levels. The piezometric levels at most of the deep well ports are calibrated within 10 ft. Correlation coefficient from regression analysis between the observed and simulated piezometric levels is greater than 0.8 for most of the well ports.

Results of the calibration appear to validate the conceptual model assumption of the existence of a layered system (aquitards) on the east and southeast of the JPL site and a relatively uniform aquifer (no aquitards) to the west of the site.

Groundwater mounding at the mouth of the Arroyo Seco is potentially due to the presence of a shallow interface with low vertical conductivity in this area. This interface also plays a significant part in inducing short-term groundwater flow reversals occasionally observed along the east end of the site.

Results of the velocity calculations indicated the vertical component of flow to be smaller than the horizontal component. Therefore, the groundwater flow in the system is primarily horizontal, except near the pumping wells.

7.0 RESULTS OF SIMULATION OF POTENTIALLY EXTREME SCENARIOS

Two cases were selected for simulation of perceived extremes. The first case is a draught case, and the other is a wet period with extreme recharge. These cases were selected to evaluate the flow of groundwater and the behavior of the model during extreme climatological conditions. The changes in recharge and pumping rates are based on experience with the basin but are not statistically derived.

7.1 SIMULATION OF DRAUGHT

In this simulation, recharge was reduced by 66 percent, to one third of its average value during the 1995 to 1996 period, and average municipal pumping was increased by 20 percent. Increase in pumping usually occurs in draught years due to reduced availability of imported water. The results of this simulation for a 16-month period are shown in Figures 7-1a to h.

As expected, water levels drop dramatically during a draught simulation period.

7.2 SIMULATION OF EXTREME RECHARGE

In this simulation, the average recharge was increased by 70 percent, and average pumping was reduced by 40 percent. The results show an overall rise in the piezometric level in all layers (Figures 7-2a to h).

8.0 CONCLUSIONS

The results of the model calibration indicate the three-dimensional model, setup for a relatively large area encompassing the JPL site and surrounding area using MODFLOW, can be manipulated to provide a relatively good prediction of piezometric level fluctuations in JPL monitoring wells.

In the vicinity of the JPL site, calibration was satisfactory. The available data indicated that there was as much as 150 feet of difference in piezometric level between the bottom and top of the layers modeled in this report. These differences were the result of a combination of layering in this aquifer and transient responses to various natural and artificial stresses imposed on the aquifer. Despite large vertical piezometric level differences, the flow field was mainly horizontal. That is, overall the vertical component of the velocity vector was not significant compared with the horizontal components.

Groundwater mounding at the mouth of the Arroyo Seco is apparently due to the presence of a shallow interface with low vertical conductivity in this area. This interface also plays a significant part in inducing occasional short-term groundwater flow reversals observed at this part of the site. An interface with low vertical conductivity is also present deeper in the aquifer. This interface, together with several other interfaces with similar conductivities beneath the JPL site, were related to substantial differences in piezometric levels (150 ft) between screens in the deep wells during pumping periods.

Two scenarios for the basin were tested to evaluate the long term response of the flow system during modeling. The scenarios included a period of draught and a very wet period. Water levels dropped substantially during the draught period. Piezometric levels rose significantly during the wet period. Direction of groundwater flow in the vicinity of the JPL site varied substantially in both scenarios, and it was primarily dependent on the recharge at the mouth of the Arroyo Seco and pumping in the Pasadena wells.

9.0 REFERENCES

- CH2MHill, 1990. *Phase 1 Report: Devil's Gate Multi-Use Project*. Prepared for City of Pasadena, Water and Power Department, in cooperation with the Metropolitan Water District of Southern California, Santa Aria, January 26, 1990.
- CH2MHill, 1992. *Phase 2 Report: Devil's Gate Multi-Use Project*. Prepared for City of Pasadena, Water and Power Department, in cooperation with the Metropolitan Water District of Southern California, Santa Aria, July 14, 1992.
- Ebasco, 1994. *JPL Groundwater Elevation Data Report Number 2: July 1993 through December 1993*. February 1994.
- Enserch, 1995a. *QA/QC Plan for JPL Groundwater Modeling Study*. Prepared for the National Aeronautics and Space Administration Jet Propulsion Laboratory, Pasadena, CA. Prepared by Enserch Environmental Corporation, Santa Ana, CA.
- Enserch, 1995b. *MODFLOW Model Testing Report*. Prepared for the National Aeronautics and Space Administration Jet Propulsion Laboratory, Pasadena, CA. Prepared by Enserch Environmental Corporation, Santa Ana, CA.
- Foster Wheeler, 1996. *Report on the Preliminary Evaluation of Groundwater Data Collected at JPL Prior to the CERCLA RI/FS*. Prepared for the National Aeronautics & Space Administration Jet Propulsion Laboratory.
- Foster Wheeler, 1999. *Final Remedial Investigation Report for Operable Units 1 and 3: On-Site and Off-Site Groundwater*. Prepared for the National Aeronautics & Space Administration Jet Propulsion Laboratory.
- Hill, M. C., 1993, *A Computer Program (MODFLOWP) For Estimating Parameters of a Transient, Three-Dimensional, Ground-Water Flow Model Using Non-Linear Regression*, U.S. Geological Survey, Open File Report 91-484, 358 p.
- McDonald, M. G., and A. W. Harbaugh, 1988. *A Modular Three-Dimensional Finite-Difference Ground-Water Flow Model*, U.S. Geological Survey, Techniques of Water Resources Investigations Book 06-A1.
- MET, 1996. *Development and Calibration of the Two-Dimensional Groundwater Flow Model of Jet Propulsion Laboratory, Pasadena, California*. Prepared for Foster Wheeler Environmental Corporation.

- MET, 1997. *Development and Calibration of the Three-Dimensional Groundwater Flow Model of Jet Propulsion Laboratory, Pasadena, California*. Prepared for Foster Wheeler Environmental Corporation.
- Smith, D.P., and E.C. Sprotte, 1986. *Structural Contour Map of the Top of Crystalline Basement Rocks, North Half of the Pasadena Quadrangle, Los Angeles County, California*. Open File Report 864 LA, Plate 3. California Division of Mines and Geology. Prepared in cooperation with the County of Los Angeles, Department of County Engineer Facilities, and the Los Angeles County Flood Control District.
- Watermaster, 1983. *Watermaster Service in the Raymond Basin for the Period of July 1, 1983 through June 30, 1984*. Prepared for the Raymond Basin Water Management Board by the State of California, Department of Water Resources.
- Watermaster, 1988. *Watermaster Service in the Raymond Basin for the Period of July 1, 1988 through June 30, 1989*. Prepared for the Raymond Basin Water Management Board by the State of California, Department of Water Resources.
- Watermaster, 1992. *Watermaster Service in the Raymond Basin for the Period of July 1, 1992 through June 30, 1993*. Prepared for the Raymond Basin Water Management Board by the State of California, Department of Water Resources.
- Watermaster, 1993. *Watermaster Service in the Raymond Basin for the Period of July 1, 1993 through June 30, 1994*. Prepared for the Raymond Basin Water Management Board by the Foothills Municipal Water District and the State of California, Department of Water Resources.
- Watermaster, 1994. *Watermaster Service in the Raymond Basin for the Period of July 1, 1994 through June 30, 1995*. Prepared for the Raymond Basin Water Management Board by the Foothills Municipal Water District and the State of California, Department of Water Resources.

TABLES

TABLE 3-1

**RESULTS OF AQUIFER TESTS IN SHALLOW JPL WELLS
JET PROPULSION LABORATORY**

Well Number	Representative Depth Interval	Estimated Hydraulic Conductivity				Model Calibrated Hydraulic Conductivity
		Slug Test		Bail Test		
	(ft/bgs)	(ft/day)	(gpd/ft2)	(ft/day)	(gpd/ft2)	(ft/day)
MW-1	70-110	7	56	--	--	1
		9	71	5	41	
MW-5	85-135	16	120	--	--	2
		21	159	16	123	
MW-6	195-245	2	18	6	41	1
		3	22	6	42	
MW-7	225-275	41	309	26	197	2
		21	155	22	165	
MW-8	155-205	9	71	--	--	2
		24	179	13	100	
MW-9	18-68	2	13	--	--	1
		2	14	2	14	
MW-10	105-155	19	145	--		3
		29	217	21	158	
MW-13	180-230	13	96	--	--	1
		13	97	15	110	
MW-15	20.5-70.5	3	25	5	41	1
		4	28	6	42	

Notes:

(1): "--" denotes data were not reliable

TABLE 3-2

**RESULTS OF AQUIFER TESTS IN DEEP JPL MULTI-PORT WELLS
JET PROPULSION LABORATORY**

Well Number	Screen Number	Representative Depth Interval (ft/bgs)	Estimated Hydraulic Conductivity (ft/day)	Estimated Hydraulic Conductivity (gpd/ft ²)	Calibrated Hydraulic Conductivity (ft/day)
MW-3	1	170-180	7	49	1
	2	250-260	7	55	1
	3	344-354	1	5	1
	4	555-565	6	48	1
	5	650-660	2	12	1
	Average		4	34	
MW-4	1	146.8-156.8	6	44	1
	2	237.2-247.2	4	27	1
	3	319.6-329.6	4	34	1
	4	388.9-398.9	4	28	1
	5	509.4-519.4	3	19	1
	Average		4	30	
MW-11	1	140-150	0.4	3	1
	2	250-260	0.1	0.7	1
	3	420-430	0.1	0.5	1
	4	515-525	0.1	0.6	1
	5	630-640	0.1	0.5	1
	Average		0.2	1	
MW-12	1(1)	135-145	NA(2)	NA(2)	
	2	240-250	5	36	1
	3	315-325	4	30	1
	4	430-440	2	13	1
	5	546-556	5	35	1
	Average		4	29	
MW-14	1	205-215	10	72	1
	2	275-285	11	79	1
	3	380-390	11	82	1
	4	453-463	16	116	1
	5	538-548	6	42	1
	Average		10	78	
MW-17	1	246-256	6	42	4
	2	366-376	7	53	4
	3	466-476	0.9	6	4
	4	578-588	0.4	3	4
	5	723-733	5	40	4
	Average		6	47	
MW-18	1	266-276	4	26	2
	2	326-336	3	25	2
	3	421-431	7	55	2
	4	561-571	5	34	2
	5	681-691	4	29	2
	Average		5	34	
MW-19	1	240-250	0.6	4	7
	2	310-320	8	58	7
	3	390-400	1	9	7
	4	442-452	14	102	7
	5	492-502	3	25	7
	Average		5	40	
MW-20	1	228-238	9	64	4
	2	388-398	7	54	4
	3	558-568	16	116	4
	4	698-708	11	83	4
	5	898-908	3	20	4
	Average		8	68	
MW-21	1	86-96	5	35	3
	2	156-166	5	35	3
	3	236-246	5	37	3
	4	306-316	9	68	3
	5	366-376	5	40	3
	Average		6	43	

Notes:

(1): Piezometric head very close to measurement port, test data could not be analyzed with desired accuracy.

(2): NA - Not applicable.

GROUNDWATER ELEVATION DATA IN JPL AND CITY OF PASADENA WELLS
JET PROPULSION LABORATORY

(Elevation in feet above Mean Sea Level)

City, Monitoring Wells Date	8/1/05	9/1/05	10/1/05	11/1/05	12/1/05	1/1/06	2/1/06	3/1/06	4/1/06	5/1/06	6/1/06	7/1/06	8/1/06	9/1/06	10/1/06	11/1/06	12/1/06
MW-1	1095.08	1094.22	1093.23	1095.31	1095.27	1095.18	1095.11	1095.55	1099.57	1099.79	1098.86	1094.37	N/A	1084.45	1086.12	1093	N/A
MW-3-1	983.08	973.08	964.36	962.32	962.87	N/A	985.64	992.19	1001.21	989.98	977.43	966.38	960.38	950.76	946.93	947.09	961.03
MW-3-2	966.03	957.09	949.16	945.62	946.59	N/A	978.67	971.71	984.58	975.65	961.21	952.08	947.51	938.12	938.10	938.07	944.14
MW-3-3	961.89	952.90	944.81	940.87	941.53	N/A	979.27	966.52	980.79	972.82	956.46	946.37	942.31	932.03	934.99	934.45	941.72
MW-3-4	896.36	886.36	873.17	867.22	864.80	N/A	975.16	901.39	928.62	918.23	880.47	865.71	863.42	844.14	880.47	869.26	882.50
MW-3-5	872.59	861.71	848.57	841.82	837.19	N/A	971.93	880.82	879.25	893.45	854.71	838.78	833.27	815.53	869.19	843.43	873.00
MW-4-1	996.39	984.79	974.69	971.13	970.79	N/A	988.13	1008.04	1016.88	1005.62	991.57	976.95	960.58	958.58	952.38	953.05	965.41
MW-4-2	974.94	966.03	957.33	953.26	953.50	N/A	981.21	978.50	992.07	984.88	969.30	958.47	954.18	943.76	944.04	944.57	949.25
MW-4-3	971.95	962.75	954.28	950.29	950.43	N/A	980.67	974.21	988.60	981.91	965.16	954.73	951.13	940.45	942.79	943.77	948.20
MW-4-4	962.33	953.68	945.02	940.77	940.64	N/A	981.01	965.21	981.16	974.21	955.15	944.57	940.27	929.83	935.48	935.92	927.51
MW-4-5	895.25	884.52	872.31	866.80	864.77	N/A	975.46	899.63	928.94	918.78	879.12	865.12	862.01	843.37	882.32	871.26	881.02
MW-5	998.59	986.43	975.67	970.37	969.06	970.17	983.75	1006.07	1016.35	1006.24	991.51	975.98	969.31	958.66	951.28	953.98	960.60
MW-6	1003.22	996.68	988.32	983.76	982.98	983.55	990.42	1000.04	1009.95	1007.19	997.00	N/A	N/A	N/A	970.98	977.23	975.47
MW-7	998.37	987.14	976.58	970.20	969.25	970.28	978.99	996.85	1011.33	1009.06	995.53	N/A	971.69	961.45	N/A	N/A	N/A
MW-8	999.32	987.89	N/A	972.59	971.19	972.96	983.94	N/A	N/A	1007.34	994.36	980.48	972.81	961.72	954.94	954.73	961.71
MW-9	1087.47	1086.21	1088.44	1089.82	1088.91	1090.04	1091.90	1088.98	1092.99	1093.06	1092.41	1088.83	1085.17	1080.39	1081.56	1088.91	1089.09
MW-10	997.03	986.59	977.38	971.43	969.20	970.02	979.40	N/A	N/A	N/A	990.55	976.77	971.11	960.49	955.44	957.03	961.38
MW-11-1	1028.48	1023.36	1019.55	1018.93	1019.73	N/A	1023.17	1028.32	1036.21	1034.31	1028.01	1024.23	1021.14	1015.33	1012.58	1012.68	1016.11
MW-11-2	989.71	980.83	973.14	969.40	969.09	N/A	989.55	993.09	1005.11	998.62	985.68	974.76	969.35	959.88	957.99	958.87	964.50
MW-11-3	974.47	966.00	958.28	953.90	953.37	N/A	985.40	977.83	991.50	984.80	968.04	957.30	952.48	941.45	945.45	946.84	952.22
MW-11-4	969.75	961.81	953.75	949.24	948.16	N/A	987.79	977.20	988.96	981.38	962.50	951.35	946.35	934.84	942.14	947.14	950.66
MW-11-5	912.29	902.41	891.44	885.79	883.70	N/A	976.49	917.43	941.93	932.26	898.87	885.25	881.18	863.97	894.21	885.49	896.38
MW-12-1	999.92	987.83	977.85	978.03	977.95	N/A	988.24	1013.89	985.87	1009.12	996.00	981.99	974.88	963.57	N/A	N/A	975.81
MW-12-2	977.97	968.00	959.59	955.41	955.84	N/A	981.93	981.65	994.37	986.40	972.03	961.32	966.46	945.80	944.65	945.53	961.20
MW-12-3	972.47	962.92	954.73	950.60	951.22	N/A	981.38	975.85	989.38	981.79	968.46	956.26	952.04	941.34	942.14	942.15	948.26
MW-12-4	958.78	949.55	941.51	936.81	937.18	N/A	981.12	961.98	978.00	970.75	951.14	941.05	936.55	925.61	933.32	932.11	937.91
MW-12-5	905.12	893.71	882.20	876.38	874.59	N/A	975.99	909.38	935.48	925.32	890.79	876.60	873.35	855.05	888.26	878.20	889.25
MW-13	998.75	987.51	979.40	974.01	972.28	973.19	980.99	996.93	1010.53	1005.38	993.36	979.70	972.99	962.54	956.79	958.12	961.87
MW-14-1	1003.44	996.99	990.18	985.99	985.23	N/A	993.38	1001.39	1010.29	1007.49	997.97	988.17	983.16	974.64	972.61	976.94	978.21
MW-14-2	1001.80	995.20	988.90	985.45	984.55	N/A	993.95	1001.49	1010.84	1006.29	995.90	986.48	981.86	972.39	971.25	975.94	977.84
MW-14-3	1000.88	994.54	988.58	985.59	984.74	N/A	996.67	1001.84	1010.96	1005.91	995.04	985.93	981.45	972.11	971.58	976.73	978.18
MW-14-4	1000.78	994.52	988.81	985.65	984.77	N/A	995.39	1001.88	1011.01	1005.78	994.92	985.95	981.49	972.06	971.65	977.78	978.66
MW-14-5	999.73	993.45	987.75	984.99	984.21	N/A	996.62	999.16	1010.71	1004.89	993.56	984.95	980.36	970.92	971.67	976.56	978.30
MW-15	1093.06	1091.42	1092.08	1093.49	1093.53	1093.70	1093.84	1093.35	1098.18	1098.17	1097.30	1092.53	1088.16	1082.92	1084.62	N/A	1093.03
MW-16	998.41	987.30	977.50	972.17	970.48	971.68	982.05	997.37	1011.40	1005.35	N/A	N/A	972.55	962.13	955.94	956.62	960.80
MW-17-1	990.27	979.19	975.69	960.76	969.38	N/A	988.87	994.36	1008.64	996.09	983.06	970.41	963.45	952.54	946.06	N/A	N/A
MW-17-2	963.28	955.15	948.24	942.18	946.40	N/A	971.04	968.68	982.00	970.10	958.53	949.44	939.73	933.53	932.42	931.71	936.50
MW-17-3	958.52	950.40	944.77	930.36	938.71	N/A	967.58	959.40	973.95	959.60	944.56	939.68	927.58	918.17	919.02	918.55	923.60
MW-17-4	896.98	887.80	882.48	870.33	868.94	N/A	968.77	905.10	928.93	917.29	886.80	871.82	866.07	851.59	878.51	873.27	883.09
MW-17-5	878.07	869.51	858.14	850.13	846.67	N/A	960.82	891.36	913.01	899.68	889.68	859.46	853.41	837.64	871.21	871.50	877.66
MW-18-1	981.40	972.73	963.83	958.39	957.00	N/A	964.64	978.11	993.50	986.76	975.87	966.00	960.23	N/A	N/A	N/A	N/A
MW-18-2	977.83	969.25	960.79	955.74	955.17	N/A	971.53	975.80	989.55	982.51	971.70	962.33	956.45	947.36	942.86	939.65	942.15
MW-18-3	963.74	955.76	947.80	943.16	945.45	N/A	971.75	967.01	980.05	971.09	968.40	949.20	943.29	934.02	932.97	931.64	937.83
MW-18-4	937.82	928.67	921.16	914.67	918.11	N/A	988.98	942.27	968.34	948.93	928.68	915.06	910.19	898.98	908.55	907.95	914.56
MW-18-5	926.14	917.71	909.70	902.74	903.54	N/A	963.01	940.16	951.35	938.57	918.08	899.28	893.12	882.37	893.96	904.38	907.39
MW-19-1	981.86	973.58	964.11	957.51	955.77	N/A	987.79	978.54	991.14	985.18	971.76	960.69	955.61	946.45	942.53	942.28	946.66
MW-19-2	961.57	956.31	947.62	942.29	941.77	N/A	969.63	958.88	976.18	970.42	952.40	943.75	939.97	931.64	933.53	935.53	936.67
MW-19-3	957.19	952.37	943.32	937.77	937.53	N/A	971.60	955.66	972.25	968.67	948.25	938.57	935.15	925.77	930.23	932.65	932.95
MW-19-4	867.93	864.09	850.43	842.30	840.23	N/A	970.90	871.39	906.17	895.81	861.18	837.81	835.74	816.41	851.45	851.73	846.14
MW-19-5	864.38	860.62	846.71	838.59	836.49	N/A	970.89	867.84	902.74	892.21	847.50	834.09	832.07	812.71	850.01	848.06	842.31
MW-20-1	987.12	961.33	955.90	952.76	952.87	N/A	955.93	962.59	971.82	967.62	961.14	951.50	946.38	938.03	N/A	N/A	939.27
MW-20-2	966.33	960.24	954.40	951.91	952.17	N/A	955.34	962.88	972.67	967.18	958.65	948.42	944.21	936.98	932.01	936.49	939.50
MW-20-3	943.03	936.67	931.19	939.93	940.54	N/A	960.82	954.76	966.11	947.71	935.04	923.24	920.84	918.59	914.77	928.41	931.22
MW-20-4	930.98	923.09	920.07	916.00	919.50	N/A	953.24	956.84	960.16	940.83	923.69	908.90	901.95	890.01	893.64	919.07	918.20
MW-20-5	968.62	962.61	956.67	951.53	950.59	N/A	958.92	963.45	965.89	968.66	961.19	947.76	946.38	938.13	935.40	939.05	941.39
MW-21-1	999.85	993.19	984.22	978.94	978.91	N/A	982.92	994.43	1005.59	1001.10	994.31	982.59	977.80	N/A	N/A	N/A	N/A
MW-21-2	998.00	990.97	983.21	978.03	978.63	N/A	985.21	994.60	1004.92	1000.97	990.81	980.27	975.38	966.12	963.72	966.36	969.06
MW-21-3	996.83	990.09	982.51	977.65	978.26	N/A	986.06	994.27	1004.55	1000.23	989.64	979.51	974.85	965.57	963.74	966.46	969.04
MW-21-4	996.32	989.61	982.35	977.53	978.27	N/A	986.10	994.18	1004.43	999.83	989.05	979.18	974.60	965.27	963.86	966.56	969.00
MW-21-5	996.33	989.49	982.59	977.42	978.07	N/A	986.31	994.11	1004.48	999.91	989.06	979.21	974.50	965.25	963.77	966.64	969.10
City of Pasadena Wells																	
Arroyo	962.85	939.65	961.65	938.65	938.65	934.65	982.15	1004.45	1002.05	947.65	935.05	934.05	931.45	905.85	941.45		
Pasadena #52	826.31	824.31	827.31	825.31	825.31	825.31	977.91	995.01	991.21	824.51							

Notes:

Notes:
N/A = Not Available

NW = No Water Above Port

Groundwater elevations are shown in feet above MSL.

In multi-port wells, ports are numbered from 1 to 5, from shallow to deep.

TABLE 3-4

**GROUNDWATER EXTRACTION DATA FROM MUNICIPAL WELLS
JET PROPULSION LABORATORY**

Groundwater Extraction Rates in cubic feet per day								
Pasadena	Jan-95	422	Rubio	Jan-95	422	Rubio	Jan-95	141
Well No. 2	Feb-95	467	Well 4	Feb-95	0	Well 7	Feb-95	156
	Mar-95	2529		Mar-95	0		Mar-95	141
	Apr-95	10600		Apr-95	145		Apr-95	134020
	May-95	8009		May-95	0		May-95	176488
	Jun-95	13213		Jun-95	10745		Jun-95	241903
	Jul-95	8431		Jul-95	52553		Jul-95	287496
	Aug-95	20937		Aug-95	7166		Aug-95	307449
	Sep-95	18150		Sep-95	4937		Sep-95	293740
	Oct-95	10820		Oct-95	11803		Oct-95	226231
	Nov-95	7405		Nov-95	16117		Nov-95	189486
	Dec-95	1686		Dec-95	0		Dec-95	0
	Jan-96	1967		Jan-96	0		Jan-96	141
	Feb-96	0		Feb-96	0		Feb-96	0
	Mar-96	843		Mar-96	0		Mar-96	0
	Apr-96	4066		Apr-96	10019		Apr-96	109771
	May-96	8712		May-96	31476		May-96	241407
	Jun-96	13213		Jun-96	68244		Jun-96	268475
	Jul-96	18970		Jul-96	103841		Jul-96	272320
	Aug-96	20656		Aug-96	136160		Aug-96	251524
	Sep-96	12487		Sep-96	120516		Sep-96	219978
	Oct-96	7166		Oct-96	73068		Oct-96	134755
	Nov-96	145		Nov-96	0		Nov-96	145
	Dec-96	281		Dec-96	0		Dec-96	141
Lincoln#5	Jan-95	0	Valley#1	Jan-95	141	Valley#2	Jan-95	422
	Feb-95	0		Feb-95	0		Feb-95	156
	Mar-95	141		Mar-95	422		Mar-95	562
	Apr-95	145		Apr-95	145		Apr-95	106286
	May-95	0		May-95	0		May-95	130399
	Jun-95	145		Jun-95	145		Jun-95	164657
	Jul-95	0		Jul-95	49462		Jul-95	201360
	Aug-95	0		Aug-95	137003		Aug-95	204591
	Sep-95	145		Sep-95	97429		Sep-95	201538
	Oct-95	0		Oct-95	14895		Oct-95	183655
	Nov-95	0		Nov-95	0		Nov-95	86539
	Dec-95	0		Dec-95	0		Dec-95	0
	Jan-96	0		Jan-96	141		Jan-96	422
	Feb-96	0		Feb-96	0		Feb-96	300
	Mar-96	0		Mar-96	0		Mar-96	281
	Apr-96	0		Apr-96	0		Apr-96	290
	May-96	141		May-96	141		May-96	193912
	Jun-96	92057		Jun-96	145		Jun-96	195439
	Jul-96	187167		Jul-96	141		Jul-96	187167
	Aug-96	30773		Aug-96	281		Aug-96	181125
	Sep-96	0		Sep-96	0		Sep-96	174240
	Oct-96	0		Oct-96	0		Oct-96	46511
	Nov-96	0		Nov-96	290		Nov-96	436
	Dec-96	0		Dec-96	0		Dec-96	141

TABLE 3-4

**GROUNDWATER EXTRACTION DATA FROM MUNICIPAL WELLS
JET PROPULSION LABORATORY**

Groundwater Extraction Rates in cubic feet per day								
Arroyo	Jan-95	0	Pasadena	Jan-95	0	Ventura	Jan-95	0
	Feb-95	242847		Feb-95	246736		Feb-95	152927
	Mar-95	531854		Mar-95	415366		Mar-95	260938
	Apr-95	514879		Apr-95	400897		Apr-95	229271
	May-95	524406		May-95	406654		May-95	270494
	Jun-95	422387		Jun-95	352110		Jun-95	233336
	Jul-95	470307		Jul-95	386841		Jul-95	180142
	Aug-95	479019		Aug-95	414944		Aug-95	247589
	Sep-95	459122		Sep-95	411061		Sep-95	230578
	Oct-95	450495		Oct-95	403562		Oct-95	224826
	Nov-95	413675		Nov-95	414836		Nov-95	245678
	Dec-95	400330		Dec-95	414944		Dec-95	242109
	Jan-96	387122		Jan-96	399066		Jan-96	236770
	Feb-96	0		Feb-96	0		Feb-96	0
	Mar-96	145013		Mar-96	82061		Mar-96	68291
	Apr-96	486275		Apr-96	303323		Apr-96	0
	May-96	491104		May-96	324452		May-96	122109
	Jun-96	466963		Jun-96	320602		Jun-96	289529
	Jul-96	403984		Jul-96	399066		Jul-96	202203
	Aug-96	359159		Aug-96	287074		Aug-96	269791
	Sep-96	339478		Sep-96	292578		Sep-96	270943
	Oct-96	317285		Oct-96	126465		Oct-96	233959
	Nov-96	335702		Nov-96	27007		Nov-96	145636
	Dec-96	348761		Dec-96	0		Dec-96	282156

TABLE 3-4

**GROUNDWATER EXTRACTION DATA FROM MUNICIPAL WELLS
JET PROPULSION LABORATORY**

Groundwater Extraction Rates in cubic feet per day								
Las Flores	Jan-95	281	La Canad	Jan-95	0	Lincoln #3	Jan-95	0
Well No. 2	Feb-95	0		Feb-95	0		Feb-95	0
	Mar-95	1827		Mar-95	0		Mar-95	281
	Apr-95	47045		Apr-95	0		Apr-95	160882
	May-95	58876		May-95	141		May-95	189275
	Jun-95	65195		Jun-95	48642		Jun-95	153622
	Jul-95	120844		Jul-95	9696		Jul-95	188151
	Aug-95	120422		Aug-95	0		Aug-95	181125
	Sep-95	118919		Sep-95	145		Sep-95	175837
	Oct-95	74755		Oct-95	141		Oct-95	169322
	Nov-95	726		Nov-95	145		Nov-95	155219
	Dec-95	843		Dec-95	0		Dec-95	0
	Jan-96	0		Jan-96	0		Jan-96	0
	Feb-96	751		Feb-96	0		Feb-96	0
	Mar-96	0		Mar-96	0		Mar-96	0
	Apr-96	11906		Apr-96	145		Apr-96	0
	May-96	88385		May-96	141		May-96	128291
	Jun-96	104689		Jun-96	75649		Jun-96	99607
	Jul-96	113537		Jul-96	23185		Jul-96	0
	Aug-96	113115		Aug-96	37658		Aug-96	143607
	Sep-96	108464		Sep-96	0		Sep-96	138521
	Oct-96	94286		Oct-96	0		Oct-96	159486
	Nov-96	3485		Nov-96	0		Nov-96	160156
	Dec-96	422		Dec-96	0		Dec-96	160048
Valley#3	Jan-95	141	Valley#4	Jan-95	141	Windsor	Jan-95	0
	Feb-95	0		Feb-95	156		Feb-95	123368
	Mar-95	0		Mar-95	281		Mar-95	207261
	Apr-95	0		Apr-95	290		Apr-95	205748
	May-95	0		May-95	0		May-95	209510
	Jun-95	1016		Jun-95	145		Jun-95	177144
	Jul-95	562		Jul-95	141		Jul-95	194615
	Aug-95	0		Aug-95	0		Aug-95	199392
	Sep-95	145		Sep-95	145		Sep-95	192390
	Oct-95	0		Oct-95	0		Oct-95	184217
	Nov-95	0		Nov-95	0		Nov-95	184114
	Dec-95	422		Dec-95	0		Dec-95	180985
	Jan-96	0		Jan-96	141		Jan-96	179299
	Feb-96	0		Feb-96	0		Feb-96	0
	Mar-96	0		Mar-96	0		Mar-96	54380
	Apr-96	0		Apr-96	145		Apr-96	198053
	May-96	141		May-96	77986		May-96	202062
	Jun-96	145		Jun-96	160736		Jun-96	191519
	Jul-96	141		Jul-96	160469		Jul-96	181828
	Aug-96	144591		Aug-96	31195		Aug-96	157238
	Sep-96	178306		Sep-96	5372		Sep-96	158558
	Oct-96	96254		Oct-96	141		Oct-96	158081
	Nov-96	290		Nov-96	290		Nov-96	173369
	Dec-96	0		Dec-96	0		Dec-96	195036

TABLE 4-1

**SCREEN ELEVATIONS AND THEIR LAYER LOCATIONS IN THE 3-D MODEL
JET PROPULSION LABORATORY**

(Layer and Screen Elevations in feet above Mean Sea Level)

Well Number	First Layer 1102 - 904 ft		Second Layer 903 - 813 ft		Third Layer 812 - 735 ft		Fourth Layer 736 - 636 ft		Fifth Layer 635 - 528 ft		Sixth Layer 527 - 257 ft		Groundwater Elevations (ft. MSL)	
	Screen Top	Screen Bottom	Screen Top	Screen Bottom	Screen Top	Screen Bottom	Screen Top	Screen Bottom	Screen Top	Screen Bottom	Screen Top	Screen Bottom	Max	Min
La Canada Irr. #1	1000	950	899	894	810	796								
	929	927	869	867	758	752								
			842	840	748	735								
			832	824			726	720						
			819	816										
Valley #1	1025	---	---	---	---	748								
Valley #2	1015	---	---	---	---	---	---	720						
Valley #3	986	---	---	---	---	---	---	---	581					
Valley #4	980	---	---	---	---	---	---	720						
Arroyo	1030	---	---	858	790	785	700	668	819	803			1004	906
			851	826	759	756	659	654	589	563				
							649	636	559	533				
Ventura	1055	1018			747	---	---	689					873	776
	993	939												
	918	---	---	846										
Pasadena #52	907	---	---	---	---	797							995	824
					797	790								
					785	---			---	528				
Windsor			837	813	783	773	731	707					900	790
							683	672						
							680	---	---	572				
Lincoln #5					810	---	---	668						
							660	644						
MW-1	1045	1005											1100	1084
MW-2	1042	1002												
MW-3	930	920	850	840	756	746			545	535	450	440	1001	818
MW-4	936	926	846	836	765	755	694	684	574	564			1017	843
MW-5	987	937											1018	951
MW-6	994	944											1010	971
MW-7	988	938											1011	961
MW-8	985	935											1007	955
MW-9	1088	1038											1093	1080
MW-10	983	933											997	955
MW-11	998	989	889	879			719	709	624	614	509	499	1036	864
MW-12	967	957	862	852	787	777	672	662	556	546			1014	855
MW-13	1003	953											1011	957
MW-14	958	958	898	888	793	783	720	710	635	625			1010	971
MW-15	1102	1052											1098	1083
MW-16	1006	956											1011	956
MW-17	945	935	825	815			725	715	613	603	468	458	1009	838
MW-18	959	949	899	889	804	794	684	654	544	534			994	882
MW-19			903	893	753	743	701	691					991	813
			833	823			651	641						
MW-20	937	927			777	767			607	597	467	457	973	890
											267	257		
MW-21	973	963	903	893	753	743	693	683					1006	964
			823	813										

TABLE 4-2

**SCREEN LOCATIONS BY NODE AND LAYER NUMBER FOR ALL MONITORING WELLS
JET PROPULSION LABORATORY**

Well Number	X-Location Easting ft	y-Location Northing ft	z (elevation in ft)	Piezometric (elevation in feet) (2/1/96)	Row	Column	Layer
						in Model	
MW-1	6000	5980	1045	1095	19	44	1
MW-3-1	5635	4730	930	986	35	46	1
MW-3-2	5635	4730	850	979	35	46	2
MW-3-3	5635	4730	756	979	35	46	3
MW-3-4	5635	4730	545	975	35	46	5
MW-3-5	5635	4730	450	972	35	46	6
MW-4-1	5020	4640	936	988	39	39	1
MW-4-2	5020	4640	846	981	39	39	2
MW-4-3	5020	4640	765	981	39	39	3
MW-4-4	5020	4640	694	981	39	39	4
MW-4-5	5020	4640	573	975	39	39	5
MW-5	4680	4000	987	984	48	38	1
MW-6	3000	5345	994	990	40	17	1
MW-7	4870	5880	988	979	25	31	1
MW-8	5110	5435	985	984	29	36	1
MW-9	5850	5550	1088	1092	24	45	1
MW-10	4130	4130	983	979	49	31	1
MW-11-1	5530	5570	999	1023	25	41	1
MW-11-2	5530	5570	889	990	25	41	2
MW-11-3	5530	5570	719	985	25	41	4
MW-11-4	5530	5570	624	988	25	41	5
MW-11-5	5530	5570	509	976	25	41	6
MW-12-1	5530	5230	967	986	29	42	1
MW-12-2	5530	5230	862	982	29	42	2
MW-12-3	5530	5230	787	981	29	42	3
MW-12-4	5530	5230	672	981	29	42	4
MW-12-5	5530	5230	556	976	29	42	5
MW-13	4230	5400	1003	981	33	26	1
MW-14-1	2710	4925	968	993	46	17	1
MW-14-2	2710	4925	898	994	46	17	2
MW-14-3	2710	4925	793	997	46	17	3
MW-14-4	2710	4925	720	995	46	17	4
MW-14-5	2710	4925	635	997	46	17	5
MW-15	5850	5750	1102	1094	22	44	1
MW-16	4365	5835	1006	982	28	26	1
MW-17-1	6640	3330	945	969	46	64	1
MW-17-2	6640	3330	825	971	46	64	2
MW-17-3	6640	3330	725	968	46	64	4
MW-17-4	6640	3330	613	969	46	64	5
MW-17-5	6640	3330	468	961	46	64	6
MW-18-1	7175	4875	959	965	26	63	1
MW-18-2	7175	4875	899	972	26	63	2
MW-18-3	7175	4875	804	972	26	63	3
MW-18-4	7175	4875	664	969	26	63	4
MW-18-5	7175	4875	544	963	26	63	5
MW-19-1	5780	1615	903	968	70	62	2
MW-19-2	5780	1615	833	970	70	62	2
MW-19-3	5780	1615	753	972	70	62	3
MW-19-4	5780	1615	701	971	70	62	4
MW-19-5	5780	1615	651	971	70	62	4
MW-20-1	8340	1360	937	956	61	86	1
MW-20-2	8340	1360	777	958	61	86	3
MW-20-3	8340	1360	607	961	61	86	5
MW-20-4	8340	1360	467	953	61	86	6
MW-20-5	8340	1360	267	959	61	86	6
MW-21-1	3115	2875	973	983	68	25	1
MW-21-2	3115	2875	903	985	68	25	2
MW-21-3	3115	2875	823	986	68	25	2
MW-21-4	3115	2875	753	986	68	25	3
MW-21-5	3115	2875	693	986	68	25	4

TABLE 4-3**MONITORING WELL PORT (SCREEN) DESIGNATIONS IN 3-D MODEL****Shallow Wells**

Monitoring Well	Port	Layer of Port in 6-Layer Model	Layer of Port in 3-Layer Model
MW-01	1	1	1
MW-05	1	1	1
MW-06	1	1	1
MW-07	1	1	1
MW-08	1	1	1
MW-09	1	1	1
MW-10	1	1	1
MW-13	1	1	1
MW-15	1	1	1
MW-16	1	1	1

Deep Wells

Monitoring Well	Port	Layer of Port in 6-Layer Model	Layer of Port in 3-Layer Model
MW-03	1, 2, 4	1, 2, 5	1, 2, 3
MW-04	1, 2, 5	1, 2, 5	2, 2, 3
MW-11	1, 3, 4	1, 4, 5	1, 2, 3
MW-12	1, 2, 5	1, 2, 5	1, 2, 3
MW-14	1, 2, 4	1, 2, 4	1, 2, 3
MW-17	1, 2, 4	1, 2, 5	1, 2, 3
MW-18	1, 3, 4	1, 3, 4	1, 2, 3
MW-19	1, 2, 4	1, 2, 4	1, 2, 3
MW-20	1, 2, 3	1, 3, 5	1, 2, 3
MW-21	1, 2, 4	1, 2, 3	1, 2, 3
Note > Two ports in one layer			

Notes:

6-Layer Model = Discretization with 6 layers

3-Layer Model = Discretization with 3 layers

TABLE 4-4

SCREEN ELEVATIONS AND LAYER DESIGNATIONS IN REFINED THREE LAYER MODEL

Well Number	Screen Elevation (feet)	UTM-x	UTM-y	Layer 1		Layer 2		Layer 3	
				top of screen	bottom of screen	top of screen	bottom of screen	top of screen	bottom of screen
MW-1	1027	392507	3785254	1045	1005				
MW-3-1	928	392394	3784893	930	920				
MW-3-2	848	392394	3784893			850	840		
MW-3-3	754	392394	3784893			756	746		
MW-3-4	542	392394	3784893					545	535
MW-3-5	447	392394	3784893					450	440
MW-4-1	933	392170	3784815			936	926		
MW-4-2	843	392170	3784815			846	836		
MW-4-3	761	392170	3784815			765	755		
MW-4-4	691	392170	3784815			694	684		
MW-4-5	570	392170	3784815					574	564
MW-5	962	392064	3784637	987	937				
MW-6	969	391541	3785032	994	944				
MW-7	963	392129	3785211	988	938				
MW-8	960	392220	3785087	985	935				
MW-9	1053	392442	3785113	1088	1038				
MW-10	958	391894	3784670	983	933				
MW-11-1	990	392340	3785124	999	989				
MW-11-2	880	392340	3785124			889	879		
MW-11-3	710	392340	3785124			719	709		
MW-11-4	615	392340	3785124			624	614		
MW-11-5	500	392340	3785124					509	499
MW-12-1	962	392339	3785005	967	957				
MW-12-2	859	392339	3785005			862	852		
MW-12-3	779	392339	3785005			787	777		
MW-12-4	666	392339	3785005			672	662		
MW-12-5	554	392339	3785005					556	546
MW-13	978	391936	3785063	1003	953				
MW-14-1	966	391452	3784899	968	958				
MW-14-2	896	391452	3784899			898	888		
MW-14-3	791	391452	3784899			793	783		
MW-14-4	717	391452	3784899					720	710
MW-14-5	633	391452	3784899					635	625
MW-15	1077	392445	3785178	1102	1052				
MW-16	981	391977	3785193	1006	956				
MW-17-1	941	392675	3784428	945	935				
MW-17-2	821	392675	3784428			825	815		
MW-17-3	723	392675	3784428			725	715		
MW-17-4	609	392675	3784428					613	603
MW-17-5	465	392675	3784428					468	458

TABLE 4-4

SCREEN ELEVATIONS AND LAYER DESIGNATIONS IN REFINED THREE LAYER MODEL

Well Number	Screen Elevation (feet)	UTM-x	UTM-y	Layer 1		Layer 2		Layer 3	
				top of screen	bottom of screen	top of screen	bottom of screen	top of screen	bottom of screen
MW-18-1	955	392825	3784907	959	949				
MW-18-2	895	392825	3784907	899	889				
MW-18-3	801	392825	3784907			804	794		
MW-18-4	661	392825	3784907					664	654
MW-18-5	541	392825	3784907					544	534
MW-19-1	901	392376	3783950	903	893				
MW-19-2	829	392376	3783950			833	823		
MW-19-3	751	392376	3783950			753	743		
MW-19-4	699	392376	3783950					701	691
MW-19-5	645	392376	3783950					651	641
MW-20-1	935	393186	3783826	937	927				
MW-20-2	773	393186	3783826			777	767		
MW-20-3	603	393186	3783826					607	597
MW-20-4	465	393186	3783826					467	457
MW-20-5	265	393186	3783826					267	257
MW-21-1	969	391583	3784268	973	963				
MW-21-2	898	391583	3784268			903	893		
MW-21-3	819	391583	3784268			823	813		
MW-21-4	749	391583	3784268					753	743
MW-21-5	687	391583	3784268					693	683
MW-22-1	932	391763	3785041	938	928				
MW-22-2	848	391763	3785041			853	843		
MW-22-3	788	391763	3785041			793	783		
MW-22-4	710	391763	3785041					713	703
MW-22-5	589	391763	3785041					593	583
MW-23-1	934	391845	3784851	938	928				
MW-23-2	854	391845	3784851			858	848		
MW-23-3	789	391845	3784851			793	783		
MW-23-4	663	391845	3784851					668	658
MW-23-5	566	391845	3784851					568	558
MW-24-1	922	392078	3785152	926	916				
MW-24-2	828	392078	3785152			831	821		
MW-24-3	766	392078	3785152			771	761		
MW-24-4	647	392078	3785152					651	641
MW-24-5	523	392078	3785152					526	516

TABLE 6-1

**SUMMARY OF CORRELATION COEFFICIENTS OF OBSERVED VS. SIMULATED DATA
FOR INDIVIDUAL WELLS AND OVERALL SIMULATION
JET PROPULSION LABORATORY**

Calibration over the period from Aug/95 to Apr/96				
Monitoring Well	Port Number	Correlation Factor	Number of Observations/Simulations	R ²
MW-01	1	-0.49028	9	0.24
MW-05	1	0.970621	9	0.94
MW-06	1	0.904073	9	0.82
MW-07	1	0.929354	9	0.86
MW-08	1	0.943698	9	0.89
MW-09	1	-0.622658	9	0.39
MW-10	1	0.828523	8	0.69
MW-13	1	0.931291	9	0.87
MW-15	1	-0.363804	9	0.13
MW-16	1	0.92992	9	0.86
MW-03	1	0.770972	8	0.59
MW-03	2	0.536719	8	0.29
MW-03	4	0.96178	7	0.93
MW-04	1	0.954918	8	0.91
MW-04	2	0.613698	8	0.38
MW-04	5	0.980782	7	0.96
MW-11	1	0.316565	8	0.10
MW-11	3	0.700282	8	0.49
MW-11	4	0.742126	8	0.55
MW-12	1	0.282055	8	0.08
MW-12	2	0.565714	8	0.32
MW-12	5	0.978131	7	0.96
MW-14	1	0.915328	8	0.84
MW-14	2	0.851848	8	0.73
MW-14	4	0.800191	8	0.64
MW-17	1	0.975774	9	0.95
MW-17	2	0.715647	9	0.51
MW-17	4	0.968282	8	0.94
MW-18	1	0.936182	9	0.88
MW-18	3	0.641145	9	0.41
MW-18	4	0.377222	8	0.14
MW-19	1	0.850375	9	0.72
MW-19	2	0.482356	9	0.23
MW-19	4	0.947203	8	0.90
MW-20	1	0.680887	9	0.46
MW-20	2	0.104705	9	0.01
MW-20	3	-0.77402	9	0.60
MW-21	1	0.853531	9	0.73
MW-21	2	0.975159	9	0.95
MW-21	4	0.960271	9	0.92
OVERALL		0.964083	338	0.93

TABLE 6-2

**SUMMARY OF VERIFIED CORRELATION COEFFICIENTS OF OBSERVED VS. SIMULATED DATA
WITH A NEW DATA SET FOR INDIVIDUAL WELLS AND OVERALL SIMULATION
JET PROPULSION LABORATORY**

Verification over the period from Aug/97 to Apr/98				
Monitoring Well	Port Number	Correlation Factor	Number of Observations/Simulations	R ²
MW-01	1	-0.976463	8	0.95
MW-05	1	0.925552	8	0.86
MW-06	1	0.916788	8	0.84
MW-07	1	0.943566	8	0.89
MW-08	1	0.931083	8	0.87
MW-09	1	-0.839757	8	0.71
MW-10	1	0.874063	7	0.76
MW-13	1	0.945503	8	0.89
MW-15	1	-0.975203	8	0.95
MW-16	1	0.950918	8	0.90
MW-03	1	0.807007	8	0.65
MW-03	2	0.856812	8	0.73
MW-03	4	0.853227	8	0.73
MW-04	1	0.888752	8	0.79
MW-04	2	0.712853	8	0.51
MW-04	5	0.806738	8	0.65
MW-11	1	0.019574	8	0.00
MW-11	3	0.823665	8	0.68
MW-11	4	0.821429	8	0.67
MW-12	1	0.552541	5	0.31
MW-12	2	0.832372	8	0.69
MW-12	5	0.807195	8	0.65
MW-14	1	0.914013	8	0.84
MW-14	2	0.490103	8	0.24
MW-14	4	0.450381	8	0.20
MW-17	1	0.942798	5	0.89
MW-17	2	0.548379	8	0.30
MW-17	4	0.868348	8	0.75
MW-18	1	1.000022	2	1.00
MW-18	3	0.952276	8	0.91
MW-18	4	0.863762	8	0.75
MW-19	1	0.890923	8	0.79
MW-19	2	0.144053	8	0.02
MW-19	4	0.908096	8	0.82
MW-20	1	0.686612	5	0.47
MW-20	2	-0.803863	8	0.65
MW-20	3	-0.947572	8	0.90
MW-21	1	0.974505	3	0.95
MW-21	2	0.783827	8	0.61
MW-21	4	0.744948	8	0.55
MW-22	1	0.938536	8	0.88
MW-22	2	0.75591	8	0.57
MW-22	4	0.716552	8	0.51
MW-23	1	0.943658	8	0.89
MW-23	2	0.759557	8	0.58
MW-23	4	0.555023	8	0.31
MW-24	1	0.956562	8	0.92
MW-24	2	0.844924	8	0.71
MW-24	4	0.795935	8	0.63
OVERALL		0.920942	371	0.85

FIGURES

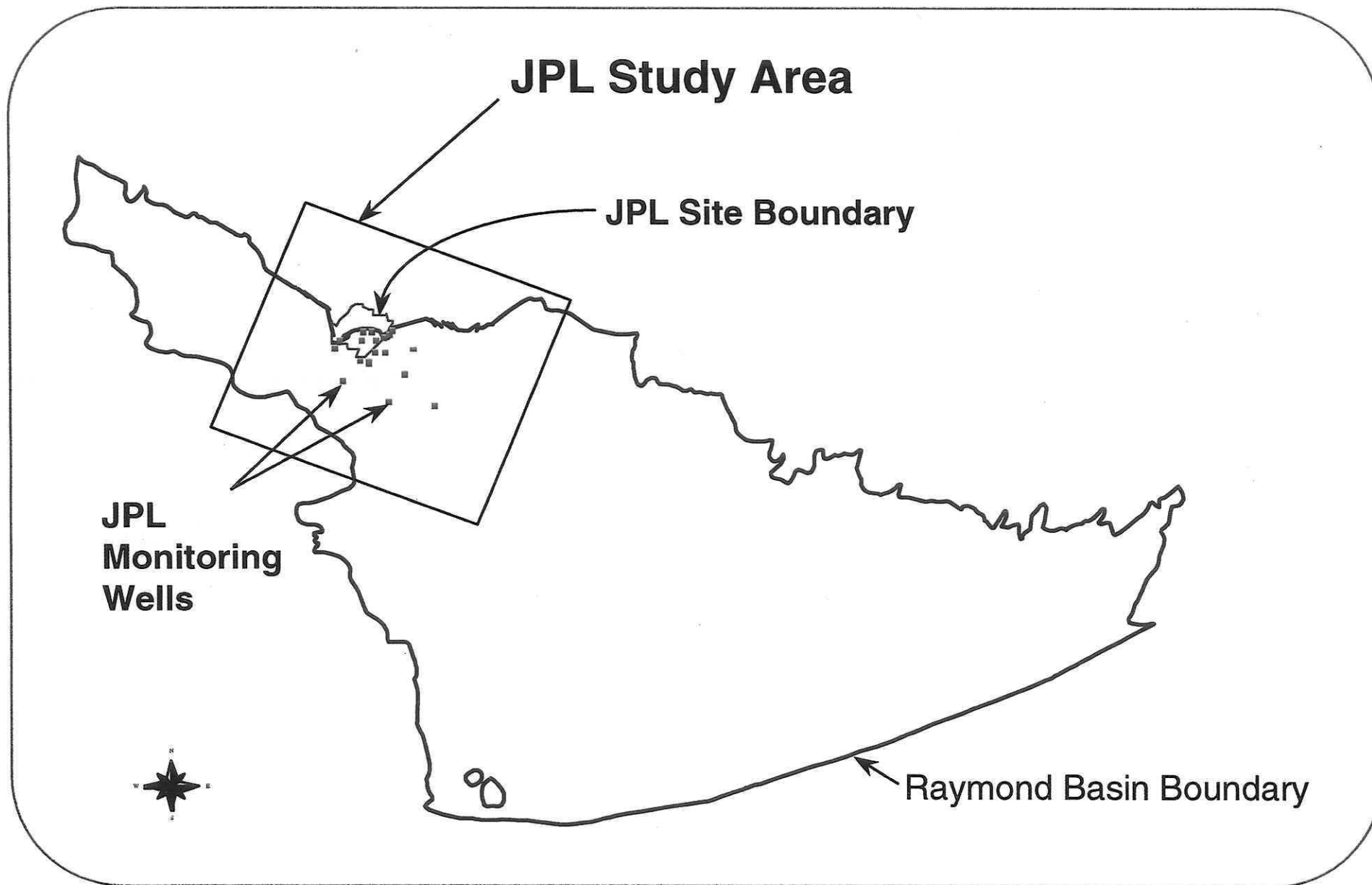


Figure 1-1
LOCATION OF THE JPL MODELED AREA IN RAYMOND BASIN

